Chapter 13

Geometrical Theory of Diffraction (GTD)

Advantages of GTD/UTD

1. It is simple to apply
2. It can be used to solve complicated problems that do not have exact solutions
3. It provides physical insight
4. It yields accurate results that compare well with experiments and other methods
5. It can be combined (hybridized) with other techniques, such as the Moment Method

Application Approach

Decompose a complex structure into simpler parts each of which resembles that of a canonical problem the solution of which is known.

Canonical Problems

Simpler boundary-value problems, which have the same local geometry at the points of diffraction as the object at the points of interest.

Examples of canonical problems include a wedge, cylinder, cone, corner, etc.

One of the main interests of diffraction by wedges is that engineers and scientists have investigated how the shape and material properties of complex structures affect their backscattering characteristics. The attraction in this area is primarily aimed toward designs of low-profile (stealth) technology by using appropriate shaping along with lossy or coated materials to reduce the radar visibility, as represented by radar cross section (RCS), of complex radar targets, such as aircraft, spacecraft and missiles. A good example is the F-117 shown in Figure 13-1, whose surface is primarily structured by a number of faceted wedges because, as will become evident from the developments, formulations, examples and problems of this chapter (see also Problem 13.50), the backscatter from exterior wedges is lower than that of convex curved surfaces. While in this chapter we will focus on the diffraction by PEC wedges, the diffraction by wedges with impedance surfaces, to represent lossy and composite wedge surfaces, will be the subject of Chapter 14.

F-117 Nighthawk

Printed with permission from Lockheed Martin.

Fig. 13-1

Geometrical Optics (GO)

Amplitude Spreading Factor

Geometrical Optics (GO) is an approximate high-frequency method for determining wave propagation for incident, reflected, and refracted fields. Because it uses ray concepts, it is often referred to as ray optics.

Originally GO was developed to analyze the propagation of light at sufficiently high frequencies where it was not necessary to consider the wave nature of light. Instead the transport of energy from one point to another in an isotropic lossless medium is accomplished using the conservation of energy flux in a tube of rays. For reflection problems, GO approximates the scattered fields only toward the specular directions as determined by *Snell's Law of Reflection.*

Geometrical Optics (GO)

- Direct Rays
- Reflected Rays
  (Snell's Law of Reflection)
- Refracted Rays
  (Snell's Law of Refraction)

$$n(s) = \frac{\beta(s)}{\beta_o} = \frac{\omega\sqrt{\mu_o \varepsilon(s)}}{\omega\sqrt{\mu_o \varepsilon_o}} = \sqrt{\frac{\varepsilon(s)}{\varepsilon_o}} = \sqrt{\varepsilon_r(s)}$$

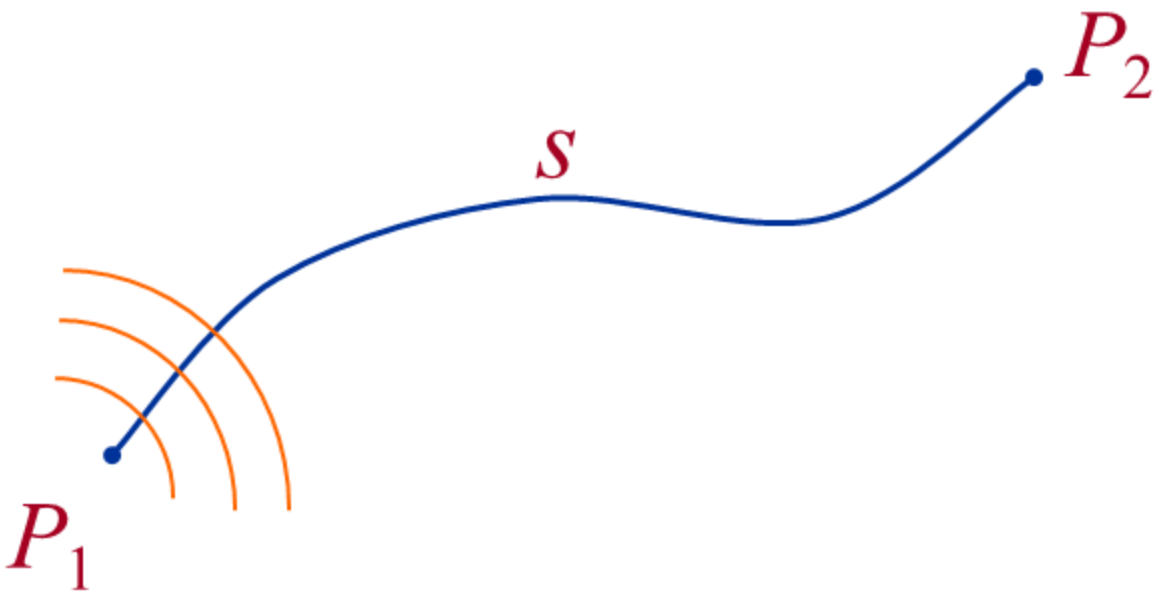

Fermat's Principle

Calculus of Variation

$$\delta \int_{P_1}^{P_o} n(s)\, ds = \text{Extremum} \quad \begin{matrix}\text{Maximum} \\ \underline{\text{or}} \\ \text{Minimum}\end{matrix} \qquad (13\text{-}1)$$

In our case a minimum

$n(s)$ = index of refraction

$n(s) = n$ = constant for homogeneous medium

δ = variational differential

Eikonal Surfaces

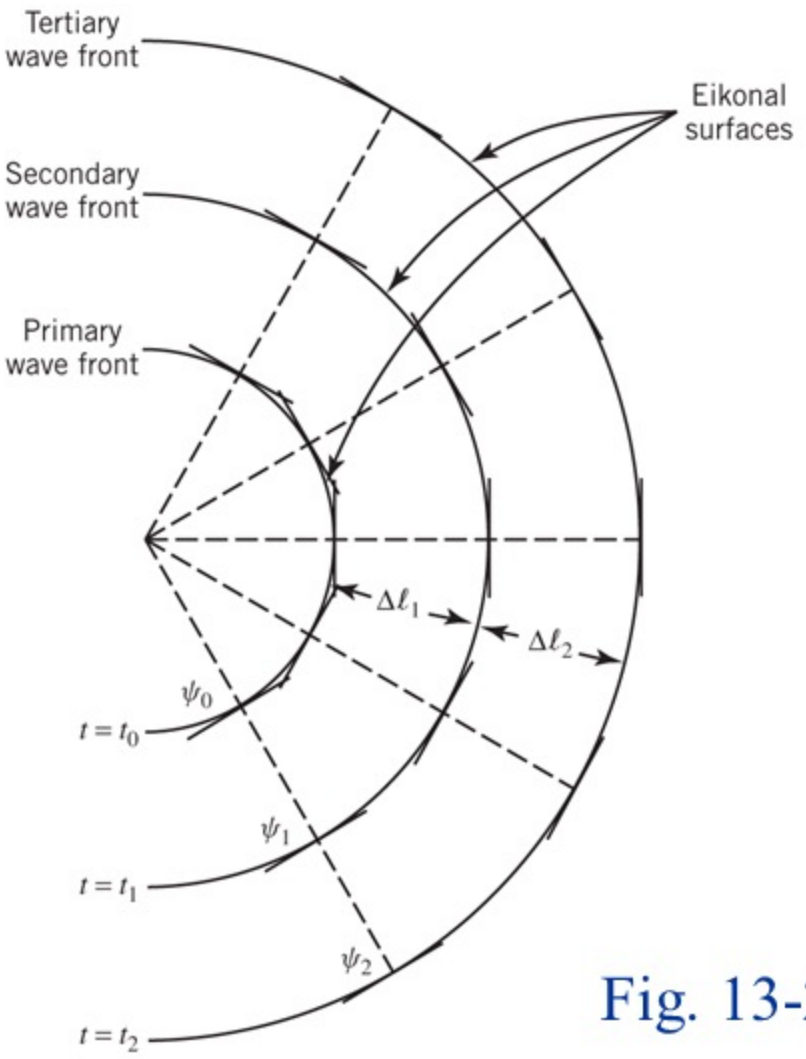

Fig. 13-2

Objectives

(Given the primary wavefront $\psi_o @ t_o$)

1. Determine the secondary wavefront surfaces ψ_n at $t = t_{n+1} > t_n$, $n = 0,1, ..$
2. To determine the power density field intensity on the secondary wavefront to those of the primary or previous wavefronts

The family of wavefront surfaces $\psi_n(x,y,z)$, $n = 0, 1, 2, .,$ that are normal to each of the radial rays is referred to as the Eikonal Surfaces, and they can be determined using the Eikonal Equation.

Equation for Eikonal Surfaces

Eikonal Equation

$$\left|\nabla \psi_n(x,y,z)\right|^2 = n^2(s)$$

$$\left(\frac{\partial \psi_n}{\partial x}\right)^2 + \left(\frac{\partial \psi_n}{\partial y}\right)^2 + \left(\frac{\partial \psi_n}{\partial z}\right)^2 = n^2(s)$$

(13-2)

Eikonal Surfaces for a Plane Wave

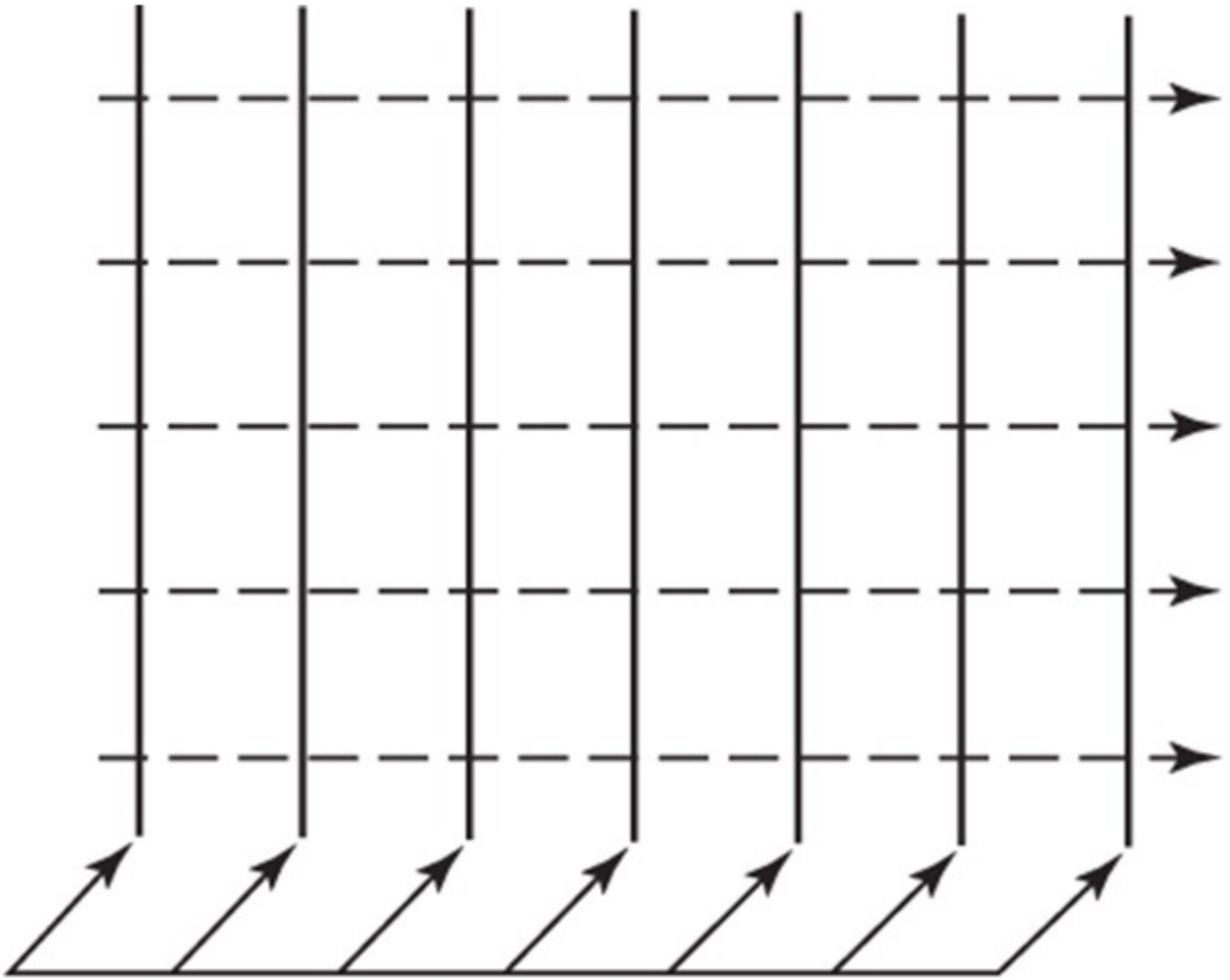

Fig. 13-3(a)

Eikonal Surfaces for a Cylindrical Wave

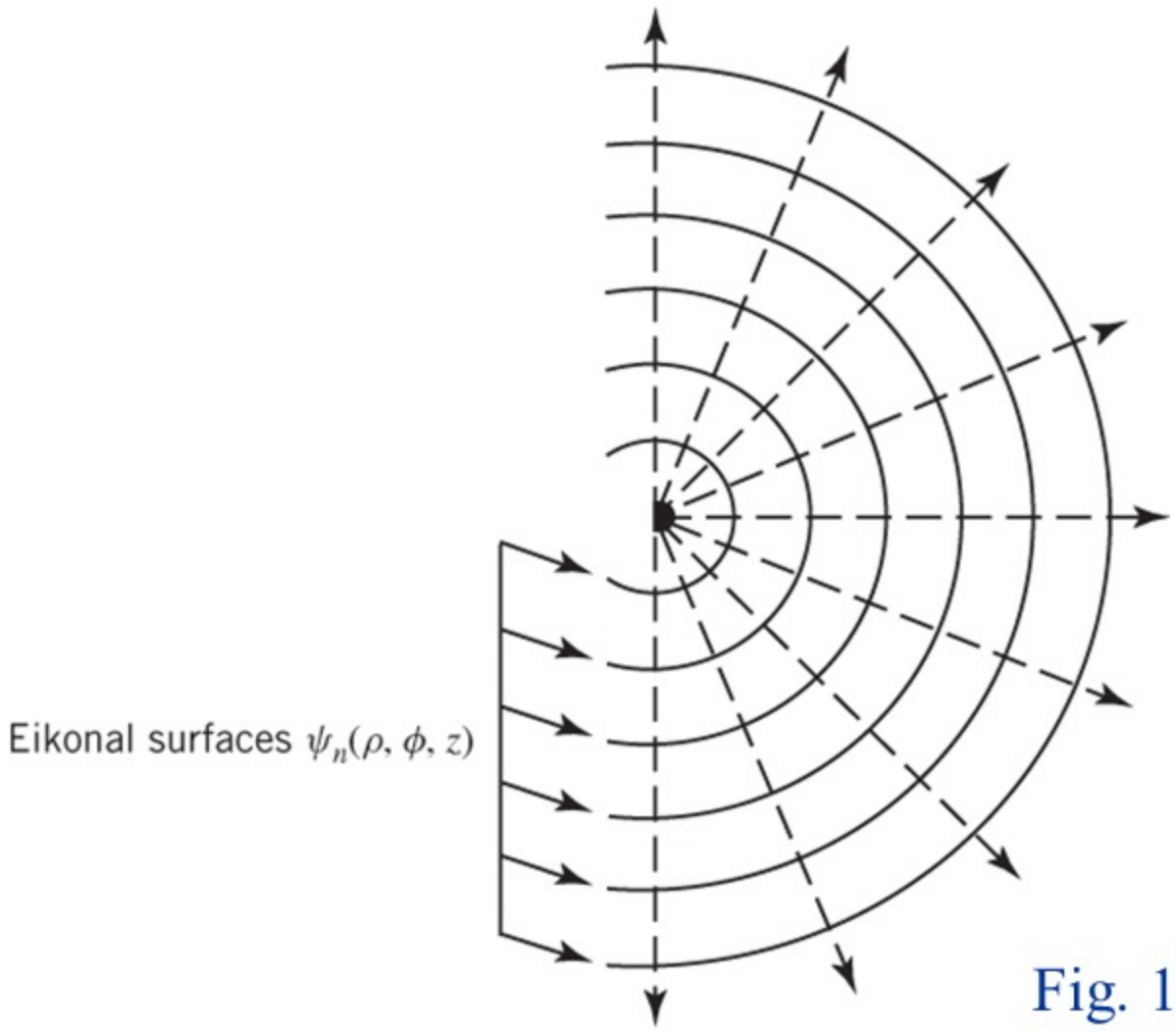

Fig. 13-3(b)

Eikonal Surfaces for a Spherical Wave

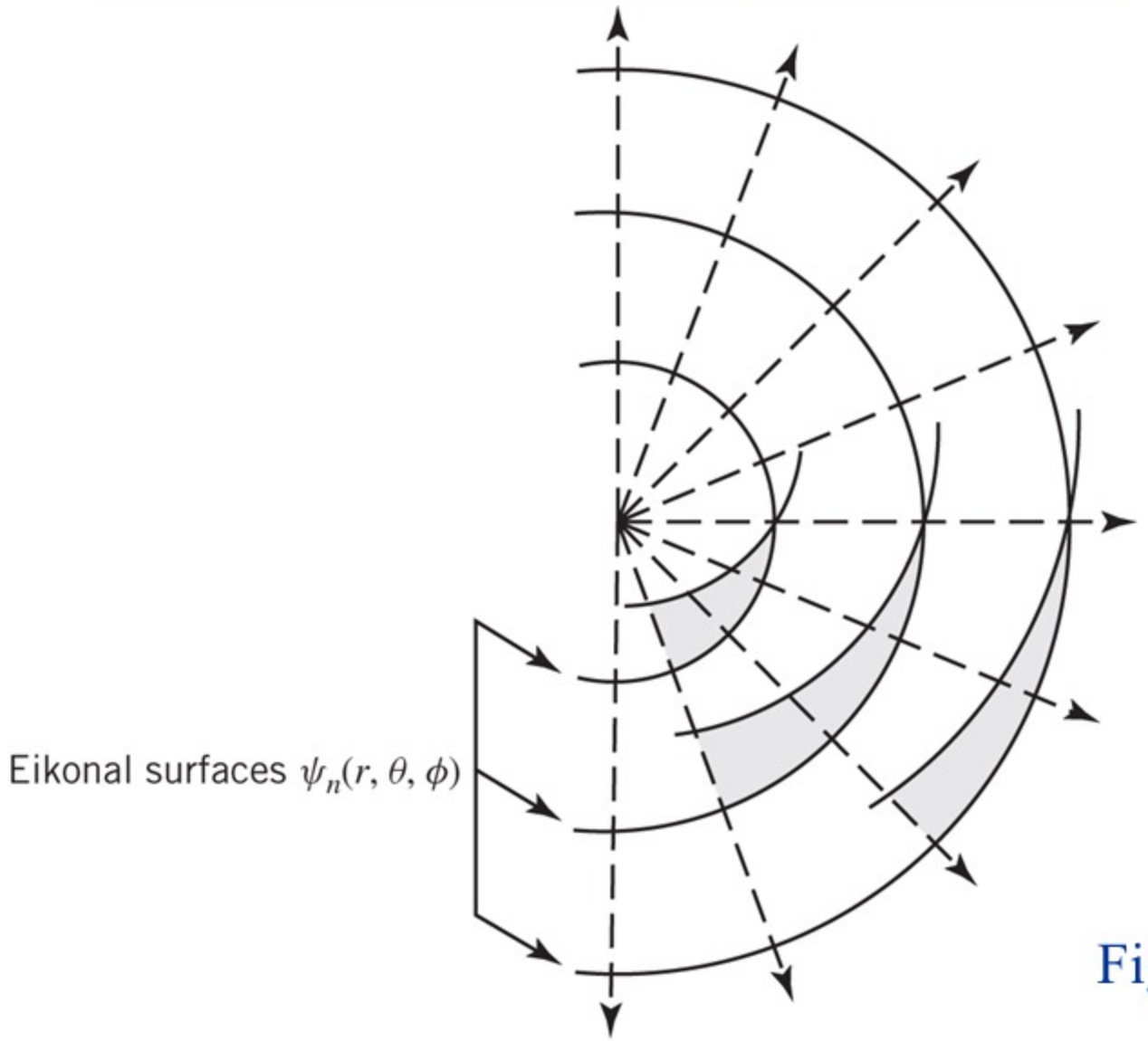

Fig. 13-3(c)

It is evident that the eikonal surfaces for:

a. Plane waves are planar surfaces perpendicular to the direction of wave travel
b. Cylindrical waves are cylindrical surfaces perpendicular to the cylindrical radial vectors
c. Spherical waves are spherical surfaces perpendicular to the spherical radial vectors

Tube of Rays for a Spherical Wave

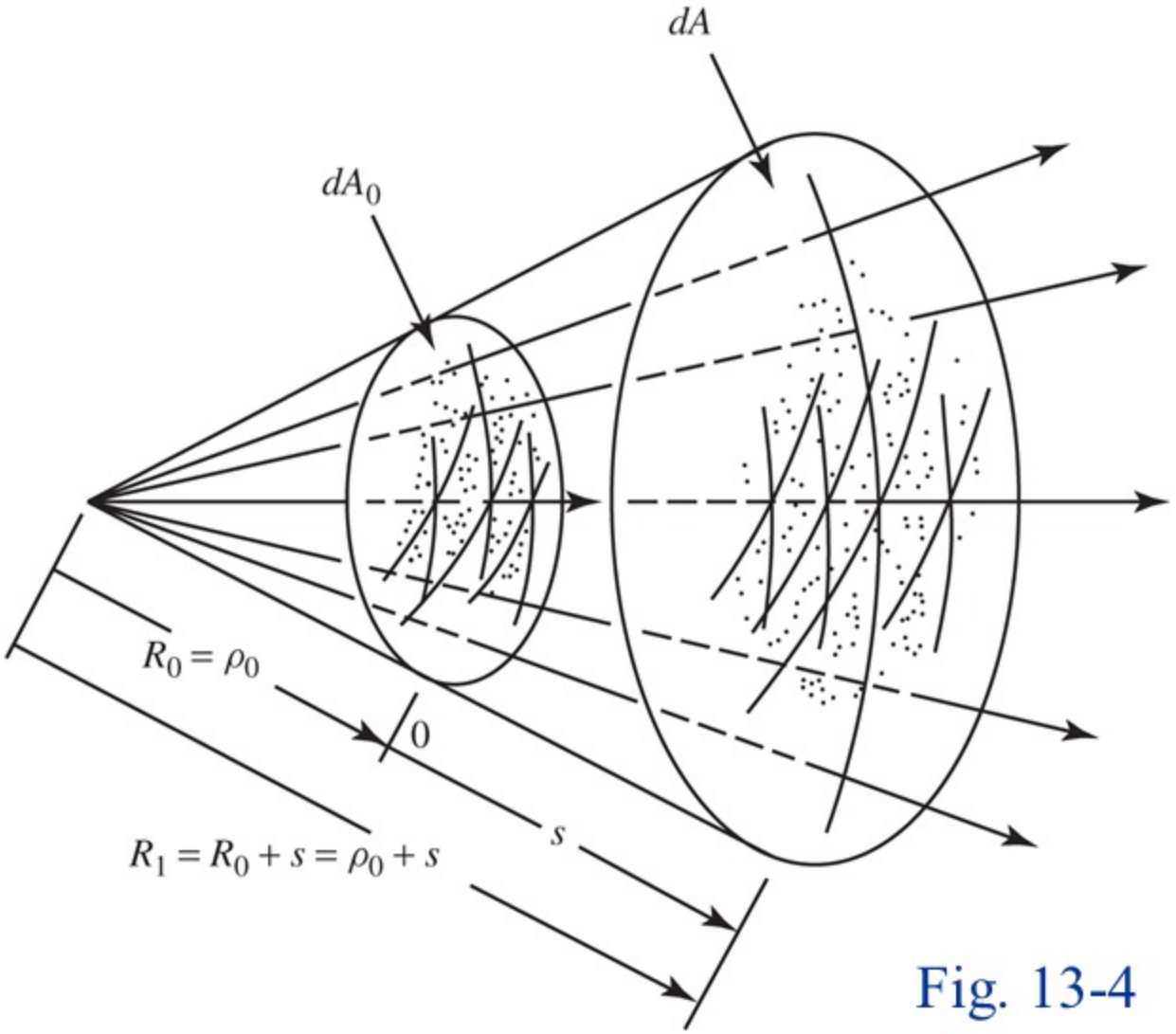

Fig. 13-4

Amplitude Spreading Factor

$$S_o dA_o = S\ dA \Rightarrow \frac{S(s)}{S_o} = \frac{dA_o}{dA} \qquad (13\text{-}3a,b)$$

$$\underline{S}(r,\theta,\phi) = \frac{1}{2}\mathrm{Re}\left[\underline{E} \times \underline{H}^*\right]$$

$$\underline{H} \cong \hat{a}_r \times \frac{\underline{E}}{\eta}$$

$$\underline{S}(r,\theta,\phi) \cong \hat{a}_r \frac{1}{2\eta}\left|\underline{E}(r,\theta,\phi)\right|^2 \qquad (13\text{-}4)$$

$$S(r,\theta,\phi) \cong \frac{1}{2\eta}\left|\underline{E}(r,\theta,\phi)\right|^2 = \frac{1}{2}\sqrt{\frac{\varepsilon}{\mu}}\left|\underline{E}(r,\theta,\phi)\right|^2 \qquad (13\text{-}4)$$

$$\frac{S(s)}{S_o} = \frac{dA_o}{dA} = \frac{\frac{1}{2\eta}|E|^2}{\frac{1}{2\eta}|E_o|^2} = \frac{|E|^2}{|E_o|^2}$$

$$\frac{dA_o}{dA} = \frac{|E|^2}{|E_o|^2}$$

$$\frac{|E|^2}{|E_o|^2} = \frac{dA_o}{dA}$$

$$\frac{|E|}{|E_o|} = \sqrt{\frac{dA_o}{dA}} \qquad (13\text{-}5a)$$

Spatial Attenuation (*Divergence*) Factor

❶ Planar Wavefront:

$$\frac{|\underline{E}|}{|\underline{E}_0|} = \sqrt{\frac{dA_o}{dA}} = \sqrt{\frac{dA_o}{dA_o}} = \boxed{1} = \boxed{\text{Constant}} \qquad (13\text{-}8)$$

❷ Cylindrical Wavefront:

$$\frac{|\underline{E}|}{|\underline{E}_0|} = \sqrt{\frac{dA_0}{dA}} = \sqrt{\frac{2\pi\ R_0/C_2}{2\pi\ R_1/C_2}} = \sqrt{\frac{R_0}{R_1}} = \boxed{\sqrt{\frac{\rho_0}{\rho_0 + s}}} \qquad (13\text{-}7)$$

❸ Spherical Wavefront:

$$\frac{|\underline{E}|}{|\underline{E}_0|} = \sqrt{\frac{dA_0}{dA}} = \sqrt{\frac{4\pi\ R_0^2/C_1}{4\pi\ R_1^2/C_1}} = \sqrt{\frac{R_0^2}{R_1^2}} = \frac{R_0}{R_1} = \boxed{\frac{\rho_0}{\rho_0 + s}} \qquad (13\text{-}6)$$

General Wavefront

Astigmatic Tube of Rays

Eikonal Surface

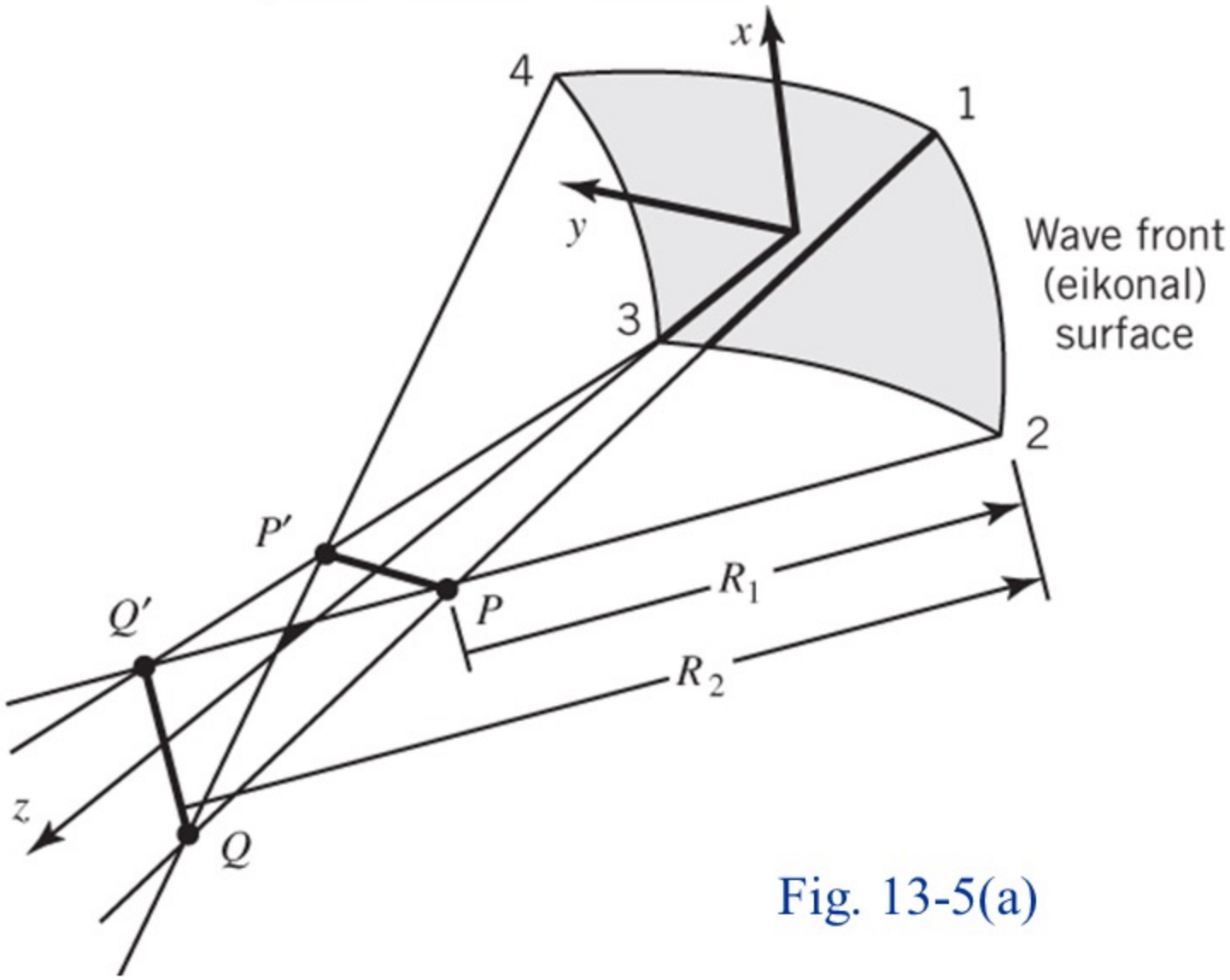

Fig. 13-5(a)

Caustic Lines

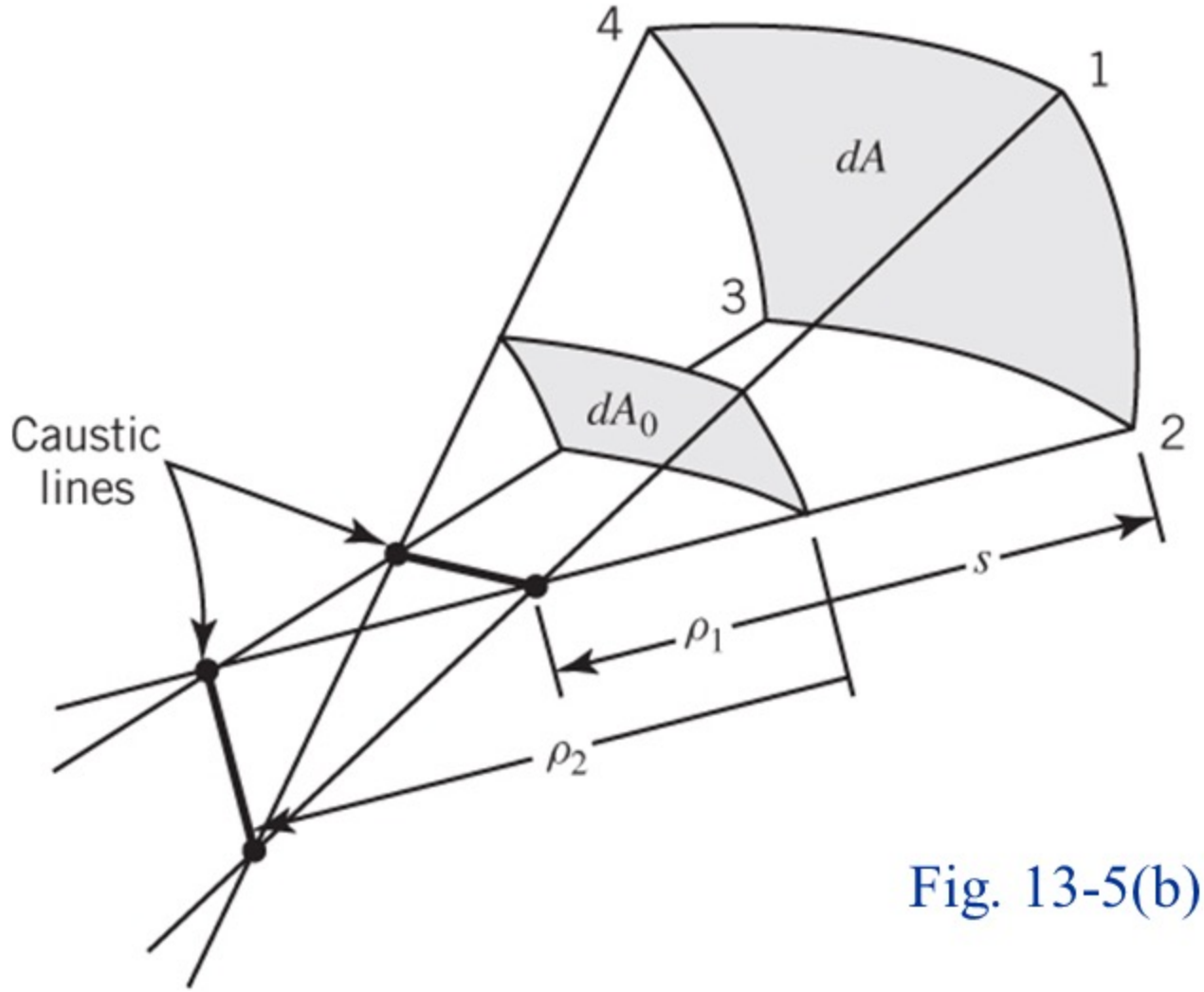

Fig. 13-5(b)

- A *caustic* is a point, a line, or a surface through which all the rays of a wave pass.
- Examples of it are the focal point of a paraboloid and the focal line of a parabolic cylinder.
- The field at a caustic is infinite, in principle, because an infinite number of rays pass through it.

Astigmatic Tube of Rays:

$$\frac{|\underline{E}|}{|\underline{E}_0|} = \sqrt{\frac{dA_0}{dA}} = \sqrt{\frac{(\rho_1 d\theta)\ \ (\rho_2 d\phi)}{(\rho_1 + s)\ d\theta\ (\rho_2 + s)\ d\phi}}$$

$$\frac{|\underline{E}|}{|\underline{E}_0|} = \sqrt{\frac{dA_0}{dA}} = \sqrt{\frac{\rho_1 \rho_2}{(\rho_1 + s)\ \ (\rho_2 + s)}}$$

(13-9)

Non Spherical Wavefront:

$$\frac{|\underline{E}|}{|\underline{E}_0|} = \sqrt{\frac{dA_0}{dA}} = \sqrt{dA_0\left(\frac{1}{dA}\right)}$$

$$= \sqrt{\left[\frac{1}{(\rho_1+s)(\rho_2+s)}\right](\rho_1\rho_2)} = \sqrt{\frac{\rho_1\rho_2}{(\rho_1+s)(\rho_2+s)}}$$

$$\frac{|\underline{E}|}{|\underline{E}_0|} = \sqrt{\frac{\rho_1\rho_2}{(\rho_1+s)(\rho_2+s)}} \qquad (13\text{-}9)$$

❶ If the incident field is spherical

$$\rho_1 = \rho_2 = \rho_O$$

❷ If the incident field is cylindrical

$$\rho_1 = \rho_o, \quad \rho_2 = \infty \quad \text{or} \quad \rho_1 = \infty, \quad \rho_2 = \rho_o$$

❸ If the incident field is a plane wave

$$\rho_1 = \rho_2 = \infty$$

For classical geometrical optics the transport of energy from one point to another in an isotropic lossless medium is accomplished using the conservation of energy flux in a tube of rays.

This accounts only for the amplitude and it does not include the wave nature of the wave; That is, it does not include phase and polarization.

Phase And Polarization

Phase and polarization information can be introduced by examining the approach introduced by Luneberg and Kline to develop high-frequency solutions of EM problems.

Luneberg (1944)- Kline (1951) Series Expansion of the E-Field for Large ω

$$\underline{E}(\underline{R},\omega) = e^{-j\beta_o \psi(\underline{R})} \sum_{m=0}^{\infty} \frac{\underline{E}_m(\underline{R})}{(j\omega)^m} \qquad (13\text{-}10)$$

$$\nabla^2 \underline{E} + \beta^2 \underline{E} = 0 \quad \text{- Wave Equation} \qquad (13\text{-}11)$$

$$\nabla \cdot \underline{E} = 0 \quad \text{- Maxwell's Equation} \qquad (13\text{-}12)$$

a. Eikonal Equation
b. Transport Equations (first- & higher-orders)
c. Conditional Equations (first- & higher-orders)

a. Eikonal Equation

$$|\nabla \psi|^2 = n^2 \quad \text{where} \begin{cases} \psi = \text{eikonal surface} \\ n = \text{index of refraction} \end{cases} \qquad (13\text{-}13a)$$

b. Transport Equations

1. $$\frac{\partial \underline{E}_0}{\partial s} + \frac{1}{2}\left(\frac{\nabla^2 \psi}{n}\right)\underline{E}_0 = 0 \quad \Longleftrightarrow \quad \text{first-order term} \qquad (13\text{-}13b)$$

2. $$\frac{\partial \underline{E}_m}{\partial s} + \frac{1}{2}\left(\frac{\nabla^2 \psi}{n}\right)\underline{E}_m = \frac{v_p}{2}\nabla^2 \underline{E}_{m-1} \quad \Longleftrightarrow \quad \text{higher-order terms} \qquad (13\text{-}13c)$$

$m = 1, 2, 3\ldots$ $\quad v_p$ = velocity of light in medium

c. Conditional Equations

1. $$\hat{s} \cdot \underline{E}_0 = 0 \quad \Longleftrightarrow \quad \text{first-order term} \qquad (13\text{-}13d)$$

2. $$\hat{s} \cdot \underline{E}_m = v_p \nabla \cdot \underline{E}_{m-1} \quad \Longleftrightarrow \quad \text{higher-order terms} \qquad (13\text{-}13e)$$

$m = 1, 2, 3\ldots$ where $\hat{s} = \dfrac{\nabla \psi}{n} =$ unit vector in the direction of propagation (normal to ψ)

s = distance along the ray path

Seeking solution of the form

$$\underline{E}(s) \cong e^{-j\beta_o \psi(s)}\, \underline{E}_0\,(s=0) \qquad (13\text{-}14)$$

By integrating first-order transport equation along s, it can be shown that

$$\underline{E}(s) = \underline{E}_o(0)\, e^{-j\beta_o\psi(0)} \sqrt{\frac{\rho_1\,\rho_2}{(\rho_1+s)\;(\rho_2+s)}}\; e^{-j\,\beta\,s} \qquad (13\text{-}15)$$

or

$$\underline{E}(s) = \underbrace{\underline{E}'_o(0)\, e^{-j\phi_o(0)}}_{\text{Field at reference point } (s=0)} \underbrace{\sqrt{\frac{\rho_1\,\rho_2}{(\rho_1+s)\;(\rho_2+s)}}}_{\text{Spatial Attenuation (divergence) factor}} \underbrace{e^{-j\beta s}}_{\text{Phase Factor}} \qquad (13\text{-}15a)$$

$\underline{E}'_o(0)$ = field amplitude at reference point $(s=0)$

$\phi_o(0)$ = field phase at reference point $(s=0)$

Extended Geometrical Optics

$$\underline{E}(s) = \underbrace{\underline{E}_o(0)}_{RF} \underbrace{\sqrt{\frac{\rho_1 \rho_2}{(\rho_1 + s)(\rho_2 + s)}}}_{ASF} \underbrace{e^{-j\beta s}}_{PF} \qquad (13\text{-}15a)$$

$RF = \underline{E}_o(0) =$ Field at Reference Point $s=0$

$ASF =$ Amplitude Spreading Factor

$PF =$ Phase Factor

It is evident that the leading term of the Luneberg-Kline series expansion solution for large ω predicts the spatial attenuation relation between the electric fields of two points as obtained by classical geometrical optics.

It also predicts the phase and polarization of the fields between the two points. This is only a high-frequency approximation, and it becomes more accurate as the frequency approaches infinity. However, for many practical engineering problems it does predict quite accurate results.

In principle, more accurate expressions to the GO approximation can be obtained by retaining higher-order terms in the Luneberg-Kline series expansion. However such a procedure is very difficult. In addition, the resulting terms do not remove the discontinuities introduced by GO along the incident and reflection boundaries.

GO (Luneberg-Kline Series)

1. They *improve* the high-frequency field approximations if the observation specular point is not near edges, shadow boundaries, or other surface discontinuities.
2. They *become singular* as the observation specular point approaches a shadow boundary on the surface.
3. They *do not correct* GO discontinuities along incident and reflection shadow boundaries.
4. They *do not describe* the diffracted fields in the shadow region.

Extended Geometrical Optics

$$\underline{E}(s) = \underbrace{\underline{E}_o(0)}_{RF} \underbrace{\sqrt{\frac{\rho_1 \rho_2}{(\rho_1 + s)(\rho_2 + s)}}}_{ASF} \underbrace{e^{-j\beta s}}_{PF} \qquad \text{(13-15a)}$$

$RF = \underline{E}_o(0) =$ Field at Reference Point $s=0$

$ASF =$ Amplitude Spreading Factor

$PF =$ Phase Factor

It should be noted that when the observation is chosen so the $s = -\rho_1$ the equation for the extended GO possesses singularities representing the congruence of the rays at the caustic lines *PP'* and *QQ'*. Therefore this equation is not valid along caustics and not very accurate near them, and it should not be used in those regions.

Eikonal Surface

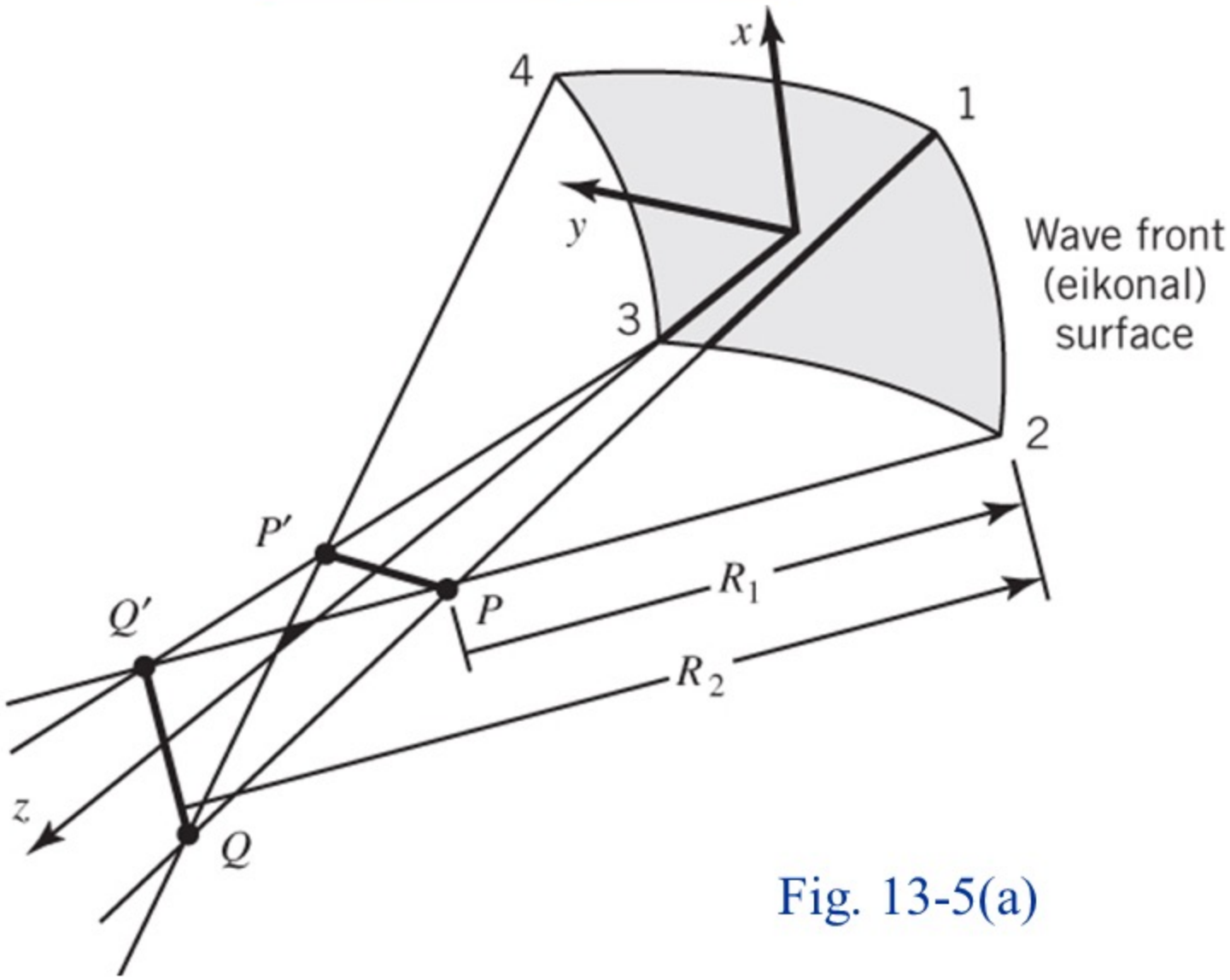

Fig. 13-5(a)

Caustic Lines

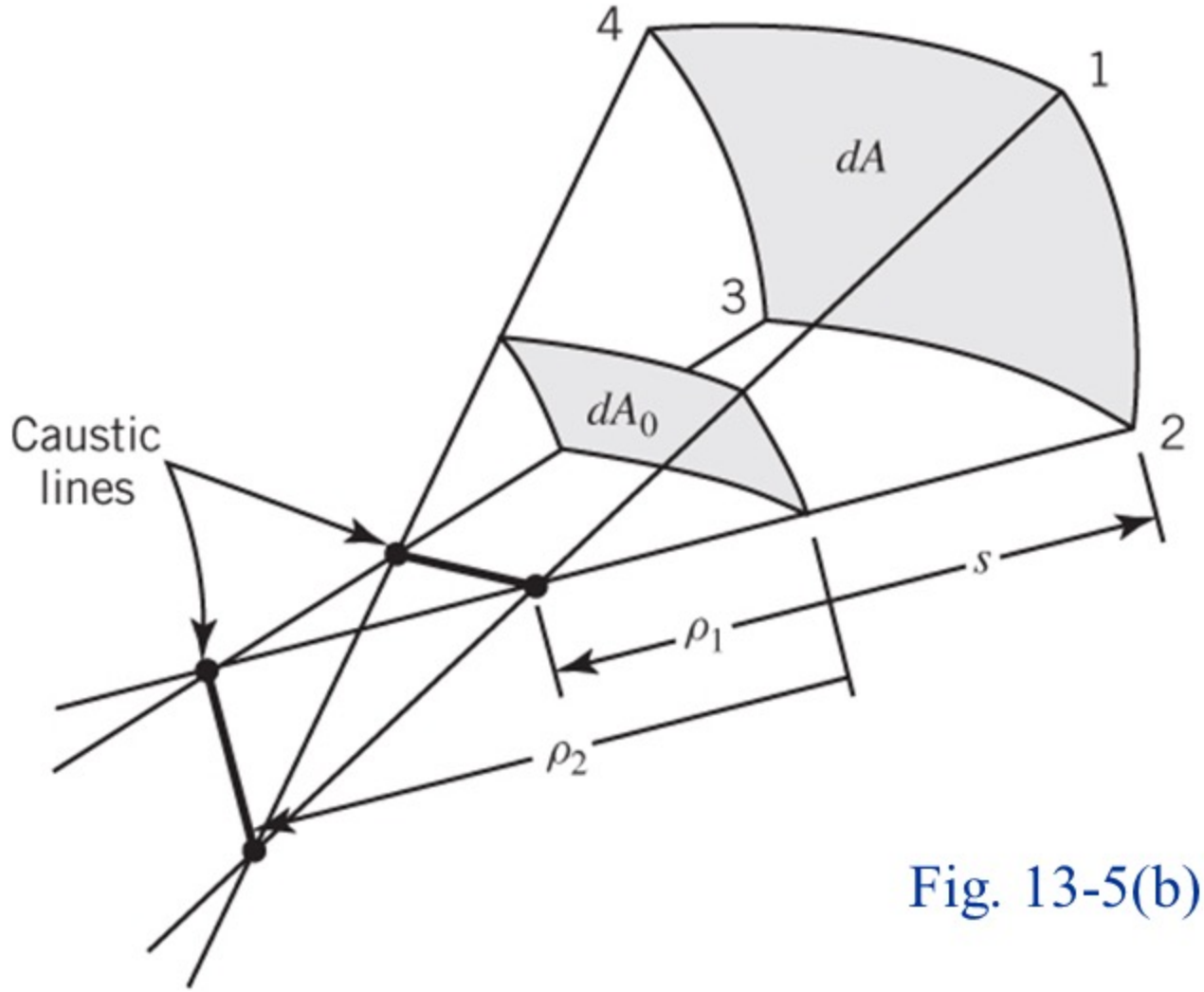

Fig. 13-5(b)

In addition, it is observed that when $-\rho_2 < s < -\rho_1$ the sign in the ρ_1+s term of the denominator changes. Similar changes of sign occur in the ρ_1+s and ρ_2+s terms when $s < -\rho_2 < -\rho_1$. Therefore the extended GO equation correctly predicts the $+90^o$ phase jumps each time a caustic is crossed in the direction of propagation.

Reflected Fields
(Reflection from Surfaces)

Reflection From a Curved Surface

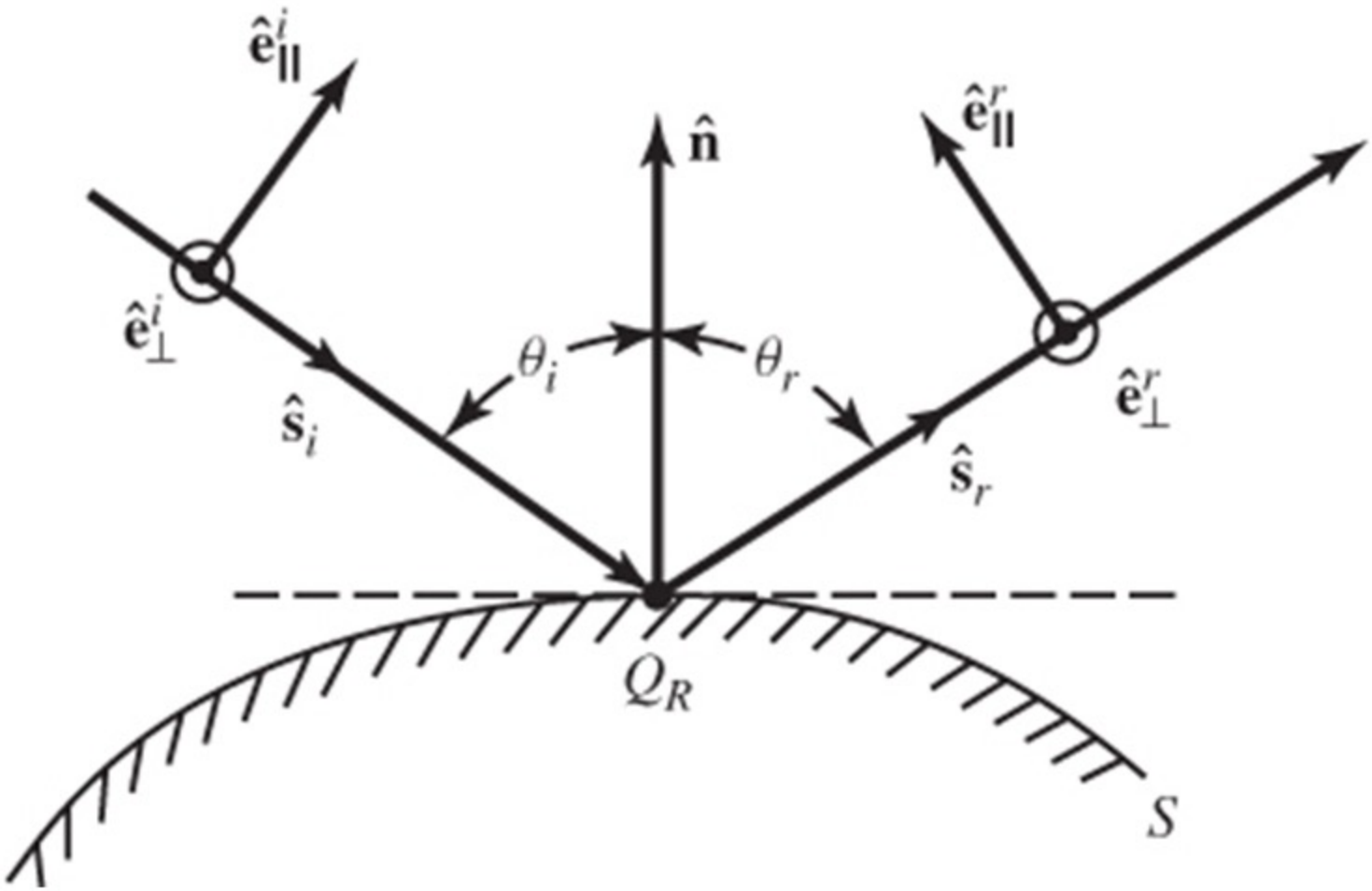

(a) Reflection point

Fig. 13-6

Reflected Field

$$\underline{E}^r = \underline{E}^i(Q_R) \cdot \tilde{R}\, A\, e^{-j\beta s}$$

$\underline{E}^i(Q_R)$ = incident field at point of reflection Q_R

$\tilde{R}$ = dyadic reflection coefficient

A = amplitude spreading factor $\left(\sqrt{\dfrac{\rho_1^r\ \rho_2^r}{(\rho_1^r + s)\ (\rho_2^r + s)}} \right)$

$e^{-j\beta s}$ = phase factor

Reflection From a Curved Surface

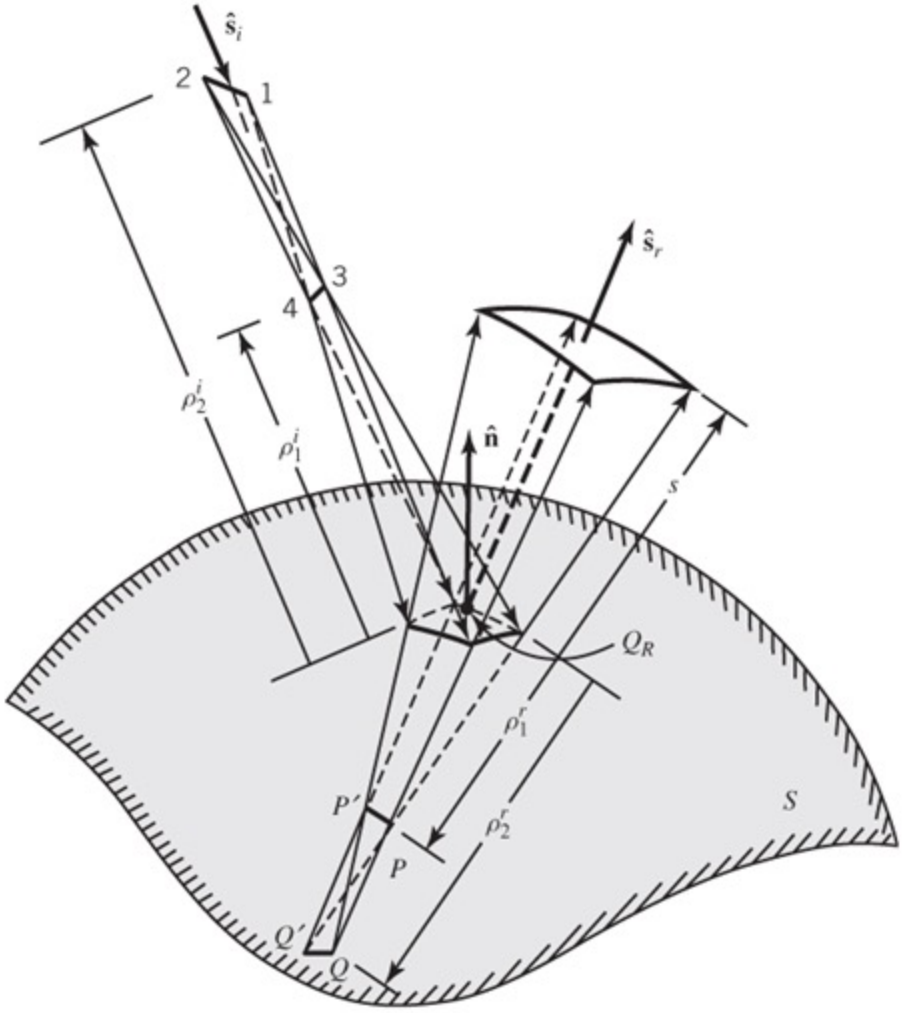

(b) Astigmatic tube of rays

Fig. 13-6

$$\hat{e}_{\perp}^{i} \times \hat{s}^{i} = \hat{e}_{\parallel}^{i} \tag{13-16a}$$

$$\hat{e}_{\perp}^{r} \times \hat{s}^{r} = \hat{e}_{\parallel}^{r} \tag{13-16b}$$

$$\mathbf{E}_0^i\left(s=0\right) = \hat{e}_{\parallel}^{i} E_{0\parallel}^{i} - \hat{e}_{\perp}^{r} E_{0\perp}^{r} \tag{13-17a}$$

$$\mathbf{E}_0^r\left(s=0\right) = \hat{e}_{\parallel}^{r} E_{0\parallel}^{i} - \hat{e}_{\perp}^{r} E_{0\perp}^{r} \tag{13-17b}$$

$$\begin{aligned} \underline{E}^{r}\left(s=0\right) &= \underline{E}^{i}\left(Q_R\right)\cdot\widetilde{R} \\ &= \left(\hat{e}_{\parallel}^{i} E_{\parallel}^{i} + \hat{e}_{\perp}^{i} E_{\perp}^{i}\right)\cdot\left(\hat{e}_{\parallel}^{i} e_{\parallel}^{r} - \hat{e}_{\perp}^{i} e_{\perp}^{r}\right) \end{aligned} \tag{13-18}$$

$$\widetilde{R} = \hat{e}_{\parallel}^{i}\hat{e}_{\parallel}^{r} - \hat{e}_{\perp}^{i}\hat{e}_{\perp}^{r}$$

$$= \text{Dyadic Reflection Coefficient}$$

In Matrix Form

$$\begin{pmatrix} E_{\parallel}^{r} \\ E_{\perp}^{r} \end{pmatrix} = \begin{bmatrix} E_{\parallel}^{i} & E_{\perp}^{i} \end{bmatrix} \begin{bmatrix} R_{\parallel,\parallel} & R_{\parallel,\perp} \\ R_{\perp,\parallel} & R_{\perp,\perp} \end{bmatrix} = \begin{bmatrix} E_{\parallel}^{i} & E_{\perp}^{i} \end{bmatrix} \begin{bmatrix} 1 & 0 \\ 0 & -1 \end{bmatrix}$$

or

$$E_{\parallel}^{r}(0) = E_{\parallel}^{i} \underbrace{R_{\parallel,\parallel}}_{=1} + E_{\perp}^{i} \underbrace{R_{\perp,\parallel}}_{=0} = E_{\parallel}^{i}(0)$$

$$E_{\perp}^{r}(0) = E_{\parallel}^{i} \underbrace{R_{\parallel,\perp}}_{=0} + E_{\perp}^{i} \underbrace{R_{\perp,\perp}}_{=-1} = -E_{\perp}^{i}(0)$$

Determine Reflected Field (First-Order, $\underline{E}_o$)

$$\underline{E}_o^i = \hat{e}_\parallel^i E_{o\parallel}^i + \hat{e}_\perp^i E_{o\perp}^i \quad \text{- Incident Field}$$

$$\underline{E}_o^r = \hat{e}_\parallel^r E_{o\parallel}^r + \hat{e}_\perp^r E_{o\perp}^r \quad \text{- Reflected Field}$$

A. Reflected Field $\boldsymbol{E}_o^r(s=0^+)$ at point of Reflection $(s=0^+)$

$$\underline{E}_o^r(s=0^+) = \underline{E}^i(Q_R)\cdot\tilde{R} = \left[\underline{E}_o^i(Q_R)\right]\cdot\left[\hat{e}_\parallel^i\hat{e}_\parallel^r - \hat{e}_\perp^i\hat{e}_\perp^r\right] \qquad (13\text{-}18)$$

$\underline{E}^r{}_o(s=0^+)$ = reflected field at point of reflection Q_R
(reference point is taken at $s=0^+$)

$\underline{E}^i{}_o(Q_R)$ = incident field at point of reflection Q_R

$\tilde{R}$ = dyadic reflection coefficient

$$\underline{E}_o^r(s=0) = \left[\underline{E}_o^i(Q_R)\right]\cdot\left[\hat{e}_{\parallel}^i\hat{e}_{\parallel}^r - \hat{e}_{\perp}^i\hat{e}_{\perp}^r\right]$$

$$= \left[\hat{e}_{\parallel}^i E_{o\parallel}^i - \hat{e}_{\perp}^i E_{o\perp}^i\right]\cdot\left[\hat{e}_{\parallel}^i\hat{e}_{\parallel}^r - \hat{e}_{\perp}^i\hat{e}_{\perp}^r\right]$$

$$\underline{E}_o^r(s=0) = \underset{1}{\left(\hat{e}_{\parallel}^i\cdot\hat{e}_{\parallel}^i\right)}\hat{e}_{\parallel}^r E_{o\parallel}^i - \underset{0}{\left(\hat{e}_{\parallel}^i\cdot\hat{e}_{\perp}^i\right)}\hat{e}_{\perp}^r E_{o\parallel}^i$$

$$+\underset{0}{\left(\hat{e}_{\perp}^i\cdot\hat{e}_{\parallel}^i\right)}\hat{e}_{\parallel}^r E_{o\perp}^i - \underset{1}{\left(\hat{e}_{\perp}^i\cdot\hat{e}_{\perp}^i\right)}\hat{e}_{\perp}^r E_{o\perp}^i$$

$$\underline{E}_o^r(s=0) = \hat{e}_{\parallel}^r E_{o\parallel}^i - \hat{e}_{\perp}^r E_{o\perp}^i$$

In matrix form

$$[R] = \begin{bmatrix} 1 & 0 \\ 0 & -1 \end{bmatrix}$$

B. Reflected Field $\boldsymbol{E}_o^r(s)$ at s

$$\underline{E}^r(s) = \underbrace{\underline{E}^i(Q_R)}_{\substack{\text{Incident} \\ \text{Field @ } QR}} \cdot \underbrace{\tilde{\underline{R}}}_{\substack{\text{Reflection} \\ \text{Coefficient}}} \underbrace{\sqrt{\frac{\rho_1^r \ \rho_2^r}{\left(\rho_1^r + s\right)\left(\rho_2^r + s\right)}}}_{\substack{\text{Amplitude Spreading} \\ \text{Factor}}} \underbrace{e^{-j\beta s}}_{\substack{\text{Phase} \\ \text{Factor}}} \qquad (13\text{-}20)$$

ρ_1^r, ρ_2^r = principal radii of curvature of reflected wavefront at the point of reflection Q_R

Extended Geometrical Optics

$$\underline{E}(s) = \underbrace{\underline{E}_o(s=0)}_{RF} \underbrace{\sqrt{\frac{\rho_1\ \rho_2}{(\rho_1+s)\ \ (\rho_2+s)}}}_{ASF} \underbrace{e^{-j\beta\ s}}_{PF}$$

$RF = \underline{E}_o(0) =$ Field at reference point s=0

$ASF =$ Amplitude spreading factor

$PF =$ Phase Factor

Determine Reflected Field (First-Order, $\underline{E}_o$)

$$\underline{E}_o^i = \hat{e}_\parallel^i E_{o\parallel}^i + \hat{e}_\perp^i E_{o\perp}^i \quad \text{-Incident Field}$$

$$\underline{E}_o^r = \hat{e}_\parallel^r E_{o\parallel}^r + \hat{e}_\perp^r E_{o\perp}^r \quad \text{-Reflected Field}$$

A. Reflected Field $\boldsymbol{E}_o^r$ ($s=0^+$) at point of Reflection ($s=0^+$)

$$\underline{E}_o^r(s=0) = \underline{E}^i(Q_R)\cdot\tilde{R} = \left[\underline{E}_o^i(Q_R)\right]\cdot\left[\hat{e}_\parallel^i\hat{e}_\parallel^r - \hat{e}_\perp^i\hat{e}_\perp^r\right]$$

$\underline{E}^r{}_o(s=0)$ = reflected field at point of reflection Q_R
(reference point is taken at $s=0$)

$\underline{E}^i{}_o(Q_R)$ = incident field at point of reflection Q_R

$\tilde{R}$ = dyadic reflection coefficient

$$\underline{E}_o^r(s=0) = \underline{E}^i(Q_R)\cdot\widetilde{R} = \left[\underline{E}^i(Q_R)\right]\cdot\left[\hat{e}_{||}^i\hat{e}_{||}^r - \hat{e}_{\perp}^i\hat{e}_{\perp}^r\right]$$

In Matrix Form

$$E_o^r(s=0) = \left[\underline{E}^i(Q_R)\right]\cdot\left[R\right]$$

$$\begin{bmatrix} E_{o||}^r(s=0) \\ E_{o\perp}^r(s=0) \end{bmatrix} = \begin{bmatrix} E_{||}^i(Q_R) & E_{\perp}^i(Q_R) \end{bmatrix} \begin{bmatrix} R_{||,||} & R_{||,\perp} \\ R_{\perp,||} & R_{\perp,\perp} \end{bmatrix}$$

$$E_{o||}^r(s=0) = E_{||}^i(Q_R)\,\cancel{R_{||,||}}^{\,1} + E_{\perp}^i(Q_R)\,\cancel{R_{\perp,||}}^{\,0}$$

$$E_{o\perp}^r(s=0) = E_{||}^i(Q_R)\,\cancel{R_{||,\perp}}^{\,0} + E_{\perp}^i(Q_R)\,\cancel{R_{\perp,\perp}}^{\,-1}$$

In matrix form

$$[R]=\begin{bmatrix}1 & 0\\ 0 & -1\end{bmatrix}$$

B. Reflected Field $\boldsymbol{E}_o^r(s)$ at s

$$\underline{E}^r(s)=\underbrace{\underline{E}^i(Q_R)}_{\substack{\text{Incident}\\ \text{Field @ } QR}}\cdot\underbrace{\underline{\tilde{R}}}_{\substack{\text{Reflection}\\ \text{Coefficient}}}\underbrace{\sqrt{\frac{\rho_1^r\ \rho_2^r}{\left(\rho_1^r+s\right)\ \left(\rho_2^r+s\right)}}}_{\substack{\text{Amplitude Spreading}\\ \text{Factor}}}\underbrace{e^{-j\beta\ s}}_{\substack{\text{Phase}\\ \text{Factor}}} \qquad (13\text{-}20)$$

ρ_1^r, ρ_2^r = principal radii of curvature of reflected wavefront at the point of reflection Q_R

Reflected Field

$$\underline{E}^r = \underline{E}^i(Q_R) \cdot \tilde{R}\, A\, e^{-j\beta s} \qquad (13\text{-}20)$$

$\underline{E}^i(Q_R)$ = incident field at point of reflection Q_R

$\tilde{R}$ = dyadic reflection coefficient

A = amplitude spreading factor $\left(\sqrt{\dfrac{\rho_1^r\ \rho_2^r}{(\rho_1^r + s)\ (\rho_2^r + s)}} \right)$

$e^{-j\beta s}$ = phase factor

Reflection From A General Curved Surface

Reflection from a 3-D Curved Surface

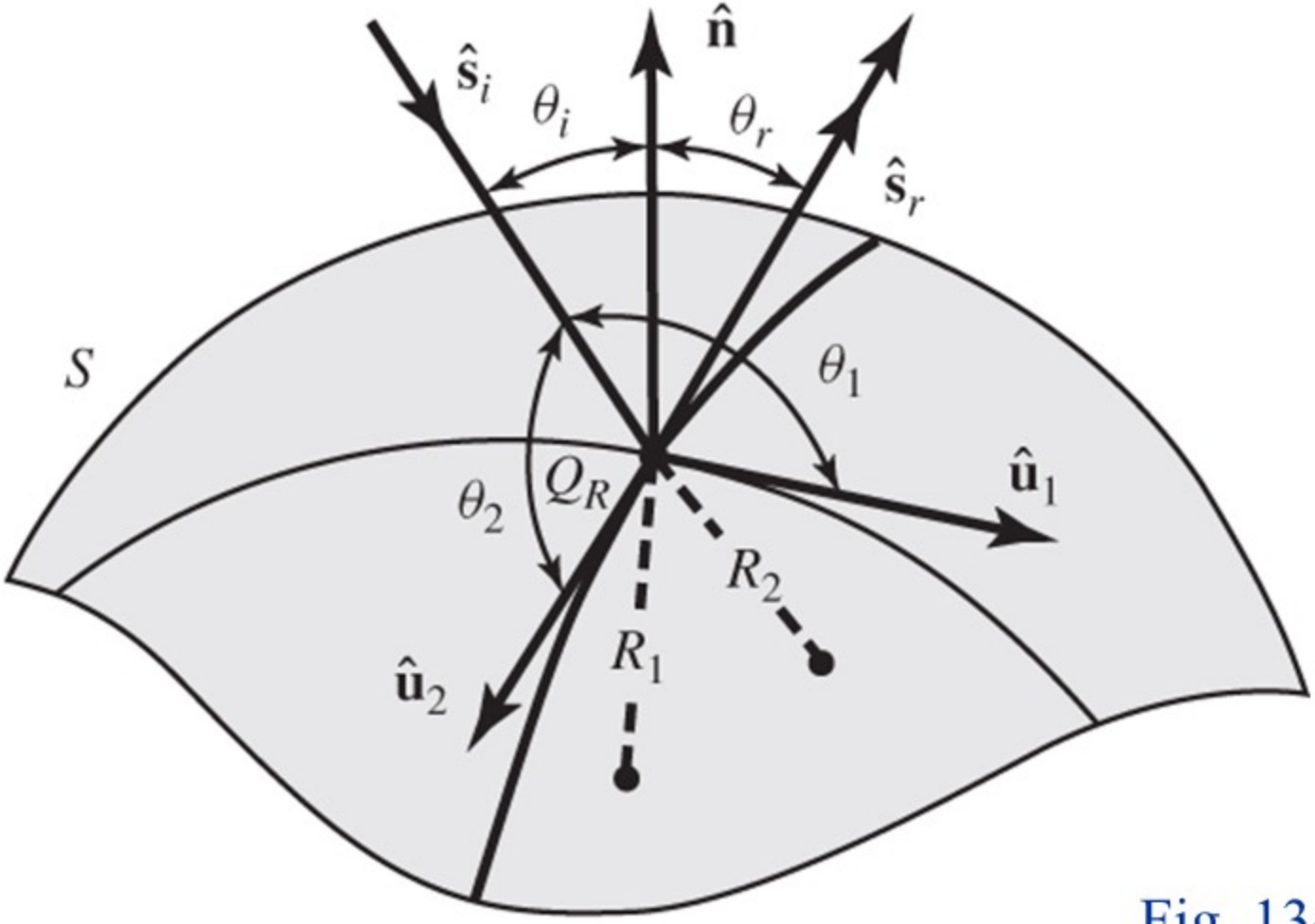

Fig. 13-7

(a) Principal radii of curvature

Reflected Field

$$\underline{E}^r = \underline{E}^i(Q_R) \cdot \tilde{R}\, A\, e^{-j\beta s} \qquad (13\text{-}20)$$

$\underline{E}^i(Q_R)$ = incident field at point of reflection Q_R

$\tilde{R}$ = dyadic reflection coefficient

ASF = amplitude spreading factor $\left(\sqrt{\dfrac{\rho_1^r\ \rho_2^r}{(\rho_1^r + s)\ (\rho_2^r + s)}} \right)$

$e^{-j\beta s}$ = phase factor

Principal Radii of Curvature of Reflected Wavefront (ρ_1^r, ρ_2^r)

$$\left.\begin{aligned} \frac{1}{\rho_1^r} &= \frac{1}{2}\left(\frac{1}{\rho_1^i}+\frac{1}{\rho_2^i}\right)+\frac{1}{f_1} \\ \frac{1}{\rho_2^r} &= \frac{1}{2}\left(\frac{1}{\rho_1^i}+\frac{1}{\rho_2^i}\right)+\frac{1}{f_2} \end{aligned}\right\} \quad \rho_1^i, \rho_2^i = \text{Principal radii of curvature of incident wavefront}$$

(13-21a)

(13-21b)

These equations are similar in form to the simple lens and mirror formulas of elementary physics. In fact, when the incident wave is spherical, f_1 and f_2 represent focal distances that are independent of the source range that is creating the spherical wave.

For incident spherical wavefront $\left(\rho_1^i = \rho_2^i = s'\right)$

$$\frac{1}{f_1} = \frac{1}{\cos\theta_i}\left(\frac{\sin^2\theta_2}{R_1} + \frac{\sin^2\theta_1}{R_2}\right) \oplus \sqrt{\frac{1}{\cos^2\theta_i}\left(\frac{\sin^2\theta_2}{R_1} + \frac{\sin^2\theta_1}{R_2}\right)^2 - \frac{4}{R_1 R_2}} \qquad \text{(13-22a)}$$

$$\frac{1}{f_2} = \frac{1}{\cos\theta_i}\left(\frac{\sin^2\theta_2}{R_1} + \frac{\sin^2\theta_1}{R_2}\right) \ominus \sqrt{\frac{1}{\cos^2\theta_i}\left(\frac{\sin^2\theta_2}{R_1} + \frac{\sin^2\theta_1}{R_2}\right)^2 - \frac{4}{R_1 R_2}} \qquad \text{(13-22b)}$$

where:

R_1, R_2 = radii of curvature of the reflecting surface

θ_1 = angle between the direction of the incident ray $\hat{s}^i$ and $\hat{u}_1$

θ_2 = angle between the direction of the incident ray $\hat{s}^i$ *and* $\hat{u}_2$

$\hat{u}_1$ = unit vector in the principal direction of S at Q_R *with principal radius of curvature* R_1

$\hat{u}_2$ = unit vector in the principal direction of S at Q_R with principal radius of curvature R_2

❶ If the incident field is spherical

$$\rho_1^i = \rho_2^i = s' = \text{distance from the source to the point of reflection } Q_R$$

❷ If the incident field is cylindrical

$$\rho_1^i = \rho', \quad \rho_2^i = \infty \quad \text{or} \quad \rho_1^i = \infty, \quad \rho_2^i = \rho'$$

where ρ' = distance from the source to the point of reflection Q_R

❸ If the incident field is a plane wave

$$\rho_1^i = \rho_2^i = \infty$$

Then $$\frac{1}{\rho_1^r \rho_2^r} = \frac{1}{f_1 f_2} = \frac{4}{R_1 R_2} \quad \text{or} \quad \rho_1^r \rho_2^r = \frac{R_1 R_2}{4} \qquad (13\text{-}23,a)$$

Reflection from a 3-D Curved Surface

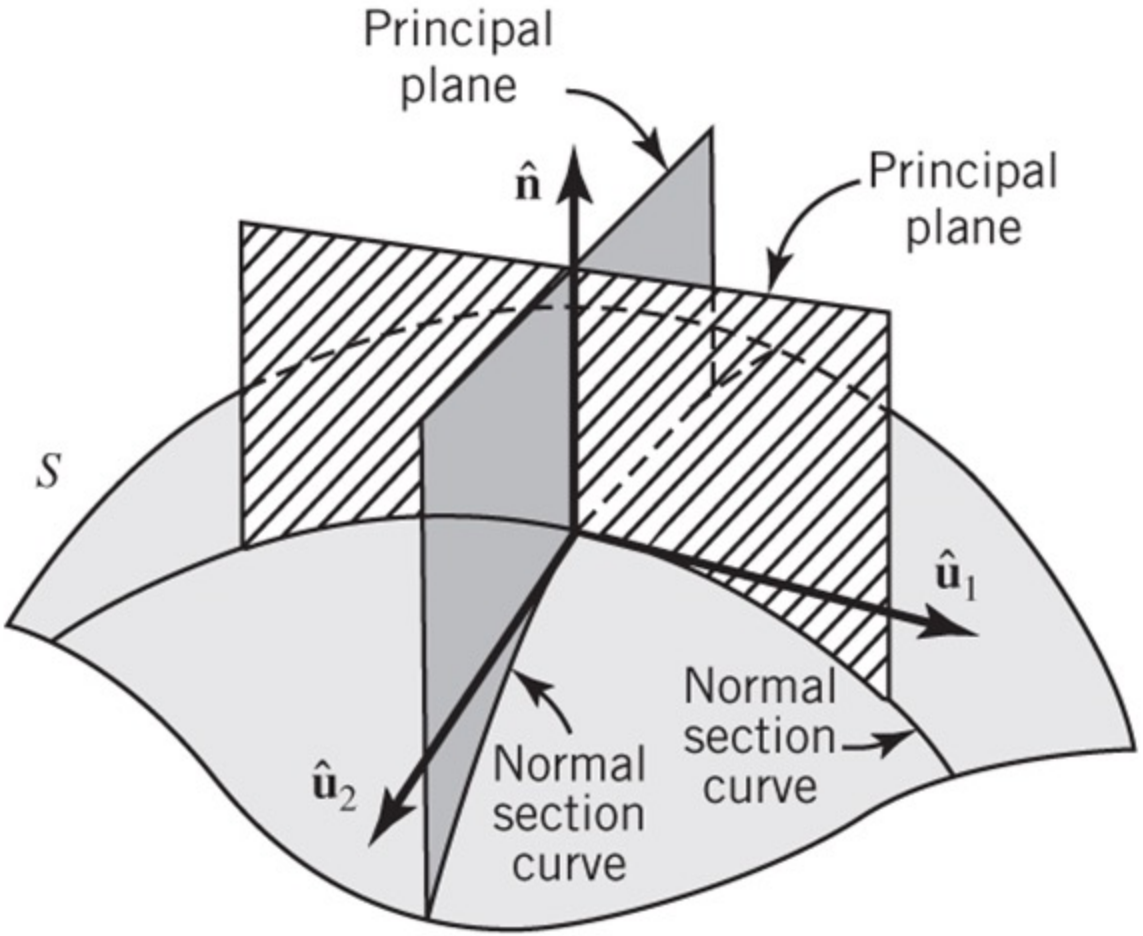

(b) Normal section curves and principal planes

Fig. 13-7

To give some physical insight into the principal radii of curvature R_1 and R_2 of a reflecting surface, let us assume that the reflecting surface is well behaved (smooth and continuous). At each point on the surface there exists a unit normal vector. If through that point a plane intersects the reflecting surface, it generates on the reflecting surface a curve as shown in the figure. If in addition the intersecting plane contains the unit vector to the surface at that point, the curve generated on the reflecting surface by the intersecting plane is known as the *normal section curve,* as shown in the figure.

If the intersecting plane is rotated about the surface normal at that point, a number of unique normal sections are generated, one on each orientation of the intersecting plane. Associated with each normal section curve, there is a radius of curvature. It can be shown that for each point on an arbitrary well behaved curved reflecting surface, there is one intersecting plane that maximizes the radius of curvature of its corresponding normal section curve while there is another intersecting plane at the same point that minimizes the radius of curvature of its corresponding normal section curve.

For each point on the reflecting surface there are two normal section radii of curvature, denoted as R_1 and R_2 and referred to as the *principal radii of curvature,* and the two corresponding planes are known as the *principal planes*. For an arbitrary surface, the two principal planes are perpendicular to each other.

Plane Wave Incidence

$$\underline{E}^r(s) = \underline{E}^i(Q_R) \cdot \tilde{R} \sqrt{\frac{\rho_1^r \ \rho_2^r}{\left(\rho_1^r + s\right)\left(\rho_2^r + s\right)}} \ e^{-j\beta s}$$

When $s >> \rho_1^r, \ \rho_2^r$

$$\underline{E}^r(s) = \underline{E}^i(Q_R) \cdot \tilde{R} \sqrt{\frac{\frac{\rho_1^r}{s} \ \frac{\rho_2^r}{s}}{\left(\frac{\rho_1^r}{s} + 1\right)\left(\frac{\rho_2^r}{s} + 1\right)}} \ e^{-j\beta s}$$

$$\underset{s>>\rho_2^r}{\overset{s>>\rho_1^r}{\cong}} \underline{E}^i(Q_R) \cdot \tilde{R} \sqrt{\frac{\rho_1^r}{s} \ \frac{\rho_2^r}{s}} \ e^{-j\beta s}$$

$$\underline{E}^r(s) \underset{s>>\rho_2^r}{\overset{s>>\rho_1^r}{\cong}} \underline{E}^i(Q_R) \cdot \tilde{R} \ \frac{\sqrt{\rho_1^r \rho_2^r}}{s} \ e^{-j\beta s}$$

Example 13-1:
Plane wave Scattering From A PEC Sphere

Example 13 – 1:

A linearly polarized uniform plane wave of amplitude E_o is incident on a conducting sphere of radius a.

Use geometrical optics methods.

1. Determine the far-zone ($s >> \rho_1^r \; and \; \rho_2^r$) fields that are reflected from the surface of the sphere.

2. Determine the bascatter radar cross sections.

Solution:

It follows.

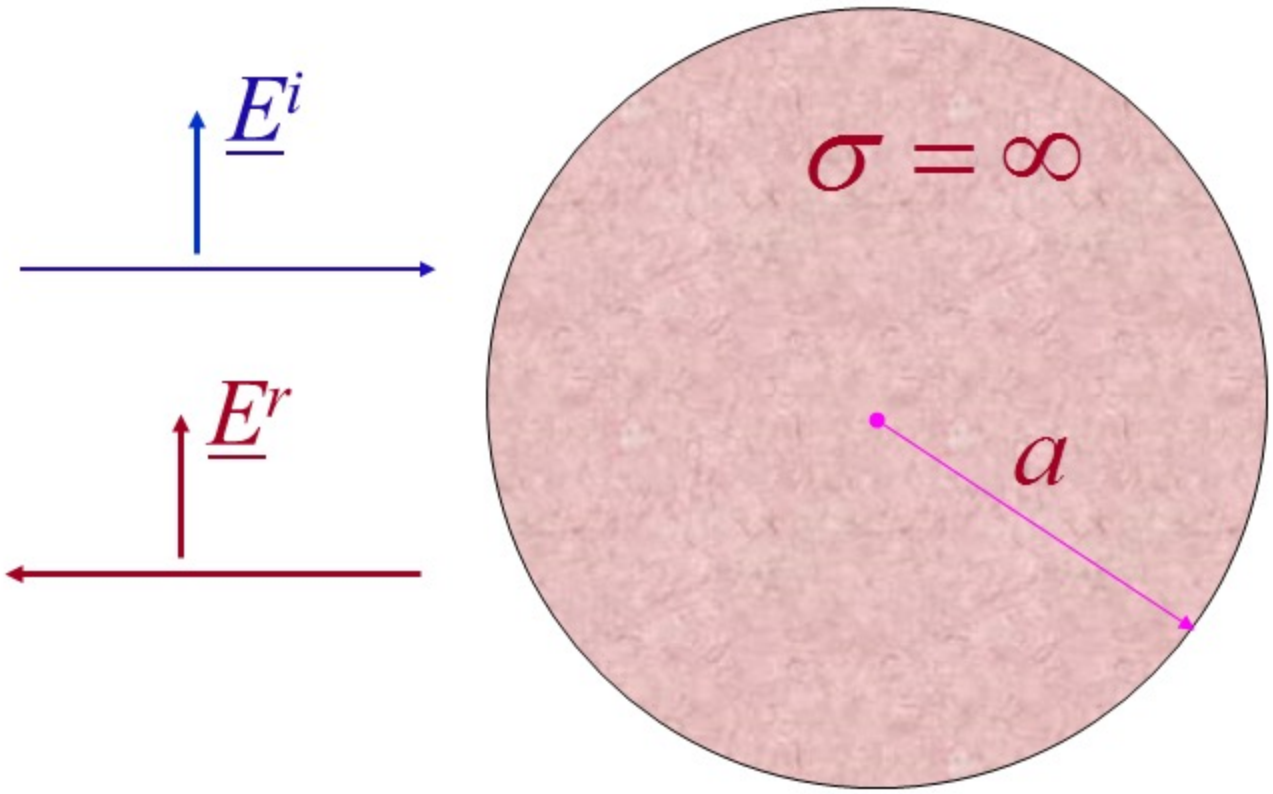

$$\underline{E}^r(s) = \underline{E}^i(Q_R) \cdot \tilde{R} \sqrt{\frac{\rho_1^r \, \rho_2^r}{\left(\rho_1^r + s\right)\left(\rho_2^r + s\right)}} \, e^{-j\beta s}$$

When $s >> \rho_1^r, \ \rho_2^r$

$$\underline{E}^r(s) = \underline{E}^i(Q_R) \cdot \tilde{R} \sqrt{\frac{\left(\frac{\rho_1^r}{s}\right)\left(\frac{\rho_2^r}{s}\right)}{\left(\frac{\rho_1^r}{s}+1\right)\left(\frac{\rho_2^r}{s}+1\right)}} \, e^{-j\beta s}$$

$$\underset{s>>\rho_2^r}{\overset{s>>\rho_1^r}{\approx}} \underline{E}^i(Q_R) \cdot \tilde{R} \sqrt{\frac{\rho_1^r}{s}\,\frac{\rho_2^r}{s}} \, e^{-j\beta s}$$

$$\underline{E}^r(s) \underset{s>>\rho_2^r}{\overset{s>>\rho_1^r}{\approx}} \underline{E}^i(Q_R) \cdot \tilde{R} \, \frac{\sqrt{\rho_1^r \rho_2^r}}{s} \, e^{-j\beta s}$$

Since $\rho_1^r \ \rho_2^r = \dfrac{a^2}{4}$ when $\rho_1^i = \rho_2^i = \infty$

Then

$$\underline{E}^r(s) \cong \underline{E}^i(Q_R) \cdot \tilde{R} \frac{\sqrt{\rho_1^r \rho_2^r}}{s} e^{-j\beta s}$$

$$E^r(s) \cong E_o^i(Q_R)(-1)\left(\frac{a}{2\ s}\right) e^{-j\beta s}$$

$$E^r(s) \cong E_o(-1)\left(\frac{a}{2}\right)\frac{e^{-j\beta s}}{s} = -E_o\left(\frac{a}{2}\right)\frac{e^{-j\beta s}}{s}$$

$$\sigma = \lim_{s\to\infty}\left[4\pi\ s^2 \frac{\left|E^r(s)\right|^2}{\left|E^i(Q_R)\right|^2}\right] \cong 4\pi\ s^2 \frac{\left|\dfrac{a}{2}\dfrac{E_o}{s}\right|^2}{\left|E_o\right|^2} = \pi\ a^2$$

Two-Dimensional Scattering from a Curved Surface

Line Source Near a 2-D Curved Surface

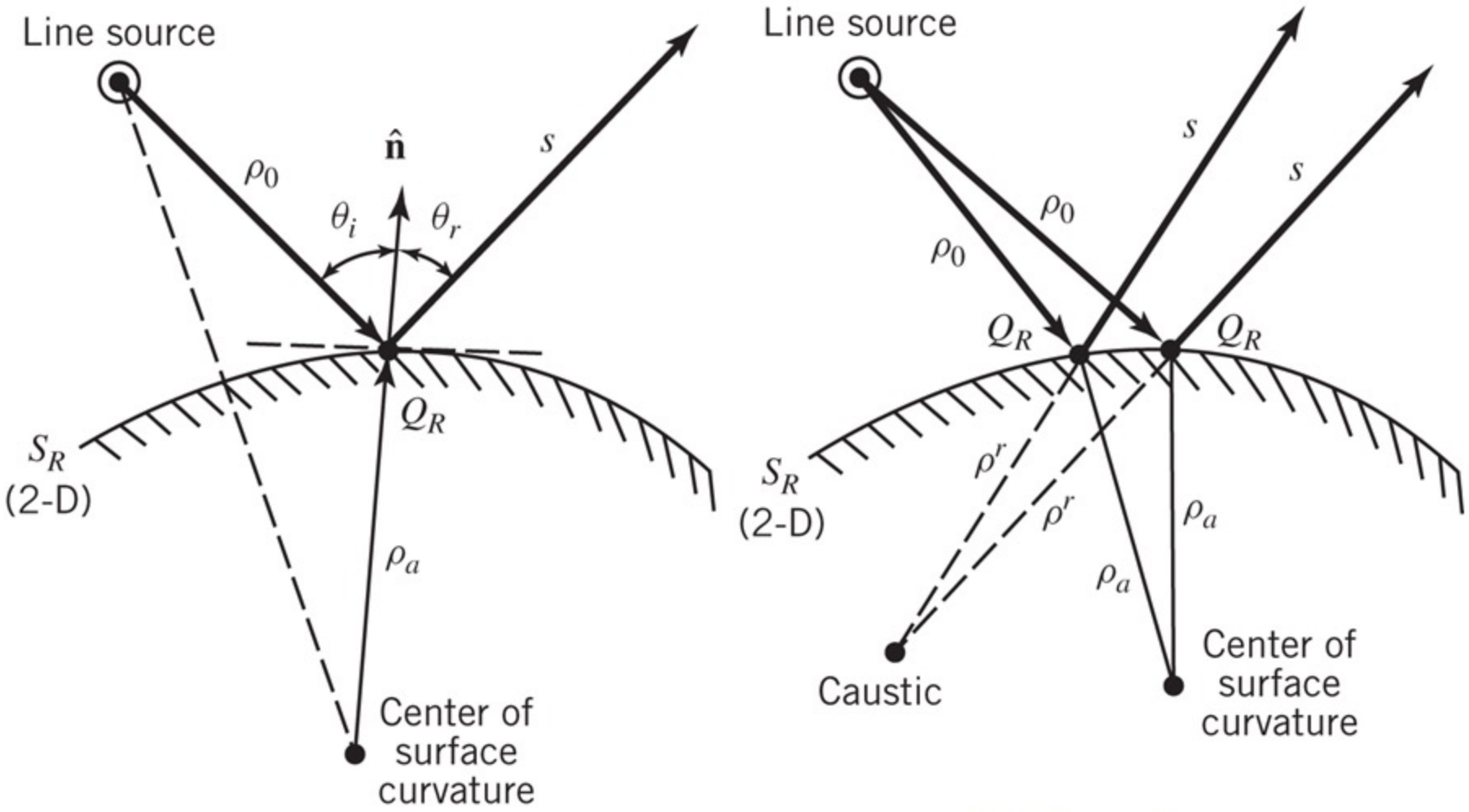

(a) Reflection point

Fig. 13-8

(b) Caustic

$$A = \sqrt{\frac{\rho_1^r \ \rho_2^r}{\left(\rho_1^r + s\right)\ \left(\rho_2^r + s\right)}} = \sqrt{\frac{\rho_1^r}{\left(\rho_1^r + s\right)\ \left(1 + \frac{s}{\rho_2^r}\right)}}$$

$$A \underset{\rho_2^r = \infty}{\overset{\rho_1^r = \rho^r}{=\!=}} \sqrt{\frac{\rho^r}{\rho^r + s}}$$

$$\underline{E}^r(s) = \underline{E}^i(Q_R) \cdot \tilde{R} \sqrt{\frac{\rho_1^r \ \rho_2^r}{\left(\rho_1^r + s\right)\left(\rho_2^r + s\right)}} \, e^{-j\beta s}$$

$$\underline{E}^r(s) = \underline{E}^i(Q_R) \cdot \tilde{R} \sqrt{\frac{\rho_1^r}{\left(\rho_1^r + s\right)\left(1 + \frac{s}{\rho_2^r}\right)}} \, e^{-j\beta s}$$

$$\underline{E}^r(s) \underset{\rho_1^r = \rho^r}{\overset{\rho_2^r \to \infty}{\simeq}} \underline{E}^i(Q_R) \cdot \tilde{R} \sqrt{\frac{\rho^r}{(\rho^r + s)}} \, e^{-j\beta s} \qquad (13\text{-}29)$$

$$\frac{1}{\rho^r} = \frac{1}{\rho_o} + \frac{2}{\rho_a \cos\theta_i} \qquad (13\text{-}30)$$

Strip

Geometrical Optics (GO)

Image Theory

Example 13-2
Reflection From a Flat PEC Surface

Example 13 – 2 :

An electric line source of infinite length and constant current I_o is placed symmetrically a distance h above a PEC strip of width w and infinite legnth, as shown in Figure 13-9a. The length of the line is placed parallel to the z axis. Assuming a free-space medium and far-field observations ($\rho \gg w,\ \rho \gg h$), derive expressions for the incident and reflected electric field components. Then compute and plot the normalized amplitude distribution (in dB) of the incident, reflected, and incident + reflected GO fields for $h = 0.50\lambda$ when $w =$ infinite and $w = 2\lambda$. Normalize the fields with respect to the maximum of the total GO field.

Solution:

It follows.

Line Source Above Strip

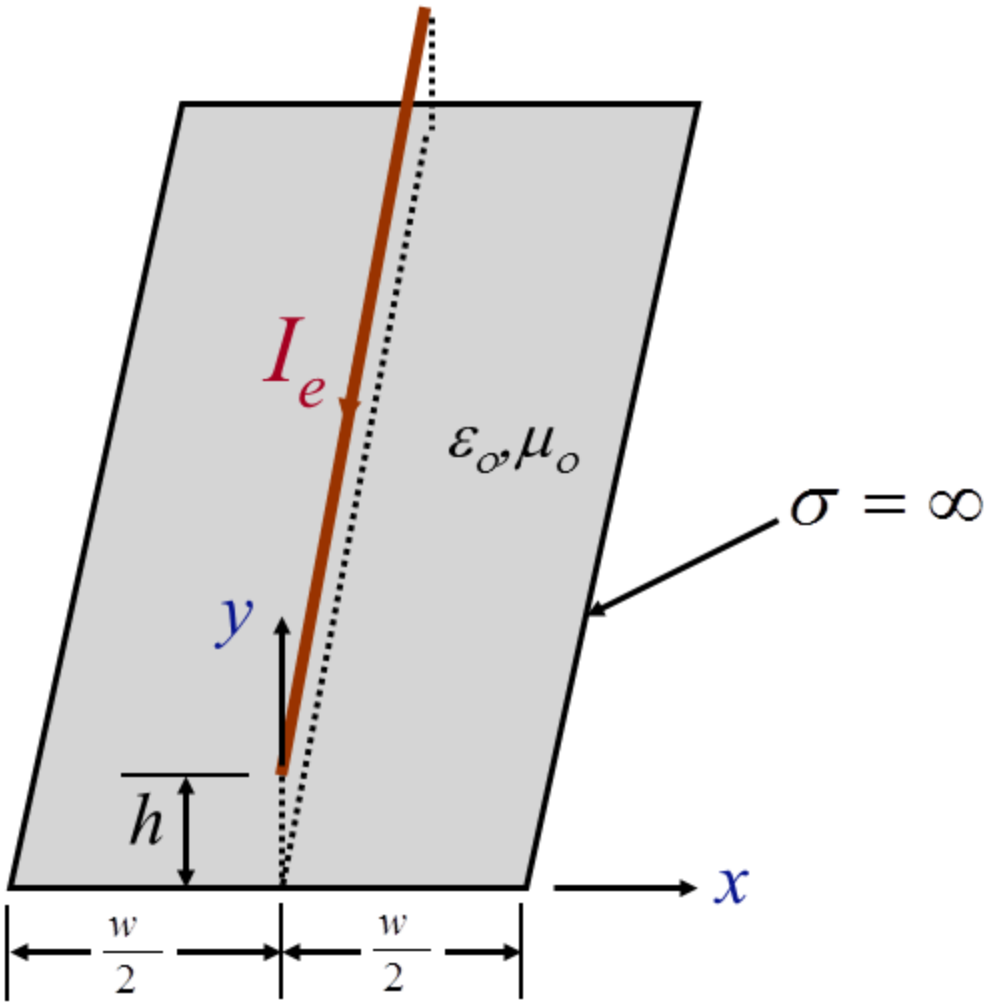

Reflection from a Flat Surface

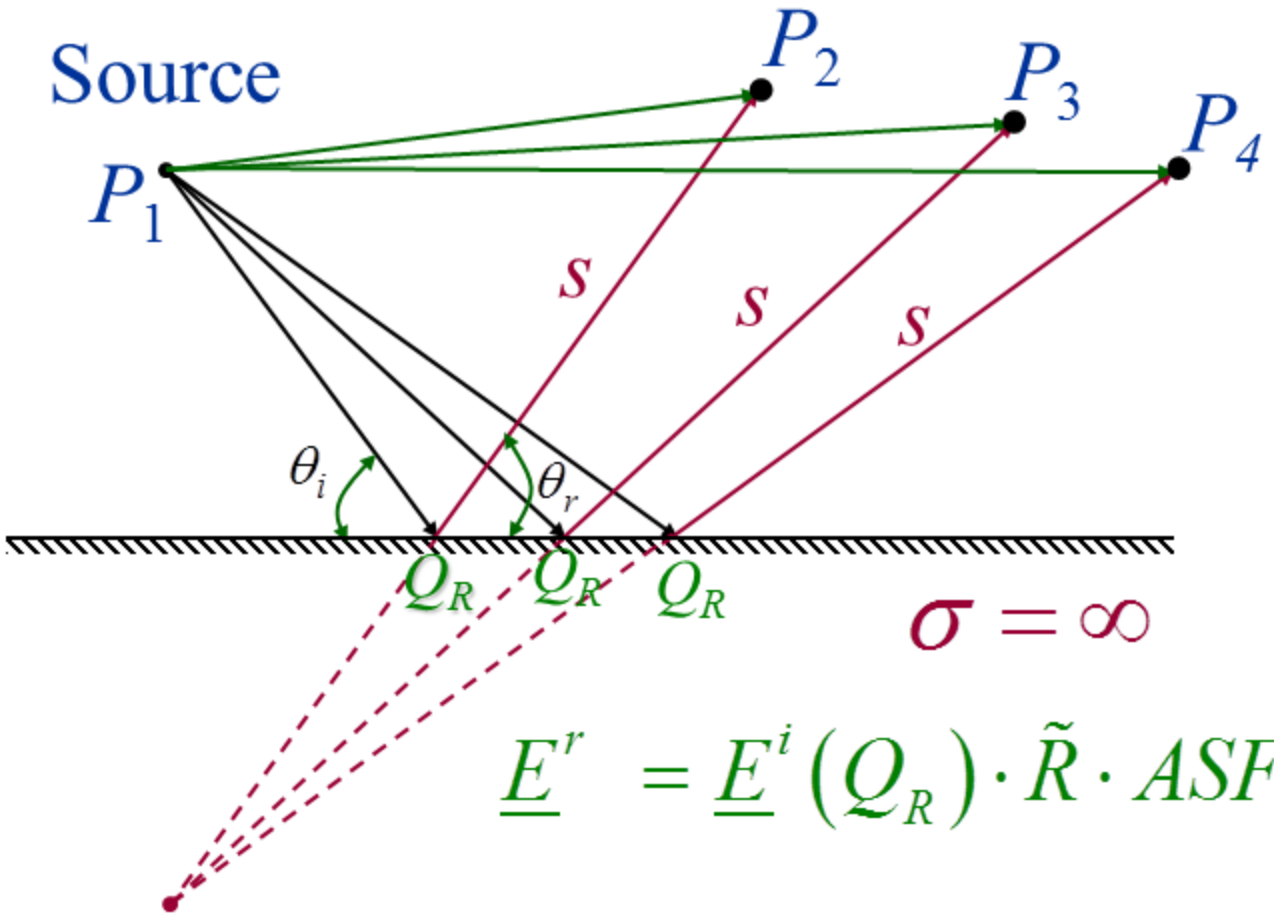

Line Source: Coordinate System

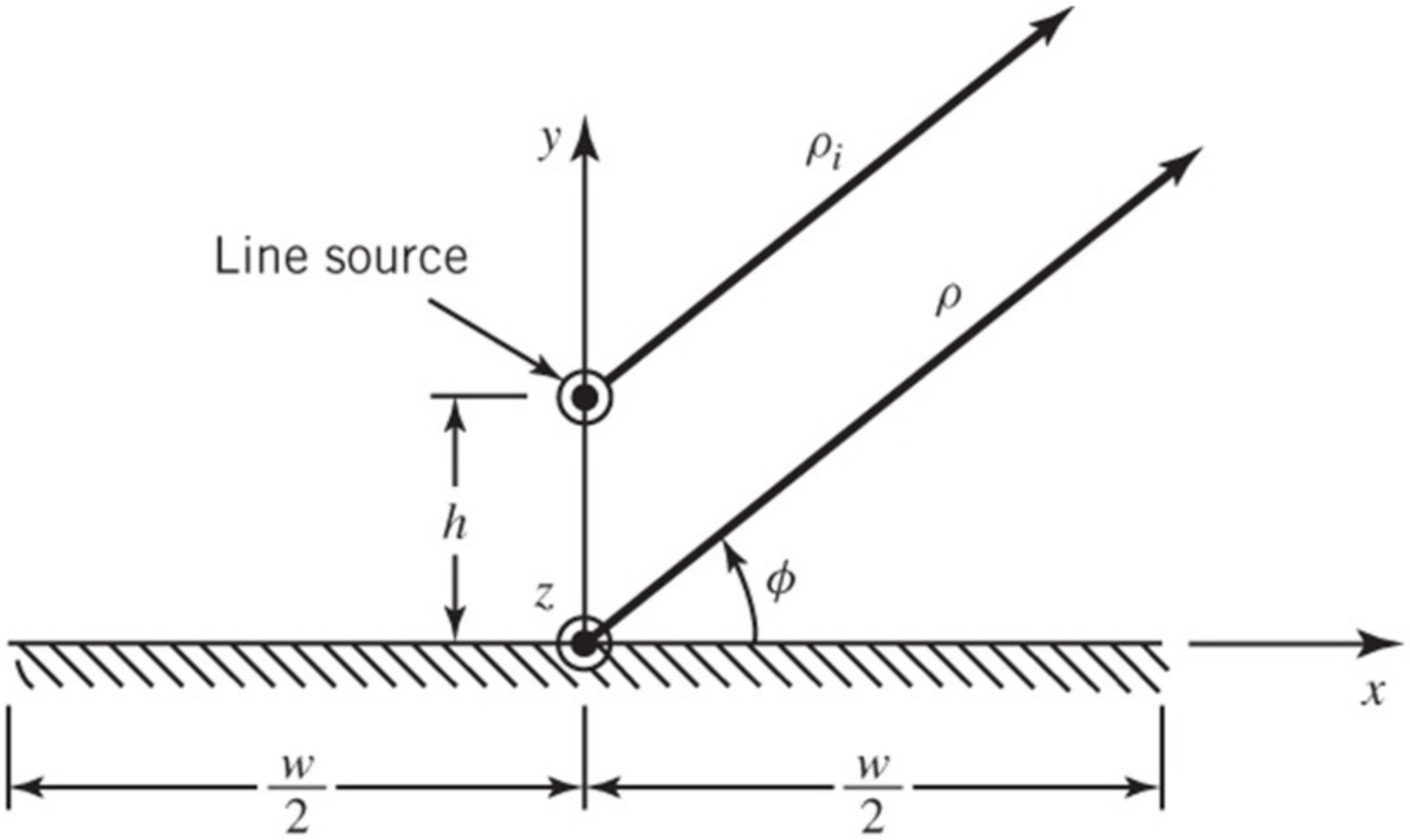

Fig. 13-9(a)

Reflection from a Flat Surface

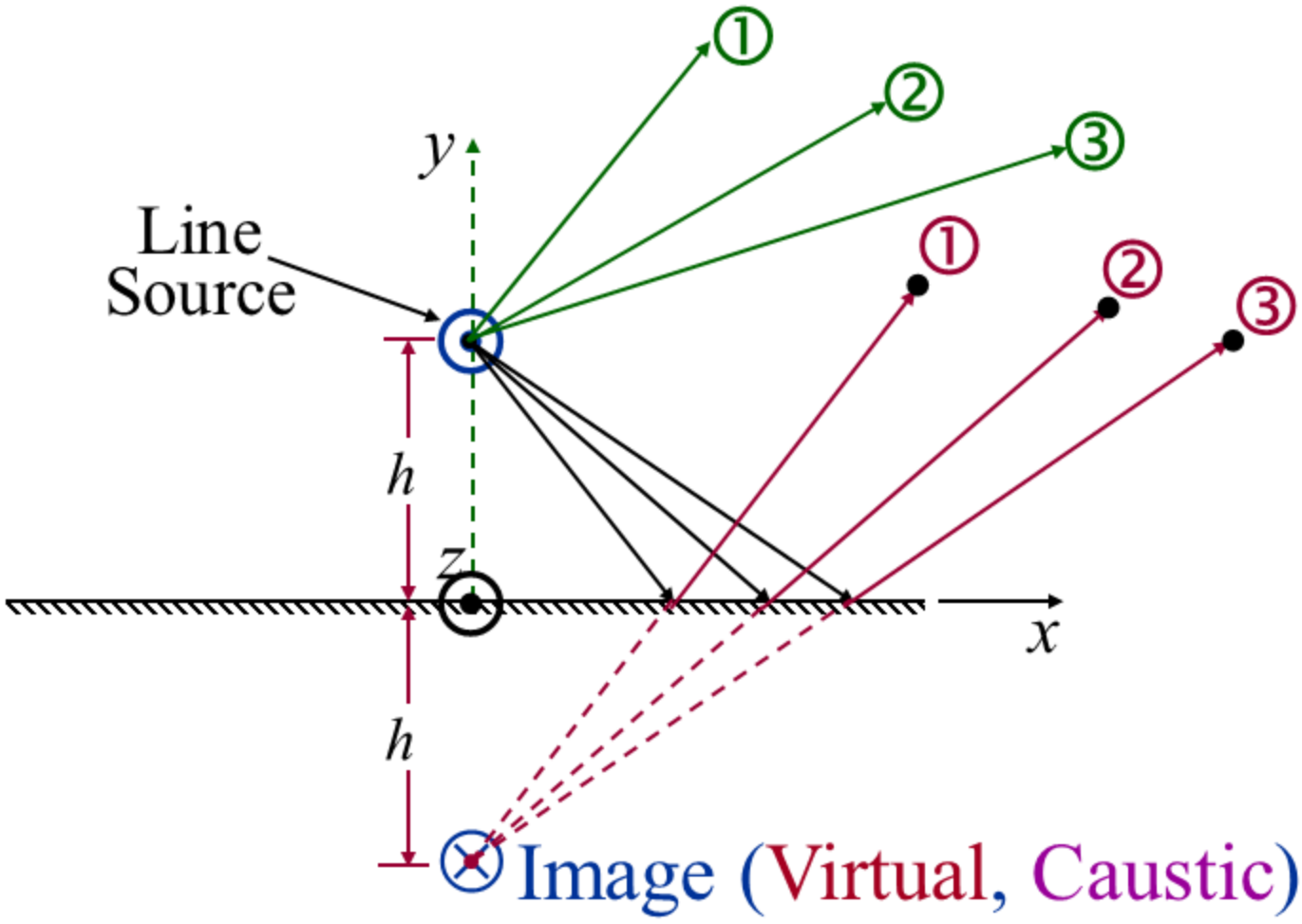

Region Separation

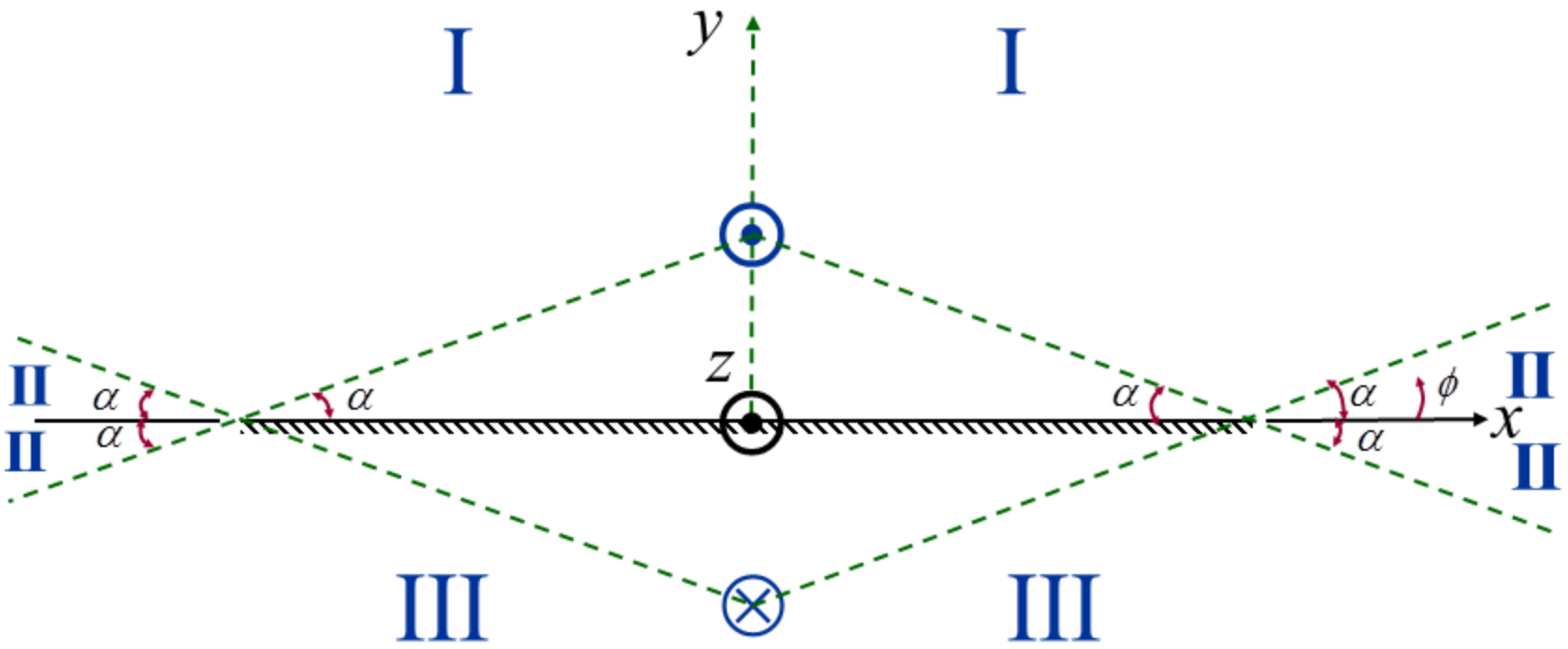

Regions	Range (ϕ)
I	$\alpha \le \phi \le \pi - \alpha$
II	$\pi - \alpha \le \phi \le \pi + \alpha,\ 2\pi - \alpha \le \phi \le 2\pi,\ 0 \le \phi \le \alpha$
III	$\pi + \alpha \le \phi \le 2\pi - \alpha$

Reflection Geometry

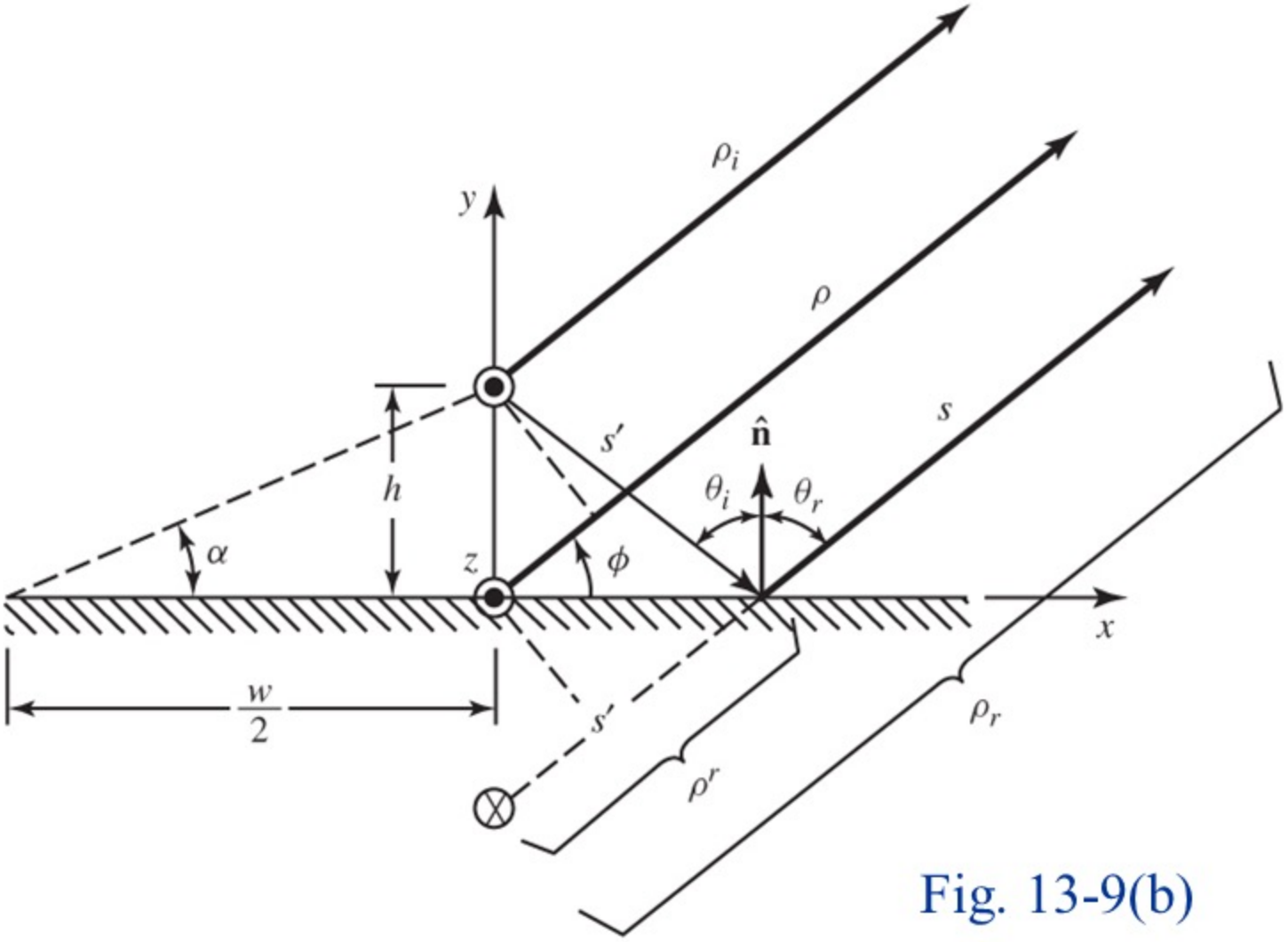

Fig. 13-9(b)

$$\underline{E}^r(s) = \underline{E}^i(Q_R)\cdot\tilde{R}\sqrt{\frac{\rho_1^r\ \rho_2^r}{\left(\rho_1^r+s\right)\ \left(\rho_2^r+s\right)}}\ e^{-j\beta s}$$

$$\underline{E}^r(s) = \underline{E}^i(Q_R)\cdot\tilde{R}\sqrt{\frac{\rho_1^r}{\left(\rho_1^r+s\right)\left(1+\dfrac{s}{\rho_2^r}\right)}}\ e^{-j\beta s}$$

$$\underline{E}^r(s) \underset{\rho_1^r=\rho^r}{\overset{\rho_2^r\to\infty}{\simeq}} \underline{E}^i(Q_R)\cdot\tilde{R}\sqrt{\frac{\rho^r}{(\rho^r+s)}}\ e^{-j\beta s}$$

$$\frac{1}{\rho^r} = \frac{1}{\rho_o} + \frac{2}{\rho_a\cos\theta_i}$$

$$\underline{E}^{i} = \hat{a}_z E_o \frac{e^{-j\beta\rho_i}}{\sqrt{\rho_i}}$$

$$\underline{E}^{r}(s) = \underline{E}^{i}(Q_R) \cdot \tilde{R} \sqrt{\frac{\rho^r}{\left(\rho^r + s\right)}}\, e^{-j\beta s}$$

$$\underline{E}^{r}(s) = \hat{a}_z\, E_o \frac{e^{-j\beta s'}}{\sqrt{s'}}(-1)\sqrt{\frac{s'}{(s'+s)}}\, e^{-j\beta s}$$

$$\underline{E}^{r}(s) = -\hat{a}_z E_o \frac{e^{-j\beta(s'+s)}}{\sqrt{s'+s}} = -\hat{a}_z E_o \frac{e^{-j\beta\rho_r}}{\sqrt{\rho_r}}$$

$$\underline{E}^{r}(s) = -\hat{a}_z\, E_o \frac{e^{-j\,\beta\,\rho_r}}{\sqrt{\rho_r}}$$

$$\rho_i \cong \rho - h\cos\left(\frac{\pi}{2} - \phi\right) = \rho - h\sin\phi$$

$$\rho_r \cong \rho + h\cos\left(\frac{\pi}{2} - \phi\right) = \rho + h\sin\phi$$

} For ϕ variations

$$\rho_i \cong \rho_r \cong \rho$$

} For amplitude variations

$$\underline{E}_z^i \cong \hat{a}_z\, E_o\, e^{+j\beta h\sin\phi}\, \frac{e^{-j\beta\rho}}{\sqrt{\rho}}$$

$$\underline{E}_z^r \cong \hat{a}_z\, E_o\, e^{-j\beta h\sin\phi}\, \frac{e^{-j\beta\rho}}{\sqrt{\rho}}$$

$$\underline{E}_z^t = \underline{E}_z^i + \underline{E}_z^r = \hat{a}_z\, E_o\,(2j)\,\sin(\beta h\sin\phi)\, \frac{e^{-j\beta\rho}}{\sqrt{\rho}}$$

GO Patterns: Infinite and Finite Strip

$w = 2\lambda,\ h = 0.5\lambda$

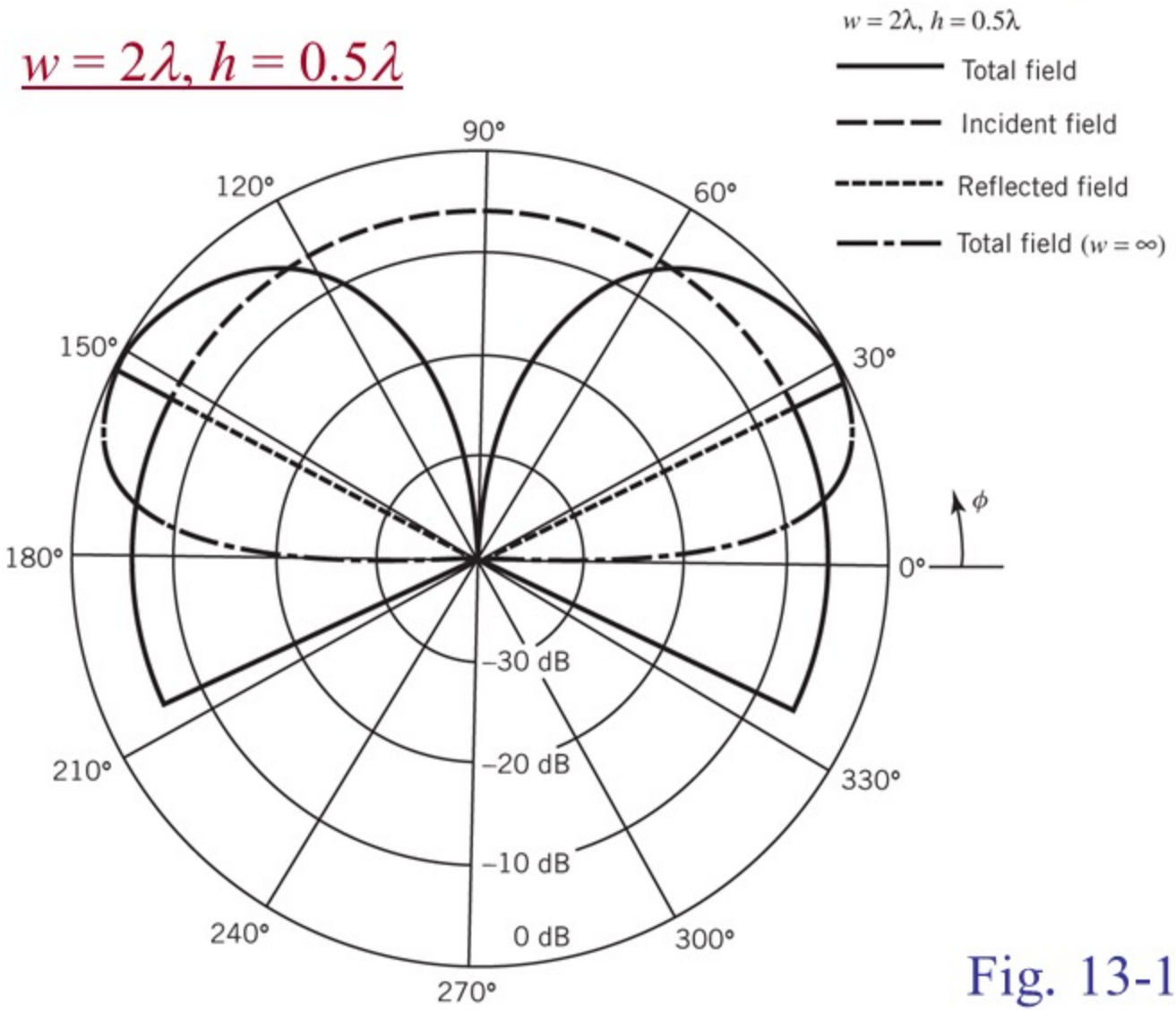

Fig. 13-10

Geometrical Theory of Diffraction (GTD)

At high frequencies diffraction, like reflection and refraction, is a local phenomenon, and it depends on:

1. The geometry of the object at the point of diffraction (edge, vertex, curved surface)
2. The amplitude, phase and polarization of the incident field at the point of diffraction

- The diffracted field is determined by a generalization of Fermat's Principle
- The total diffracted field at a point is the sum of the rays at that point
- The phase of the field on a ray is assumed to be equal to the product of the optical length of the ray from some reference point and the wave number of the medium.

Diffraction by a Curved Edge

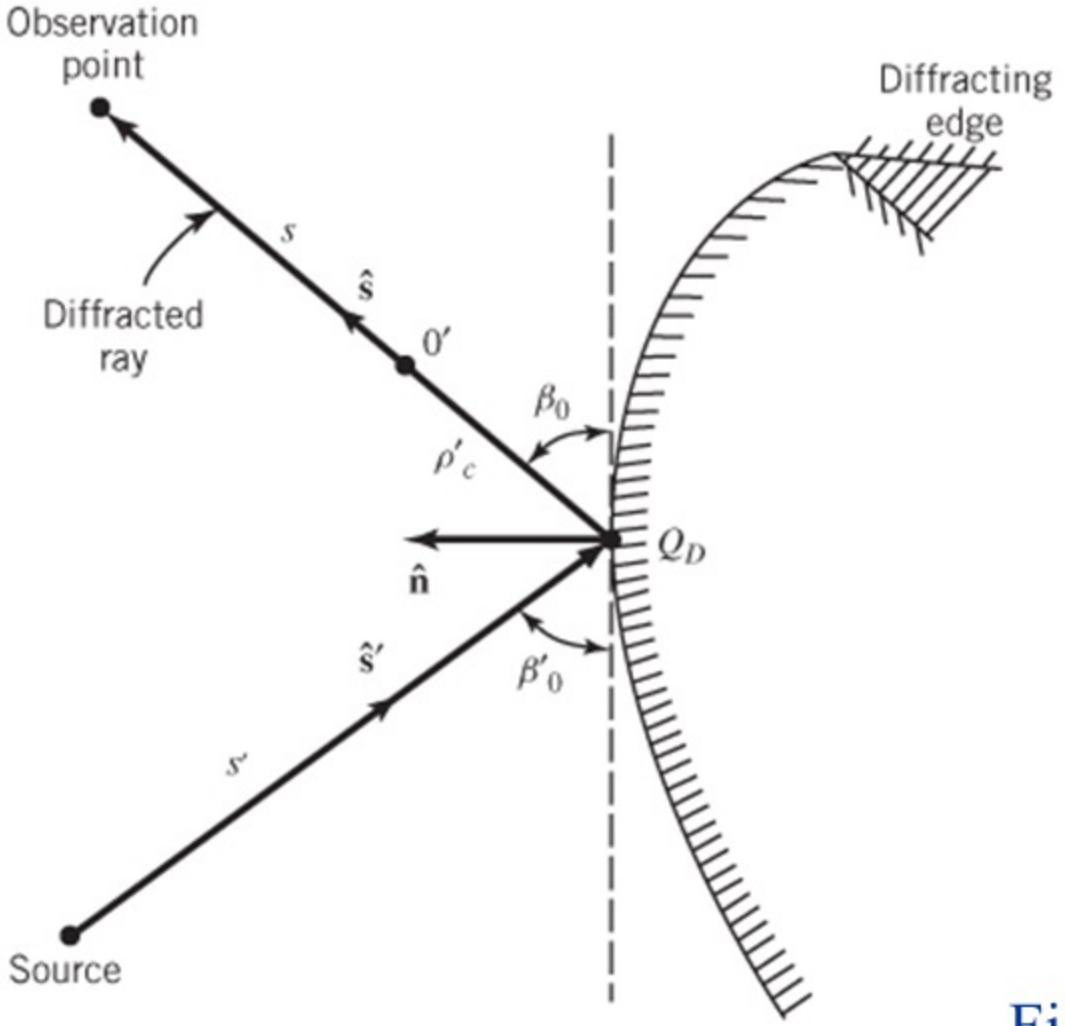

(a) Diffraction point

Fig. 13-11

$$\underline{E}^d(\underline{R}) \simeq \frac{e^{-j\beta\psi_d(\underline{R})}}{\sqrt{\beta}}\underline{A}(\underline{R}), \quad \beta = \omega\sqrt{\mu\varepsilon} \qquad (13\text{-}31)$$

$$\begin{cases} \nabla^2 \underline{E} + \beta^2 \underline{E} = 0 \\ \nabla \cdot \underline{E} = 0 \end{cases}$$

$$\underline{E}^d(s) \simeq \underbrace{\left[\frac{\underline{A}(0')}{\sqrt{\beta}} e^{-j\beta\psi(0')}\right]}_{\underline{E}^d(0')} \sqrt{\frac{\rho_c' \rho_c}{(\rho_c' + s)(\rho_c + c)}} e^{-j\beta s}$$

$$\underline{E}^d(s) = \underline{E}^d(0') \sqrt{\frac{\rho_c' \rho_c}{(\rho_c' + s)(\rho_c + c)}} e^{-j\beta s} \qquad (13\text{-}32)$$

$$\lim_{\rho_c' \to 0}\left[\underline{E}^d(0')\sqrt{\rho_c'}\right] = \text{finite} \qquad (13\text{-}33)$$

$$\lim_{\rho_c' \to 0}\left[\underline{E}^d(0')\sqrt{\rho_c'}\right] = \underline{E}^i(Q_D)\cdot\widetilde{D} \qquad (13\text{-}33a)$$

Therefore

$$\underline{E}^d(s) = \underline{E}^d(0')\sqrt{\frac{\rho_c'\rho_c}{(\rho_c'+s)(\rho_c+c)}}e^{-j\beta s}$$

$$\underline{E}^d(s) = \left[\underline{E}^d(0')\sqrt{\rho_c'}\right]\sqrt{\frac{\rho_c}{(\rho_c'+s)(\rho_c+c)}}e^{-j\beta s}$$

$$\underline{E}^d(s) = \lim_{\rho_c' \to 0} \left\{ \underbrace{\left[\underline{E}^d(0') \sqrt{\rho_c'} \right]}_{\underline{E}^i(Q_D)\cdot\tilde{D}} \sqrt{\frac{\rho_c}{(\rho_c' + s)(\rho_c + s)}} \right\} e^{-j\beta s}$$

$$\underline{E}^d(s) = \underline{E}^i(Q_D)\cdot\tilde{D} \underbrace{\sqrt{\frac{\rho_c}{s(\rho_c + s)}}}_{A(s,\rho_c)} e^{-j\beta s} \qquad (13\text{-}34)$$

$\underline{E}^i(Q_D) =$ incident field at point of diffraction Q_d

$\widetilde{D} =$ dyadic diffraction coefficient

$A(\rho_c, s) =$ amplitude spreading factor

$e^{-j\beta s} =$ phase factor

$\rho_c =$ distance between the reference Q_d $(\text{at } s = 0)$ at the edge (also first caustic of the diffracted rays) and the second caustic of the diffracted rays.

Diffraction by a Curved Edge

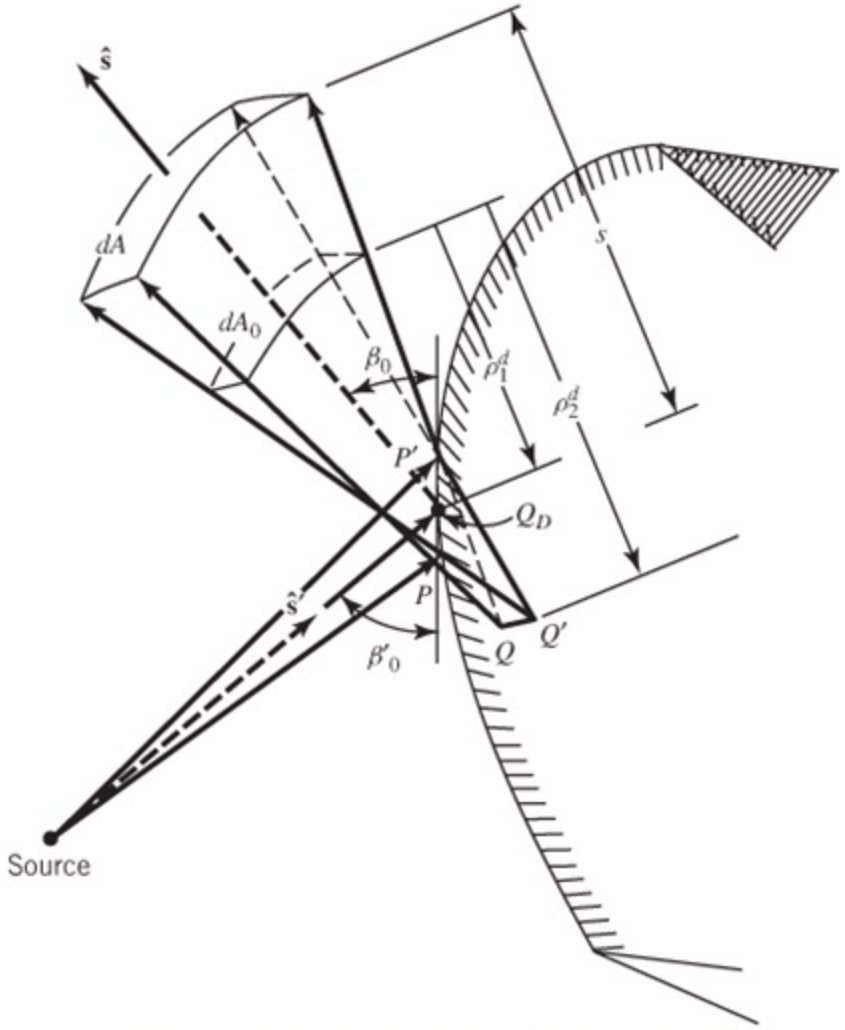

Fig. 13-11

(b) Astigmatic tube of rays

Diffracted Fields

$$\underline{E}^d = \underbrace{\underline{E}^i(Q_d)}_{\substack{\text{Field} \\ \text{at Reference}}} \cdot \underbrace{\tilde{D}}_{\substack{\text{Diffraction} \\ \text{Coefficient}}} \underbrace{A(\rho_c, s)}_{\substack{\text{Amplitude} \\ \text{Spreading} \\ \text{Factor}}} \underbrace{e^{-j\beta s}}_{\substack{\text{Phase} \\ \text{Factor}}} \qquad (13\text{-}34a)$$

$\underline{E}^i(Q_d) =$ incident field at reference point Q_d of diffraction

$\tilde{D} =$ dyadic diffraction coefficient

$A =$ amplitude spreading factor

$e^{-j\beta s} =$ phase factor

Amplitude Spreading Factor

$$A(\rho_c, s) = \sqrt{\frac{\rho_c}{s(\rho_c + s)}} \qquad (13\text{-}34b)$$

$A(\rho_c, s) =$ spatial attenuation (spreading, divergence) factor for curved surface

$\rho_c =$ distance between reference point $Q_D(s = 0)$ at the edge (also first caustic of the diffracted rays) and the second caustic of the diffracted rays.

Diffraction by a Wedge With Straight Edge

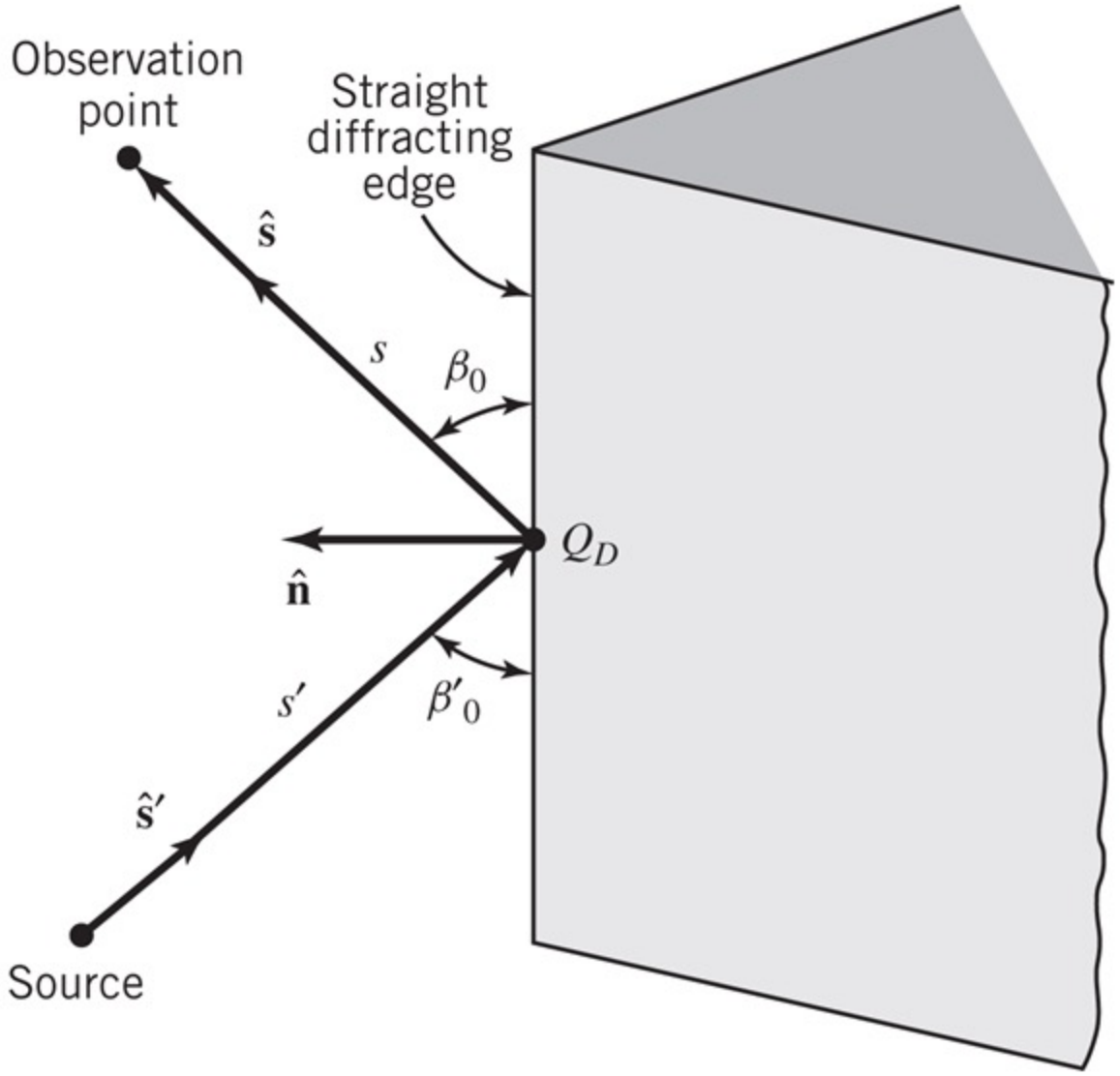

Fig. 13-12

For A Straight Diffracted Edge

$$\underline{E}^{d}(s) = \underline{E}^{i}(Q_d) \cdot \tilde{D} A(s, s') e^{-j\beta s} \tag{13-35}$$

$$A(s, s') = \begin{cases} \dfrac{1}{\sqrt{s}} & \text{for plane and conical wave incidence} \quad (13\text{-}35a) \\ \dfrac{1}{\sqrt{\rho}} & \text{for cylindrical wave incidence} \quad (13\text{-}35b) \\ \sqrt{\dfrac{s'}{s(s+s')}} \overset{s>>s'}{\simeq} \dfrac{\sqrt{s'}}{s} & \text{spherical wave incidence} \quad (13\text{-}35c) \end{cases}$$

Two-Dimensional Diffraction

$$\underline{E}^d(\rho) = \underline{E}^i(Q) \cdot \underset{\sim}{D} \frac{1}{\sqrt{\rho}} e^{-j\beta\rho}$$

$\underline{E}^i(Q)$ = incident field at diffraction point

$\underset{\sim}{D}$ = diffraction coefficient

$\frac{1}{\sqrt{\rho}}$ = ASF(cylindrical wave)

$e^{-j\beta\rho}$ = phase factor

Amplitude Spreading Factor (ASF):

$\frac{1}{\sqrt{\rho}}$ = amplitude spreading factor:

cylindrical wave

$\frac{1}{r}$ = amplitude spreading factor:

spherical wave

1 = amplitude spreading factor:

plane wave

Line Source Near a 2-D Conducting Wedge

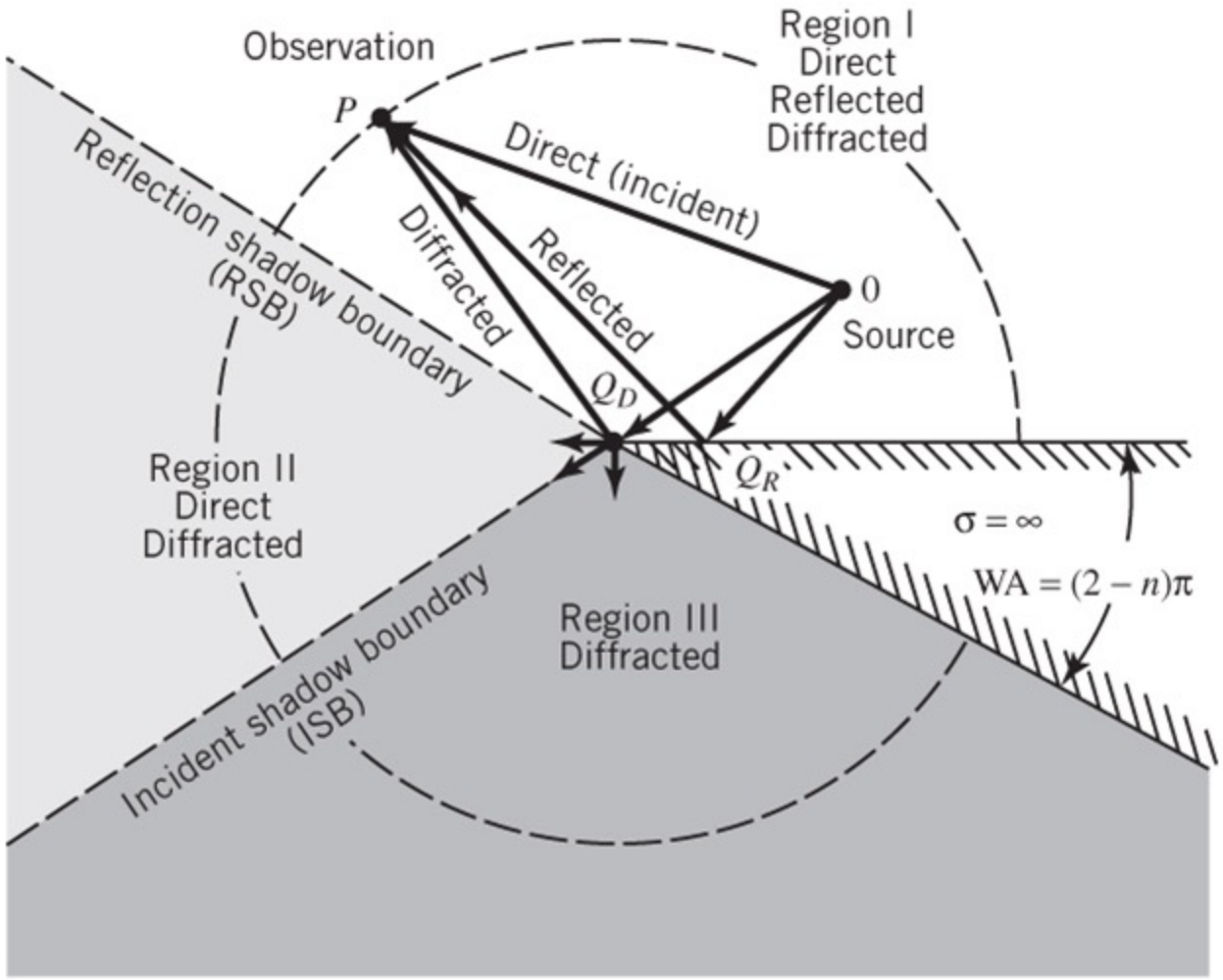

(a) Region separation

Fig. 13-13(a)

Line Source Near a 2-D Conducting Wedge

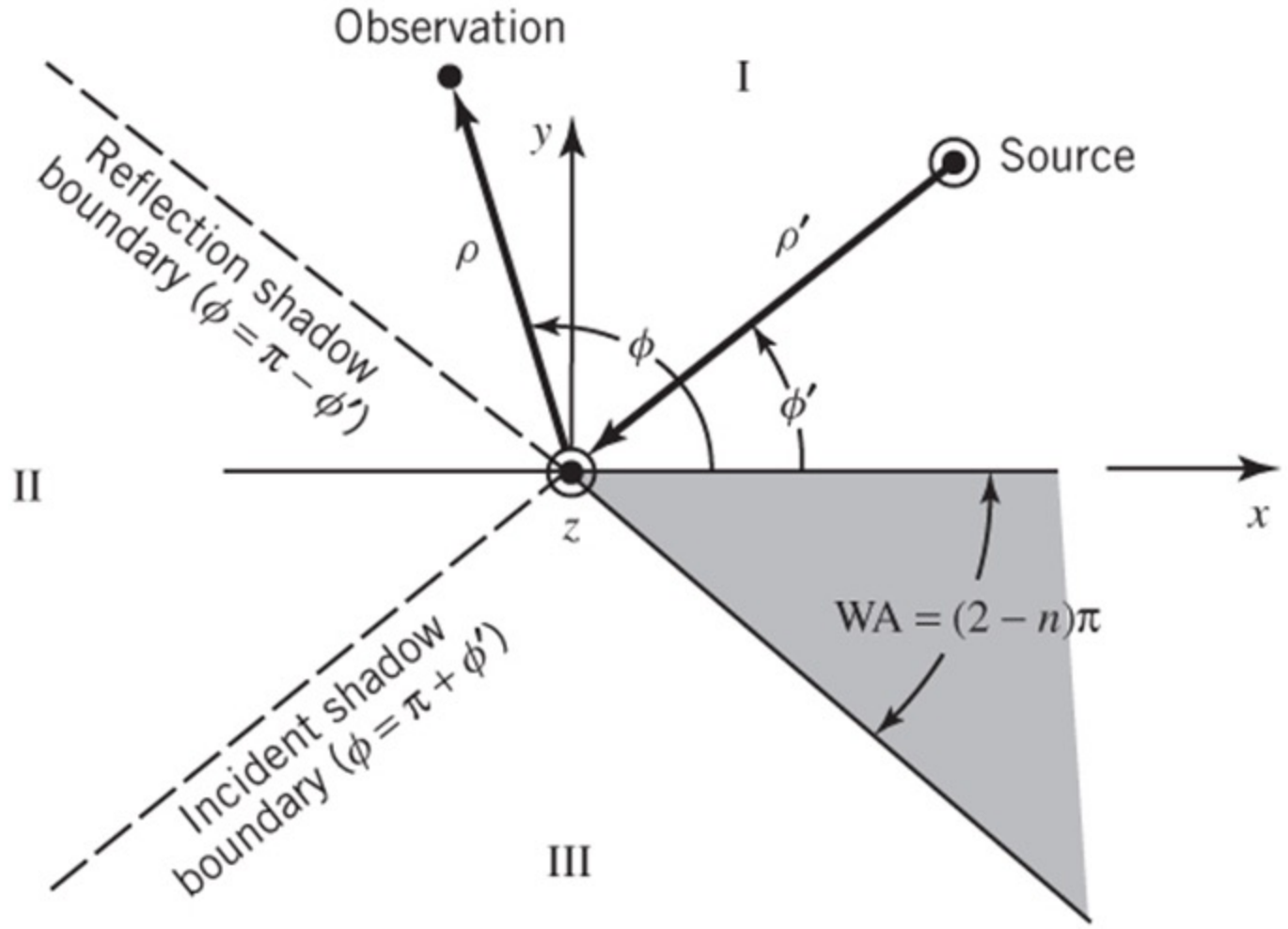

(b) Coordinate system

Fig. 13-13(b)

Wedge Diffraction: Normal Incidence

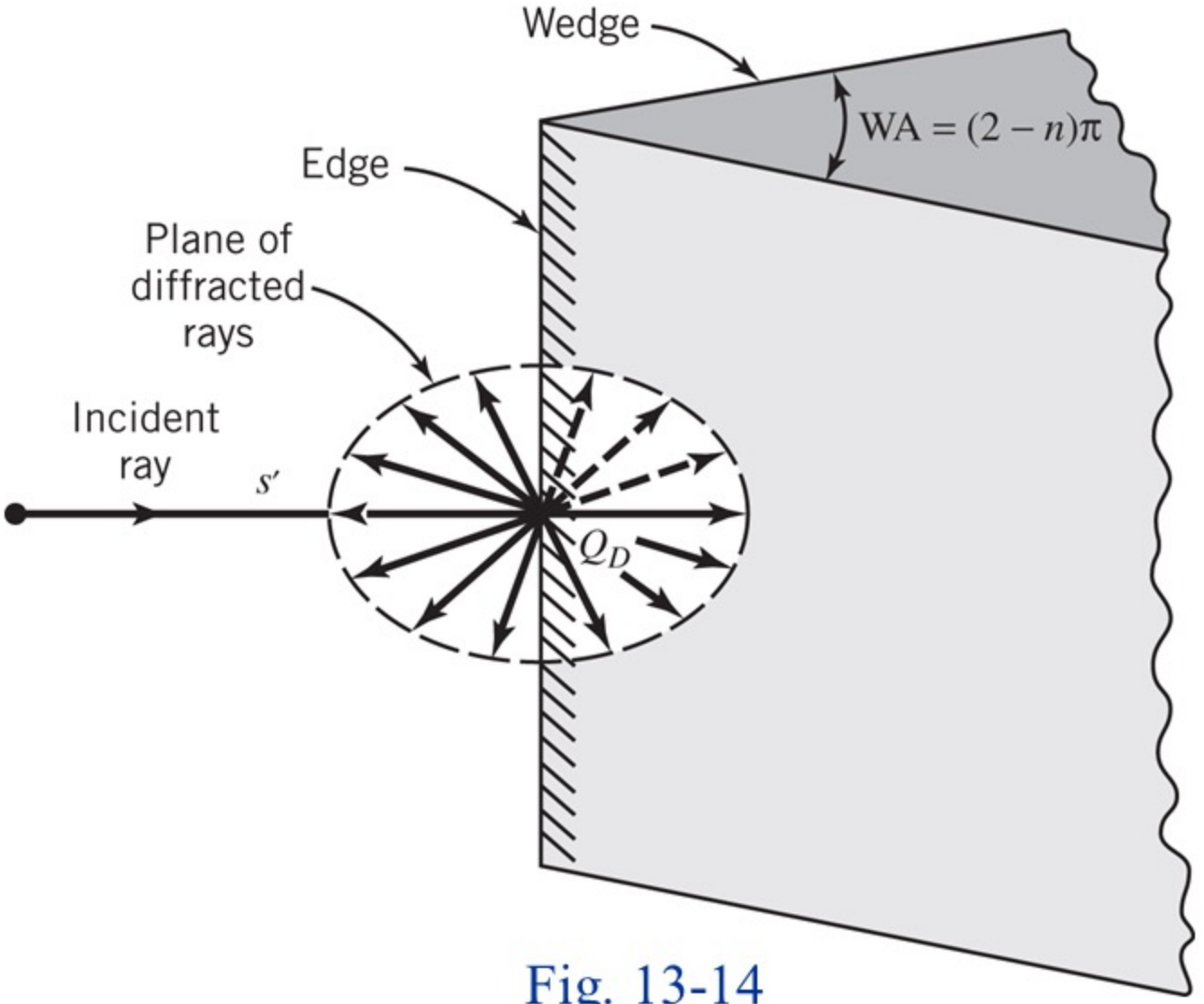

Fig. 13-14

Diffraction

Diffracted Fields

$$\underline{E}^d = \underline{E}^i(Q_d) \cdot \tilde{D} A e^{-j\beta s} \qquad (13\text{-}35)$$

$\underline{E}^i(Q_d) =$ incident field at point Q_d of diffraction

$\tilde{D} =$ dyadic diffraction coefficient

$A =$ amplitude spreading factor

$e^{-j\beta s} =$ phase factor

Table 2.2 RCS OF SOME TYPICAL TARGETS

Object	Typical RCSs [22]	
	RCS (m^2)	RCS (dBsm)
Pickup truck	200	23
Automobile	100	20
Jumbo jet airliner	100	20
Large bomber *or* commercial jet	40	16
Cabin cruiser boat	10	10
Large fighter aircraft	6	7.78
Small fighter aircraft *or* four-passenger jet	2	3
Adult male	1	0
Conventional winged missile	0.5	−3
Bird	0.01	−20
Insect	0.00001	−50
Advanced tactical fighter	0.000001	−60

F-117 Nighthawk

Printed with permission from Lockheed Martin.

Fig. 13-1

Wedge Diffraction

1. Electric Line Source
2. Magnetic Line Source

1. Electric Line Source (TM^z)

(Horizontal-Soft Polarization)

$$E_z^e = -\frac{\omega}{4}\mu I_e G \quad \Rightarrow \quad \underline{\mathrm{H}}^e = \frac{1}{-j\omega\mu}\nabla \times \underline{E}^e \qquad (13\text{-}36)$$

2. Magnetic Line Source (TE^z)

(Vertical-Hard Polarization)

$$H_z^m = +\frac{\omega}{4}\varepsilon I_m G \quad \Rightarrow \quad \underline{\mathrm{E}}^m = \frac{1}{j\omega\varepsilon}\nabla \times \underline{H}^m \qquad (13\text{-}37)$$

If $\beta\rho'$ is large $\left(\beta\rho' \to \infty\right)$

$$H_{m/n}^{(2)}\left(\beta\rho'\right) \overset{\beta\rho'\to\infty}{\simeq} \sqrt{\frac{2}{\pi\beta\rho'}} e^{-j\left(\beta\rho' - \frac{\pi}{4} - \frac{m}{n}\frac{\pi}{2}\right)} \tag{13-39}$$

$$G\left(\rho,\rho',\phi,\phi'\right) \simeq \sqrt{\frac{2}{\pi\beta\rho'}} e^{-j\left(\beta\rho' - \frac{\pi}{4}\right)} F\left(\beta\rho\right) \tag{13-40}$$

$$F\left(\beta\rho\right) = \frac{1}{n}\sum_{m=0}^{\infty} \varepsilon_m J_{m/n}\left(\beta\rho\right) e^{j\frac{m}{n}\left(\frac{\pi}{2}\right)} \left\{ \begin{array}{l} \cos\left[\frac{m}{n}\left(\phi - \phi'\right)\right] \\ \pm\cos\left[\frac{m}{n}\left(\phi + \phi'\right)\right] \end{array} \right\} \tag{13-40a}$$

\+ For Hard (TE^z) Polarization (Neumann B.C.'s) $\left(\partial G / \partial\phi\big|_{\substack{wedge \\ surface}} = 0 \right)$

– For Soft (TM^z) Polarization (Dirichlet B.C.'s) $\left(G\big|_{\substack{wedge \\ surface}} = 0 \right)$

$$F(\beta\rho)=\frac{1}{n}\sum_{m=0}^{\infty}\varepsilon_m J_{m/n}(\beta\rho)\,e^{j\frac{m}{n}\left(\frac{\pi}{2}\right)}\left\{\begin{array}{l}\cos\left[\dfrac{m}{n}(\phi-\phi')\right]\\ \pm\cos\left[\dfrac{m}{n}(\phi+\phi')\right]\end{array}\right\}$$

$$\varepsilon_m=\begin{cases}1 & m=0\\ 2 & m\neq 0\end{cases} \qquad \text{(13-40a)}$$

If $\beta\rho<1$, $\simeq$ 15 terms $(m=0,\ldots,14)$ for 5 significant figure accuracy

If $\beta\rho<10$, $\simeq$ 40 terms $(m=0,1,\ldots,39)$ for 5 significant figure accuracy

Diffraction Patterns by a Wedge-TE^z-Hard

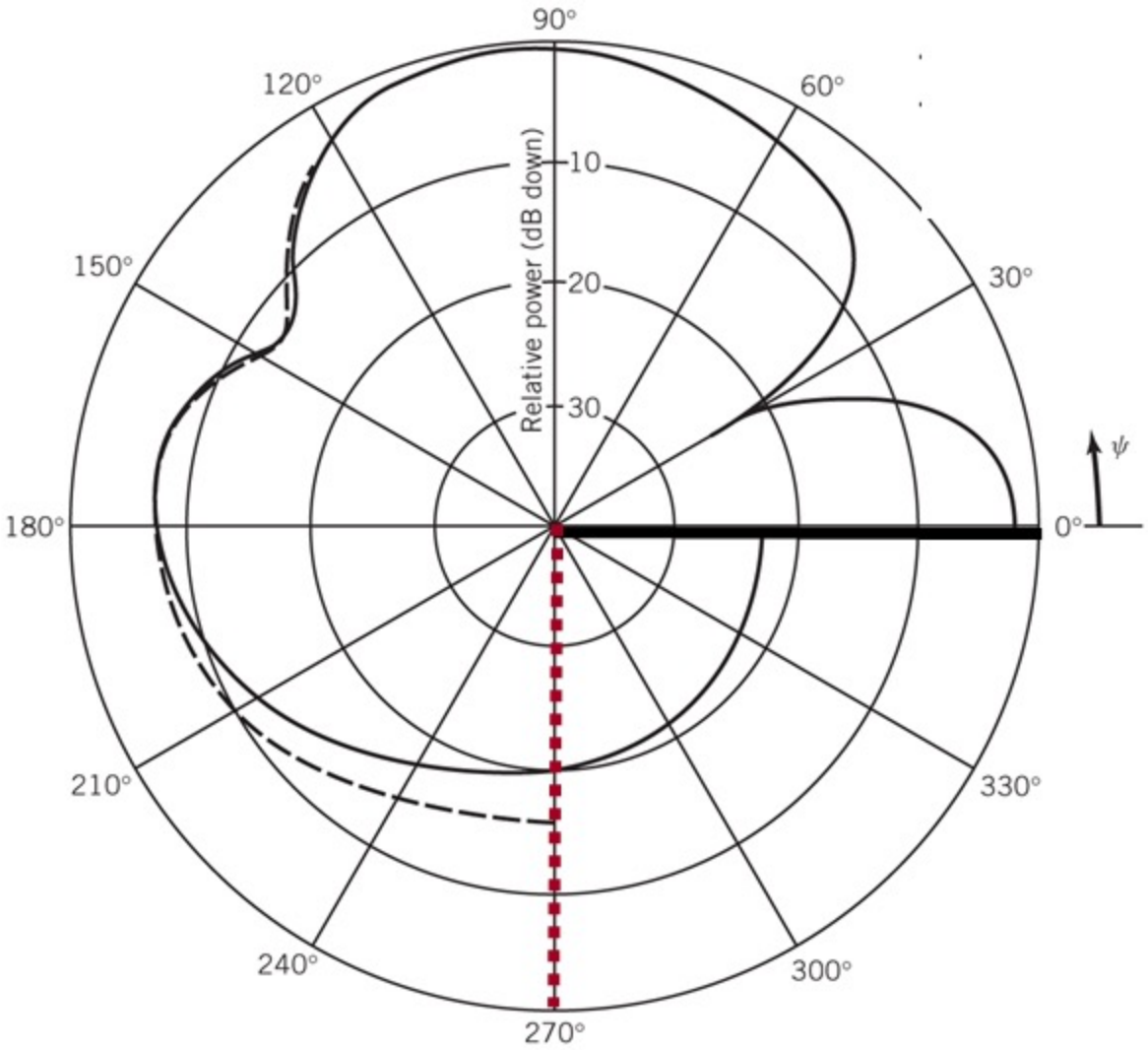

$n = 2$

$n = 1.5$

$\rho = \lambda$

$\psi' = 30°$

$\mathrm{WA} = (2 - n)\pi$

Fig. 13-15

Diffraction Patterns by a Wedge-TM^z-Soft

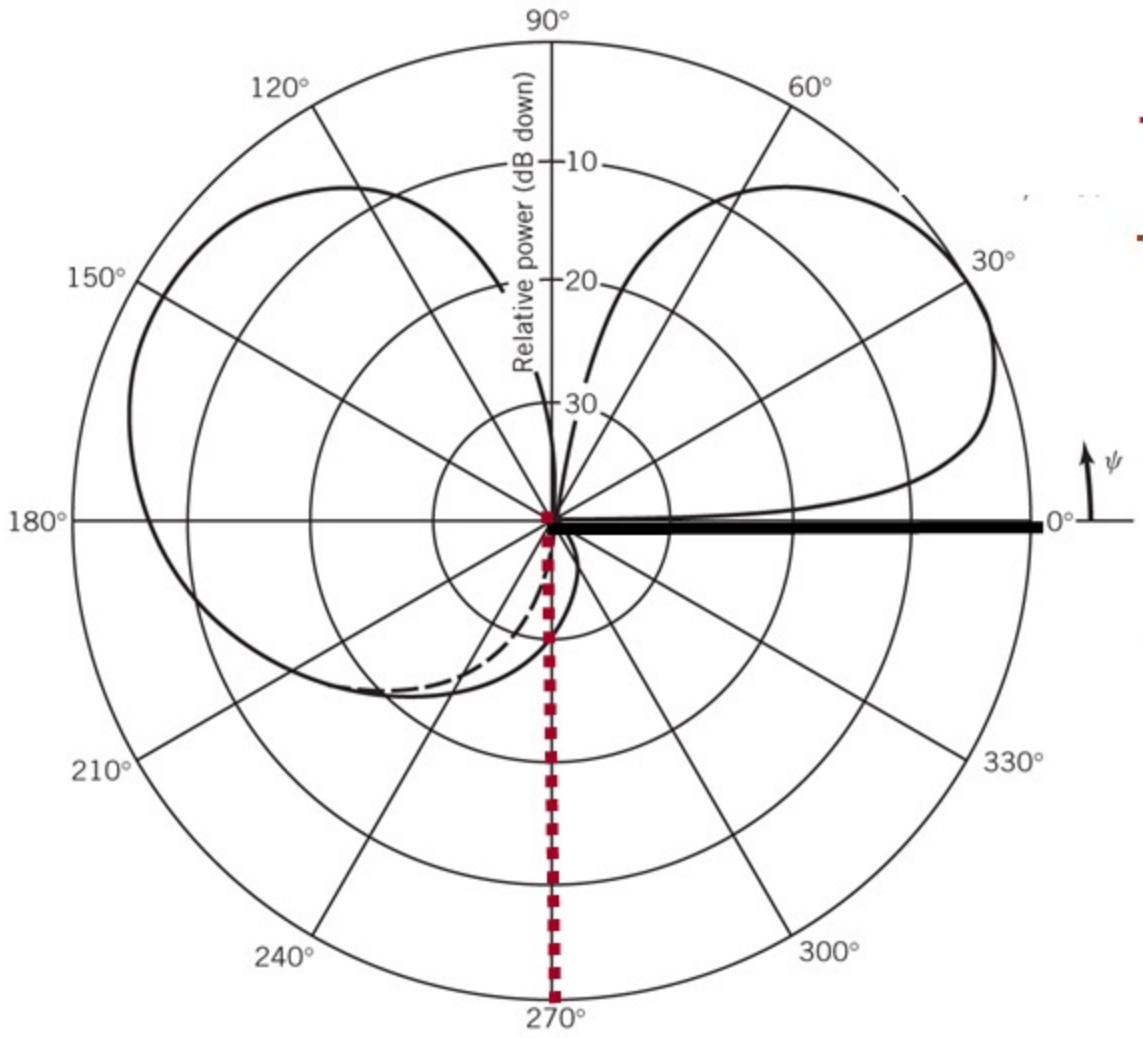

$n = 2$

$n = 1.5$

$\rho = \lambda$

$\psi' = 30°$

$\mathrm{WA} = (2 - n)\pi$

Fig. 13-16

$$F(\beta\rho)=\frac{1}{n}\sum_{m=0}^{\infty}\varepsilon_m J_{m/n}(\beta\rho)\,e^{j\frac{m}{n}\left(\frac{\pi}{2}\right)}\left\{\cos\left[\frac{m}{n}(\phi-\phi')\right]\pm\cos\left[\frac{m}{n}(\phi+\phi')\right]\right\} \tag{13-40a}$$

$$\varepsilon_m=\begin{cases}1 & m=0\\ 2 & m\neq 0\end{cases} \tag{13-38a}$$

If $\beta\rho<1$, $\simeq 15$ terms $(m=0,\ldots,14)$ for 5 sign. figure accuracy

If $\beta\rho<10$, $\simeq 40$ terms $(m=0,1,\ldots,39)$ for 5 sign. figure accuracy

Reciprocity in Wedge Diffraction

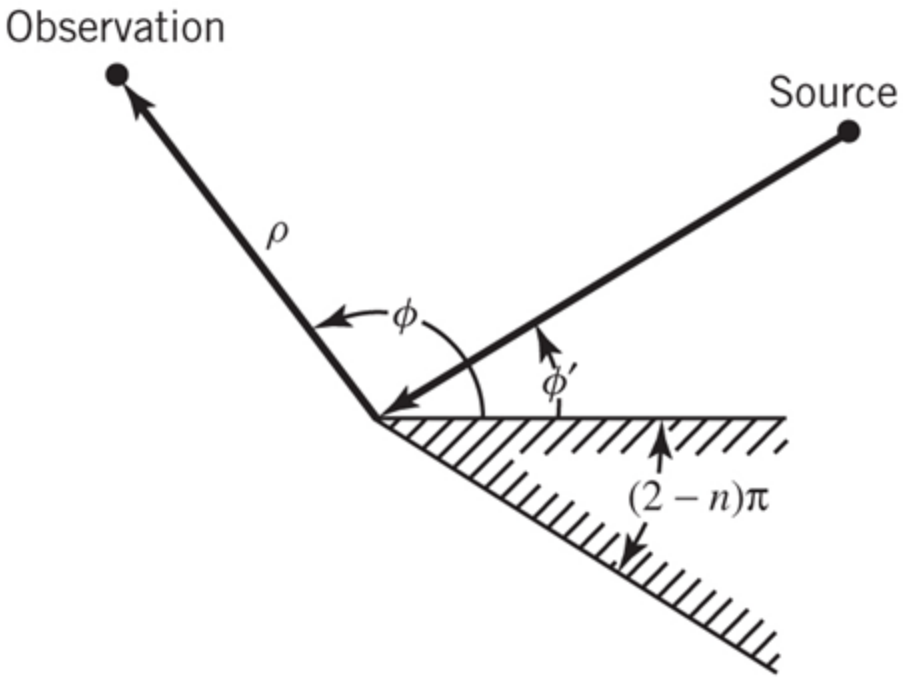

(a) Plane Wave Incidence

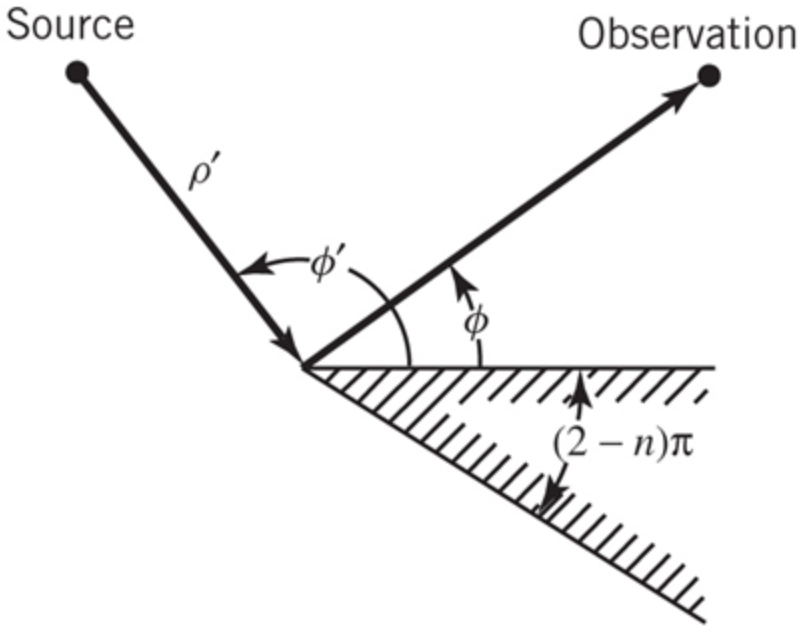

(b) Cylindrical Wave Incidence

Fig. 13-17

GTD Development

- Watson Transformation
- Method of Steepest Descent

(Saddle Point Method)

Simplification of $F(\beta\rho)$

1. Watson Transformation
   Transforms an infinite series summation into an integral
2. Method of Steepest Descent (Saddle Point Method)
   Evaluates the integral by deforming the actual line integral path to that of the steepest descent

If $\beta\rho'$ is large $\left(\beta\rho' \to \infty\right)$

$$H_{m/n}^{(2)}\left(\beta\rho'\right) \overset{\beta\rho' \to \infty}{\simeq} \sqrt{\frac{2}{\pi\beta\rho'}} e^{-j\left(\beta\rho' - \frac{\pi}{4} - \frac{m}{n}\frac{\pi}{2}\right)} \tag{13-39}$$

$$G\left(\rho, \rho', \phi, \phi'\right) \simeq \sqrt{\frac{2}{\pi\beta\rho'}} e^{-j\left(\beta\rho' - \frac{\pi}{4}\right)} F\left(\beta\rho\right) \tag{13-40}$$

$$F\left(\beta\rho\right) = \frac{1}{n}\sum_{m=0}^{\infty} \varepsilon_m J_{m/n}\left(\beta\rho\right) e^{j\frac{m}{n}\left(\frac{\pi}{2}\right)} \left\{ \begin{array}{l} \cos\left[\frac{m}{n}\left(\phi - \phi'\right)\right] \\ \pm\cos\left[\frac{m}{n}\left(\phi + \phi'\right)\right] \end{array} \right\} \tag{13-40a}$$

\+ For Hard (TE^z) Polarization (Neumann B.C.'s) $\left(\partial G / \partial \phi \big|_{\substack{wedge \\ surface}} = 0 \right)$

– For Soft (TM^z) Polarization (Dirichlet B.C.'s) $\left(G \big|_{\substack{wedge \\ surface}} = 0 \right)$

Standard Method of Steepest Descent

$$F(\beta\rho)=\frac{1}{n}\sum_{m=0}^{\infty}\varepsilon_m J_{m/n}(\beta\rho)\,e^{j\frac{m}{n}\left(\frac{\pi}{2}\right)}\begin{Bmatrix}\cos\left[\frac{m}{n}(\phi-\phi')\right]\\ \pm\cos\left[\frac{m}{n}(\phi+\phi')\right]\end{Bmatrix}\approx I_{SDP}(\beta\rho)$$

$$I_{SDP}(\beta\rho)=\int_{SDP}H(z)\,e^{\beta\rho h(z)}dz$$

$$I_{SDP}(\beta\rho)\overset{\beta\rho\to\text{large}}{\simeq}\sqrt{\frac{2\pi}{-\beta\rho h''(z_s)}}H(z_s)\,e^{\beta\rho h(z_s)};\ \text{provided}\quad h''(z_s)\neq 0$$

$$\left.\frac{dh}{dz}\right|_{z=z_s}\equiv h'(z=z_s)=h'(z_s)=0;\ z_s=\text{Saddle Point}$$

The evaluation of $F(\beta\rho)$ will be accomplished in two step. That is:

$$F(\beta\rho) = F_1(\beta\rho) + F_2(\beta\rho)$$

It will turn out that for the functions

$$F(\beta\rho) = F_1(\beta\rho) + F_2(\beta\rho)$$

simple *poles* (*no branch points*, etc.) occur at

$$z_p = -(\phi - \phi') + 2npN \quad \text{for} \quad F_1(\beta\rho)$$

$$z_p = -(\phi + \phi') + 2npN \quad \text{for} \quad F_2(\beta\rho)$$

and can be evaluated using the conventional Steepest Descent Method provided that

$$-\pi \leq z_p = -(\phi \mp \phi') + 2npN \leq +\pi$$

Steepest Descent Paths, Saddle Point, and Poles

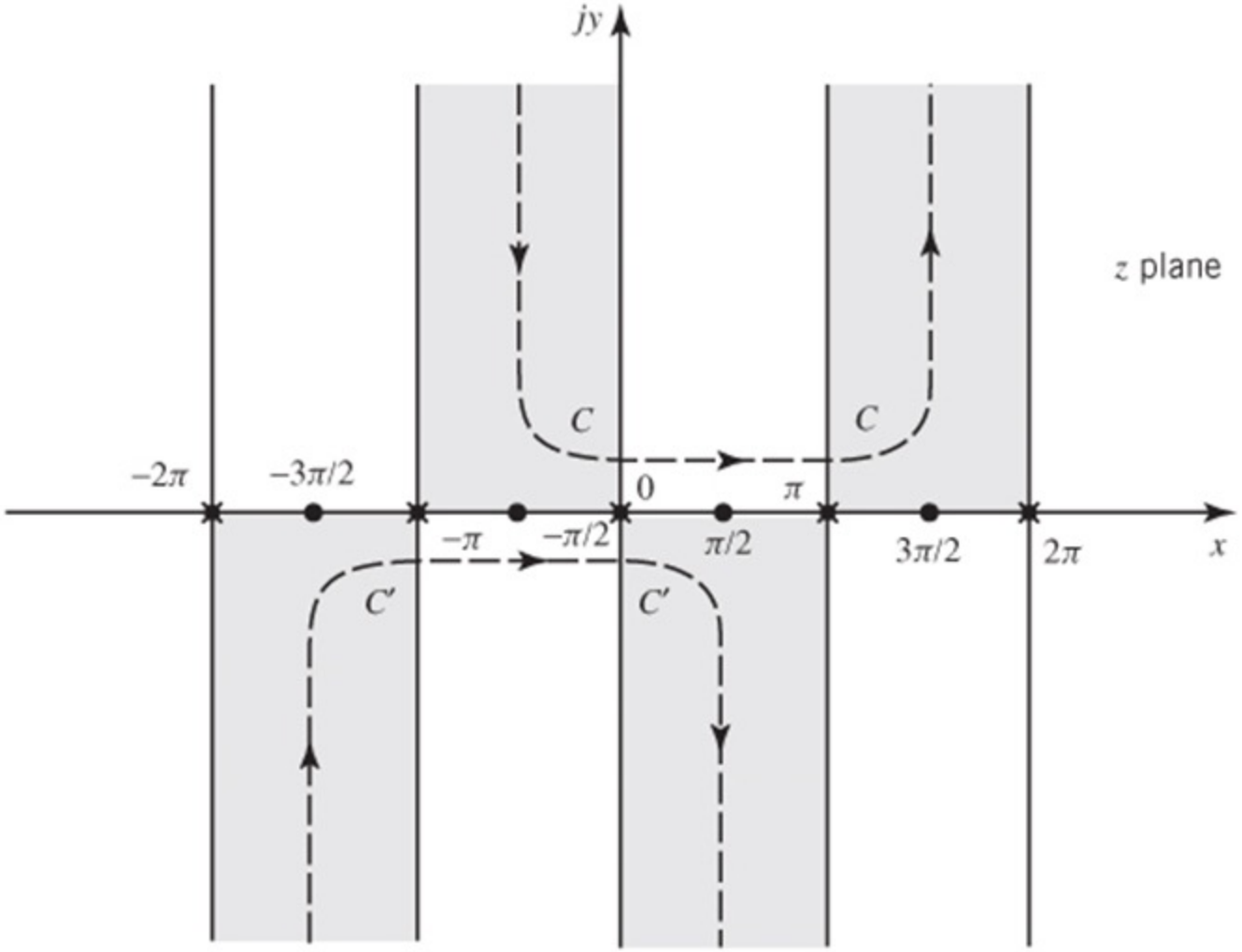

(a) Contours for Bessel function

Fig. 13-18

It will also be shown that the *saddle* points are given by

$$z_p = \pm\pi$$

When the poles are far removed the saddle points, then the evaluation along $SDP_{+\pi}$ and $SDP_{-\pi}$ can be evaluated using the conventional steepest descent method for isolated poles and saddle points.

The evaluation of $F(\beta\rho)$

$$F(\beta\rho) = F_1(\beta\rho) + F_2(\beta\rho)$$

1. Evaluating $F_1(\beta\rho)$ along $SDP_{\pm\pi}$ leads to incident diffracted field.
2. Evaluating $F_2(\beta\rho)$ along $SDP_{\pm\pi}$ leads to reflected diffracted field.

Both are valid provided observations are not made at and near, respectively, the *ISB* and *RSB*.

If the poles

$$z_p = -(\phi \mp \phi') + 2npN$$

are near the saddle points

$$z_s = \pm\pi$$

then the Pauli-Clemmow modified method of steepest descent must be used.

Shadow Boundaries and Transition Regions

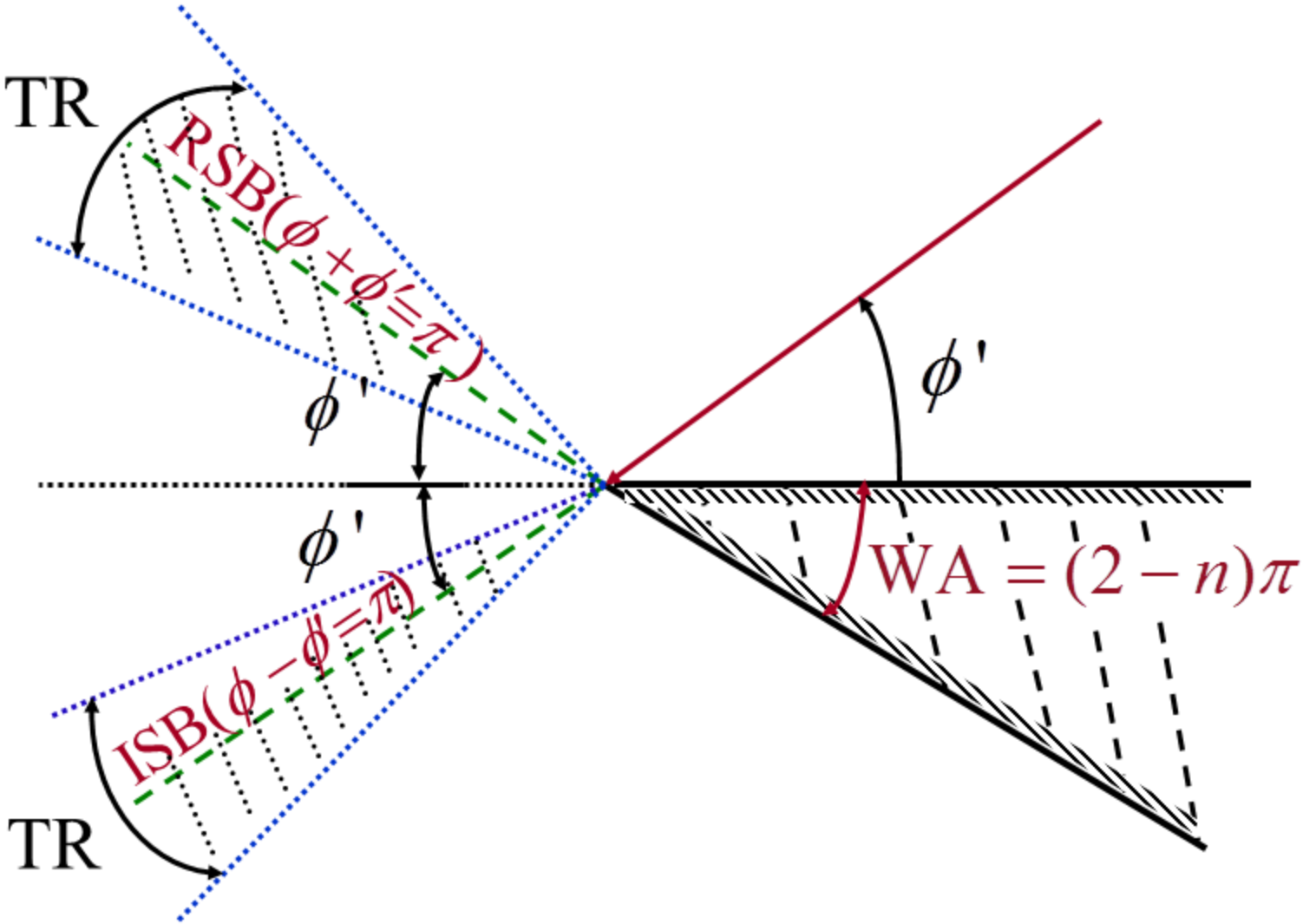

Watson Transformation

$$F(\beta\rho)=\frac{1}{n}\sum_{m=0}^{\infty}\varepsilon_m J_{m/n}(\beta\rho)\,e^{j\frac{m}{n}\left(\frac{\pi}{2}\right)}\left\{\cos\left[\frac{m}{n}(\phi-\phi')\right]\pm\cos\left[\frac{m}{n}(\phi+\phi')\right]\right\} \tag{13-40a}$$

$$\varepsilon_m=\begin{cases}1 & m=0\\ 2 & m\neq 0\end{cases} \tag{13-38a}$$

If $\beta\rho<1$, $\simeq 15$ terms $(m=0,\ldots,14)$
for 5 sign. figure accuracy

If $\beta\rho<10$, $\simeq 40$ terms $(m=0,1,\ldots,39)$
for 5 sign. figure accuracy

$$\cos\left(\frac{m}{n}\xi^{\mp}\right)=\frac{1}{2}\left[e^{j\frac{m}{n}\xi^{\mp}}+e^{-j\frac{m}{n}\xi^{\mp}}\right],\quad \xi^{\mp}=\phi\mp\phi'$$

(13-42, a)

$$J_{\frac{m}{n}}(\beta\rho)=\frac{1}{2\pi}\int_{C}e^{j\left[\beta\rho\cos z+\frac{m}{n}\left(z-\frac{\pi}{2}\right)\right]}dz$$

(13-43a)

or

$$J_{\frac{m}{n}}(\beta\rho)=\frac{1}{2\pi}\int_{C'}e^{j\left[\beta\rho\cos z-\frac{m}{n}\left(z+\frac{\pi}{2}\right)\right]}dz$$

(13-43b)

Steepest Descent Paths, Saddle Point, and Poles

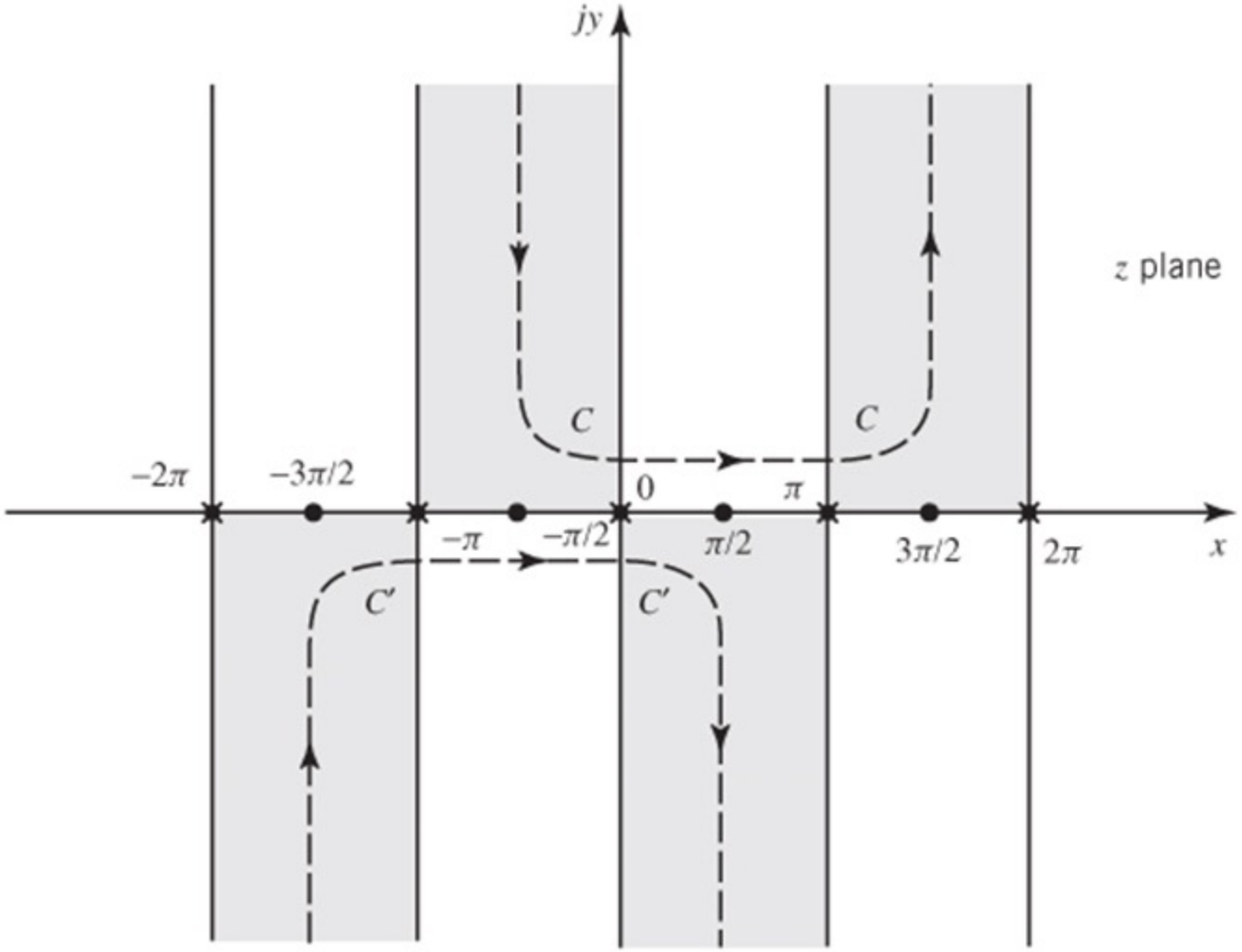

(a) Contours for Bessel function

Fig. 13-18

$$F(\beta\rho) = I(\beta\rho, \phi - \phi', n) \pm I(\beta\rho, \phi + \phi', n)$$

(13-44)

$$I(\beta\rho, \xi^{\mp}, n) = \frac{1}{2\pi n}\int_{C} e^{j\beta\rho\cos z} \sum_{m=1}^{\infty} e^{j\frac{m}{n}(\xi^{\mp}+z)}\, dz$$

(13-44a)

$$+ \frac{1}{2\pi n}\int_{C'} e^{j\beta\rho\cos z} \sum_{m=0}^{\infty} e^{-j\frac{m}{n}(\xi^{\mp}+z)}\, dz$$

$$\xi^{\mp} = \phi \mp \phi'$$

$$-\frac{1}{1-x^{-1}} = x\left(1+x+x^2+x^3+\ldots\right) = \sum_{m=1}^{\infty} x^m$$

$$\frac{1}{1-x^{-1}} = 1+x^{-1}+x^{-2}+x^{-3}+\ldots = \sum_{m=0}^{\infty} x^{-m} \tag{13-45a}$$

$$\frac{1}{1-e^{-j\left(\xi^{\mp}+z\right)/n}} = \frac{e^{j\left(\xi^{\mp}+z\right)/2n}}{e^{j\left(\xi^{\mp}+z\right)/2n}-e^{-j\left(\xi^{\mp}+z\right)/2n}} \tag{13-45b}$$

$$= \frac{1}{2}+\frac{1}{2j}\cot\left(\frac{\xi^{\mp}+z}{2n}\right) \tag{13-46}$$

$$G(\rho,\rho',\phi,\phi') \overset{\beta\rho'\to\text{large}}{\simeq} \sqrt{\frac{2}{\pi\beta\rho'}}e^{-j\left(\phi\rho'-\frac{\pi}{4}\right)}F(\beta\rho) \qquad (13\text{-}40)$$

$$F(\beta\rho)=\frac{1}{4\pi jn}\int_{C'-C}\cot\left[\frac{(\phi-\phi')+z}{2n}\right]e^{j\beta\rho\cos z}dz \pm \frac{1}{4\pi jn}\int_{C'-C}\cot\left[\frac{(\phi+\phi')+z}{2n}\right]e^{j\beta\rho\cos z}dz \qquad (13\text{-}47)$$

$$F(\beta\rho)=\frac{1}{4\pi jn}\int_{C'-C}H_1(z)e^{\beta\rho h_1(z)}dz \pm \frac{1}{4\pi jn}\int_{C'-C}H_2(z)e^{\beta\rho h_2(z)}dz$$

(13-48), (13-48a), (13-48b)

$$F(\beta\rho) = F_1(\beta\rho) + F_2(\beta\rho)$$

$$= \underbrace{\frac{1}{4\pi\, jn} \int_{C'-C} \cot\left[\frac{(\phi - \phi') + z}{2n}\right] e^{j\beta\rho\cos z}\, dz}_{F_1(\beta\rho)}$$

$$\pm \underbrace{\frac{1}{4\pi\, jn} \int_{C'-C} \cot\left[\frac{(\phi + \phi') + z}{2n}\right] e^{j\beta\rho\cos z}\, dz}_{F_2(\beta\rho)}$$

(13-48), (13-48a), (13-48b)

$$C_T = C' + SDP_{+\pi} - C + SDP_{-\pi} \qquad (13\text{-}49a)$$

or

$$C' - C = C_T - SDP_{+\pi} - SDP_{-\pi}$$

C_T = Closed path

$SDP_{+\pi}$ = Path along saddle point $+\pi$

$SDP_{-\pi}$ = Path along saddle point $-\pi$

Steepest Descent Paths, Saddle Point, and Poles

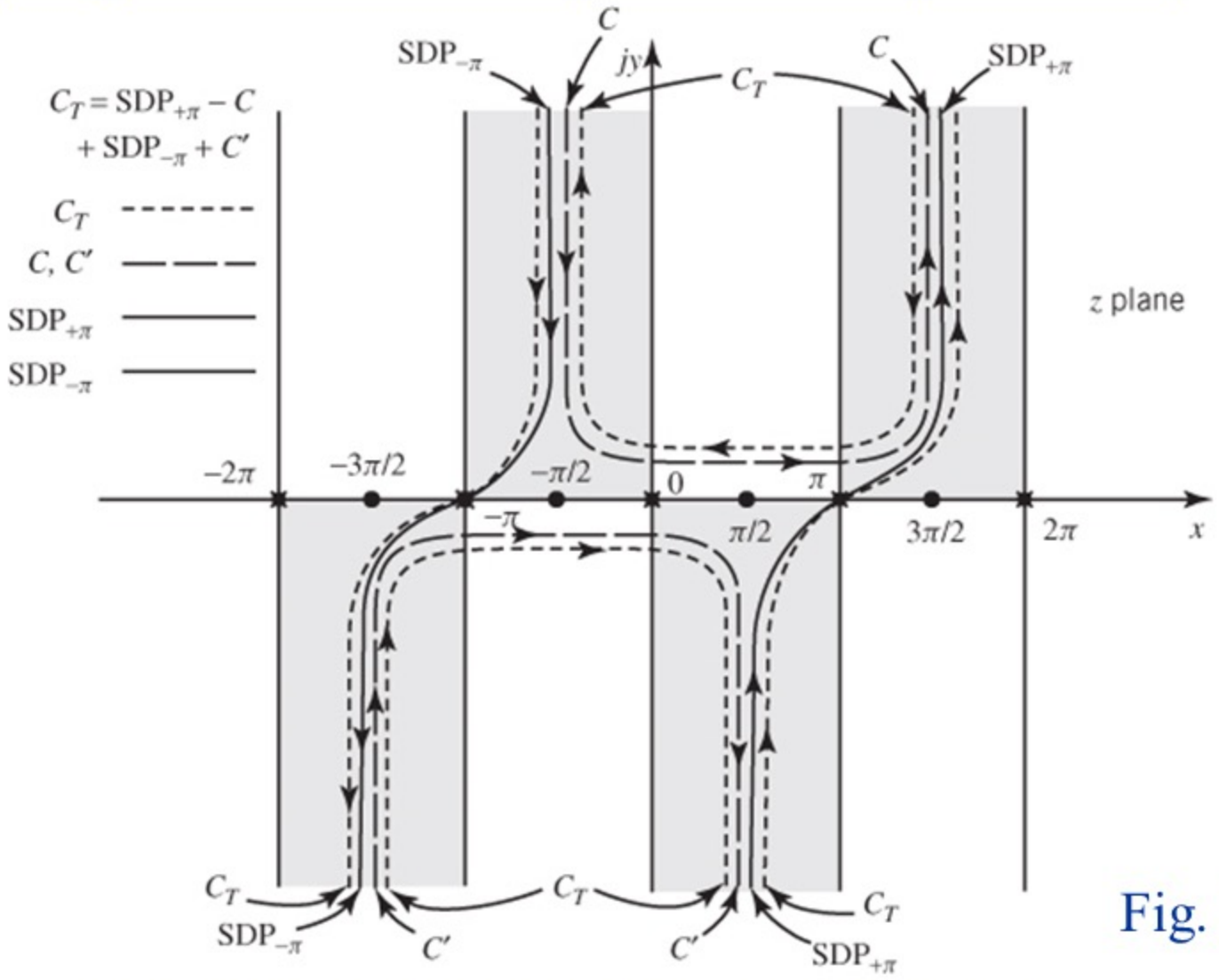

Fig. 13-18

(b) Steepest Descent paths, saddle points and poles.

Evaluate Along Closed Path C_T Using Residue Theory (complex variables) This Leads to GO

Evaluation Along $SDP_{+\pi}$ and $SDP_{-\pi}$ Leads to Incident and Reflected Diffracted Fields

$$F(\beta\rho) = F_1(\beta\rho) \pm F_2(\beta\rho) \tag{13-48}$$

$$F_1(\beta\rho) = \frac{1}{4\pi jn} \int_{C'-C} H_1(z) e^{\beta\rho h_1(z)} dz \tag{13-48a}$$

$$F_2(\beta\rho) = \frac{1}{4\pi jn} \int_{C'-C} H_2(z) e^{\beta\rho h_2(z)} dz \tag{13-48b}$$

$$H_1(z) = \cot\left[\frac{(\phi - \phi') + z}{2n}\right] = \cot\left[\frac{\xi^- + z}{2n}\right] \tag{13-48c}$$

$$H_2(z) = \cot\left[\frac{(\phi + \phi') + z}{2n}\right] = \cot\left[\frac{\xi^+ + z}{2n}\right] \tag{13-48d}$$

$$h_1(z) = h_2(z) = j\cos(z) \tag{13-48e}$$

Then

$$\frac{1}{4\pi jn}\oint_{C_T} H_1(z)\,e^{\beta\rho h_1(z)}dz = \frac{1}{4\pi jn}\int_{C'-C} H_1(z)\,e^{\beta\rho h_1(z)}dz + \frac{1}{4\pi jn}\int_{SDP_{-\pi}} H_1(z)\,e^{\beta\rho h_1(z)}dz + \frac{1}{4\pi jn}\int_{SDP_{+\pi}} H_1(z)\,e^{\beta\rho h_1(z)}dz \tag{13-49}$$

$$C_T = C' + SDP_{+\pi} - C + SDP_{-\pi} \tag{13-49a}$$

Evaluation Along $C' - C = C_T - SDP_{+\pi} - SDP_{-\pi}$

$$\frac{1}{4\pi jn}\int_{C'-C} H_1(z)e^{\beta\rho h_1(z)}dz = \frac{1}{4\pi jn}\oint_{C_T} H_1(z)e^{\beta\rho h_1(z)}dz$$

$$-\frac{1}{4\pi jn}\int_{SDP_{-\pi}} H_1(z)e^{\beta\rho h_1(z)}dz$$

$$-\frac{1}{4\pi jn}\int_{SDP_{+\pi}} H_1(z)e^{\beta\rho h_1(z)}dz$$

(13-50)

Therefore for $F_1(\beta\rho)$

$$F_1(\beta\rho) = \frac{1}{4\pi jn}\int_{C'-C} H_1(z)\,e^{\beta\rho h_1(z)}dz$$

$$= \frac{1}{4\pi jn}\oint_{C_T} H_1(z)\,e^{\beta\rho h_1(z)}dz$$

$$- \frac{1}{4\pi jn}\int_{SDP_{-\pi}} H_1(z)\,e^{\beta\rho h_1(z)}dz \qquad (13\text{-}50)$$

$$- \frac{1}{4\pi jn}\int_{SDP_{+\pi}} H_1(z)\,e^{\beta\rho h_1(z)}dz$$

Simarly for $F_2(\beta\rho)$

$$F_2(\beta\rho) = \frac{1}{4\pi jn}\int_{C'-C} H_2(z)\,e^{\beta\rho h_2(z)}dz$$

$$= \frac{1}{4\pi jn}\oint_{C_T} H_2(z)\,e^{\beta\rho h_2(z)}dz$$

$$- \frac{1}{4\pi jn}\int_{SDP_{-\pi}} H_2(z)\,e^{\beta\rho h_2(z)}dz$$

$$- \frac{1}{4\pi jn}\int_{SDP_{+\pi}} H_2(z)\,e^{\beta\rho h_2(z)}dz$$

Summary

$$\frac{1}{4\pi jn}\int_{SDP_{+\pi}} H_{1,2}(z)\,e^{\beta\rho h_{1,2}(z)}dz \overset{\beta\rho\to\text{large}}{\simeq} \frac{1}{4\pi jn}\left|\sqrt{\frac{2\pi}{-\beta\rho h''_{1,2}(z=+\pi)}}\right| \cdot e^{+j\frac{\pi}{4}} H_{1,2}(z=+\pi)\,e^{\beta\rho h_{1,2}(z=+\pi)} \tag{13-60a}$$

$$\frac{1}{4\pi jn}\int_{SDP_{-\pi}} H_{1,2}(z)\,e^{\beta\rho h_{2}(z)}dz \overset{\beta\rho\to\text{large}}{\simeq} \frac{1}{4\pi jn}\left|\sqrt{\frac{2\pi}{-\beta\rho h''_{1,2}(z=-\pi)}}\right| \cdot e^{-j\frac{3\pi}{4}} H_{1,2}(z=-\pi)\,e^{\beta\rho h_{1,2}(z=-\pi)} \tag{13-60b}$$

$$\frac{1}{4\pi jn}\oint_{C_T} H_{1,2}(z)\,e^{\beta\rho h_{2}(z)}dz = 2\pi j\sum_{p}\left[\begin{array}{c}\text{Residues of Poles}\\ \text{Enclosed by } C_T\end{array}\right] \tag{13-51}$$

Evaluate

$$F(\beta\rho) = F_1(\beta\rho) + F_2(\beta\rho)$$

Along Closed Path C_T

Using

Residue Theory

(complex variables).

This Leads to GO

Consider: Poles enclosed by C_T

$$\frac{1}{4\pi jn}\oint_{C_T} H_1(z)\, e^{\beta\rho h_1(z)}\, dz \qquad (13\text{-}52)$$

$$= \frac{1}{4\pi jn}\oint_{C_T} \cot\left[\frac{(\phi-\phi')+z}{2n}\right] e^{j\beta\rho\cos z}\, dz$$

$$\frac{1}{4\pi jn}\oint_{C_T} H_2(z)\, e^{\beta\rho h_2(z)}\, dz$$

$$= \frac{1}{4\pi jn}\oint_{C_T} \cot\left[\frac{(\phi+\phi')+z}{2n}\right] e^{j\beta\rho\cos z}\, dz$$

Evaluate (13-51)

$F_1(\beta\rho)$

Along Closed Path C_T

Using Residue Theory.

This Leads to *Incident GO*

Poles enclosed by C_T

From complex variables:

$$\frac{1}{4\pi jn}\oint_{C_T} H_1(z)\,e^{\beta\rho h_1(z)}\,dz \qquad (13\text{-}51)$$

$$= 2\pi j \sum_p \mathrm{Res}(z = z_p)$$

$$= 2\pi j \sum_p \left[\begin{array}{c}\text{Residues of Poles}\\ \text{Enclosed by } C_T\end{array}\right]$$

Poles enclosed by C_T

$$\frac{1}{4\pi jn}\oint_{C_T} H_1(z)\, e^{\beta\rho h_{1,2}(z)}\, dz \qquad (13\text{-}52)$$

$$= \frac{1}{4\pi jn}\oint_{C_T} \cot\left[\frac{(\phi-\phi')+z}{2n}\right] e^{j\beta\rho\cos z}\, dz$$

The cotangent function has poles when

$$\cot\left[\frac{(\phi-\phi')+z}{2n}\right] = \left.\frac{\cos\left[\dfrac{(\phi-\phi')+z}{2n}\right]}{\sin\left[\dfrac{(\phi-\phi')+z}{2n}\right]}\right|_{z=z_p} = \infty$$

Poles enclosed by C_T

Poles when denominator

$$\sin\left[\frac{(\phi-\phi')+z}{2n}\right]_{z=z_p}=0$$

$$\left[\frac{(\phi-\phi')+z}{2n}\right]_{z=z_p}=\pi N,\quad N=0,\pm1,\pm2,\ldots \tag{13-53}$$

$$(\phi-\phi')+z_p=2n\pi N \tag{13-53a}$$

$$z_p=-(\phi-\phi')+2n\pi N \Rightarrow z_p=-\xi^{-}+2\pi nN \tag{13-53b}$$

$$\boxed{-\pi\le z_p\le+\pi} \quad \text{or} \quad \boxed{|z_p|\le\pi}$$

Poles at

$$z_p = -(\phi - \phi') + 2\pi nN$$

For $N = 0$

$$z_p = -(\phi - \phi')$$

which are along ISB

Evaluation of $F_1(\beta\rho)$ Along C_T

$$F_1(\beta\rho)\oint_{C_T} = 2\pi j \sum_p \left[\begin{array}{c} \text{Residues of Poles} \\ \text{Enclosed by } C_T \end{array} \right] \quad (13\text{-}51)$$

Poles occur at

$$z_p = -(\phi - \phi') + 2\pi nN \quad (13\text{-}53a)$$

Also for C_T as chosen

$$-\pi \le z_p = -(\phi - \phi') + 2\pi nN \le +\pi \quad (13\text{-}53b)$$

$$F_1(\beta\rho)\oint_{C_T} = \frac{1}{4\pi jn}\oint_{C_T}\cot\left[\frac{(\phi-\phi')+z}{2n}\right]e^{j\beta\rho\cos z}dz$$

$$F_1(\beta\rho)\oint_{C_T} = \oint_{C_T}\underbrace{\frac{1}{4\pi jn}\cot\left[\frac{(\phi-\phi')+z}{2n}\right]e^{j\beta\rho\cos z}}_{N(z)/D(z)}dz$$

$$F_1(\beta\rho)\oint_{C_T} = \oint_{C_T}\frac{N(z)}{D(z)}dz \qquad (13\text{-}52)$$

$$\frac{N(z)}{D(z)} = \frac{1}{4\pi jn}\cot\left[\frac{(\phi-\phi')+z}{2n}\right]e^{j\beta\rho\cos z}$$

$$= \left.\frac{\cos\left[\dfrac{(\phi-\phi')+z}{2n}\right]e^{j\beta\rho\cos z}}{4\pi jn\ \sin\left[\dfrac{(\phi-\phi')+z}{2n}\right]}\right\} \qquad \text{(13-52a)}$$

$$\Rightarrow \begin{cases} N(z) = \cos\left[\dfrac{(\phi-\phi')+z}{2n}\right]e^{j\beta\rho\cos z} & \text{(13-52b)} \\ D(z) = 4\pi jn\ \sin\left[\dfrac{(\phi-\phi')+z}{2n}\right] & \text{(13-52c)} \end{cases}$$

$$F_1(\beta\rho)\oint_{C_T} = \oint_{C_T} \frac{N(z)}{D(z)}dz \qquad (13\text{-}51)$$

$$= 2\pi j \sum_p \text{Res}(z_p)\Big|_{\text{provided that } |z_p| \le \pi}$$

For simple poles (no branch points, etc.)

$$\mathrm{Res}(z_p) = \left.\frac{N(z)}{D'(z)}\right|_{z=z_p=-(\phi-\phi')+2\pi nN} \tag{13-54}$$

where

$$D'(z)\Big|_{z=z_p} = \left.\frac{dD(z)}{dz}\right|_{z=z_p}$$

$$N(z)\Big|_{z=z_p=-(\phi-\phi')+2\pi nN} = \cos\left[\frac{(\phi-\phi')+z}{2n}\right] e^{j\beta\rho\cos z}\Bigg|_{z=z_p}$$

$$= \cos[\pi N]\, e^{j\beta\rho\cos\left[-(\phi-\phi')+2\pi nN\right]}$$

$$N(z=z_p) = \cos(\pi N)\, e^{j\beta\rho\cos\left[-(\phi-\phi')+2\pi nN\right]} \qquad (13\text{-}54a)$$

$$D'(z)\Big|_{z=z_p} = \frac{dD(z)}{dz}\Big|_{z=z_p} = \frac{d}{dz}\left\{4\pi j \sin\left[\frac{(\phi-\phi')+z}{2n}\right]\right\}\Big|_{z=z_p}$$

$$D'(z)\Big|_{z=z_p} = \frac{4\pi jn}{2n}\cos\left[\frac{(\phi-\phi')+z}{2n}\right]\Big|_{z=z_p}$$

$$D'(z)\Big|_{z=z_p} = 2\pi j \cos\left[\frac{(\phi-\phi')+z}{2n}\right]\Big|_{z=z_p}$$

$$D'(z)\Big|_{z=z_p} = 2\pi j \cos\left(\frac{2\pi nN}{2n}\right) = 2\pi j \cos(\pi N)$$

$$D'(z=z_p) = 2\pi j \cos(\pi N) \qquad (13\text{-}54b)$$

$$-\pi \le z_p = -\left(\phi - \phi'\right) + 2\pi nN \le +\pi$$

When $z = z_p = +\pi$:

$$z_p = -\left(\phi - \phi'\right) + 2\pi nN^+ = +\pi$$

$$\boxed{2\pi nN^+ - \left(\phi - \phi'\right) = +\pi}$$

When $z = z_p = -\pi$:

$$z_p = -\left(\phi - \phi'\right) + 2\pi nN^- = -\pi$$

$$\boxed{2\pi nN^- - \left(\phi - \phi'\right) = -\pi}$$

$$\mathrm{Res}\left(z=z_p\right)=\left.\frac{N(z)}{D'(z)}\right|_{z=z_p}=\frac{N\left(z=z_p\right)}{D'\left(z=z_p\right)}$$

$$=\frac{\cos(\pi N)\,e^{j\beta\rho\cos\left[-(\phi-\phi')+2\pi nN\right]}}{2\pi j\cos(\pi N)}$$

$$\mathrm{Res}\left(z=z_p\right)=\frac{1}{2\pi j}e^{j\beta\rho\cos\left[-(\phi-\phi')+2\pi nN\right]} \qquad (13\text{-}55a)$$

Therefore

$$F_1(\beta\rho)\oint_{C_T} = \frac{1}{4\pi jn}\oint_{C_T} H_1(z)\,e^{\beta\rho h_1(z)}dz = 2\pi j\sum_p \text{Res}(z=z_p)$$

$$2\pi j\sum_p \text{Res}(z_p) = 2\pi j\left[\frac{1}{2\pi j}e^{j\beta\rho\cos\left[-(\phi-\phi')+2\pi nN\right]}\right] \qquad \text{(13-55b)}$$

$$z = z_p = -(\phi-\phi') + 2\pi nN \le \pi$$

$$F_1(\beta\rho)\oint_{C_T} = e^{j\beta\rho\cos\left[-(\phi-\phi')+2\pi nN\right]}\left\{U\left[\pi - \left|-(\phi-\phi')+2\pi nN\right|\right]\right.$$

$$\text{where } U[t-t_0] = \begin{cases} 0 & t < t_o \\ 1/2 & t = t_o \\ 1 & t > t_o \end{cases} \qquad \text{(13-56)}$$

The unit step function is introduced in (13-55b) so that (13-53b)

$$-\pi \le z_p = -\left(\phi - \phi'\right) + 2\pi nN \le +\pi \qquad \text{(13-53b)}$$

is satisfied. When $z_p = \pm\pi$, (13-55b) is expressed as

$$2\pi nN^{+} - \left(\phi - \phi'\right) = +\pi \qquad \text{for} \quad z_p = +\pi \qquad \text{(13-57a)}$$

and

$$2\pi nN^{-} - \left(\phi - \phi'\right) = -\pi \qquad \text{for} \quad z_p = -\pi \qquad \text{(13-57b)}$$

For the principal value of N ($N^{\pm} = 0$), (13-55b) reduces to

$$F_1(\beta\rho)\Big|_{C_T} = e^{j\beta\rho\cos\left[-(\phi-\phi')\right]}\left\{U\left[\pi - \left|-\left(\phi - \phi'\right)\right|\right]\right. \qquad \text{(13-58)}$$

This is referred to as the *Incident GO*

and it exists if $\left|\left(\phi - \phi'\right)\right| \le \pi$.

Using Same Procedure Evaluate

$F_2(\beta\rho)$

Along Closed Path C_T

Using Residue Theory.

This Leads to *Reflected GO*

Simarly for $F_2(\beta\rho)$,

$$F_2(\beta\rho)\oint_{C_T} = \frac{1}{4\pi jn}\oint_{C_T} H_2(z)\,e^{\beta\rho h_2(z)}dz = 2\pi j\sum_p \text{Res}(z=z_p)$$

$$2\pi j\sum_p \text{Res}(z_p) = 2\pi j\left[\frac{1}{2\pi j}e^{j\beta\rho\cos\left[-(\phi+\phi')+2\pi nN\right]}\right]$$

$$z = z_p = -(\phi+\phi')+2\pi nN \le \pi$$

$$F_2(\beta\rho)\oint_{C_T} = e^{j\beta\rho\cos\left[-(\phi+\phi')+2\pi nN\right]}\left\{U\left[\pi - \left|-(\phi+\phi')+2\pi nN\right|\right]\right.$$

$$\text{where } U[t-t_0] = \begin{cases} 0 & t < t_o \\ 1/2 & t = t_o \\ 1 & t > t_o \end{cases}$$

The unit step function is introduced in (13-55b) so that (13-53b)

$$-\pi \le z_p = -\left(\phi + \phi'\right) + 2\pi nN \le +\pi \qquad \text{(13-53b)}$$

is satisfied. When $z_p = \pm\pi$, (13-55b) is expressed as

$$2\pi nN^{+} - \left(\phi + \phi'\right) = +\pi \qquad \text{for} \quad z_p = +\pi \qquad \text{(13-57a)}$$

and

$$2\pi nN^{-} - \left(\phi + \phi'\right) = -\pi \qquad \text{for} \quad z_p = -\pi \qquad \text{(13-57b)}$$

For the principal value of N $(N^{\pm} = 0)$, $F_2\left(\beta\rho\right)$ reduces to

$$F_2\left(\beta\rho\right)\Big|_{C_T} = e^{j\beta\rho\cos\left[-\left(\phi+\phi'\right)\right]}\left\{U\left[\pi - \left|-\left(\phi+\phi'\right)\right|\right]\right. \qquad \text{(13-62b)}$$

This is referred to as the *Reflected GO*

and it exists if $\left|\left(\phi+\phi'\right)\right| \le \pi$.

Evaluation of

$$F(\beta\rho)=F_1(\beta\rho) \pm F_2(\beta\rho)$$

Along Closed Path C_T
Using Residue Theory.
This Leads to *Total GO*

Therefore, combining both $F_1(\beta\rho)+F_2(\beta\rho)=F(\beta\rho)$

$$F(\beta\rho)\oint_{C_T} = 2\pi j\sum_p \text{Res}(z_p) = 2\pi j\left[\frac{1}{2\pi j}e^{j\beta\rho\cos\left[-(\phi\pm\phi')+2\pi nN\right]}\right]$$

$$z = z_p = -(\phi\pm\phi')+2\pi nN \le \pi$$

$$F(\beta\rho)\oint_{C_T} = e^{j\beta\rho\cos\left[-(\phi\pm\phi')+2\pi nN\right]}\begin{cases} U\left[\pi-\left|-(\phi-\phi')+2\pi nN\right|\right] \\ \text{or} \\ U\left[\pi-\left|-(\phi+\phi')+2\pi nN\right|\right] \end{cases}$$

$$\text{where } U[t-t_0] = \begin{cases} 0 & t<t_o \\ 1/2 & t=t_o \\ 1 & t>t_o \end{cases}$$

which for the principal value of N $(N^{\pm}=0)$ reduce to

$$F(\beta\rho)\oint_{C_T} = \begin{cases} e^{j\beta\rho\cos\left[-(\phi-\phi')\right]} \cdot U\left[\pi-(\phi-\phi')\right] & \text{for } \left|(\phi-\phi')\right| \le \pi \\ \textit{Incident Geometrical Optics} & \\ e^{j\beta\rho\cos\left[-(\phi+\phi')\right]} \cdot U\left[\pi-(\phi+\phi')\right] & \text{for } \left|(\phi+\phi')\right| \le \pi \\ \textit{Reflected Geometrical Optics} & \end{cases}$$

If $N = 0$:

$$F(\beta\rho)\oint_{C_T} = \begin{cases} e^{j\beta\rho\cos\left[-(\phi-\phi')\right]}U\left[\pi - \left|-(\phi-\phi')\right|\right] \\ e^{j\beta\rho\cos\left[-(\phi+\phi')\right]}U\left[\pi - \left|-(\phi+\phi')\right|\right] \end{cases}$$

.....

$$F(\beta\rho)\oint_{C_T} = \begin{cases} e^{j\beta\rho\cos(\phi-\phi')}U\left[\pi-(\phi-\phi')\right] \text{ for } (\phi-\phi') \le \pi \\ \textit{Incident Geometrical Optics} \\ \\ e^{j\beta\rho\cos(\phi+\phi')}U\left[\pi-(\phi+\phi')\right] \text{ for } (\phi+\phi') \le \pi \\ \textit{Reflected Geometrical Optics} \end{cases}$$

Geometrical Optics Field

$$F_G(\beta\rho) = \begin{cases} e^{j\beta\rho\cos(\phi-\phi')} \pm e^{j\beta\rho\cos(\phi+\phi')} & 0 \le \phi < \pi - \phi' \\ e^{j\beta\rho\cos(\phi-\phi')} \pm 0 & \pi - \phi' \le \phi < \pi + \phi' \\ 0 \pm 0 & \pi + \phi' \le \phi < \underbrace{2\pi - \mathrm{WA}}_{n\pi} \end{cases}$$

$U_{GO}^{inc/dir}$	U_{GO}^{ref}	Region

(13-65)

Line Source Near a 2-D Conducting Wedge

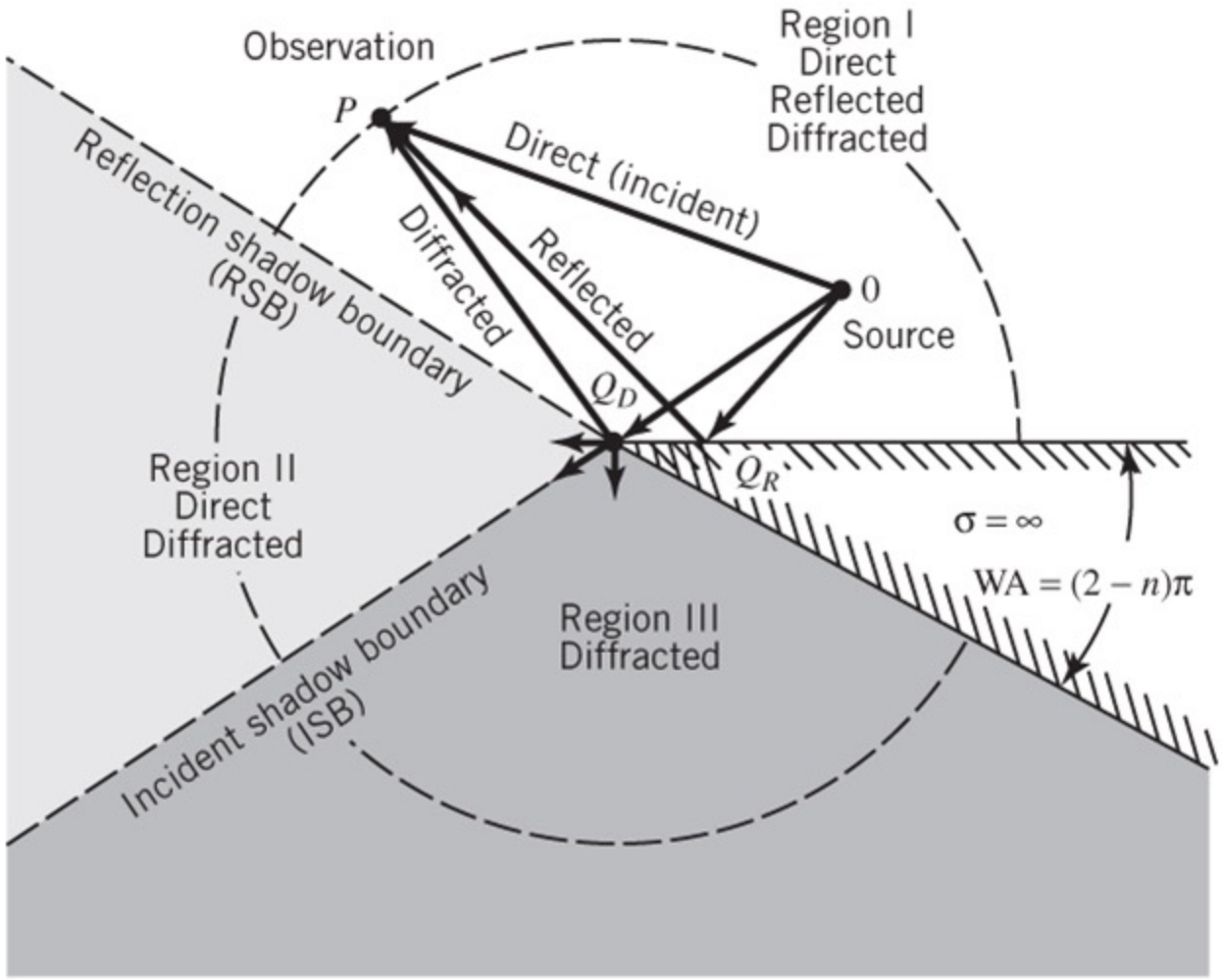

(a) Region separation

Fig. 13-13(a)

Shadow Boundaries and Transition Regions

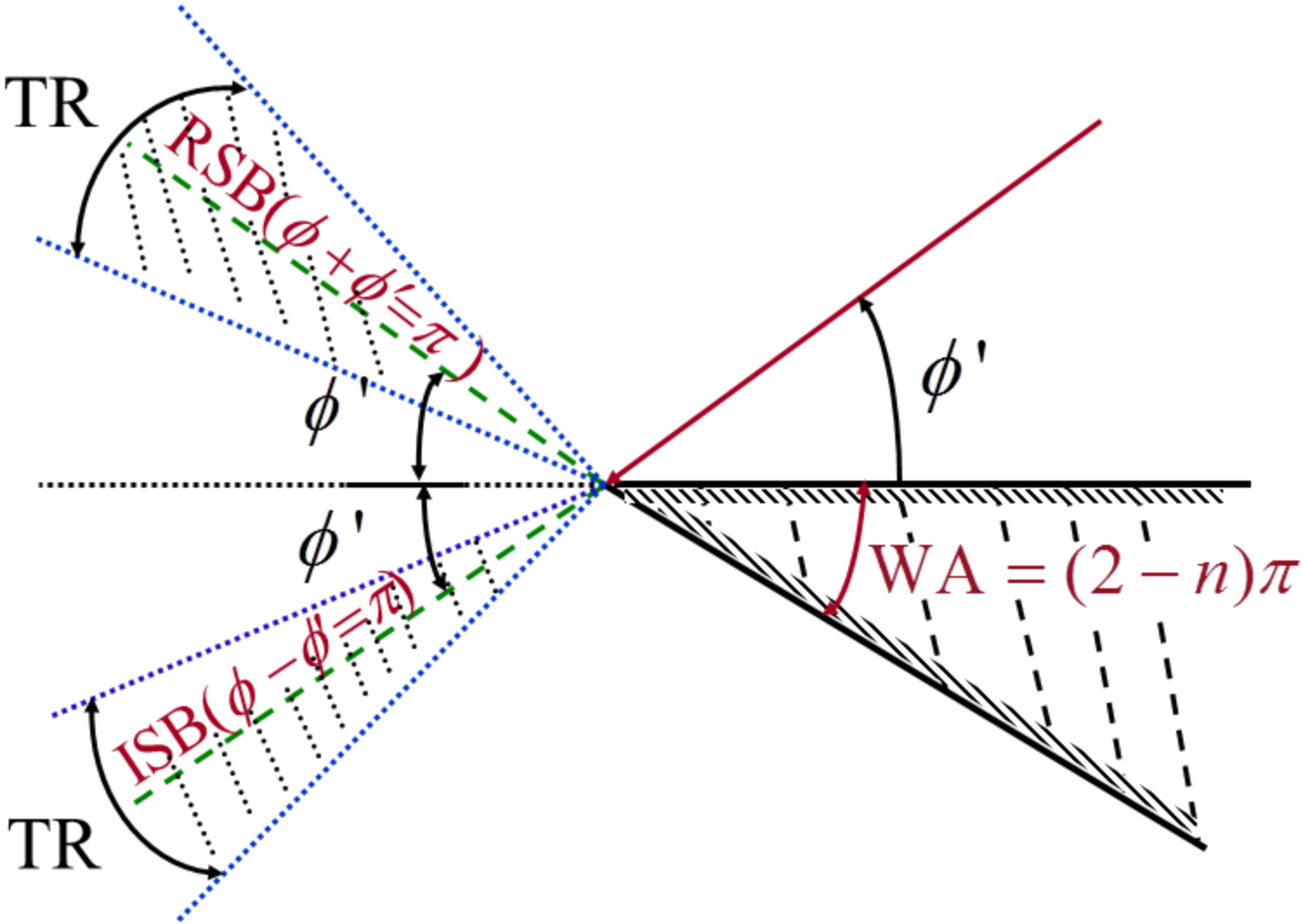

Keller's Diffraction

1. Diffraction Functions
2. Diffraction Coefficients

Evaluation Along $SDP_{+\pi}$ and $SDP_{-\pi}$ Using Method of Steepest Descent

Therefore the contributions of $F(\beta\rho)$ along the $SDP_{\pm\pi}$ are

$$F(\beta\rho)\Big|_{SDP_{\pm\pi}} = F_1(\beta\rho)\Big|_{SDP_{\pm\pi}} \pm F_2(\beta\rho)\Big|_{SDP_{\pm\pi}}$$

$$F_1(\beta\rho)\Big|_{SDP_{\pm\pi}} = \left[-\frac{1}{4\pi jn} \int_{SDP_{+\pi}} \cot\left[\frac{(\phi - \phi') + z}{2n} \right] e^{j\beta\rho\cos z} dz \right.$$

$$\left. -\frac{1}{4\pi jn} \int_{SDP_{-\pi}} \cot\left[\frac{(\phi - \phi') + z}{2n} \right] e^{j\beta\rho\cos z} dz \right]$$

(13-61)

$$F_2(\beta\rho)\Big|_{SDP_{\pm\pi}} = \left[-\frac{1}{4\pi jn} \int_{SDP_{+\pi}} \cot\left[\frac{(\phi+\phi')+z}{2n} \right] e^{j\beta\rho\cos z}\, dz \right.$$

$$\left. -\frac{1}{4\pi jn} \int_{SDP_{-\pi}} \cot\left[\frac{(\phi+\phi')+z}{2n} \right] e^{j\beta\rho\cos z}\, dz \right]$$

(13-62b)

Evaluation Along $SDP_{+\pi}$ and $SDP_{-\pi}$ Leads to Incident and Reflected Diffracted Fields

When the poles are far removed from the saddle points, the evaluation of the integrals along the $SDP_{\pm}$ paths can be performed using the *conventional steepest descent method.* This leads to Keller's diffraction functions and coefficients which possess singularities along the *ISB & RSB*.

The *poles* are given by

$$z_p = -\xi^{\mp} + 2npN$$

with $-\pi \leq z_p \leq +\pi$

The *saddle* points are given by

$$z_s = \pm\pi$$

Consider: Contributions Along $SDP_{+\pi}$ and $SDP_{-\pi}$

$$\frac{1}{4\pi jn}\int_{SDP_{+\pi}} H_1(z)\,e^{\beta\rho h_1(z)}dz =$$

$$\frac{1}{4\pi jn}\int_{SDP_{+\pi}} \cot\left[\frac{(\phi-\phi')+z}{2n}\right]e^{j\beta\rho\cos z}dz$$

$$\frac{1}{4\pi jn}\int_{SDP_{-\pi}} H_1(z)\,e^{\beta\rho h_1(z)}dz =$$

$$\frac{1}{4\pi jn}\int_{SDP_{-\pi}} \cot\left[\frac{(\phi-\phi')+z}{2n}\right]e^{j\beta\rho\cos z}dz$$

Consider: Contributions Along $SDP_{+\pi}$ and $SDP_{-\pi}$

$$\frac{1}{4\pi jn}\int_{SDP_{+\pi}} H_2(z)\,e^{\beta\rho h_2(z)}dz =$$

$$\frac{1}{4\pi jn}\int_{SDP_{+\pi}} \cot\left[\frac{(\phi+\phi')+z}{2n}\right]e^{j\beta\rho\cos z}dz$$

$$\frac{1}{4\pi jn}\int_{SDP_{-\pi}} H_2(z)\,e^{\beta\rho h_2(z)}dz =$$

$$\frac{1}{4\pi jn}\int_{SDP_{-\pi}} \cot\left[\frac{(\phi+\phi')+z}{2n}\right]e^{j\beta\rho\cos z}dz$$

Evaluation of

$$F_1(\beta\rho)/H_1(z) \quad \text{and} \quad F_2(\beta\rho)/H_2(z)$$

Along $SDP_{+\pi}$

Evaluation of

$$F_1(\beta\rho)/H_1(z)$$

Along $SDP_{+\pi}$

Consider: Contributions Along $SDP_{+\pi}$

$$\frac{1}{4\pi jn}\int_{SDP_{+\pi}} H_1(z)e^{\beta\rho h_1(z)}dz =$$

$$\frac{1}{4\pi jn}\int_{SDP_{+\pi}} \cot\left[\frac{(\phi-\phi')+z}{2n}\right]e^{j\beta\rho\cos z}dz$$

$$\int_{C'-C} H_1(z)\, e^{\beta\rho h_1(z)}\, dz$$

$$\overset{\beta\rho\to\infty}{\simeq} \sum_s H_1(z_s) \sqrt{-\frac{2\pi}{\beta\rho h_1''(z_s)}}\, e^{\beta\rho h_1(z_s)}$$

provided poles of $H_1(z)$ are *not* near saddle points

$$H_1(z) = \cot\left[\frac{(\phi-\phi') + z}{2n}\right] = \cot\left[\frac{\xi^- + z}{2n}\right]$$

$$\xi^- = \phi - \phi'$$

$$h_1(z) = j\cos z$$

To find saddle points:

$$\left.\frac{dh_1(z)}{dz}\right|_{z=z_s} = 0 = -j\sin z_s$$

$$\Rightarrow z_s = s\pi,\ s = 0, \pm 1, \pm 2, \ldots$$

Create Steepest Descent Paths (SDP), $SDP_{-\pi}$ and $SDP_{+\pi}$, passing through saddle points $z_s = -\pi$ and $z_s = +\pi$

Evaluation of

$$F_1(\beta\rho)/H_1(z)$$

Along $SDP_{+\pi}$

$$\frac{1}{4\pi jn}\int_{SDP_{+\pi}} H_1(z)\,e^{\beta\rho h_1(z)}dz$$

$$=\frac{1}{4\pi jn}\int_{SDP_{+\pi}} \cot\left[\frac{(\phi-\phi')+z}{2n}\right]e^{j\beta\rho\cos z}dz$$

$$=\frac{1}{4\pi jn}\left\{\left|\sqrt{\frac{2\pi}{-\beta\rho h_1''(z=+\pi)}}\right| \cdot e^{+j\pi/4}H_1(z=+\pi)\,e^{\beta\rho h_1(z=+\pi)}\right\}$$

$$H_1\left(z=+\pi\right)=\cot\left[\frac{\left(\phi-\phi'\right)+\pi}{2n}\right]$$

$$=\cot\left[\frac{\pi+\left(\phi-\phi'\right)}{2n}\right]$$

$$h_1\left(z\right)=j\cos\left(z\right)\Rightarrow h_1\left(z=+\pi\right)=j\cos\left(+\pi\right)=-j$$

$$h_1'\left(z\right)=-j\sin\left(z\right)$$

$$h_1''\left(z\right)=-j\cos\left(z\right)\Rightarrow h_1''\left(z=+\pi\right)=-j\cos\left(\pi\right)=+j$$

$$\frac{1}{4\pi jn}\int_{SDP_{+\pi}} \cot\left[\frac{(\phi-\phi')+z}{2n}\right] e^{j\beta\rho\cos z}\,dz$$

$$= \frac{1}{4\pi jn}\left\{\left|\sqrt{-\frac{2\pi}{j\beta\rho}}\right| e^{+j\pi/4}\cot\left[\frac{\pi+(\phi-\phi')}{2n}\right] e^{-j\beta\rho}\right\}$$

$$= \frac{1}{4\pi jn}\sqrt{\frac{2\pi}{\beta\rho}} e^{+j\pi/4}\cot\left[\frac{\pi+(\phi-\phi')}{2n}\right] e^{-j\beta\rho}$$

$$= \frac{e^{-j\left(\beta\rho+\frac{\pi}{4}\right)}}{2n\sqrt{2\pi\beta\rho}}\cot\left[\frac{\pi+(\phi-\phi')}{2n}\right] \qquad (1)$$

Evaluation of

$$F_2(\beta\rho)/H_2(z)$$

Along $SDP_{+\pi}$

Similarly:

$$\frac{1}{4\pi jn}\int_{SDP_{+\pi}} \cot\left[\frac{(\phi+\phi')+z}{2n}\right] e^{j\beta\rho\cos z}\,dz$$

$$= \frac{e^{-j\left(\beta\rho+\frac{\pi}{4}\right)}}{2n\sqrt{2\pi\beta\rho}} \cot\left[\frac{\pi+(\phi+\phi')}{2n}\right] \qquad (2)$$

Summary [(1)+(2)] $SDP_{+\pi}$: GTD

$$\frac{1}{4\pi jn}\int_{SDP_{+\pi}} \cot\left[\frac{(\phi-\phi')+z}{2n}\right] e^{j\beta\rho\cos z}\,dz$$

$$= \frac{e^{-j\pi/4}}{2n\sqrt{2\pi\beta}} \cot\left[\frac{\pi+(\phi-\phi')}{2n}\right]\frac{e^{-j\beta\rho}}{\sqrt{\rho}} \qquad (1)$$

$$\frac{1}{4\pi jn}\int_{SDP_{+\pi}} \cot\left[\frac{(\phi+\phi')+z}{2n}\right] e^{j\beta\rho\cos z}\,dz$$

$$= \frac{e^{-j\pi/4}}{2n\sqrt{2\pi\beta}} \cot\left[\frac{\pi+(\phi+\phi')}{2n}\right]\frac{e^{-j\beta\rho}}{\sqrt{\rho}} \qquad (2)$$

Evaluation of

$$F_1(\beta\rho)/H_1(z)$$

Along $SDP_{-\pi}$

$$\frac{1}{4\pi jn}\int_{SDP_{-\pi}} H_1(z)\, e^{\beta\rho h_1(z)}\, dz$$

$$= \frac{1}{4\pi jn}\int_{SDP_{-\pi}} \cot\left[\frac{(\phi-\phi')+z}{2n}\right] e^{j\beta\rho\cos z}\, dz$$

$$= \frac{1}{4\pi jn}\left\{\left|\sqrt{\frac{2\pi}{-\beta\rho h_1''(z=-\pi)}}\right| \cdot e^{-j3\pi/4} e^{\beta\rho h_1(z=+\pi)}\right\}$$

$$H_1\left(z=-\pi\right)=\cot\left[\frac{\left(\phi-\phi'\right)-\pi}{2n}\right]$$

$$=\cot\left[\frac{-\pi+\left(\phi-\phi'\right)}{2n}\right]$$

$$=-\cot\left[\frac{\pi-\left(\phi-\phi'\right)}{2n}\right]$$

$$h_1\left(z\right)=j\cos\left(z\right)\Rightarrow h_1\left(z=-\pi\right)=j\cos\left(-\pi\right)=-j$$

$$h_1'\left(z\right)=-j\sin\left(z\right)$$

$$h_1''\left(z\right)=-j\cos\left(z\right)\Rightarrow h_1''\left(z=-\pi\right)=-j\cos\left(-\pi\right)=+j$$

$$\frac{1}{4\pi jn}\int_{SDP\_\pi}\cot\left[\frac{(\phi-\phi')+z}{2n}\right]e^{j\beta\rho\cos z}dz$$

$$=-\frac{1}{4\pi jn}\left\{\left|\sqrt{-\frac{2\pi}{jk\rho}}\right|\cdot e^{-j3\pi/4}\cot\left[\frac{\pi-(\phi-\phi')}{2n}\right]e^{-j\beta\rho}\right\}$$

$$=\frac{e^{-j\pi/4}}{2n\sqrt{2\pi\beta}}\cot\left[\frac{\pi-(\phi-\phi')}{2n}\right]\frac{e^{-j\beta\rho}}{\sqrt{\rho}} \qquad (3)$$

Evaluation of

$$F_2(\beta\rho)/H_2(z)$$

Along $SDP_{-\pi}$

Similarly:

$$\frac{1}{4\pi jn}\int_{SDP_{-\pi}} \cot\left[\frac{(\phi+\phi')+z}{2n}\right] e^{j\beta\rho\cos z}\,dz$$

$$= \frac{e^{-j\pi/4}}{2n\sqrt{2\pi\beta}} \cot\left[\frac{\pi-(\phi+\phi')}{2n}\right]\frac{e^{-j\beta\rho}}{\sqrt{\rho}} \qquad (4)$$

Summary [(3)+(4)] $SDP_{-\pi}$: GTD

$$\frac{1}{4\pi jn}\int_{SDP_{-\pi}} \cot\left[\frac{(\phi-\phi')+z}{2n}\right] e^{j\beta\rho\cos z}\,dz$$

$$= \frac{e^{-j\pi/4}}{2n\sqrt{2\pi\beta}} \cot\left[\frac{\pi-(\phi-\phi')}{2n}\right]\frac{e^{-j\beta\rho}}{\sqrt{\rho}} \qquad (3)$$

$$\frac{1}{4\pi jn}\int_{SDP_{-\pi}} \cot\left[\frac{(\phi+\phi')+z}{2n}\right] e^{j\beta\rho\cos z}\,dz$$

$$= \frac{e^{-j\pi/4}}{2n\sqrt{2\pi\beta}} \cot\left[\frac{\pi-(\phi+\phi')}{2n}\right]\frac{e^{-j\beta\rho}}{\sqrt{\rho}} \qquad (4)$$

Evaluation of:

1. $F_1(\beta\rho)/H_1(z)$ Along $SDP_{+\pi}$ and $SDP_{-\pi}$ Leads to Incident Diffracted Fields

2. $F_2(\beta\rho)/H_2(z)$ Along $SDP_{+\pi}$ and $SDP_{-\pi}$ Leads to Reflected Diffracted Fields

Summary [(1)-(4)] $SDP_{+\pi}$ + $SDP_{-\pi}$: GTD

$$F(\beta\rho)\Big|_{SDP_{\pm\pi}} = -\frac{e^{-j\pi/4}}{2n\sqrt{2\pi\beta}}\frac{e^{-j\beta\rho}}{\sqrt{\rho}}$$

$$\cdot\left\{\left[\cot\left[\frac{\pi+(\phi-\phi')}{2n}\right]_{\substack{F_1(\beta\rho)\\ SDP:+\pi}} + \cot\left[\frac{\pi-(\phi-\phi')}{2n}\right]_{\substack{F_1(\beta\rho)\\ SDP:-\pi}}\right]\right.$$

$$\left.\pm\left[\cot\left[\frac{\pi+(\phi+\phi')}{2n}\right]_{\substack{F_2(\beta\rho)\\ SDP:+\pi}} + \cot\left[\frac{\pi-(\phi+\phi')}{2n}\right]_{\substack{F_2(\beta\rho)\\ SDP:-\pi}}\right]\right\}$$

Since

$$\cot(x+y)=\frac{\cos(x+y)}{\sin(x+y)}$$

$$\cot(x-y)=\frac{\cos(x-y)}{\sin(x-y)}$$

Then

$$\cot(x+y)+\cot(x-y)=\frac{\cos(x+y)}{\sin(x+y)}+\frac{\cos(x-y)}{\sin(x-y)}$$

$$=\frac{\cos(x+y)\sin(x-y)+\sin(x+y)\cos(x-y)}{\sin(x+y)\sin(x-y)}$$

Also

$$\cos(x+y)\sin(x-y)$$

$$=\frac{1}{2}\left[\sin(2x)-\sin(2y)\right]$$

$$\sin(x+y)\cos(x-y)$$

$$=\frac{1}{2}\left[\sin(2x)+\sin(2y)\right]$$

$$\sin(x+y)\sin(x-y)$$

$$=-\frac{1}{2}\left[\cos(2x)-\cos(2y)\right]$$

Thus

$$\cot(x+y)+\cot(x-y)$$

$$=\frac{\frac{1}{2}\left[\sin(2x)-\sin(2y)\right]+\frac{1}{2}\left[\sin(2x)+\sin(2y)\right]}{-\frac{1}{2}\left[\cos(2x)-\cos(2y)\right]}$$

$$\cot(x+y)+\cot(x-y) = \frac{-2\sin(2x)}{\cos(2x)-\cos(2y)}$$

$$\cot(x+y)+\cot(x-y) = -\frac{2\sin(2x)}{\cos(2x)-\cos(2y)}$$

Therefore

$$\cot\left[\underbrace{\frac{\pi}{2n}}_{x}+\underbrace{\frac{\phi-\phi'}{2n}}_{y}\right]+\cot\left[\underbrace{\frac{\pi}{2n}}_{x}+\underbrace{\frac{\phi-\phi'}{2n}}_{y}\right]=-\frac{2\sin\left(\frac{\pi}{n}\right)}{\cos\left(\frac{\pi}{n}\right)-\cos\left(\frac{\phi-\phi'}{n}\right)}$$

$$\cot\left[\underbrace{\frac{\pi}{2n}}_{x}+\underbrace{\frac{\phi+\phi'}{2n}}_{y}\right]+\cot\left[\underbrace{\frac{\pi}{2n}}_{x}-\underbrace{\frac{\phi+\phi'}{2n}}_{y}\right]=-\frac{2\sin\left(\frac{\pi}{n}\right)}{\cos\left(\frac{\pi}{n}\right)-\cos\left(\frac{\phi+\phi'}{n}\right)}$$

Finally

$$F(\beta\rho)\Big|_{SDP_{\pm\pi}} = F_1(\beta\rho)\Big|_{SDP_{\pm\pi}} + F_2(\beta\rho)\Big|_{SDP_{\pm\pi}} = -\frac{e^{-j\pi/4}e^{-j\beta\rho}}{2n\sqrt{2\pi\beta\rho}}$$

$$\cdot\left\{\frac{2\sin\left(\frac{\pi}{n}\right)}{\cos\left(\frac{\pi}{n}\right)-\cos\left(\frac{\phi-\phi'}{n}\right)}\right.$$

$$\left.\pm\left[\frac{2\sin\left(\frac{\pi}{n}\right)}{\cos\left(\frac{\pi}{n}\right)-\cos\left(\frac{\phi+\phi'}{n}\right)}\right]\right\}$$

Summary: GTD (Keller)

$$F(\beta\rho)\Big|_{SDP_{\pm\pi}} = F_1(\beta\rho)\Big|_{SDP_{\pm\pi}} + F_2(\beta\rho)\Big|_{SDP_{\pm\pi}} = -\frac{e^{-j(\beta\rho+\pi/4)}}{\sqrt{2\pi\beta\rho}}$$

$$\cdot\left\{\frac{\frac{1}{n}\sin\left(\frac{\pi}{n}\right)}{\cos\left(\frac{\pi}{n}\right)-\cos\left(\frac{\phi-\phi'}{n}\right)}\right.$$

$$\left.\pm\left[\frac{\frac{1}{n}\sin\left(\frac{\pi}{n}\right)}{\cos\left(\frac{\pi}{n}\right)-\cos\left(\frac{\phi+\phi'}{n}\right)}\right]\right\}$$

Summary
Keller's Diffraction

1. Diffraction Functions
2. Diffraction Coefficients

Decomposition of Total Field

$$E_z(H_z) \sim F(\beta\rho) = F_G + F_D$$

where

$$F_G = F_G^i \pm F_G^r$$

$$F_D = F_D^i \pm F_D^r$$

F_G^i = Incident Geometrical Optics Field

F_G^r = Reflected Geometrical Optics Field

F_D^i = Incident Diffracted Field

F_D^r = Reflected Diffracted Field

$$F(\rho,\phi,\phi',n) \simeq F_G(\rho,\phi,\phi',n) + F_D(\rho,\phi,\phi',n) \qquad (13\text{-}64)$$

F_G = Geometrical Optics Field

$$= F_G^i \pm F_G^r$$

F_D = Diffracted Field

$$= F_D^i \pm F_D^r$$

Line Source Near a 2-D Conducting Wedge

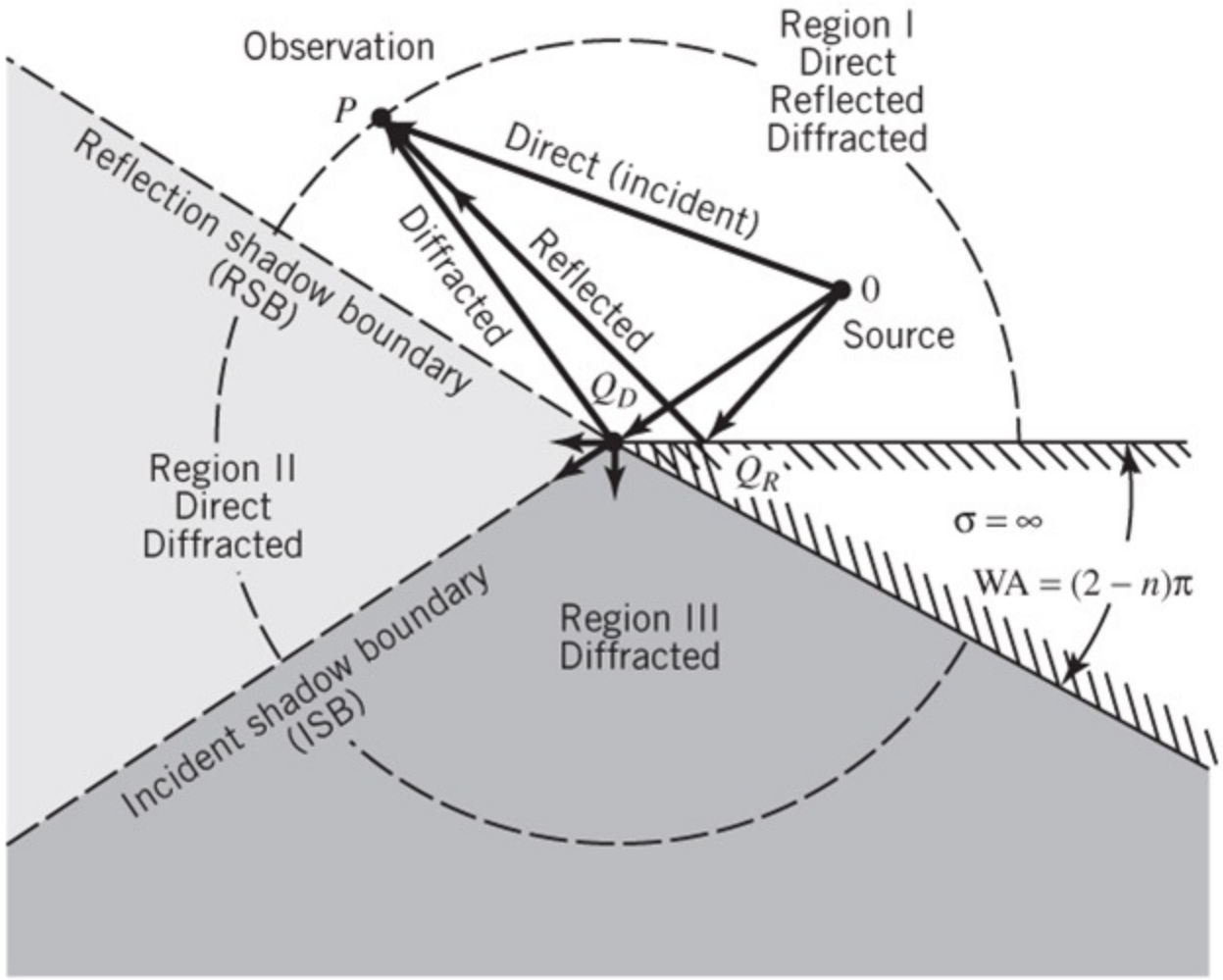

(a) Region separation

Fig. 13-13(a)

Regions of GO and Diffracted Fields

Region I $0 \le \phi \le \pi - \phi'$	Region II $\pi - \phi' \le \phi \le \pi + \phi'$	Region III $\pi + \phi' \le \phi \le 2\pi - \mathrm{WA}$
Direct GO	Direct GO	---------
Reflected GO	---------	---------
Diffracted A. Incident B. Reflected	*Diffracted* A. Incident B. Reflected	*Diffracted* A. Incident B. Reflected

Geometrical Optics Field

$$F_G(\beta\rho)=\begin{cases} e^{j\beta\rho\cos(\phi-\phi')} \pm e^{j\beta\rho\cos(\phi+\phi')} & 0\le\phi<\pi-\phi' \\ e^{j\beta\rho\cos(\phi-\phi')} \pm 0 & \pi-\phi'\le\phi<\pi+\phi' \\ 0 \pm 0 & \pi+\phi'\le\phi<\underbrace{2\pi-\mathrm{WA}}_{n\pi} \end{cases}$$

$U_{GO}^{inc/dir}$ U_{GO}^{ref} Region

(13-65)

Diffracted Field

$$F_D = F_D^i \pm F_D^r = V_B$$

$$V_B = V_B^i\left(\rho, \phi - \phi', n\right) \pm V_B^r\left(\rho, \phi + \phi', n\right)$$

$$F_D^i = V_B^i\left(\rho, \phi - \phi', n\right) = \frac{e^{-j\beta\rho}}{\sqrt{\rho}} D^i \qquad (13\text{-}66)$$

$$F_D^r = V_B^r\left(\rho, \phi + \phi', n\right) = \frac{e^{-j\beta\rho}}{\sqrt{\rho}} D^r$$

$$F_D = V_B = V_B^i \pm V_B^r$$

$$V_B^i = F_D^i = \frac{e^{-j\beta\rho}}{\sqrt{\rho}} \underbrace{\left\{ \frac{e^{-j\pi/4}\,\frac{1}{n}\sin\left(\frac{\pi}{n}\right)}{\sqrt{2\pi\beta}\left[\cos\left(\frac{\pi}{n}\right) - \cos\left(\frac{\phi-\phi'}{n}\right)\right]} \right\}}_{D^{inc}}$$

$$V_B^i = F_D^i = \frac{e^{-j\beta\rho}}{\sqrt{\rho}} D^{inc}$$

$$F_D = V_B = V_B^i \pm V_B^r$$

$$V_B^r = F_D^r = \frac{e^{-j\beta\rho}}{\sqrt{\rho}} \underbrace{\left\{ \frac{e^{-j\pi/4}}{\sqrt{2\pi\beta}} \frac{\frac{1}{n}\sin\left(\frac{\pi}{n}\right)}{\left[\cos\left(\frac{\pi}{n}\right) - \cos\left(\frac{\phi+\phi'}{n}\right)\right]} \right\}}_{D^{ref}}$$

$$V_B^r = F_{DIF}^{ref} = \frac{e^{-j\beta\rho}}{\sqrt{\rho}} D^{ref}$$

Away from Shadow Boundaries

$$D^i\left(\phi-\phi',n\right)=\frac{e^{-j\pi/4}}{\sqrt{2\pi\beta}}\frac{\frac{1}{n}\sin\left(\frac{\pi}{n}\right)}{\cos\left(\frac{\pi}{n}\right)-\cos\left(\frac{\phi-\phi'}{n}\right)}$$

$$D^r\left(\phi+\phi',n\right)=\frac{e^{-j\pi/4}}{\sqrt{2\pi\beta}}\frac{\frac{1}{n}\sin\left(\frac{\pi}{n}\right)}{\cos\left(\frac{\pi}{n}\right)-\cos\left(\frac{\phi+\phi'}{n}\right)}$$

Away from Shadow Boundaries

$$V_B^{h,s}\left(\rho,\phi\mp\phi',n\right)\simeq\frac{e^{-j\left(\beta\rho+\frac{\pi}{4}\right)}}{\sqrt{2\pi\beta\rho}}\frac{1}{n}\sin\left(\frac{\pi}{n}\right)$$

$$\cdot\left\{\frac{1}{\cos\left(\frac{\pi}{n}\right)-\cos\left(\frac{\phi-\phi'}{n}\right)}\pm\frac{1}{\cos\left(\frac{\pi}{n}\right)-\cos\left(\frac{\phi+\phi'}{n}\right)}\right\}$$

(13-67)

Away from Shadow Boundaries

$$V_B^{h,s}\left(\rho,\phi\mp\phi',n\right)\simeq\frac{e^{-j\left(\beta\rho+\frac{\pi}{4}\right)}}{\sqrt{2\pi\beta\rho}}\frac{1}{n}\sin\left(\frac{\pi}{n}\right)$$

$$\cdot\left\{\frac{1}{\cos\left(\frac{\pi}{n}\right)-\cos\left(\frac{\phi-\phi'}{n}\right)}\pm\frac{1}{\cos\left(\frac{\pi}{n}\right)-\cos\left(\frac{\phi+\phi'}{n}\right)}\right\}$$

$$V_B^{h,s}\left(\rho,\phi\mp\phi',n\right)\simeq\frac{e^{-j\beta\rho}}{\sqrt{\rho}}D^{h,s}\qquad(13\text{-}67)$$

Away from Shadow Boundaries

$$D^h \simeq \frac{e^{-j\pi/4}}{\sqrt{2\pi\beta}}\left[\frac{\frac{1}{n}\sin\left(\frac{\pi}{n}\right)}{\cos\left(\frac{\pi}{n}\right)-\cos\left(\frac{\phi-\phi'}{n}\right)}+\frac{\frac{1}{n}\sin\left(\frac{\pi}{n}\right)}{\cos\left(\frac{\pi}{n}\right)-\cos\left(\frac{\phi+\phi'}{n}\right)}\right]$$

$$D^s \simeq \frac{e^{-j\pi/4}}{\sqrt{2\pi\beta}}\left[\frac{\frac{1}{n}\sin\left(\frac{\pi}{n}\right)}{\cos\left(\frac{\pi}{n}\right)-\cos\left(\frac{\phi-\phi'}{n}\right)}-\frac{\frac{1}{n}\sin\left(\frac{\pi}{n}\right)}{\cos\left(\frac{\pi}{n}\right)-\cos\left(\frac{\phi+\phi'}{n}\right)}\right]$$

$$D^h = D^i + D^r$$

$$D^s = D^i - D^r$$

Away from Shadow Boundaries

$$V_B(\rho,\phi,\phi',n) = V_B^i(\rho,\phi-\phi',n) \pm V_B^r(\rho,\phi+\phi',n) = F(\beta\rho)\Big|_{SDP_{\pm\pi}}$$

$$V_B^i(\rho,\phi-\phi',n) = \frac{e^{-j\pi/4}}{\sqrt{2\pi\beta}} \frac{\frac{1}{n}\sin\left(\frac{\pi}{n}\right)}{\cos\left(\frac{\pi}{n}\right)-\cos\left(\frac{\phi-\phi'}{n}\right)} \frac{e^{-j\beta\rho}}{\sqrt{\rho}}$$

$$= \underbrace{[1]}_{1} \underbrace{\left[\frac{e^{-j\pi/4}}{\sqrt{2\pi\beta}} \frac{\frac{1}{n}\sin\left(\frac{\pi}{n}\right)}{\cos\left(\frac{\pi}{n}\right)-\cos\left(\frac{\phi-\phi'}{n}\right)}\right]}_{2} \underbrace{\left[\frac{1}{\sqrt{\rho}}\right]}_{3} \underbrace{\left[e^{-j\beta\rho}\right]}_{4}$$

$$V_B^i(\rho,\phi-\phi',n) = [1] \cdot \quad [D^i] \quad [A] \quad [e^{-j\beta\rho}]$$

At RSB ($\phi = \pi - \phi'$)

$$\phi - \phi' = \pi - \phi' - \phi' = \pi - 2\phi'$$

$$\phi + \phi' = \pi - \phi' + \phi' = \pi$$

At ISB ($\phi = \pi + \phi'$)

$$\phi - \phi' = \pi + \phi' - \phi' = \pi$$

$$\phi + \phi' = \pi + \phi' + \phi' = \pi + 2\phi'$$

$$V_B^r(\rho,\phi+\phi',n)=\frac{e^{-j\pi/4}}{\sqrt{2\pi\beta}}\frac{\frac{1}{n}\sin\left(\frac{\pi}{n}\right)}{\cos\left(\frac{\pi}{n}\right)-\cos\left(\frac{\phi+\phi'}{n}\right)}\frac{e^{-j\beta\rho}}{\sqrt{\rho}}$$

$$=\underbrace{[1]}_{1}\underbrace{\left[\frac{e^{-j\pi/4}}{\sqrt{2\pi\beta}}\frac{\frac{1}{n}\sin\left(\frac{\pi}{n}\right)}{\cos\left(\frac{\pi}{n}\right)-\cos\left(\frac{\phi+\phi'}{n}\right)}\right]}_{2}\underbrace{\left[\frac{1}{\sqrt{\rho}}\right]}_{3}\underbrace{\left[e^{-j\beta\rho}\right]}_{4}$$

$$V_B^r(\rho,\phi+\phi',n)=[1]\cdot\left[\quad D^r \quad\right]\ [A]\ \left[e^{-j\beta\rho}\right]$$

1 : $[1]$ = Amplitude of Incident field at Edge

2 : D^i, D^r = Incident, Reflection Diffraction Coefficient

3 : $A=\frac{1}{\sqrt{\rho}}$ = Amplitude Spreading Factor (for plane & cylindrical inc.)

4 : $e^{-j\beta\rho}$ = phase Factor

$$V_B = V_B^i \pm V_B^r$$

Incident Diffracted Field

$$V_B^i = \frac{e^{-j\beta\rho}}{\sqrt{\rho}} \underbrace{\left\{ \frac{e^{-j\pi/4}}{\sqrt{2\pi\beta}} \frac{\frac{1}{n}\sin\left(\frac{\pi}{n}\right)}{\left[\cos\left(\frac{\pi}{n}\right) - \cos\left(\frac{\phi-\phi'}{n}\right)\right]} \right\}}_{D^i}$$

$$V_B^i = \frac{e^{-j\beta\rho}}{\sqrt{\rho}} D^i$$

$$V_B = V_B^i \pm V_B^r$$

Reflected Diffracted Field

$$V_B^{ref} = \frac{e^{-j\beta\rho}}{\sqrt{\rho}} \underbrace{\left\{ \frac{e^{-j\pi/4}}{\sqrt{2\pi\beta}} \frac{\frac{1}{n}\sin\left(\frac{\pi}{n}\right)}{\left[\cos\left(\frac{\pi}{n}\right) - \cos\left(\frac{\phi+\phi'}{n}\right)\right]} \right\}}_{D^r}$$

$$V_B^r = \frac{e^{-j\beta\rho}}{\sqrt{\rho}} D^r$$

Shadow Boundaries and Transition Regions

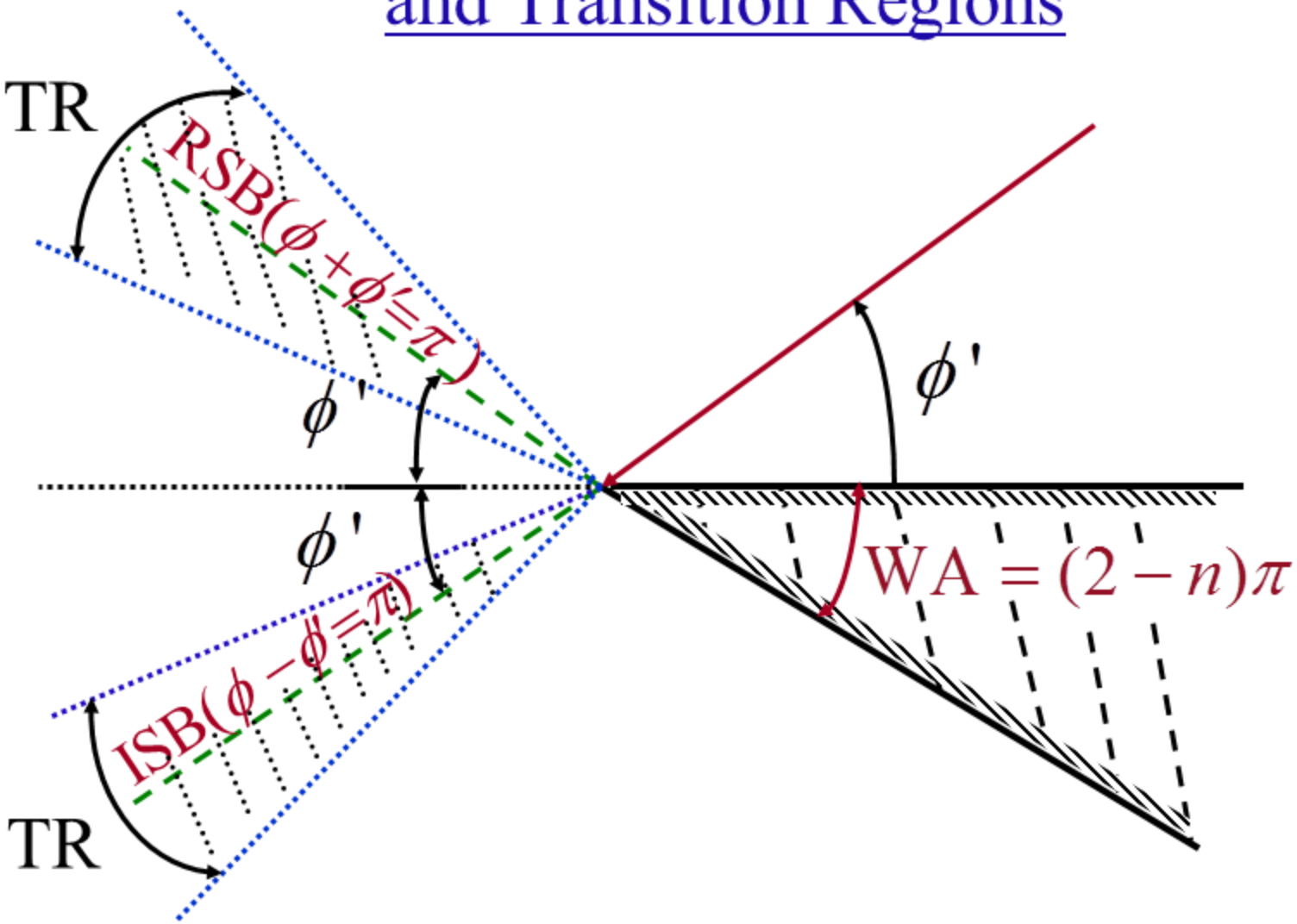

Away from Shadow Boundaries
Keller's Diffractions Coefficients

$$D^i\left(\phi-\phi',n\right)=\frac{e^{-j\pi/4}}{\sqrt{2\pi\beta}}\frac{\frac{1}{n}\sin\left(\frac{\pi}{n}\right)}{\cos\left(\frac{\pi}{n}\right)-\cos\left(\frac{\phi-\phi'}{n}\right)}$$

$$D^r\left(\phi+\phi',n\right)=\frac{e^{-j\pi/4}}{\sqrt{2\pi\beta}}\frac{\frac{1}{n}\sin\left(\frac{\pi}{n}\right)}{\cos\left(\frac{\pi}{n}\right)-\cos\left(\frac{\phi+\phi'}{n}\right)}$$

Polarization of Incident and Diffracted Fields

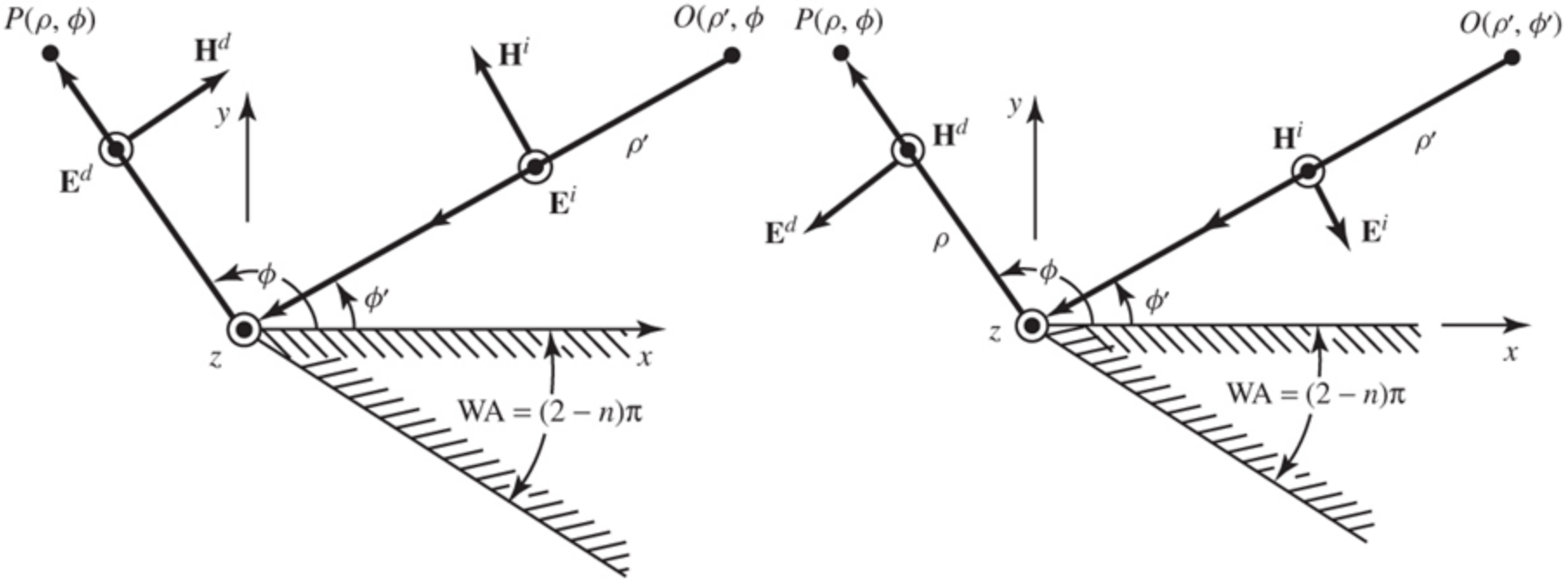

(a) Soft Polarization

(b) Hard Polarization

Fig. 13-22

Pauli-Clemmow Modified Method of Steepest Descent

Standard Method of Steepest Descent

$$V(\beta\rho)=\frac{1}{n}\sum_{m=0}^{\infty}\varepsilon_m J_{m/n}(\beta\rho)\,e^{j\frac{m}{n}\left(\frac{\pi}{2}\right)}\left\{\begin{array}{l}\cos\left[\frac{m}{n}(\phi-\phi')\right]\\ \pm\cos\left[\frac{m}{n}(\phi+\phi')\right]\end{array}\right\}$$

$$I_{SDP}(\beta\rho)=\int_{SDP}H(z)\,e^{\beta\rho h(z)}dz$$

$$I_{SDP}(\beta\rho)\overset{\beta\rho\to\text{large}}{\simeq}\sqrt{\frac{2\pi}{-\beta\rho h''(z_s)}}H(z_s)\,e^{\beta\rho h(z_s)}$$

Pauli-Clemmow Modified Method of Steepest Descent

Pauli-Clemmow

Method of Steepest Descent

$$I(\beta\rho)=\int_C H(z)e^{\beta\rho h(z)}dz \overset{\beta\rho\to\text{large}}{\simeq} \sqrt{\frac{2\pi}{-\beta\rho h''(z_s)}}H(z_s)e^{\beta\rho h(z_s)} \times \{F[\beta\rho g]\}$$

$$F(\beta\rho g)=2j\left|\sqrt{\beta\rho g}\right|e^{+j\beta\rho g}\int_{\left|\sqrt{\beta\rho g}\right|}^{\infty} e^{-j\tau^2}d\tau$$

$g \equiv j\left[h(z_s)-h(z_p)\right]$ = represents separation between saddle points and poles

z_s = represents the saddle points

z_p = represents the poles

Geometrical Optics Field

1. Incident

2. Reflected

$$\frac{1}{4\pi\, jn}\oint_{C_T} H_{1,2}\, e^{h_{1,2}(z)}\, dz$$

Incident Diffracted Field

$$F_1(\beta\rho)\Big|_{SDP_{\pm\pi}} = \frac{1}{4\pi jn}\left[\int_{SDP_{-\pi}} H_1(z)\,e^{\beta\rho h_1(z)}dz + \int_{SDP_{+\pi}} H_1(z)\,e^{\beta\rho h_1(z)}dz\right] \qquad (13\text{-}61)$$

Reflected Diffracted Field

$$F_2(\beta\rho)\Big|_{SDP_{\pm\pi}} = \frac{1}{4\pi jn}\left[\int_{SDP_{-\pi}} H_2(z)\,e^{\beta\rho h_2(z)}dz + \int_{SDP_{+\pi}} H_2(z)\,e^{\beta\rho h_2(z)}dz\right] \qquad (13\text{-}62b)$$

For Evaluation of $H_1(z)_{\pm\pi}$

$$\frac{1}{4\pi jn}\int_{SDP_{+\pi}} H_1(z)\,e^{\beta\rho h_1(z)}dz$$

$$=\frac{1}{4\pi jn}\int_{SDP_{+\pi}} \cot\left[\frac{(\phi-\phi')+z}{2n}\right]e^{j\beta\rho\cos z}dz$$

$$z_s\big|_{s=1}=z_1=+\pi$$

$$z_p^+=-(\phi-\phi')+2\pi nN^+$$

$$g^+(\xi^-)=g^+(\phi-\phi')$$

$$g^+(\xi^-)=j\left\{j\cos(\pi)-j\cos\left[(\phi-\phi')-2\pi nN^+\right]\right\}$$

$$g^+(\xi^-)=1+\cos\left[(\phi-\phi')-2\pi nN^+\right]$$

$$\frac{1}{4\pi jn}\int_{SDP_{+\pi}} \cot\left[\frac{(\phi-\phi')+z}{2n}\right] e^{j\beta\rho\cos z}\,dz$$

$$= \frac{e^{-j\pi/4}}{2n\sqrt{2\pi\beta}}\frac{e^{-j\beta\rho}}{\sqrt{\rho}} \cot\left[\frac{\pi+(\phi-\phi')}{2n}\right] F\left[\beta\rho g^{+}\left(\xi^{-}\right)\right]$$

$$F\left[\beta\rho g^{+}\left(\xi^{-}\right)\right] = F\left[\beta\rho g^{+}\left(\phi-\phi'\right)\right]$$

$$= 2j\left|\sqrt{\beta\rho g^{+}\left(\phi-\phi'\right)}\right| \int_{\left|\sqrt{\beta\rho g^{+}(\phi-\phi')}\right|}^{\infty} e^{-j\tau^{2}}\,d\tau$$

$$g^{+}\left(\phi-\phi'\right) = 1+\cos\left[\left(\phi-\phi'\right)-2\pi nN^{+}\right]$$

where $2\pi nN^{+}-\left(\phi-\phi'\right)=+\pi$

$$\frac{1}{4\pi jn}\int_{SDP_{-\pi}} H_1(z)\,e^{\beta\rho h_1(z)}dz$$

$$=\frac{1}{4\pi jn}\int_{SDP_{-\pi}} \cot\left[\frac{(\phi-\phi')+z}{2n}\right]e^{j\beta\rho\cos z}dz$$

$$z_s\big|_{s=1}=z_1=-\pi$$

$$z_p^-=-(\phi-\phi')+2\pi nN^-$$

$$g^-(\xi^-)=g^-(\phi-\phi')$$

$$=j\left\{j\cos(-\pi)-j\cos\left[(\phi-\phi')-2\pi nN^-\right]\right\}$$

$$g^-(\xi^-)=1+\cos\left[(\phi-\phi')-2\pi nN^-\right]$$

$$\frac{1}{4\pi jn}\int_{SDP_{-\pi}} \cot\left[\frac{(\phi-\phi')+z}{2n}\right] e^{j\beta\rho\cos z}\,dz$$

$$= \frac{e^{-j\pi/4}}{2n\sqrt{2\pi\beta}}\frac{e^{-j\beta\rho}}{\sqrt{\rho}}\cot\left[\frac{\pi-(\phi-\phi')}{2n}\right]F\left[\beta\rho g^{-}\left(\xi^{-}\right)\right]$$

$$F\left[\beta\rho g^{-}\left(\xi^{-}\right)\right] = F\left[\beta\rho g^{-}\left(\phi-\phi'\right)\right]$$

$$= 2j\left|\sqrt{\beta\rho g^{-}\left(\phi-\phi'\right)}\right| \int_{\left|\sqrt{\beta\rho g^{-}(\phi-\phi')}\right|}^{\infty} e^{-j\tau^{2}}\,d\tau$$

$$g^{-}\left(\phi-\phi'\right) = 1+\cos\left[\left(\phi-\phi'\right)-2\pi nN^{-}\right]$$

where $2\pi nN^{-}-\left(\phi-\phi'\right)=-\pi$

For Evaluation of $H_2(z)_{\pm\pi}$

$$\frac{1}{4\pi jn}\int_{SDP_{+\pi}} H_2(z)\,e^{\beta\rho h_1(z)}dz$$

$$=\frac{1}{4\pi jn}\int_{SDP_{+\pi}} \cot\left[\frac{(\phi+\phi')+z}{2n}\right]e^{j\beta\rho\cos z}dz$$

$$z_s\big|_{s=1}=z_1=+\pi$$

$$z_p^+=-(\phi+\phi')+2\pi nN^+$$

$$g^+(\xi^+)=g^+(\phi+\phi')$$

$$=j\left\{j\cos(\pi)-j\cos\left[(\phi+\phi')-2\pi nN^+\right]\right\}$$

$$g^+(\xi^+)=1+\cos\left[(\phi+\phi')-2\pi nN^+\right]$$

$$\frac{1}{4\pi jn}\int_{SDP_{+\pi}} \cot\left[\frac{(\phi+\phi')+z}{2n}\right] e^{j\beta\rho\cos z}\,dz$$

$$= \frac{e^{-j\pi/4}}{2n\sqrt{2\pi\beta}}\frac{e^{-j\beta\rho}}{\sqrt{\rho}}\cot\left[\frac{\pi+(\phi+\phi')}{2n}\right] F\left[\beta\rho g^{+}\left(\xi^{+}\right)\right]$$

$$F\left[\beta\rho g^{+}\left(\xi^{+}\right)\right] = F\left[\beta\rho g^{+}\left(\phi+\phi'\right)\right]$$

$$= 2j\left|\sqrt{\beta\rho g^{+}\left(\phi+\phi'\right)}\right| \int_{\left|\sqrt{\beta\rho g^{+}(\phi+\phi')}\right|}^{\infty} e^{-j\tau^{2}}\,d\tau$$

$$g^{+}\left(\phi+\phi'\right) = 1+\cos\left[\left(\phi+\phi'\right)-2\pi nN^{+}\right]$$

where $2\pi nN^{+}-\left(\phi+\phi'\right)=+\pi$

$$\frac{1}{4\pi jn}\int_{SDP_{-\pi}} H_2(z)\,e^{\beta\rho h_1(z)}dz$$

$$=\frac{1}{4\pi jn}\int_{SDP_{-\pi}} \cot\left[\frac{(\phi+\phi')+z}{2n}\right]e^{j\beta\rho\cos z}dz$$

$$z_s\big|_{s=1}=z_1=-\pi$$

$$z_p^-=-(\phi+\phi')+2\pi nN^-$$

$$g^-(\xi^+)=g^-(\phi+\phi')$$

$$=j\left\{j\cos(-\pi)-j\cos\left[(\phi+\phi')-2\pi nN^-\right]\right\}$$

$$g^-(\xi^+)=1+\cos\left[(\phi+\phi')-2\pi nN^-\right]$$

$$\frac{1}{4\pi jn}\int_{SDP_{-\pi}} \cot\left[\frac{(\phi+\phi')+z}{2n}\right] e^{j\beta\rho\cos z}\,dz$$

$$= \frac{e^{-j\pi/4}}{2n\sqrt{2\pi\beta}}\frac{e^{-j\beta\rho}}{\sqrt{\rho}}\cot\left[\frac{\pi-(\phi+\phi')}{2n}\right]F\left[\beta\rho g^{-}\left(\xi^{+}\right)\right]$$

$$F\left[\beta\rho g^{-}\left(\xi^{+}\right)\right] = F\left[\beta\rho g^{-}\left(\phi+\phi'\right)\right]$$

$$= 2j\left|\sqrt{\beta\rho g^{-}\left(\phi+\phi'\right)}\right| \int_{\left|\sqrt{\beta\rho g^{-}(\phi+\phi')}\right|}^{\infty} e^{-j\tau^{2}}\,d\tau$$

$$g^{-}\left(\phi-\phi'\right) = 1+\cos\left[\left(\phi+\phi'\right)-2\pi nN^{-}\right]$$

where $2\pi nN^{-}-\left(\phi+\phi'\right)=-\pi$

Values of N^- as a Function of ξ and n

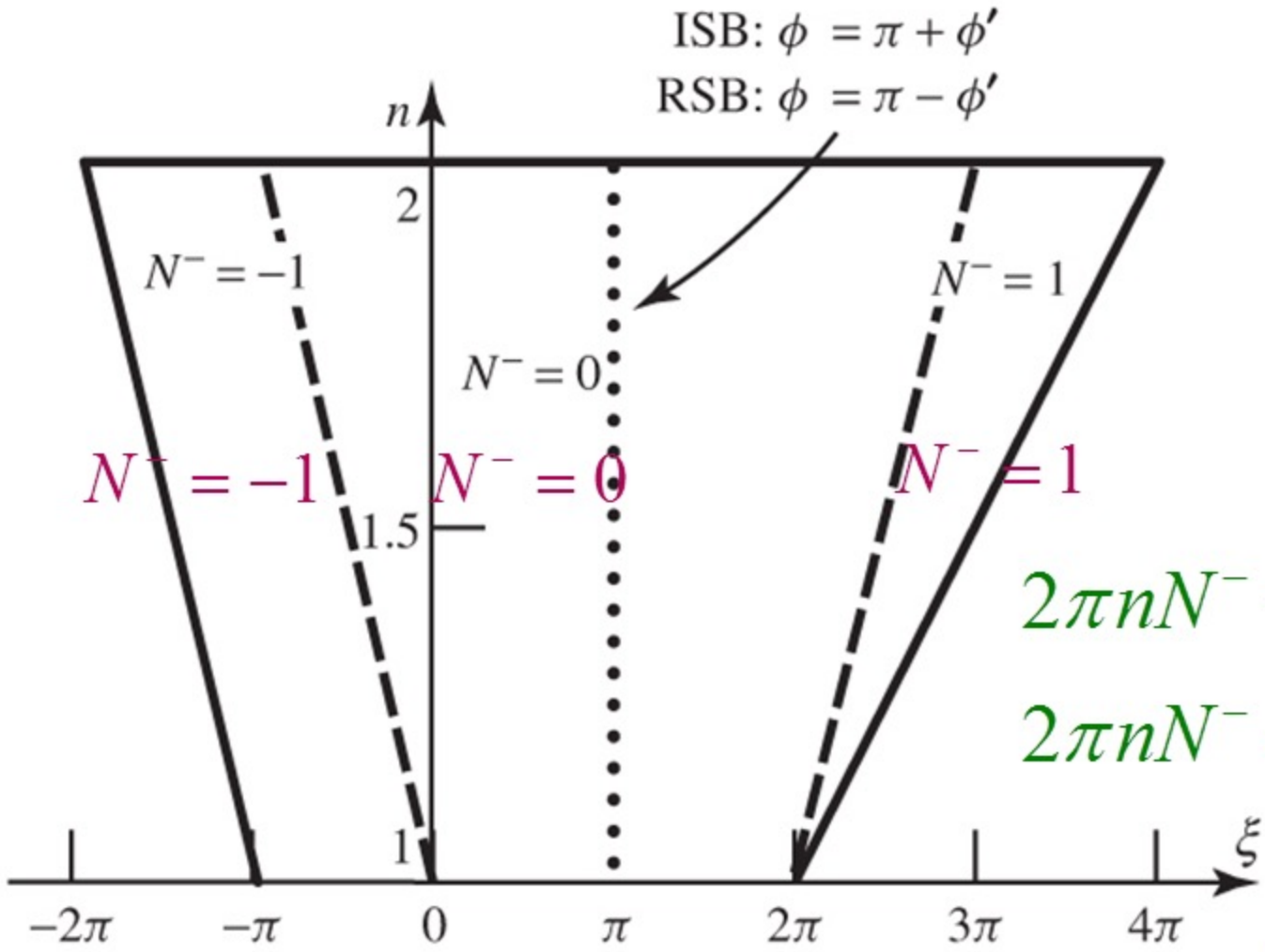

$$2\pi n N^- - \xi = -\pi$$

$$2\pi n N^- = \xi - \pi \tag{13-19}$$

(a) N^-

Values of N^+ as a Function of ξ and n

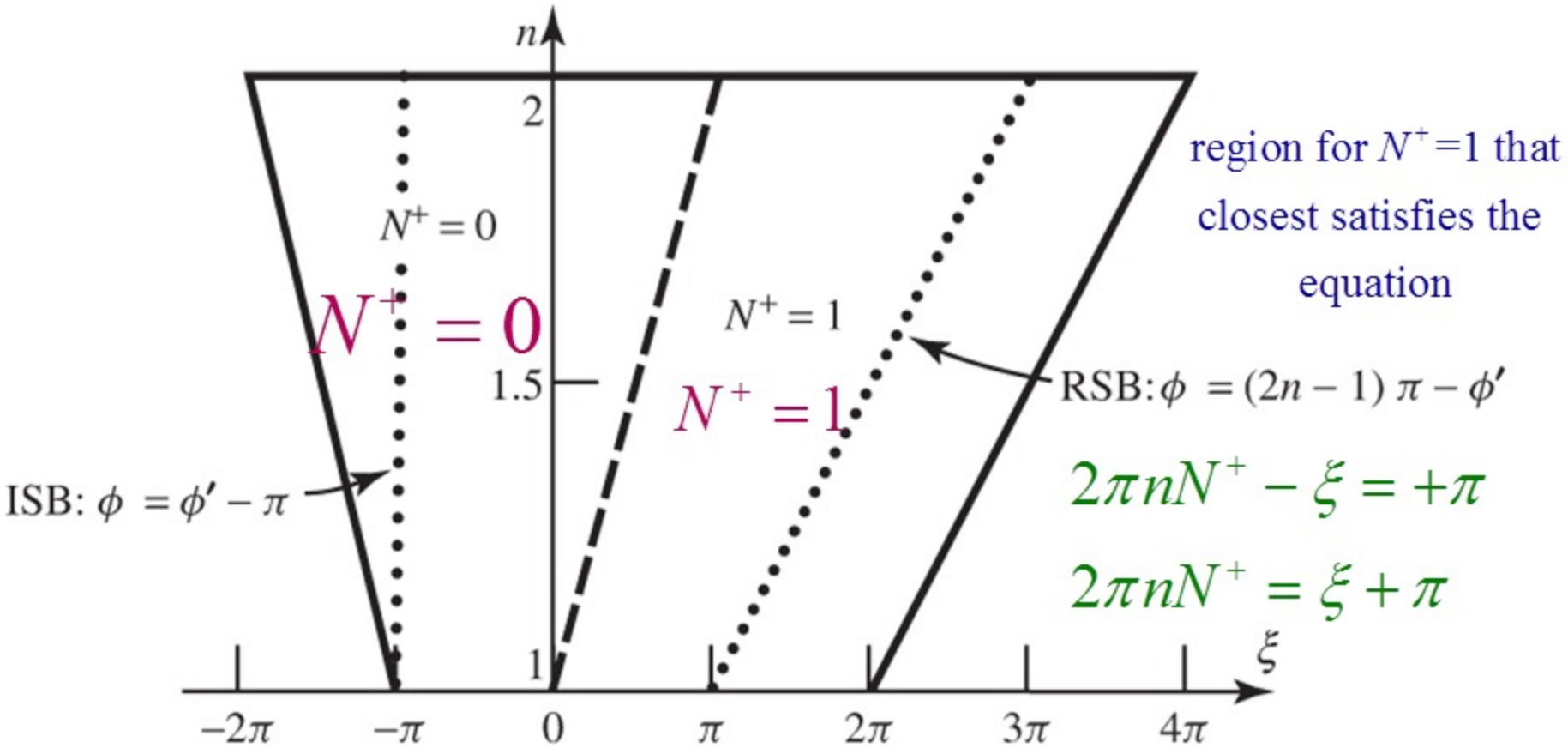

region for $N^+=1$ that closest satisfies the equation

$$2\pi n N^+ - \xi = +\pi$$

$$2\pi n N^+ = \xi + \pi$$

(b) N^+

(13-19)

If the poles

$$z_p = -(\phi \pm \phi') + 2n\pi N$$

are near the saddle points

$$z_s = \pm\pi$$

then the Pauli-Clemmow modified method of steepest descent must be used. This leads to UTD.

Values of $N^{\pm}$

$$2\pi nN^{-} - (\phi - \phi') = -\pi$$

$$2\pi nN^{-} - (\phi + \phi') = -\pi$$

$$2\pi nN^{+} - (\phi - \phi') = +\pi$$

$$2\pi nN^{+} - (\phi + \phi') = +\pi$$

$$2\pi n N^- = \xi - \pi$$

$\underline{n=1} \quad \Rightarrow \quad 2\pi N^- = \xi - \pi$

a. $\xi = \pi \quad 2\pi N^- = 0 \Rightarrow N^- = 0$

b. $\xi = \pi/2 \quad 2\pi N^- = \dfrac{\pi}{2} - \pi = -\dfrac{\pi}{2}$

1. $N^- = 0 \quad 0 = -\dfrac{\pi}{2}$

2. $N^- = 1 \quad 2\pi = -\dfrac{\pi}{2}$

3. $N^- = -1 \quad -2\pi = -\dfrac{\pi}{2}$

$\Rightarrow$ Closest: $N^- = 0$

c. $\xi = 0 \qquad 2\pi N^- = -\pi$

$$\left.\begin{aligned} &1.\ N^- = 0 \quad 0 = -\pi \\ &2.\ N^- = 1 \quad 2\pi = -\pi \\ &3.\ N^- = -1 \quad -2\pi = -\pi \end{aligned}\right\} \Rightarrow \text{Closest: } \begin{aligned} N^- &= 0 \\ N^- &= -1 \end{aligned}$$

d. $\xi = 2\pi \qquad 2\pi N^- = 2\pi - \pi = \pi$

$$\left.\begin{aligned} &1.\ N^- = 0 \quad 0 = \pi \\ &2.\ N^- = 1 \quad 2\pi = \pi \\ &3.\ N^- = -1 \quad -2\pi = \pi \end{aligned}\right\} \Rightarrow \text{Closest: } \begin{aligned} N^- &= 0 \\ N^- &= 1 \end{aligned}$$

$$2\pi nN^- - \xi = -\pi \Leftrightarrow 2\pi nN^- = \xi - \pi$$

$$n = \frac{1}{2\pi N^-}\left[\xi - \pi\right]$$

$N^- = 1:$ $\quad n = \dfrac{1}{2\pi}\left[\xi - \pi\right]$

$N^- = 0:$ $\quad \xi = \pi\left(\text{any value of } n\right)$

$N^- = -1:$ $\quad n = -\dfrac{1}{2\pi}\left[\xi - \pi\right] = \dfrac{1}{2\pi}\left[\pi - \xi\right]$

$$2\pi nN^+ - \xi = +\pi \Leftrightarrow 2\pi nN^+ = \xi + \pi$$

$$n = \frac{1}{2\pi N^+}\left[\xi + \pi\right]$$

$N^+ = 1$: $n = \dfrac{1}{2\pi}\left[\xi + \pi\right]$

$N^+ = 0$: $\xi = -\pi$ (any value of n)

Width of Transition Region

Shadow Boundaries and Transition Regions

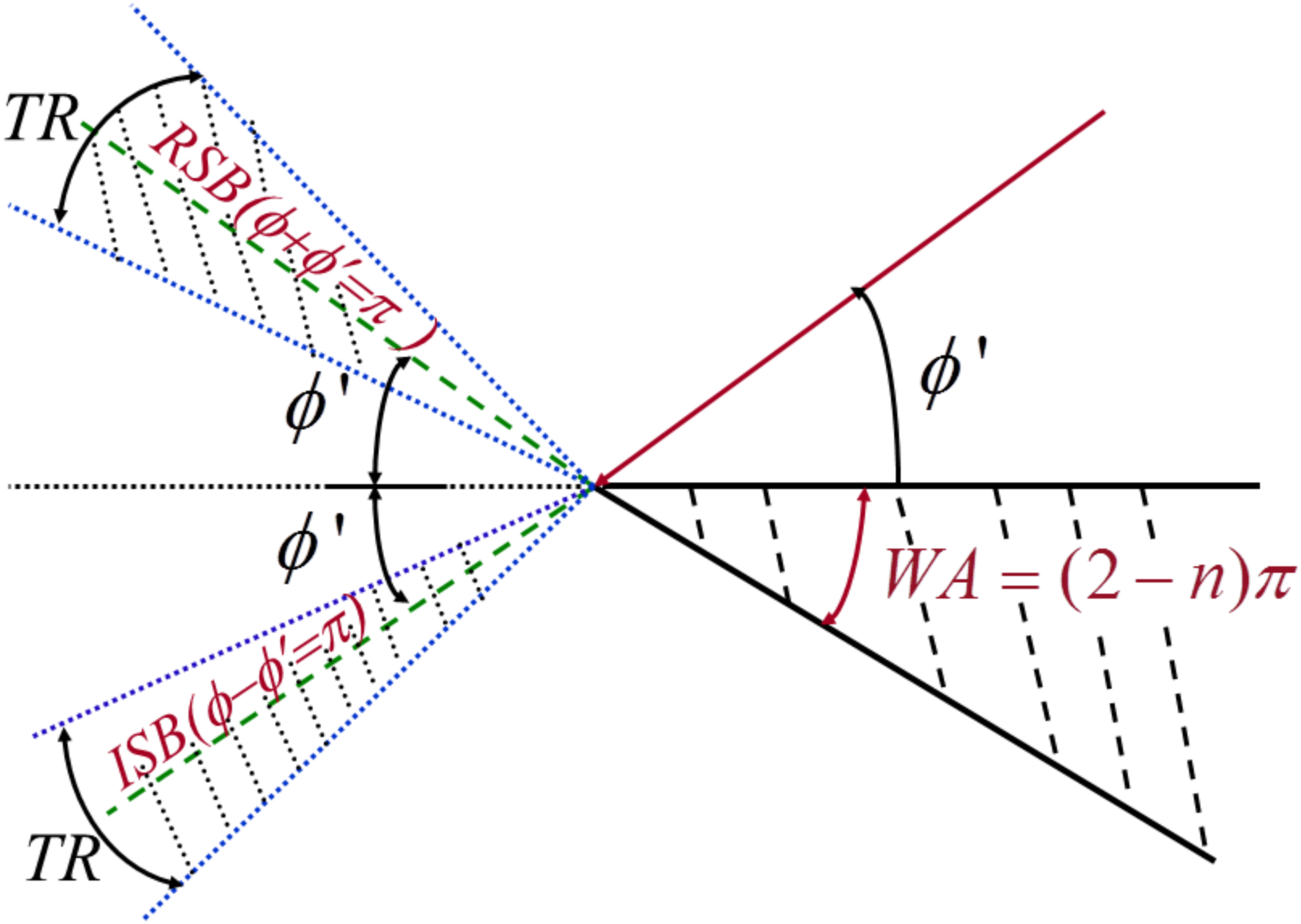

$$g^{+} = 1 + \cos(\xi - 2\pi n N^{+})$$

$$2\pi n N^{+} - \xi = +\pi \quad (\text{for } g^{+})$$

$$g^{-} = 1 + \cos(\xi - 2\pi n N^{-})$$

$$2\pi n N^{-} - \xi = -\pi \quad (\text{for } g^{-})$$

g^+ and g^- are representative of the angular separation between the observation point and the *ISB* or *RSB*.

In fact, when the observations are made along the *ISB* or *RSB*, the $g^{\pm}$ functions are equal to zero.

In order for the Keller diffraction functions and coefficients to be valid $\beta\rho g^{\pm} >> 1$. This can be achieved by one of the following conditions:

1. $\beta\rho$ and $g^{\pm}$ are large. These are satisfied if the distance ρ to the observation point is large and the observation angle ϕ is far away from either of the two shadow boundaries.

2. $\beta\rho$ large and $g^{\pm}$ small. This is satisfied if the distance ρ to the observation point is large and observation angle ϕ is near either one or both of the shadow boundaries.

3. $\beta\rho$ small and $g^{\pm}$ large. This is satisfied if the distance ρ to the observation point is small and observation angle ϕ is far away from either of the two shadow boundaries.

Plane Wave Incident Upon Half Plane

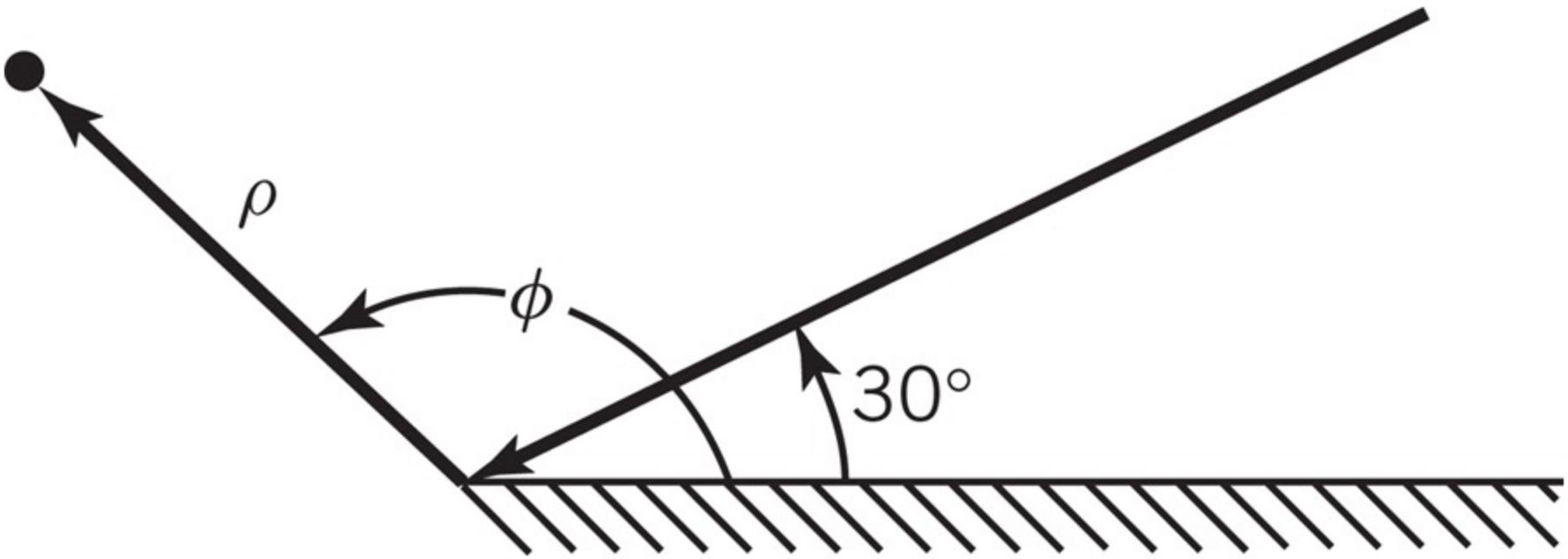

Fig. 13-20

Example: Plane Wave Diffraction

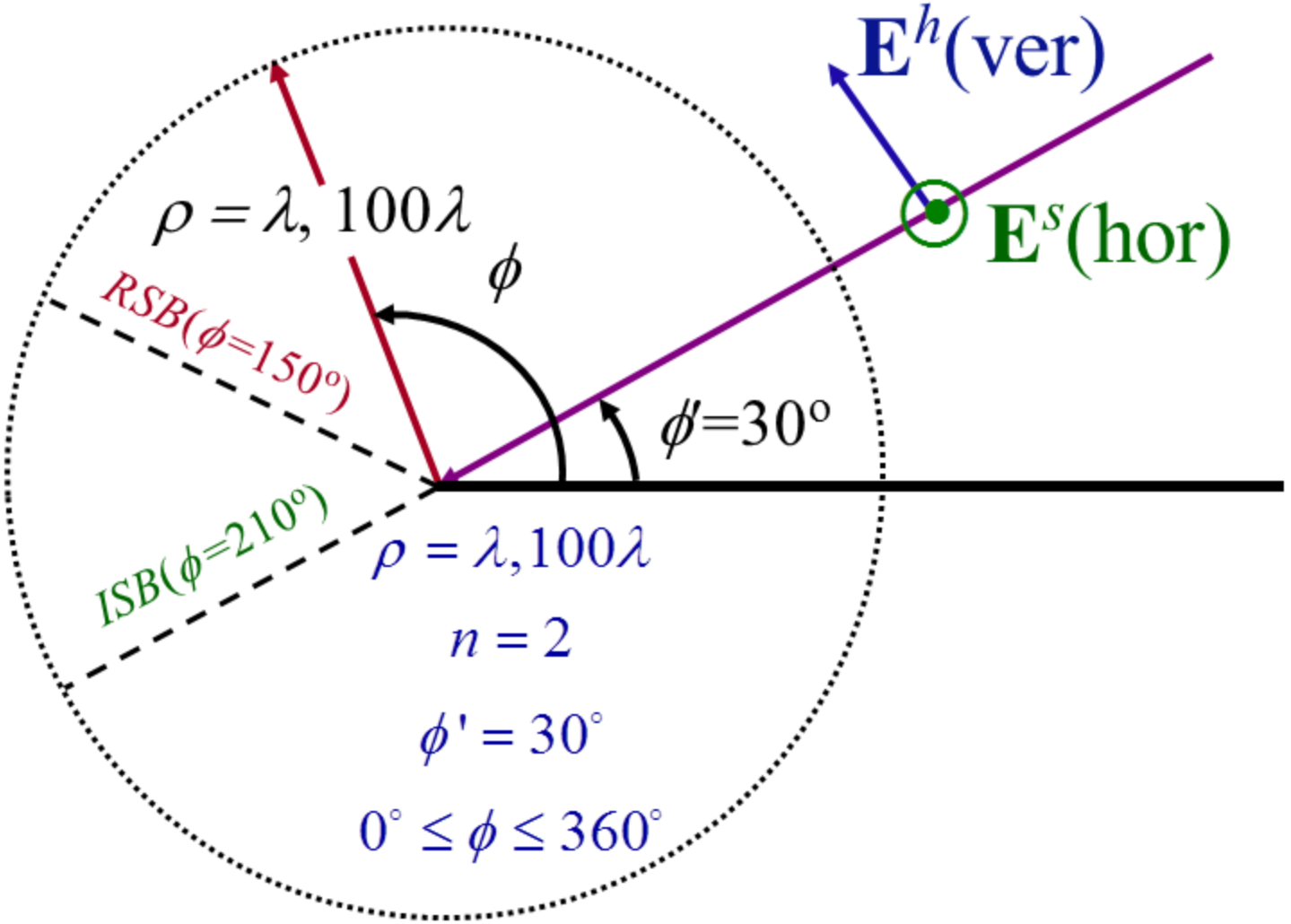

Incident Diffracted Field

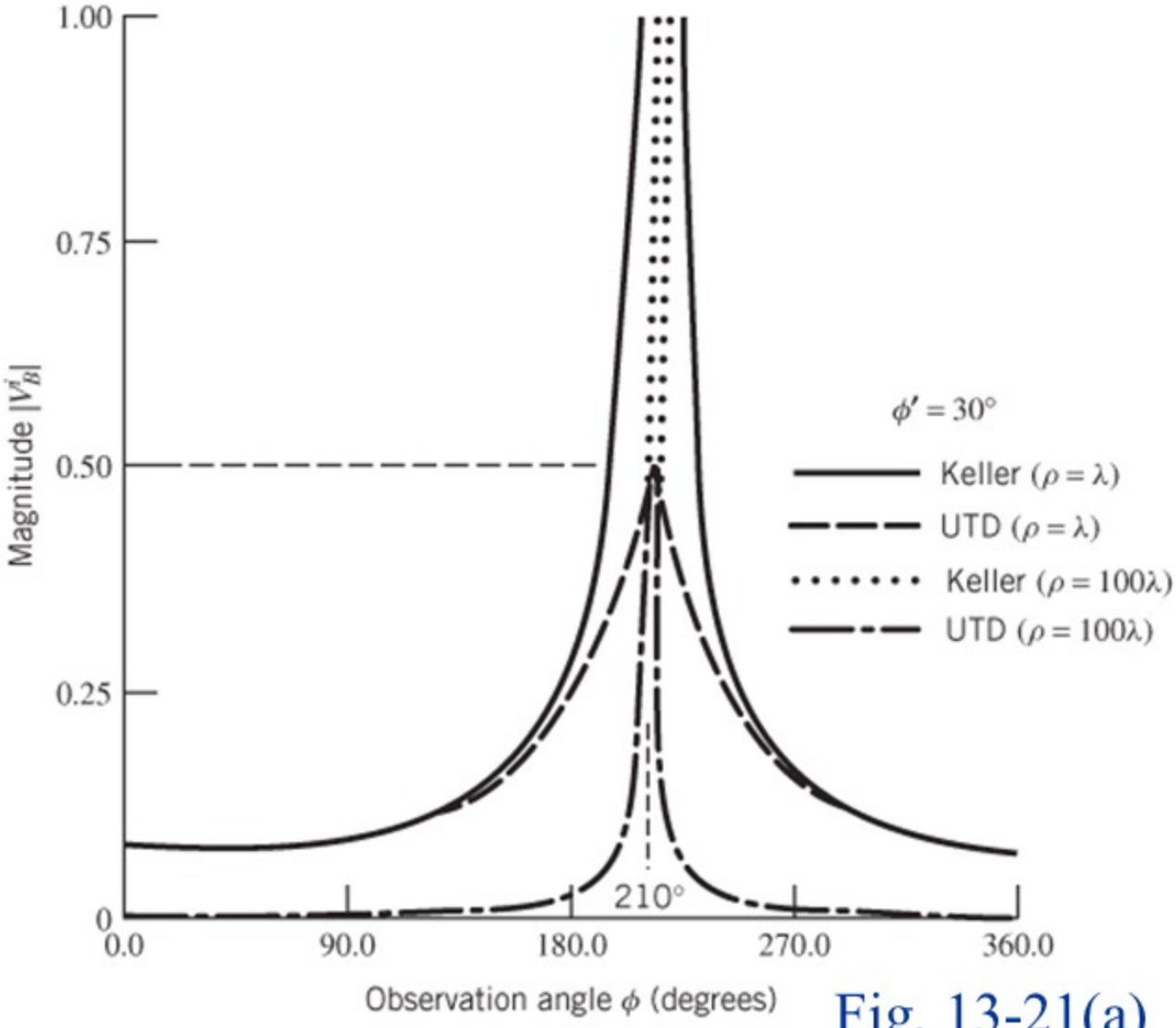

Fig. 13-21(a)

Reflected Diffracted Field

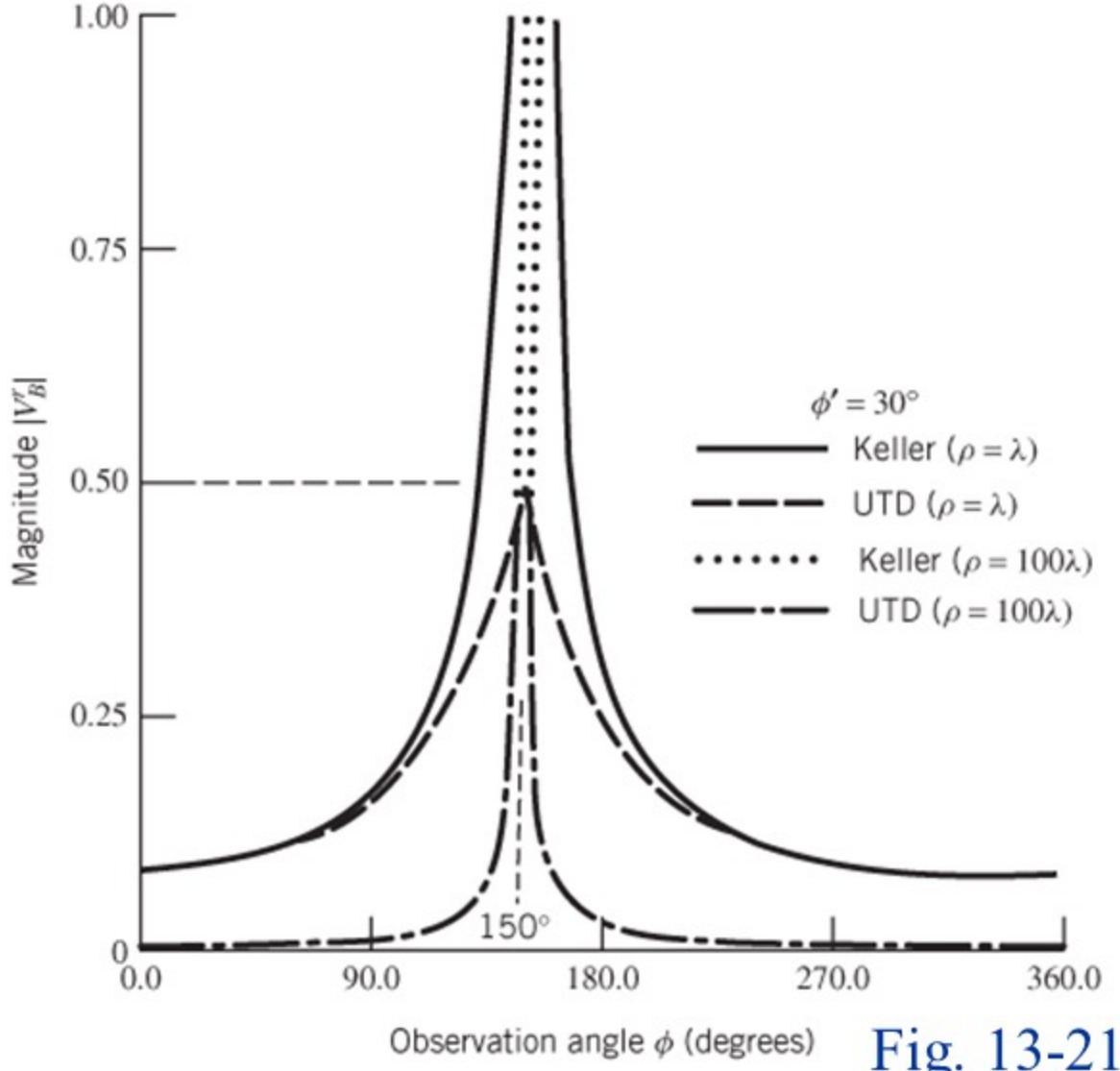

Fig. 13-21(b)

Shadow Boundaries and Transition Regions

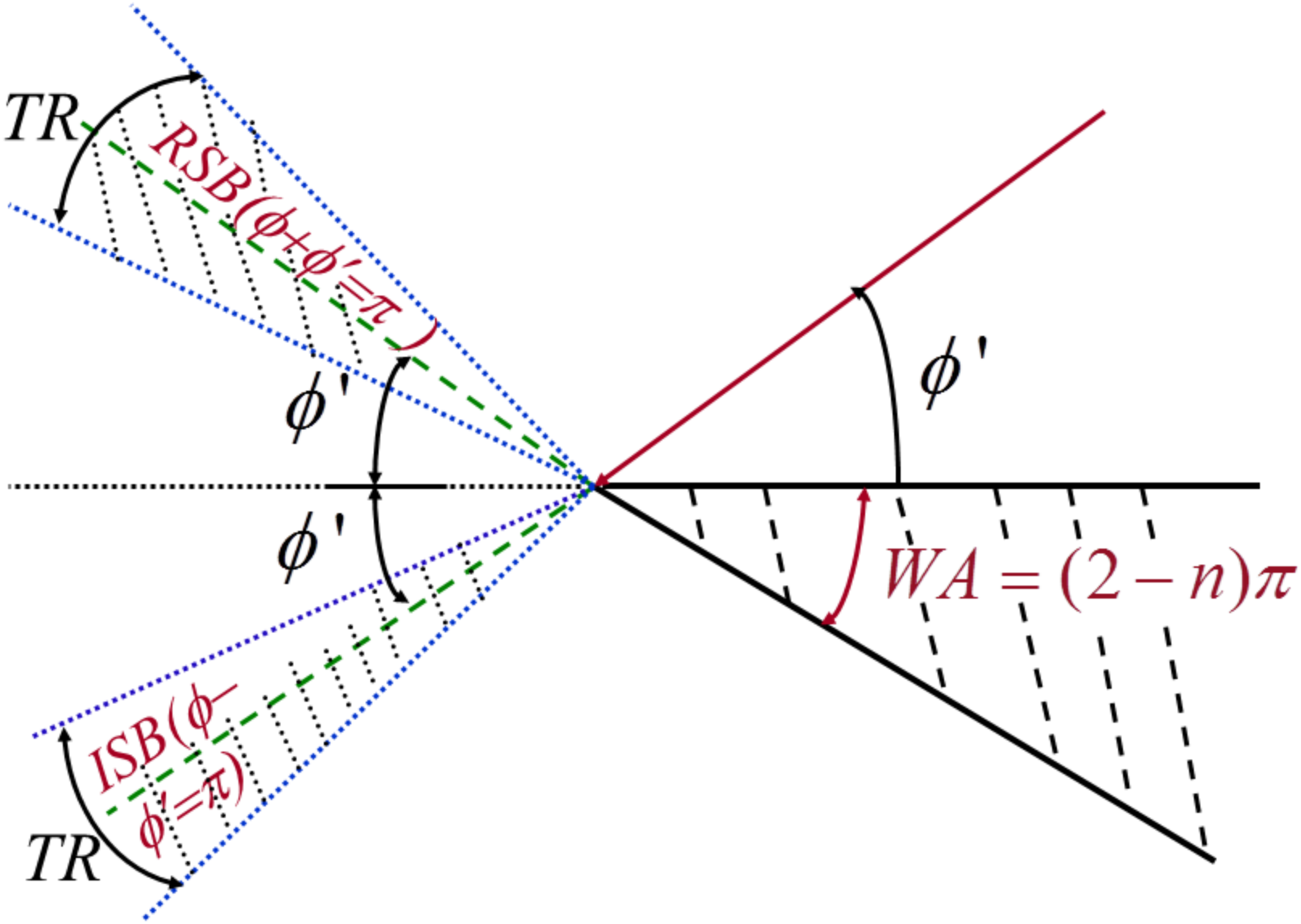

Uniform Theory of Diffraction (UTD)

1. Diffraction Functions
2. Diffraction Coefficients

$$V_B^{i,r}(\rho,\xi,n) = I_{+\pi}(\rho,\xi,n) + I_{-\pi}(\rho,\xi,n)$$

$$V_B^{i,r}(\rho,\xi,n) = -\frac{e^{-j\pi/4}}{2n\sqrt{2\pi\beta}}\left\{\left[C^+(\xi)F^+(\xi)\right] + \left[C^-(\xi)F^-(\xi)\right]\right\}\frac{e^{-j\beta\rho}}{\sqrt{\rho}}$$

For $V_B^i \Rightarrow \xi = \xi^- = \phi - \phi'$

For $V_B^r \Rightarrow \xi = \xi^+ = \phi + \phi'$

$$I_{+\pi}(\rho,\phi-\phi',n)=\frac{e^{-j\beta\rho}}{\sqrt{\rho}}\left\{-\frac{e^{-j\pi/4}}{2n\sqrt{2\pi\beta}}\left[C^{+}(\phi-\phi')F^{+}(\phi-\phi')\right]\right\}$$

$$I_{-\pi}(\rho,\phi-\phi',n)=\frac{e^{-j\beta\rho}}{\sqrt{\rho}}\left\{-\frac{e^{-j\pi/4}}{2n\sqrt{2\pi\beta}}\left[C^{-}(\phi-\phi')F^{-}(\phi-\phi')\right]\right\}$$

$$I_{+\pi}(\rho,\phi+\phi',n)=\frac{e^{-j\beta\rho}}{\sqrt{\rho}}\left\{-\frac{e^{-j\pi/4}}{2n\sqrt{2\pi\beta}}\left[C^{+}(\phi+\phi')F^{+}(\phi+\phi')\right]\right\}$$

$$I_{-\pi}(\rho,\phi+\phi',n)=\frac{e^{-j\beta\rho}}{\sqrt{\rho}}\left\{-\frac{e^{-j\pi/4}}{2n\sqrt{2\pi\beta}}\left[C^{-}(\phi+\phi')F^{-}(\phi+\phi')\right]\right\}$$

$$C^{+}(\xi) = \cot\left(\frac{\pi + \xi}{2n}\right); \qquad C^{-}(\xi) = \cot\left(\frac{\pi - \xi}{2n}\right)$$

(13-69c) (13-69d)

$$F^{+}(\xi) = 2j\sqrt{\beta\rho g^{+}(\xi)} \int_{\sqrt{\beta\rho g^{+}(\xi)}}^{\infty} e^{-j\tau^2} d\tau \qquad (13\text{-}69e)$$

$$F^{-}(\xi) = 2j\sqrt{\beta\rho g^{-}(\xi)} \int_{\sqrt{\beta\rho g^{-}(\xi)}}^{\infty} e^{-j\tau^2} d\tau \qquad (13\text{-}69f)$$

$$\xi = \xi^{-} = \phi - \phi'; \qquad \xi = \xi^{+} = \phi + \phi'$$

(13-71c) (13-71d)

$$V_B^{h,s}(\rho,\xi,n) = -\frac{e^{-j\pi/4}}{2n\sqrt{2\pi\beta}}\frac{e^{-j\beta\rho}}{\sqrt{\rho}}$$

$$\cdot\left\langle\left\{\left[C^+(\xi^-)F^+(\xi^-)\right]+\left[C^-(\xi^-)F^-(\xi^-)\right]\right\}\right.$$

$$\left.\pm\left\{\left[C^+(\xi^+)F^+(\xi^+)\right]+\left[C^-(\xi^+)F^-(\xi^+)\right]\right\}\right\rangle$$

$$\xi^- = \phi - \phi'$$

$$\xi^+ = \phi + \phi'$$

Summary $SDP_{+\pi}$ + $SDP_{-\pi}$: UTD

$$V_B^{h,s}(\rho,\xi,n) = -\frac{e^{-j\pi/4}}{2n\sqrt{2\pi\beta}}\frac{e^{-j\beta\rho}}{\sqrt{\rho}}$$

$$\cdot\left\langle \left\{\left[\cot\left(\frac{\pi+(\phi-\phi')}{2n}\right)F^{+}(\phi-\phi')\right]\right.\right.$$

$$\left.\left.+\left[\cot\left(\frac{\pi-(\phi-\phi')}{2n}\right)F^{-}(\phi-\phi')\right]\right\}\right.$$

$$\left.\pm\left\{\left[\cot\left(\frac{\pi+(\phi+\phi')}{2n}\right)F^{+}(\phi+\phi')\right]\right.\right.$$

$$\left.\left.+\left[\cot\left(\frac{\pi-(\phi+\phi')}{2n}\right)F^{-}(\phi+\phi')\right]\right\}\right\rangle$$

Summary $SDP_{+\pi}$ + $SDP_{-\pi}$: GTD

$$F(\beta\rho)\Big|_{SDP_{\pm\pi}} = V_B^{h,s}(\rho,\xi,n) = -\frac{e^{-j\pi/4}}{2n\sqrt{2\pi\beta}}\frac{e^{-j\beta\rho}}{\sqrt{\rho}}$$

$$\cdot\left\{\left[\cot\left[\frac{\pi+(\phi-\phi')}{2n}\right]_{\substack{F_1(\beta\rho)\\ SDP:+\pi}} + \cot\left[\frac{\pi-(\phi-\phi')}{2n}\right]_{\substack{F_1(\beta\rho)\\ SDP:-\pi}}\right]\right.$$

$$\left.\pm\left[\cot\left[\frac{\pi+(\phi+\phi')}{2n}\right]_{\substack{F_2(\beta\rho)\\ SDP:+\pi}} + \cot\left[\frac{\pi-(\phi+\phi')}{2n}\right]_{\substack{F_2(\beta\rho)\\ SDP:-\pi}}\right]\right\}$$

Incident and Reflected Diffracted Fields

$$V_B^i(\rho,\xi^-,n)=\frac{e^{-j\beta\rho}}{\sqrt{\rho}}\underbrace{\left\{-\frac{e^{-j\pi/4}}{2n\sqrt{2\pi\beta}}\left\{\left[\cot\left(\frac{\pi+(\phi-\phi')}{2n}\right)F^+(\phi-\phi')\right]+\left[\cot\left(\frac{\pi-(\phi-\phi')}{2n}\right)F^-(\phi-\phi')\right]\right\}\right\}}_{D^i}$$

$$V_B^r(\rho,\xi^+,n)=\frac{e^{-j\beta\rho}}{\sqrt{\rho}}\underbrace{\left\{-\frac{e^{-j\pi/4}}{2n\sqrt{2\pi\beta}}\left\{\left[\cot\left(\frac{\pi+(\phi+\phi')}{2n}\right)F^+(\phi+\phi')\right]+\left[\cot\left(\frac{\pi-(\phi+\phi')}{2n}\right)F^-(\phi+\phi')\right]\right\}\right\}}_{D^r}$$

Polarization of Incident and Diffracted Fields

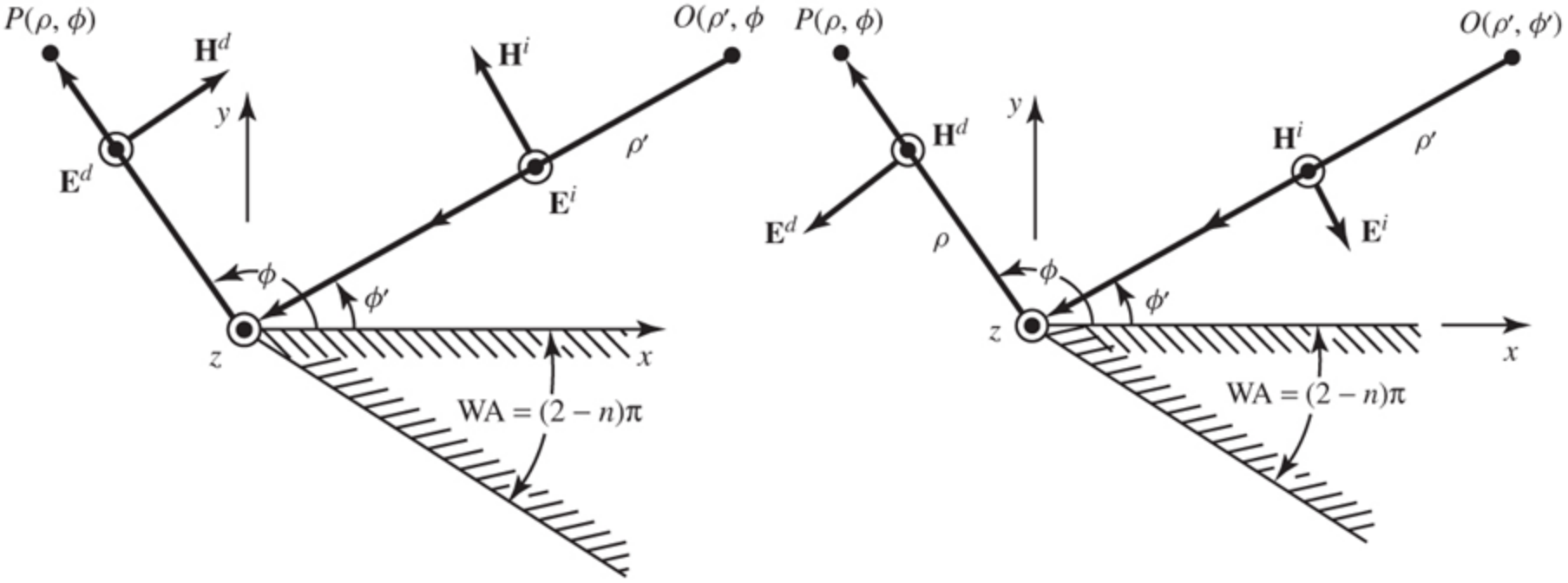

(a) Soft Polarization

(b) Hard Polarization

Fig. 13-22

$$D^i(\rho,\phi-\phi',n)=-\frac{e^{-j\pi/4}}{2n\sqrt{2\pi\beta}}$$

$$\cdot\left[C^+(\phi-\phi')F^+(\phi-\phi')+C^-(\phi-\phi')F^-(\phi-\phi')\right]$$

(13-68b)

$$D^r(\rho,\phi+\phi',n)=-\frac{e^{-j\pi/4}}{2n\sqrt{2\pi\beta}}$$

$$\cdot\left[C^+(\phi+\phi')F^+(\phi+\phi')+C^-(\phi+\phi')F^-(\phi+\phi')\right]$$

(13-69a)

$$D_s(\rho,\phi,\phi',n) = D^i(\rho,\phi-\phi',n)$$

$$-D^r(\rho,\phi+\phi',n)$$

(13-70c)

$$D_h(\rho,\phi,\phi',n) = D^i(\rho,\phi-\phi',n)$$

$$+D^r(\rho,\phi+\phi',n)$$

(13-71d)

$$D_s(\rho,\phi,\phi',n) = -\frac{e^{-j\pi/4}}{2n\sqrt{2\pi\beta}}$$

$$\cdot\left\{\left[C^+(\phi-\phi')F^+(\phi-\phi')+C^-(\phi-\phi')F^-(\phi-\phi')\right]\right.$$

$$\left.\mp\left[C^+(\phi+\phi')F^+(\phi+\phi')+C^-(\phi+\phi')F^-(\phi+\phi')\right]\right\}$$

(13-71a)

$$D_h(\rho,\phi,\phi',n) = -\frac{e^{-j\pi/4}}{2n\sqrt{2\pi\beta}}$$

$$\cdot\left\{\left[C^+(\phi-\phi')F^+(\phi-\phi')+C^-(\phi-\phi')F^-(\phi-\phi')\right]\right.$$

$$\left.\oplus\left[C^+(\phi+\phi')F^+(\phi+\phi')+C^-(\phi+\phi')F^-(\phi+\phi')\right]\right\}$$

(13-71b)

Uniform Theory Of Diffraction (UTD)

$$D^i = -\frac{e^{-j\pi/4}}{2n\sqrt{2\pi\beta}}\left\{\cot\left[\frac{\pi+(\phi-\phi')}{2n}\right]F\left[\beta\rho\, g^+(\phi-\phi')\right]\right.$$

$$\left.+\cot\left[\frac{\pi-(\phi-\phi')}{2n}\right]F\left[\beta\rho\, g^-(\phi-\phi')\right]\right\} \quad \text{(13-68b)}$$

$$D^r = -\frac{e^{-j\pi/4}}{2n\sqrt{2\pi\beta}}\left\{\cot\left[\frac{\pi+(\phi+\phi')}{2n}\right]F\left[\beta\rho\, g^+(\phi+\phi')\right]\right.$$

$$\left.+\cot\left[\frac{\pi-(\phi+\phi')}{2n}\right]F\left[\beta\rho\, g^-(\phi+\phi')\right]\right\} \quad \text{(13-69b)}$$

UTD Diffraction Coefficients

$$D^i(\rho,\phi-\phi',n)=D^i(\rho,\xi^-,n)$$

$$=-\frac{e^{-j\pi/4}}{2n\sqrt{2\pi\beta}}\left\{\left[C^+(\xi^-)F^+(\xi^-)+C^-(\xi^-)F^-(\xi^-)\right]\right\}$$

$$\xi^-=\phi-\phi' \qquad \text{(13-68b)}$$

$$C^+(\xi^-)=\cot\left(\frac{\pi+\xi^-}{n}\right); \qquad \text{(13-68c)}$$

$$C^-(\xi^-)=\cot\left(\frac{\pi-\xi^-}{n}\right) \qquad \text{(13-68d)}$$

$$F^+(\xi^-)=2j\sqrt{\beta\rho g^+(\xi^-)}\int_{\sqrt{\beta\rho g^+(\xi^-)}}^{\infty}e^{-j\tau^2}d\tau \qquad \text{(13-68e)}$$

$$F^-(\xi^-)=2j\sqrt{\beta\rho g^-(\xi^-)}\int_{\sqrt{\beta\rho g^-(\xi^-)}}^{\infty}e^{-j\tau^2}d\tau \qquad \text{(13-68f)}$$

$$D^r(\rho,\phi+\phi',n)=D^r(\rho,\xi^+,n)$$

$$=-\frac{e^{-j\pi/4}}{2n\sqrt{2\pi\beta}}\left\{\left[C^+(\xi^+)F^+(\xi^+)+C^-(\xi^+)F^-(\xi^+)\right]\right\}$$

$$\xi^+=\phi+\phi' \qquad \text{(13-69b)}$$

$$C^+(\xi^+)=\cot\left(\frac{\pi+\xi^+}{n}\right); \qquad \text{(13-69c)}$$

$$C^-(\xi^+)=\cot\left(\frac{\pi-\xi^+}{n}\right) \qquad \text{(13-69d)}$$

$$F^+(\xi^+)=2j\sqrt{\beta\rho g^+(\xi^+)}\int_{\sqrt{\beta\rho g^+(\xi^+)}}^{\infty}e^{-j\tau^2}d\tau \qquad \text{(13-69e)}$$

$$F^-(\xi^+)=2j\sqrt{\beta\rho g^-(\xi^+)}\int_{\sqrt{\beta\rho g^-(\xi^+)}}^{\infty}e^{-j\tau^2}d\tau \qquad \text{(13-69f)}$$

Magnitude and Phase of Transition Function *F*

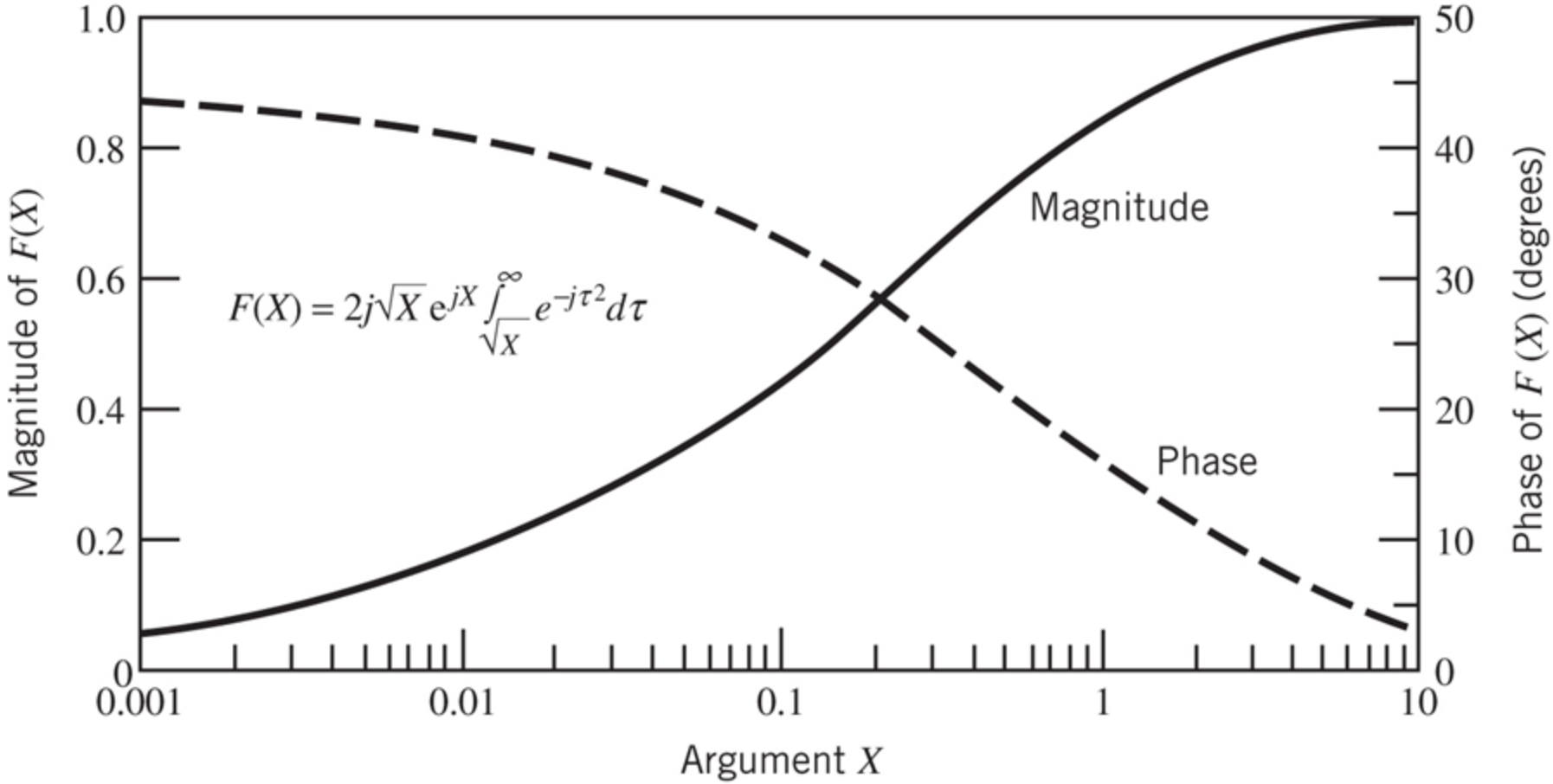

Fig. 13-23

Transition Function F

$$F(x) = 2j\sqrt{x}e^{jx}\underbrace{\int_{\sqrt{x}}^{\infty} e^{-j\tau^2}\,d\tau}_{\text{Fresnel Integral}}$$

$$x < 0.3$$

$$F(x) \simeq \left[\sqrt{\pi x} - 2xe^{j\pi/4} - \frac{2}{3}x^2 e^{-j\pi/4}\right] e^{j\left(\frac{\pi}{4}-x\right)} \qquad \text{(13-74a)}$$

$$x > 5.5$$

$$F(x) \simeq \left[1 + j\frac{1}{2x} - \frac{3}{4}\frac{1}{x^2} - j\frac{15}{8}\frac{1}{x^3} + \frac{75}{16}\frac{1}{x^4}\right] \qquad \text{(13-74b)}$$

$$V_B = F_{DIF} = \frac{e^{-j\beta\rho}}{\sqrt{\rho}} D_{s,h} = [(1)][D_{s,h}]\left[\frac{1}{\sqrt{\rho}}\right][e^{-j\beta\rho}]$$

①: (1) = Amplitude of Incident Field

②: $D_{s,h}$ = Diffraction Coefficient

③: $\frac{1}{\sqrt{\rho}}$ = Amplitude Spreading Factor

(For Incident Plane Wave)

(Also for Incident Cylindrical Wave)

④: $e^{-j\beta\rho}$ = Phase Factor

③ Amplitude Spreading Factor

$$A = \begin{cases} \dfrac{1}{\sqrt{s}}, & \text{plane wave incidence} \\ \dfrac{1}{\sqrt{\rho}}, \ \rho = s \sin \beta_0', & \text{cylindrical wave incidence} \\ \dfrac{\sqrt{s'}}{s}, & \text{spherical wave incidence} \end{cases}$$

s' = distance (source to edge)

s = distance (edge to observation)

What Happens Along Shadow Boundaries

1. Case A: $\phi' \leq (n-1)\pi$

2. Case B: $\phi' \geq (n-1)\pi$

Case A : $\phi' \leq (n-1)\pi$

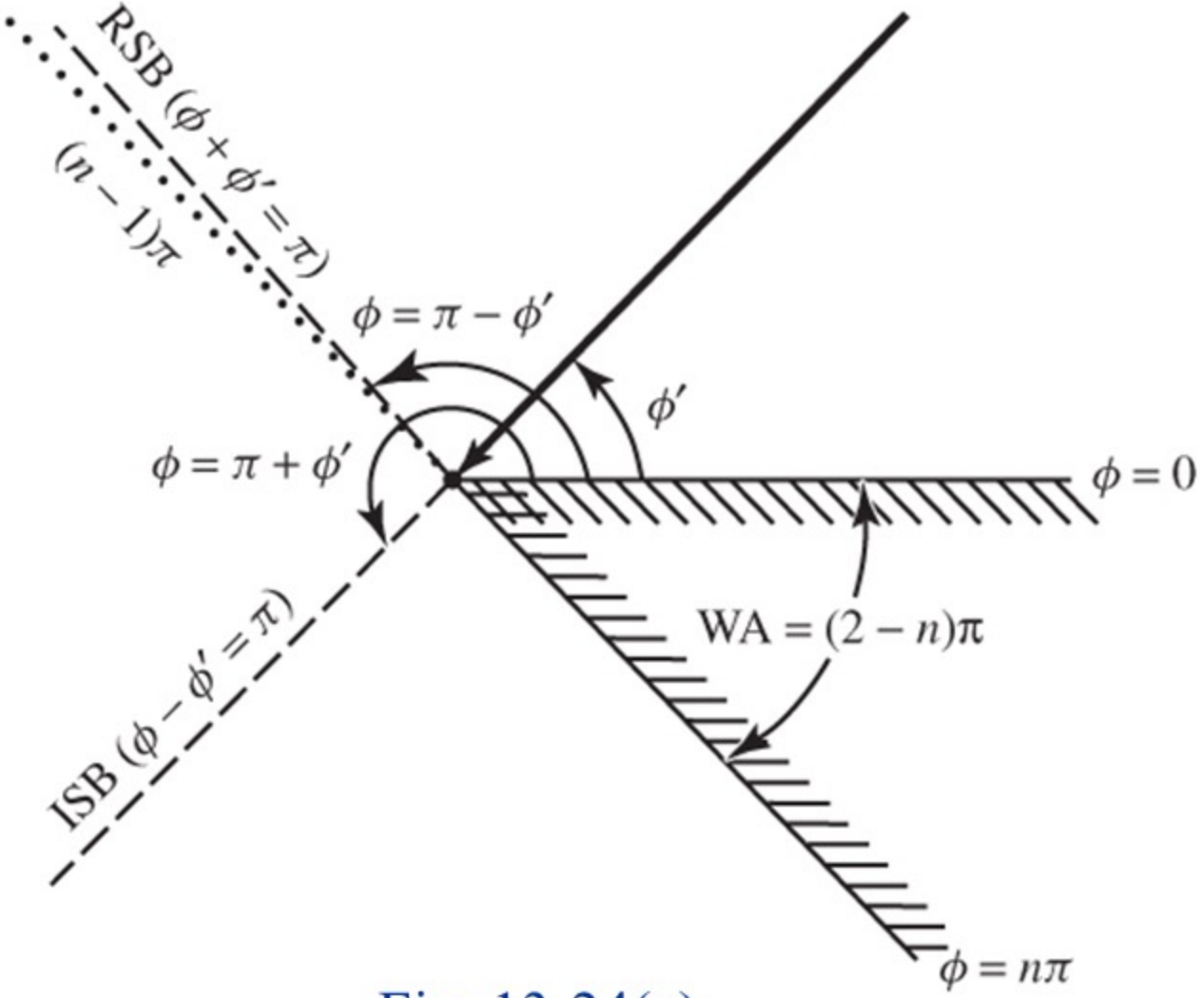

Fig. 13-24(a)

Case B : $\phi' \geq (n-1)\pi$

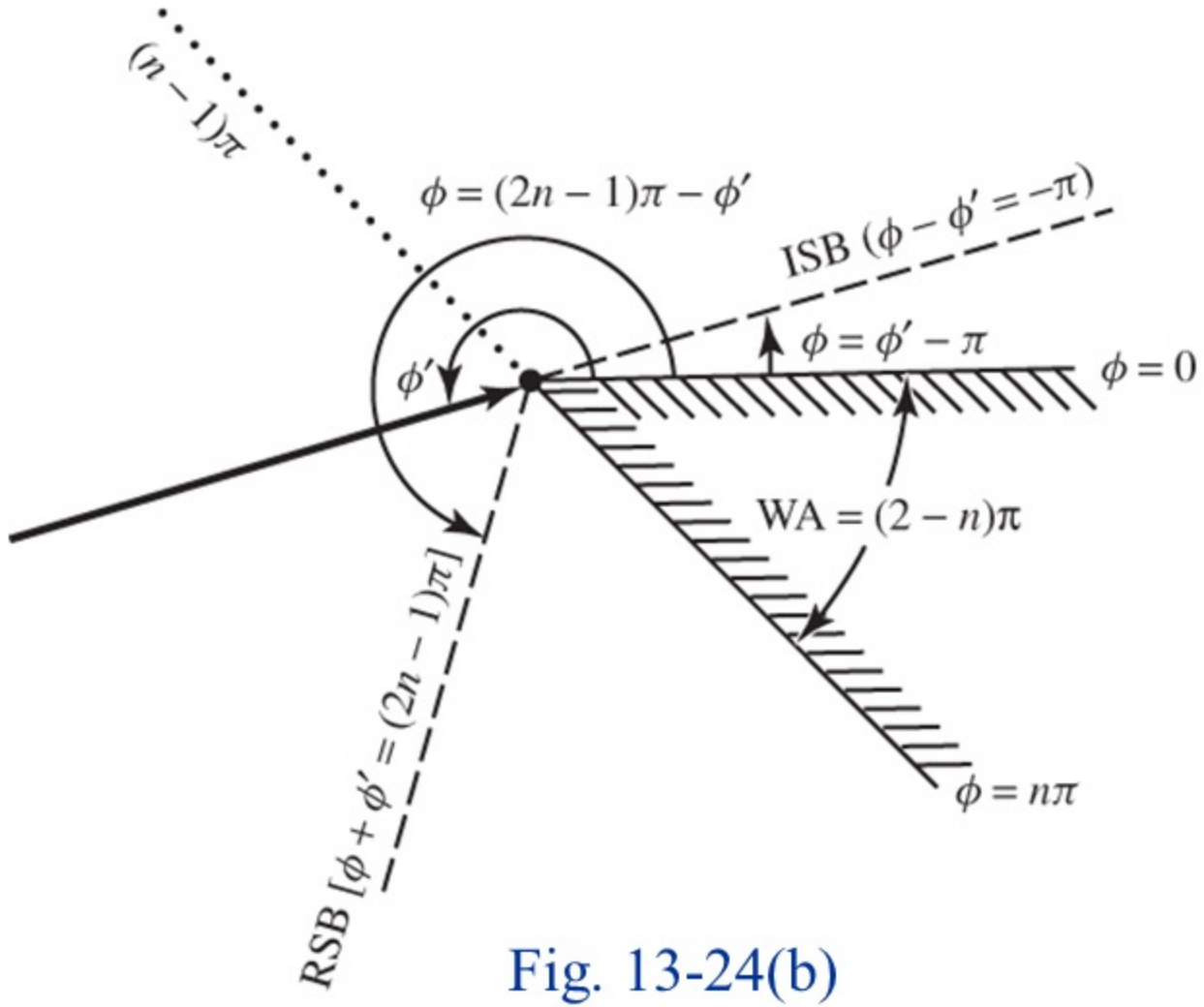

Fig. 13-24(b)

$$V_B^{i,r}(\rho,\xi,n) = I_{+\pi}(\rho,\xi,n) + I_{-\pi}(\rho,\xi,n)$$

$$V_B^{i,r}(\rho,\xi,n) = -\frac{e^{-j\pi/4}}{2n\sqrt{2\pi\beta}}\left\{\left[C^+(\xi)F^+(\xi)\right] + \left[C^-(\xi)F^-(\xi)\right]\right\}\frac{e^{-j\beta\rho}}{\sqrt{\rho}}$$

For $V_B^i \Rightarrow \xi = \xi^- = \phi - \phi'$

For $V_B^r \Rightarrow \xi = \xi^+ = \phi + \phi'$

$$V_B^{h,s}(\rho,\xi,n) = -\frac{e^{-j\pi/4}}{2n\sqrt{2\pi\beta}}\frac{e^{-j\beta\rho}}{\sqrt{\rho}}$$

$$\cdot\left\langle\left\{\left[C^+(\xi^-)F^+(\xi^-)\right]+\left[C^-(\xi^-)F^-(\xi^-)\right]\right\}\right.$$

$$\left.\pm\left\{\left[C^+(\xi^+)F^+(\xi^+)\right]+\left[C^-(\xi^+)F^-(\xi^+)\right]\right\}\right\rangle$$

$$\xi^- = \phi - \phi'$$

$$\xi^+ = \phi + \phi'$$

Summary $SDP_{+\pi}$ + $SDP_{-\pi}$: UTD

$$V_B^{h,s}(\rho,\xi,n) = -\frac{e^{-j\pi/4}}{2n\sqrt{2\pi\beta}}\frac{e^{-j\beta\rho}}{\sqrt{\rho}}$$

$$\cdot\left\langle \left\{\left[\cot\left(\frac{\pi+(\phi-\phi')}{2n}\right)F^{+}(\phi-\phi')\right]\right.\right.$$

$$\left.\left.+\left[\cot\left(\frac{\pi-(\phi-\phi')}{2n}\right)F^{-}(\phi-\phi')\right]\right\}\right.$$

$$\left.\pm\left\{\left[\cot\left(\frac{\pi+(\phi+\phi')}{2n}\right)F^{+}(\phi+\phi')\right]\right.\right.$$

$$\left.\left.+\left[\cot\left(\frac{\pi-(\phi+\phi')}{2n}\right)F^{-}(\phi+\phi')\right]\right\}\right\rangle$$

Case A : $\phi' \geq (n-1)\pi$

$$V_B^{h,s}(\rho,\xi,n) = -\frac{e^{-j\pi/4}}{2n\sqrt{2\pi\beta}}\frac{e^{-j\beta\rho}}{\sqrt{\rho}}$$

$$\cdot \Big\langle \Big\{ \Big[\cot\Big(\frac{\pi+(\phi-\phi')}{2n}\Big) F^+(\phi-\phi') \Big]$$

∞ Case A: ISB $(\phi - \phi' = \pi)$ 0

$$+ \Big[\cot\Big(\frac{\pi-(\phi-\phi')}{2n}\Big) F^-(\phi-\phi') \Big] \Big\}$$

$$\pm \Big\{ \Big[\cot\Big(\frac{\pi+(\phi+\phi')}{2n}\Big) F^+(\phi+\phi') \Big]$$

Case A: RSB $(\phi + \phi' = \pi)$

∞ 0

$$+ \Big[\cot\Big(\frac{\pi-(\phi+\phi')}{2n}\Big) F^-(\phi+\phi') \Big] \Big\} \Big\rangle$$

Case B: $\phi' \geq (n-1)\pi$

$$V_B^{h,s}(\rho,\xi,n) = -\frac{e^{-j\pi/4}}{2n\sqrt{2\pi\beta}}\frac{e^{-j\beta\rho}}{\sqrt{\rho}}$$

Case B: ISB $(\phi - \phi' = -\pi)$

$$\cdot\left\langle\left\{\left[\cot\left(\frac{\pi+(\phi-\phi')}{2n}\right)F^{+}(\phi-\phi')\right]\right.\right.$$

∞ $\qquad$ 0

$$\left.\left.+\left[\cot\left(\frac{\pi-(\phi-\phi')}{2n}\right)F^{-}(\phi-\phi')\right]\right\}\right\rangle$$

Case B: RSB $[\phi + \phi' = (2n-1)\pi]$

$$\pm\left\langle\left\{\left[\cot\left(\frac{\pi+(\phi+\phi')}{2n}\right)F^{+}(\phi+\phi')\right]\right.\right.$$

∞ $\qquad$ 0

$$\left.\left.+\left[\cot\left(\frac{\pi-(\phi+\phi')}{2n}\right)F^{-}(\phi+\phi')\right]\right\}\right\rangle$$

What Happens Along ISB and RSB Shadow Boundaries When:

1. Case A : $\phi' \leq (n-1)\pi$

Case A : $\phi' \leq (n-1)\pi$

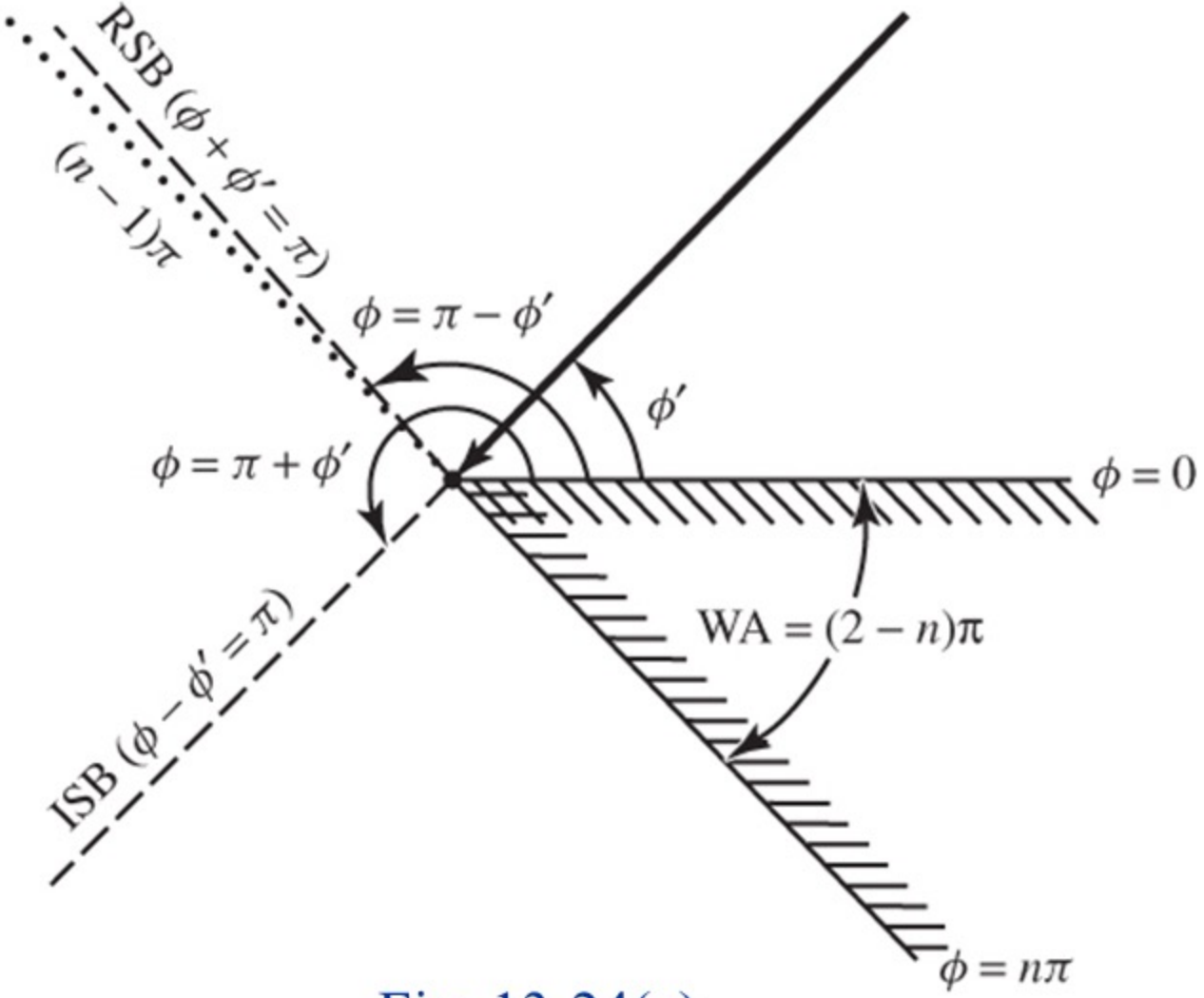

Fig. 13-24(a)

$$\phi' \le (n-1)\pi$$

ISB ($\xi^- = \phi - \phi' = \pi$)

Incident Diffracted Field

$$V_B^i(\rho,\xi^-,n) = \frac{e^{-j\beta\rho}}{\sqrt{\rho}} \underbrace{\left\{ -\frac{e^{-j\pi/4}}{2n\sqrt{2\pi\beta}} \left\{ \left[\cot\left(\frac{\pi+(\phi-\phi')}{2n} \right) F^+(\phi-\phi') \right] + \left[\cot\left(\frac{\pi-(\phi-\phi')}{2n} \right) F^-(\phi-\phi') \right] \right\} \right\}}_{D^{inc}}$$

∞ $\qquad$ 0

$$\phi' \le (n-1)\pi$$

RSB $(\xi^+ = \phi + \phi' = \pi)$

Reflected Diffracted Field

$$V_B^r(\rho, \xi^+, n) = \frac{e^{-j\beta\rho}}{\sqrt{\rho}} \underbrace{\left\{ -\frac{e^{-j\pi/4}}{2n\sqrt{2\pi\beta}} \left\{ \left[\cot\left(\frac{\pi + (\phi+\phi')}{2n} \right) F^+(\phi+\phi') \right] \right.\right.}_{D^{ref}}$$

$$\left.\left. + \left[\cot\left(\frac{\pi - (\phi+\phi')}{2n} \right) F^-(\phi+\phi') \right] \right\} \right\}$$

∞ $\qquad$ 0

$$\phi' \le (n-1)\pi$$

ISB ($\xi^- = \phi - \phi' = \pi$)

Incident Diffracted Field

$$V_B^i(\rho,\xi^-,n) = \frac{e^{-j\beta\rho}}{\sqrt{\rho}} \underbrace{\left\{ -\frac{e^{-j\pi/4}}{2n\sqrt{2\pi\beta}} \left\{ \left[\cot\left(\frac{\pi+(\phi-\phi')}{2n} \right) F^+(\phi-\phi') \right] + \left[\cot\left(\frac{\pi-(\phi-\phi')}{2n} \right) F^-(\phi-\phi') \right] \right\} \right\}}_{D^{inc}}$$

∞ $\qquad$ 0

Along ISB ($\phi = \pi + \phi'$ or $\phi - \phi' = \pi$)

Let: $\phi - \phi' = \pi - \varepsilon$

$$\cot\left[\frac{\pi - (\phi - \phi')}{2n}\right]_{\phi-\phi'=\pi-\varepsilon} = \cot\left[\frac{\pi - (\pi - \varepsilon)}{2n}\right]$$

$$= \cot\left(\frac{\varepsilon}{2n}\right) = \overset{\varepsilon\to 0}{\simeq} \frac{2n}{\varepsilon}$$

$$\cot\left[\frac{\pi - (\phi - \phi')}{2n}\right]_{\phi-\phi'=\pi-\varepsilon} \overset{\varepsilon\to 0}{\simeq} \frac{2n}{\varepsilon} = \frac{2n}{|\varepsilon|\,\mathrm{sgn}(\varepsilon)}$$

Along ISB ($\phi = \pi + \phi'$ or $\phi - \phi' = \pi$)

$$g^-(\phi-\phi') = 1+\cos\left[(\phi-\phi') - 2\pi n N^-\right]_{N^-=0}$$

$$g^-(\phi-\phi')\Big|_{\phi-\phi'=(\pi-\varepsilon)} = 1+\cos(\phi-\phi')\Big|_{\phi-\phi'=(\pi-\varepsilon)}$$

$$g^-(\phi-\phi')\Big|_{\phi-\phi'=(\pi-\varepsilon)} = 1+\cos(\pi-\varepsilon) = 1-\cos(\varepsilon)$$

$$g^-(\phi-\phi')\Big|_{\phi-\phi'=(\pi-\varepsilon)} \simeq 1-\left[1-\frac{\varepsilon^2}{2}+\ldots\right] = +\frac{\varepsilon^2}{2}$$

Along ISB ($\phi = \pi + \phi'$ or $\phi - \phi' = \pi$)

$$F^{-}\left[\beta\rho g^{-}(\phi-\phi')\right]_{\phi-\phi'=(\pi-\varepsilon)} = F^{-}\left[\frac{\beta\rho\varepsilon^{2}}{2}\right]$$

$$F(x) \overset{x\to 0}{\simeq} \left[\sqrt{\pi x} - 2xe^{j\pi/4} - \frac{2}{3}x^{2}e^{-j\pi/4}\right] e^{j\left(\frac{\pi}{4}+x\right)}$$

$$F(x) \overset{x\to 0}{\simeq} \sqrt{\pi x}\, e^{j\left(\frac{\pi}{4}+x\right)} \simeq \sqrt{\pi x}\, e^{j\frac{\pi}{4}}$$

$$F^{-}\left[\beta\rho g^{-}(\phi-\phi')\right]_{\phi-\phi'=(\pi-\varepsilon)} = F^{-}\left(\frac{\beta\rho\varepsilon^{2}}{2}\right) \simeq \sqrt{\frac{\beta\rho\pi\varepsilon^{2}}{2}}\, e^{j\pi/4}$$

$$F^{-}\left[\beta\rho g^{-}(\phi-\phi')\right]_{\phi-\phi'=(\pi-\varepsilon)} \simeq |\varepsilon| \sqrt{\frac{\pi\beta\rho}{2}}\, e^{j\frac{\pi}{4}}$$

Along ISB ($\phi = \pi + \phi'$ or $\phi - \phi' = \pi$)

$$\cot\left[\frac{\pi - (\phi - \phi')}{2n}\right] F^{-}\left[\beta\rho g^{-}(\phi - \phi')\right]\Big|_{\phi-\phi'=(\pi-\varepsilon)}$$

$$\simeq \frac{2n}{|\varepsilon|\,\mathrm{sgn}(\varepsilon)} |\varepsilon| \sqrt{\frac{\pi\beta\rho}{2}} e^{j\pi/4}$$

$$\cot\left[\frac{\pi - (\phi - \phi')}{2n}\right] F^{-}\left[\beta\rho g^{-}(\phi - \phi')\right]\Big|_{\phi-\phi'=(\pi-\varepsilon)}$$

$$\simeq n\sqrt{2\pi\beta\rho}\,\mathrm{sgn}(\varepsilon) e^{j\pi/4}$$

Incident Diffracted Fields

Along ISB ($\phi = \pi + \phi'$ or $\phi - \phi' = \pi$)

$$V_B^{inc}(\rho, \phi - \phi', n)\Big|_{\phi-\phi'=\pi-\varepsilon} = \frac{e^{-j\beta\rho}}{\sqrt{\rho}} \underbrace{\left\{ -\frac{e^{-j\pi/4}}{2n\sqrt{2\pi\beta}} \left\{ \left[\cot\left(\frac{\pi+(\phi-\phi')}{2n} \right) F^{+}(\phi-\phi') \right] \right.\right.}_{\approx 0} + \left.\left. \left[\cot\left(\frac{\pi-(\phi-\phi')}{2n} \right) F^{-}(\phi-\phi') \right] \right\} \right\}}_{D^{inc}} \Bigg|_{\phi-\phi'=\pi-\varepsilon}$$

$$V_B^{inc}(\rho, \phi - \phi', n)\Big|_{\phi-\phi'=\pi-\varepsilon} = \frac{e^{-j\beta\rho}}{\sqrt{\rho}} \underbrace{\left\{ -\frac{e^{-j\pi/4}}{2n\sqrt{2\pi\beta}} n\sqrt{2\pi\beta\rho}\, \mathrm{sgn}(\varepsilon) e^{j\pi/4} \right\}}_{D^{inc}}$$

$$V_B^{inc}(\rho, \phi - \phi', n)\Big|_{\phi-\phi'=\pi-\varepsilon} = -0.5 e^{-j\beta\rho}\, \mathrm{sgn}(\varepsilon)$$

$$\left| V_B^{inc}(\rho, \phi - \phi', n) \right|_{\phi-\phi'=\pi-\varepsilon} = 0.5$$

What Happens Along Shadow Boundaries

2. Case B : $\phi' \geq (n-1)\pi$

Case B : $\phi' \geq (n-1)\pi$

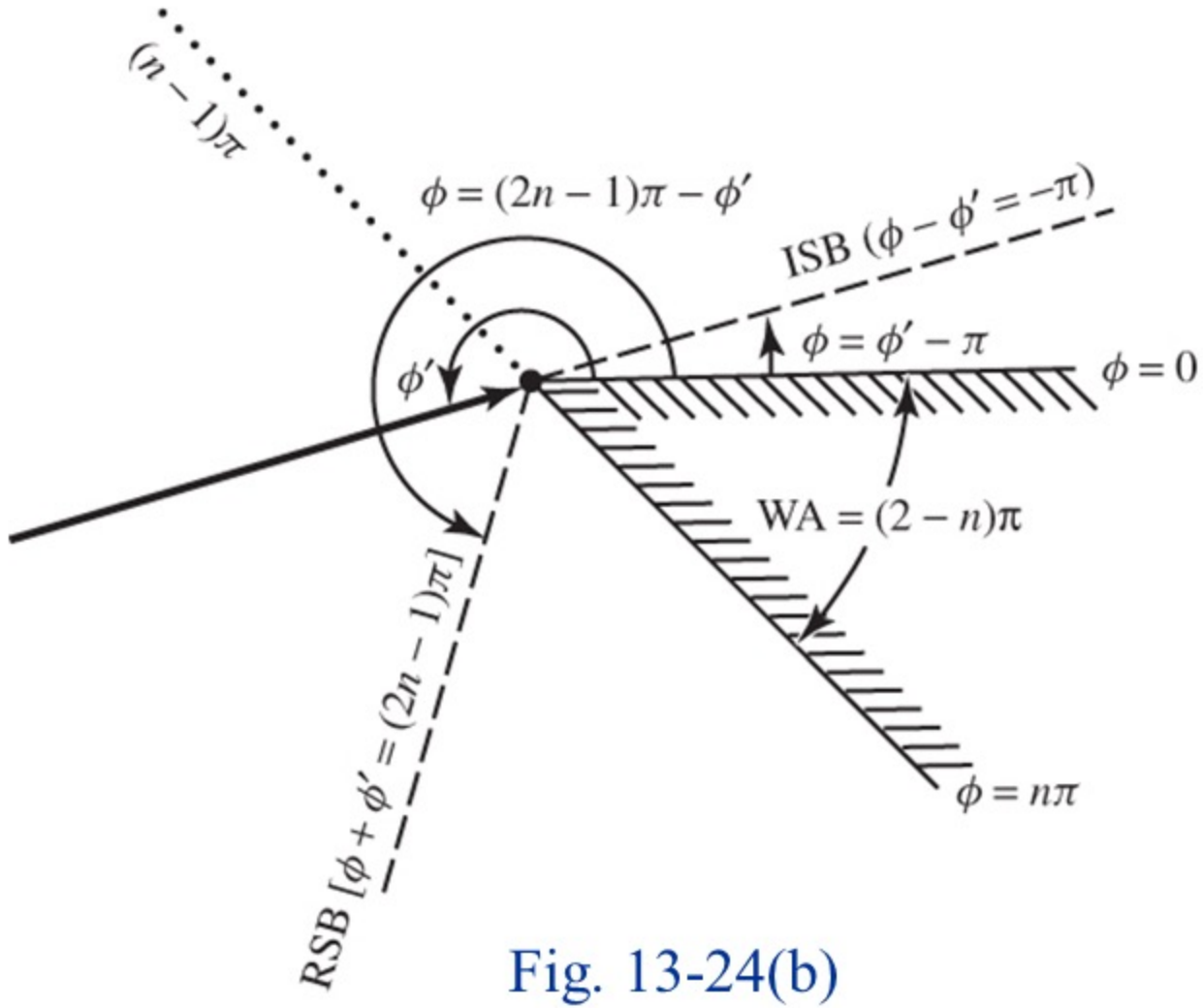

Fig. 13-24(b)

Summary $SDP_{+\pi}$ + $SDP_{-\pi}$: UTD

$$V_B^{h,s}(\rho,\xi,n) = -\frac{e^{-j\pi/4}}{2n\sqrt{2\pi\beta}}\frac{e^{-j\beta\rho}}{\sqrt{\rho}}$$

$$\cdot\left\langle \left\{\left[\cot\left(\frac{\pi+(\phi-\phi')}{2n}\right)F^{+}(\phi-\phi')\right]\right.\right.$$

$$\left.\left.+\left[\cot\left(\frac{\pi-(\phi-\phi')}{2n}\right)F^{-}(\phi-\phi')\right]\right\}\right.$$

$$\left.\pm\left\{\left[\cot\left(\frac{\pi+(\phi+\phi')}{2n}\right)F^{+}(\phi+\phi')\right]\right.\right.$$

$$\left.\left.+\left[\cot\left(\frac{\pi-(\phi+\phi')}{2n}\right)F^{-}(\phi+\phi')\right]\right\}\right\rangle$$

Case A : $\phi' \geq (n-1)\pi$

$$V_B^{h,s}(\rho,\xi,n) = -\frac{e^{-j\pi/4}}{2n\sqrt{2\pi\beta}}\frac{e^{-j\beta\rho}}{\sqrt{\rho}}$$

$$\cdot \Big\langle \Big\{ \Big[\cot\Big(\frac{\pi+(\phi-\phi')}{2n}\Big) F^+(\phi-\phi') \Big]$$

∞ Case A: ISB $(\phi - \phi' = \pi)$ 0

$$+ \Big[\cot\Big(\frac{\pi-(\phi-\phi')}{2n}\Big) F^-(\phi-\phi') \Big] \Big\}$$

$$\pm \Big\{ \Big[\cot\Big(\frac{\pi+(\phi+\phi')}{2n}\Big) F^+(\phi+\phi') \Big]$$

Case A: RSB $(\phi + \phi' = \pi)$

∞ 0

$$+ \Big[\cot\Big(\frac{\pi-(\phi+\phi')}{2n}\Big) F^-(\phi+\phi') \Big] \Big\} \Big\rangle$$

Case B: $\phi' \geq (n-1)\pi$

$$V_B^{h,s}(\rho,\xi,n) = -\frac{e^{-j\pi/4}}{2n\sqrt{2\pi\beta}}\frac{e^{-j\beta\rho}}{\sqrt{\rho}}$$

Case B: ISB ($\phi - \phi' = -\pi$)

∞ 0

$$\cdot\left\langle \left\{ \left[\cot\left(\frac{\pi+(\phi-\phi')}{2n}\right) F^{+}(\phi-\phi') \right] + \left[\cot\left(\frac{\pi-(\phi-\phi')}{2n}\right) F^{-}(\phi-\phi') \right] \right\} \right.$$

Case B: RSB [$\phi + \phi' = (2n-1)\pi$]

∞ 0

$$\left. \pm \left\{ \left[\cot\left(\frac{\pi+(\phi+\phi')}{2n}\right) F^{+}(\phi+\phi') \right] + \left[\cot\left(\frac{\pi-(\phi+\phi')}{2n}\right) F^{-}(\phi+\phi') \right] \right\} \right\rangle$$

$$2\pi nN^{-} - (\phi - \phi') = -\pi$$

$$2\pi nN^{-} - (\phi + \phi') = -\pi$$

$$2\pi nN^{+} - (\phi - \phi') = +\pi$$

$$2\pi nN^{+} - (\phi + \phi') = +\pi$$

Case A:

1. ISB $\Rightarrow N^- = 0$

$$C^-(\beta^-) = \cot\left[\frac{\pi - (\phi - \phi')}{2n}\right]$$

2. RSB $\Rightarrow N^- = 0$

$$C^-(\beta^+) = \cot\left[\frac{\pi - (\phi + \phi')}{2n}\right]$$

Case B:

1. ISB $\Rightarrow N^+ = 0$

$$C^+(\beta^-) = \cot\left[\frac{\pi + (\phi - \phi')}{2n}\right]$$

2. RSB $\Rightarrow N^+ = 1$

$$C^+(\beta^+) = \cot\left[\frac{\pi + (\phi + \phi')}{2n}\right]$$

Table 13-1: Cotangent Function Behavior for $N^{\pm}$

	Cotangent Function Becomes Singular When	Value of $N^{\pm}$ Along the SB
$\cot\left[\frac{\pi-(\phi-\phi')}{2n}\right]$	$\phi=\pi+\phi'$ or $\phi-\phi'=\pi$ **ISB** of Case **A**	$N^{-}=0$
$\cot\left[\frac{\pi-(\phi+\phi')}{2n}\right]$	$\phi=\pi-\phi'$ or $\phi+\phi'=\pi$ **RSB** of Case **A**	$N^{-}=0$
$\cot\left[\frac{\pi+(\phi-\phi')}{2n}\right]$	$\phi=\phi'+\pi$ or $\phi-\phi'=-\pi$ **ISB** of Case **B**	$N^{+}=0$
$\cot\left[\frac{\pi+(\phi+\phi')}{2n}\right]$	$\phi=(2n-1)\pi-\phi'$ or $\phi+\phi'=(2n-1)\pi$ **RSB** of Case **B**	$N^{+}=1$

Example 13-3

GO and Diffracted Fields From a PEC Half Plane (Knife Edge)

Example 13 – 3 :

A plane wave of unity amplitude is incident upon a half-plane ($n = 2$) at an incident angle of $\phi' = 30^o$, as shown in Figure 13-20. At a distance of λ ($\rho = \lambda$) from the edge of the wedge, compute and plot the amplitude and phase of the following:

1. The total (incident plus reflected) GO field.
2. The incident diffracted field.
3. The reflected diffracted field.
4. The total field (GO + diffracted).

Solution:

It follows.

Plane Wave Incident Upon Half Plane

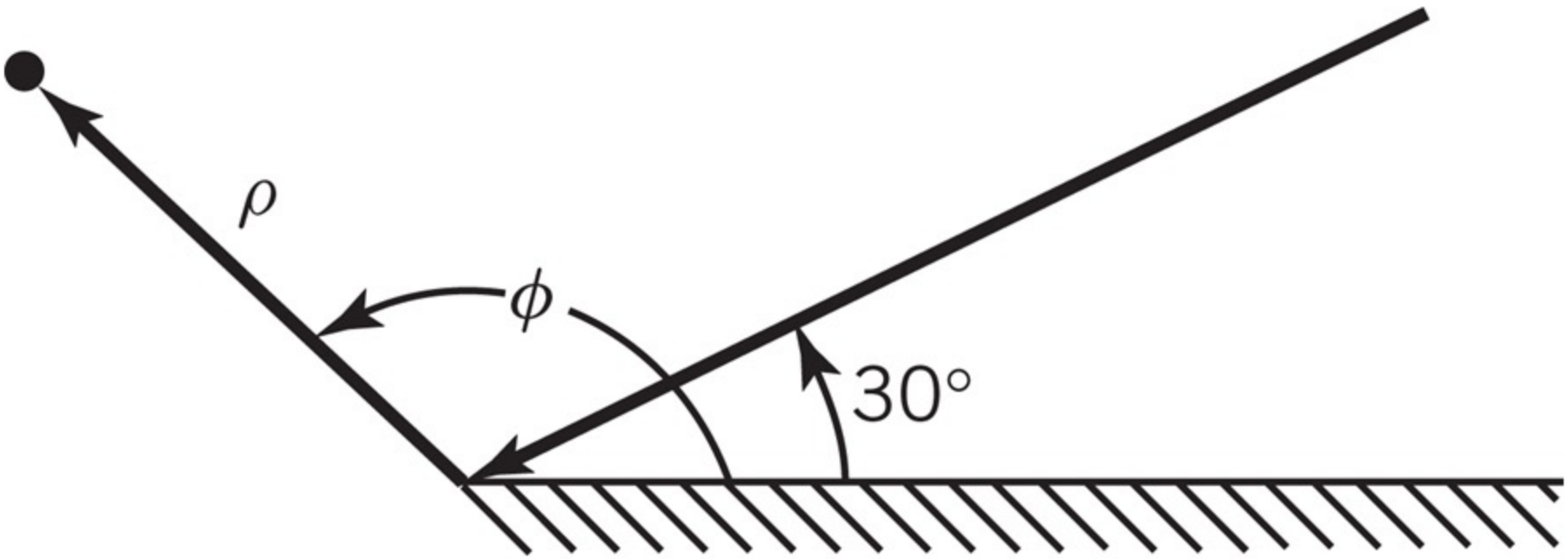

Fig. 13-20

Field Distribution of a Plane Wave Upon a Half Plane

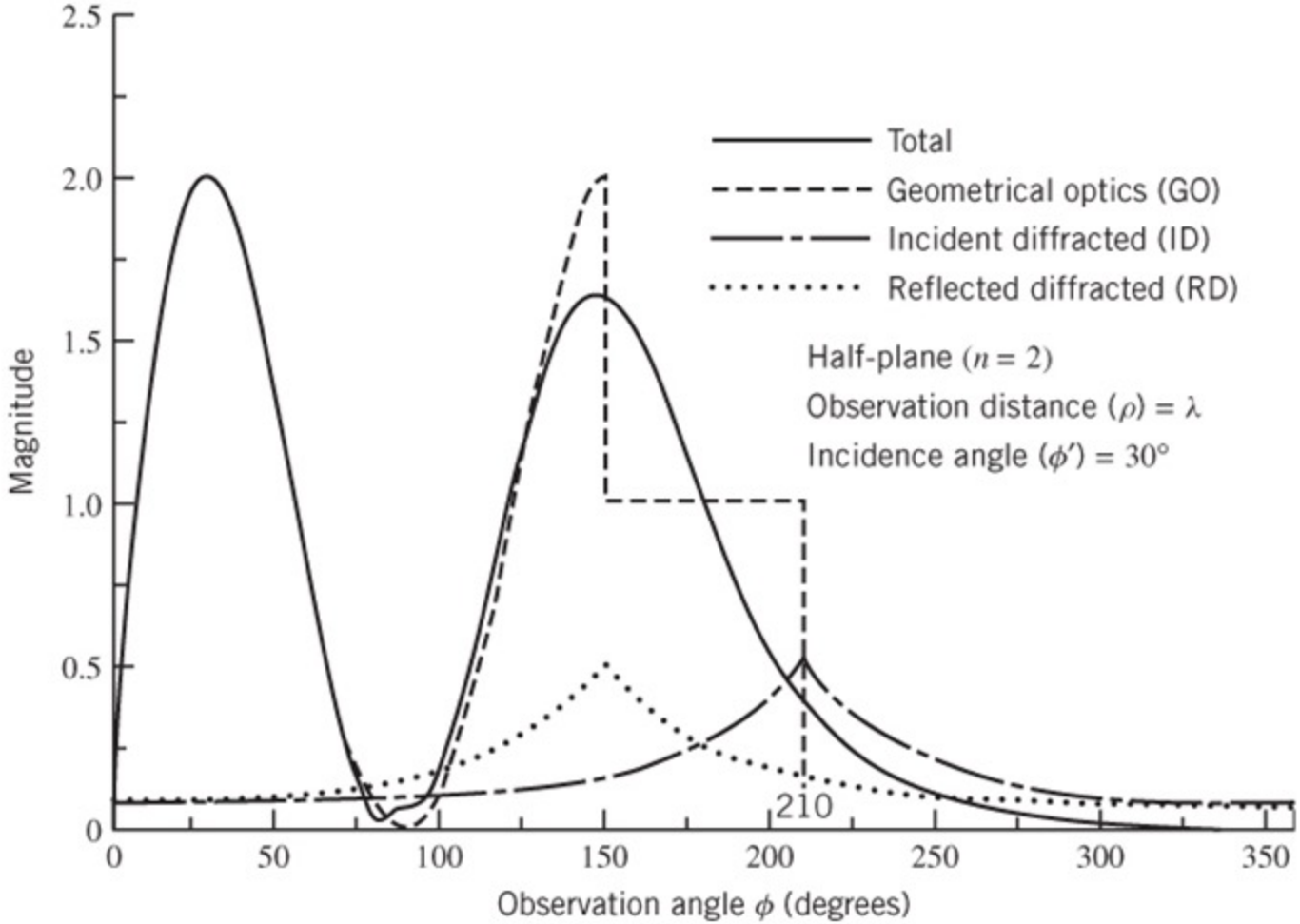

(a) Soft polarization

Fig. 13-25

Field Distribution of a Plane Wave Upon a Half Plane

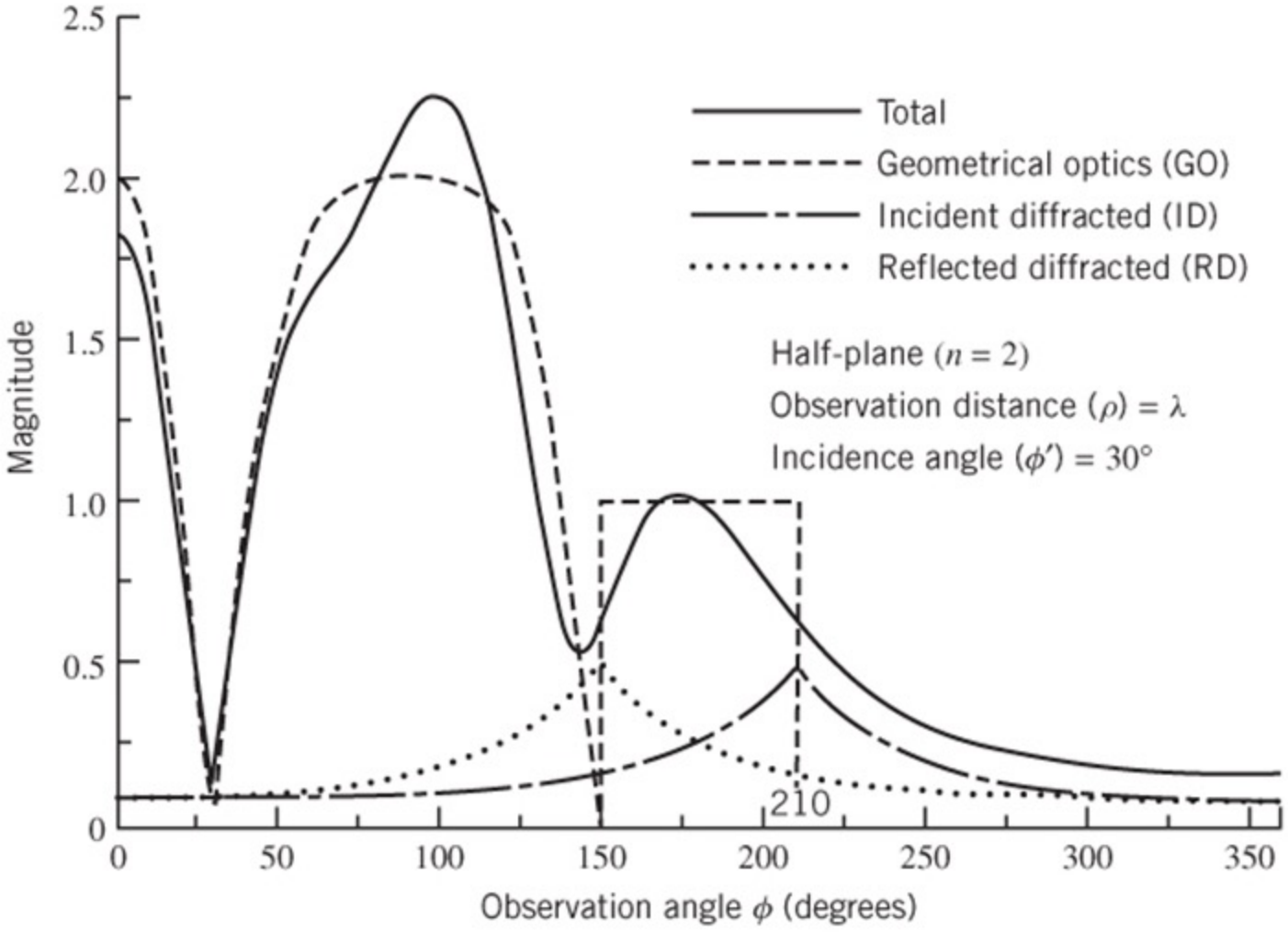

(b) Hard polarization Fig. 13-25

Summary

$$V_B^i(\rho,\phi-\phi',n)=\frac{e^{-j\beta\rho}}{\sqrt{\rho}}D^i(\rho,\phi-\phi',n)$$

$$V_B^r(\rho,\phi+\phi',n)=\frac{e^{-j\beta\rho}}{\sqrt{\rho}}D^r(\rho,\phi+\phi',n)$$

$$V_B^s=V_B^i-V_B^r=\frac{e^{-j\beta\rho}}{\sqrt{\rho}}\left\{\underbrace{D^i(\rho,\phi-\phi',n)-D^r(\rho,\phi+\phi',n)}_{D^s(\rho,\phi,\phi',n)}\right\}$$

$$V_B^h=V_B^i+V_B^r=\frac{e^{-j\beta\rho}}{\sqrt{\rho}}\left\{\underbrace{D^i(\rho,\phi-\phi',n)+D^r(\rho,\phi+\phi',n)}_{D^h(\rho,\phi,\phi',n)}\right\}$$

Computer Program (WDC)

Wedge Diffraction Coefficients

Input Parameters: R, PHID, PHIDP, BTD, FN

Output Parameters: CDCS, CDCH

Wedge Diffraction Coefficient WDC Subroutine

WDC(CDCS, CDCH, R, PHID, PHIDP, BTD, FN)

CDCS = Complex Diffraction Coefficient

(Soft Polarization)

CDCH = Complex Diffraction Coefficient

(Hard Polarization)

R = Real=Distance parameter ρ (or ρ') (in wavelengths)

PHID = Observation angle ϕ or ψ (in degrees)

PHIDP = Incidence angle ϕ' or ψ' (in degrees)

BTN = Oblique angle β (in degrees)

FN = Wedge factor n [WA=$(2-n)\pi$]

Example 13-4

Reflection From a Flat PEC Surface

Example 13 – 4 :

For the geometry of Figure 13-9 repeat the formulations of Example 13-2 including the fields diffracted from the edges of the strip.

Solution:

It follows.

Line Source Above Strip

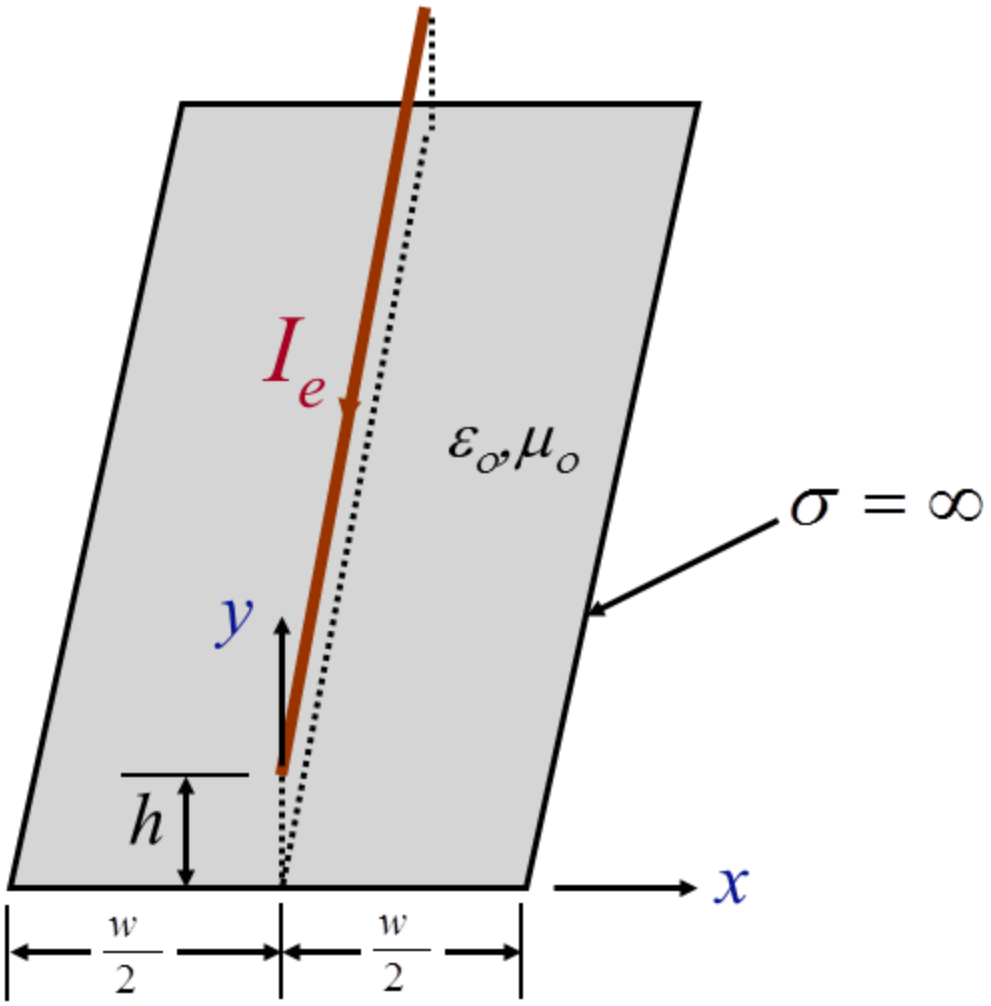

Line Source: Coordinate System

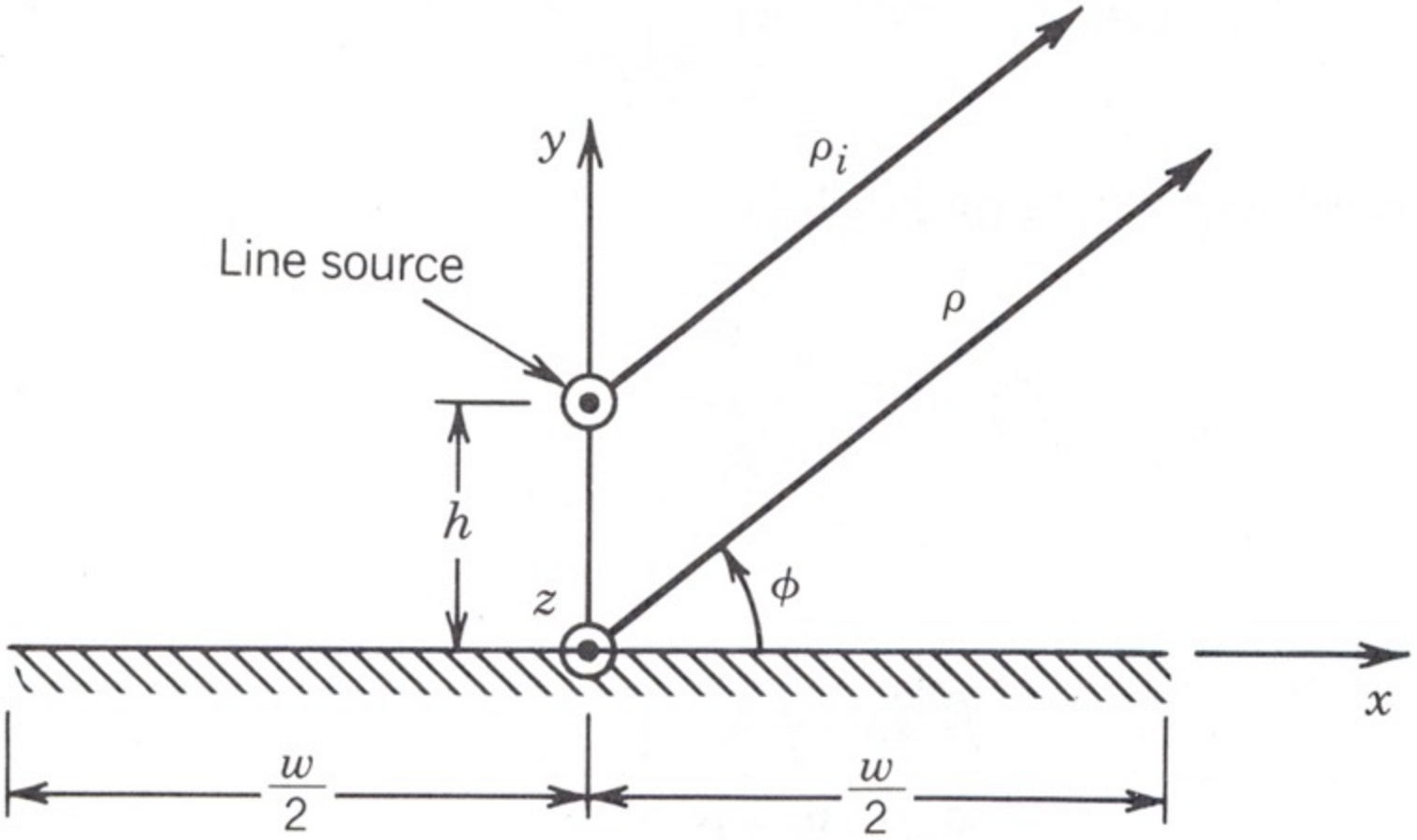

Fig. 13-9(a)

Geometrical Optics Fields

a. Incident/Direct
b. Reflected

Reflection from a Flat Surface

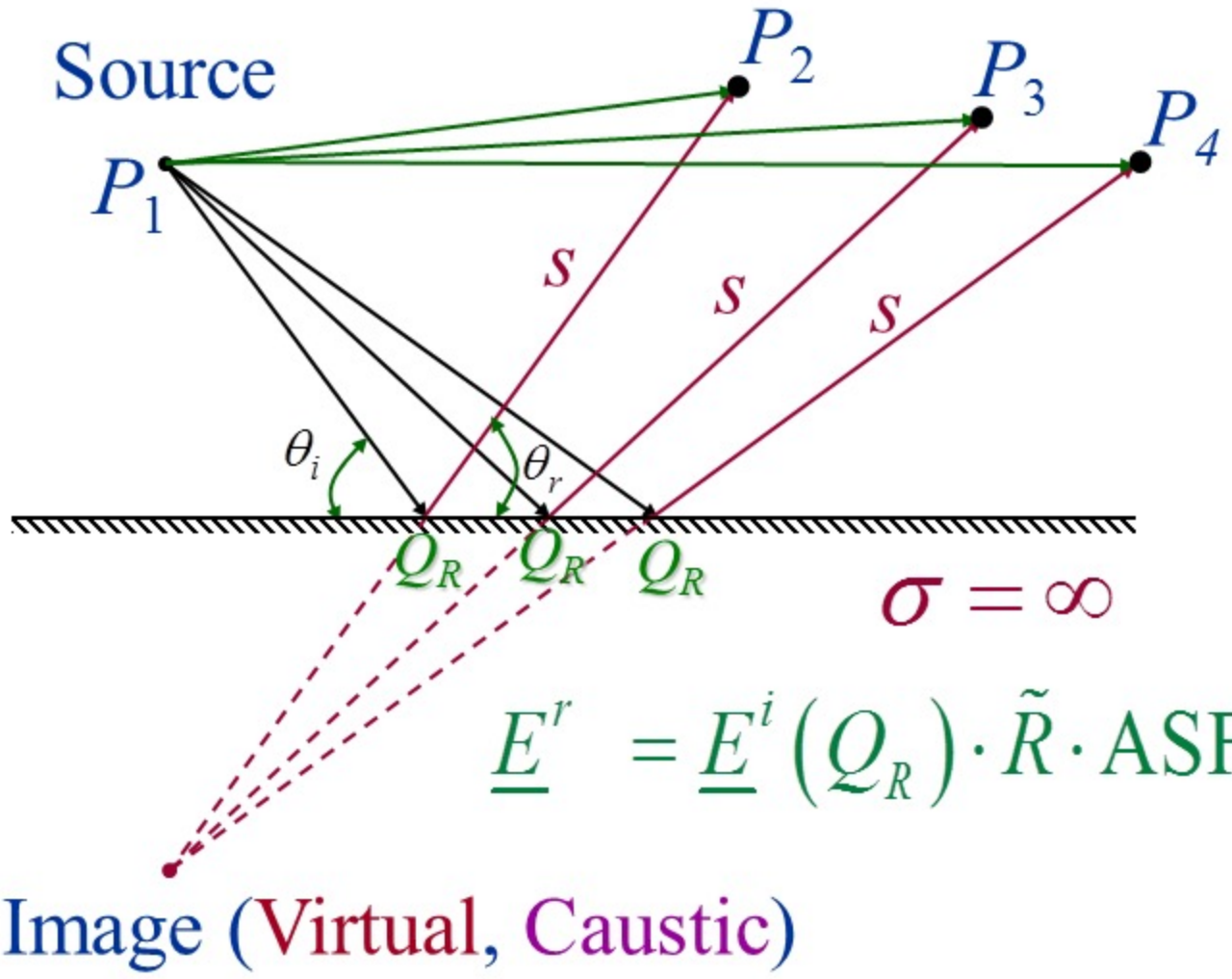

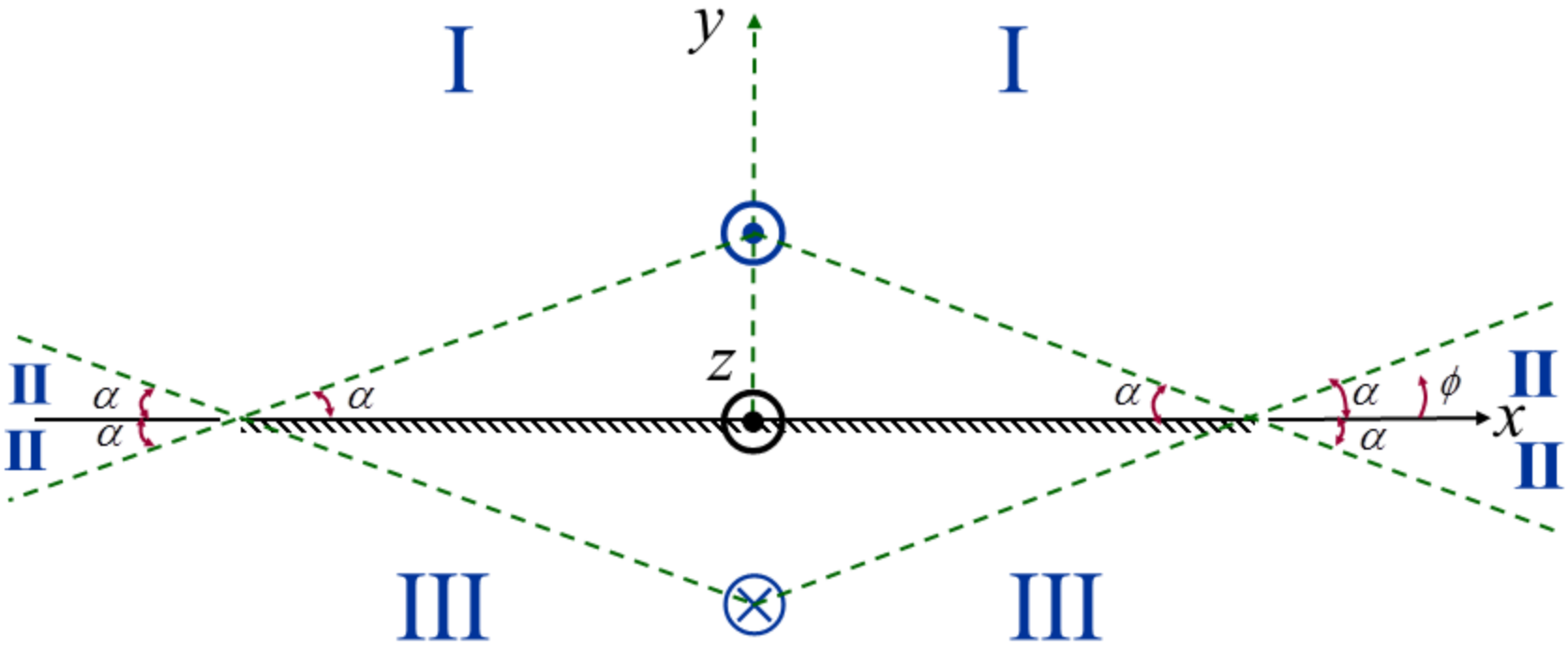

Regions	Range (ϕ)
I	$\alpha \le \phi \le \pi - \alpha$
II	$\pi - \alpha \le \phi \le \pi + \alpha,\ 2\pi - \alpha \le \phi \le 2\pi,\ 0 \le \phi \le \alpha$
III	$\pi + \alpha \le \phi \le 2\pi - \alpha$

Diffracted Fields

Region Separation for GO & Diffraction

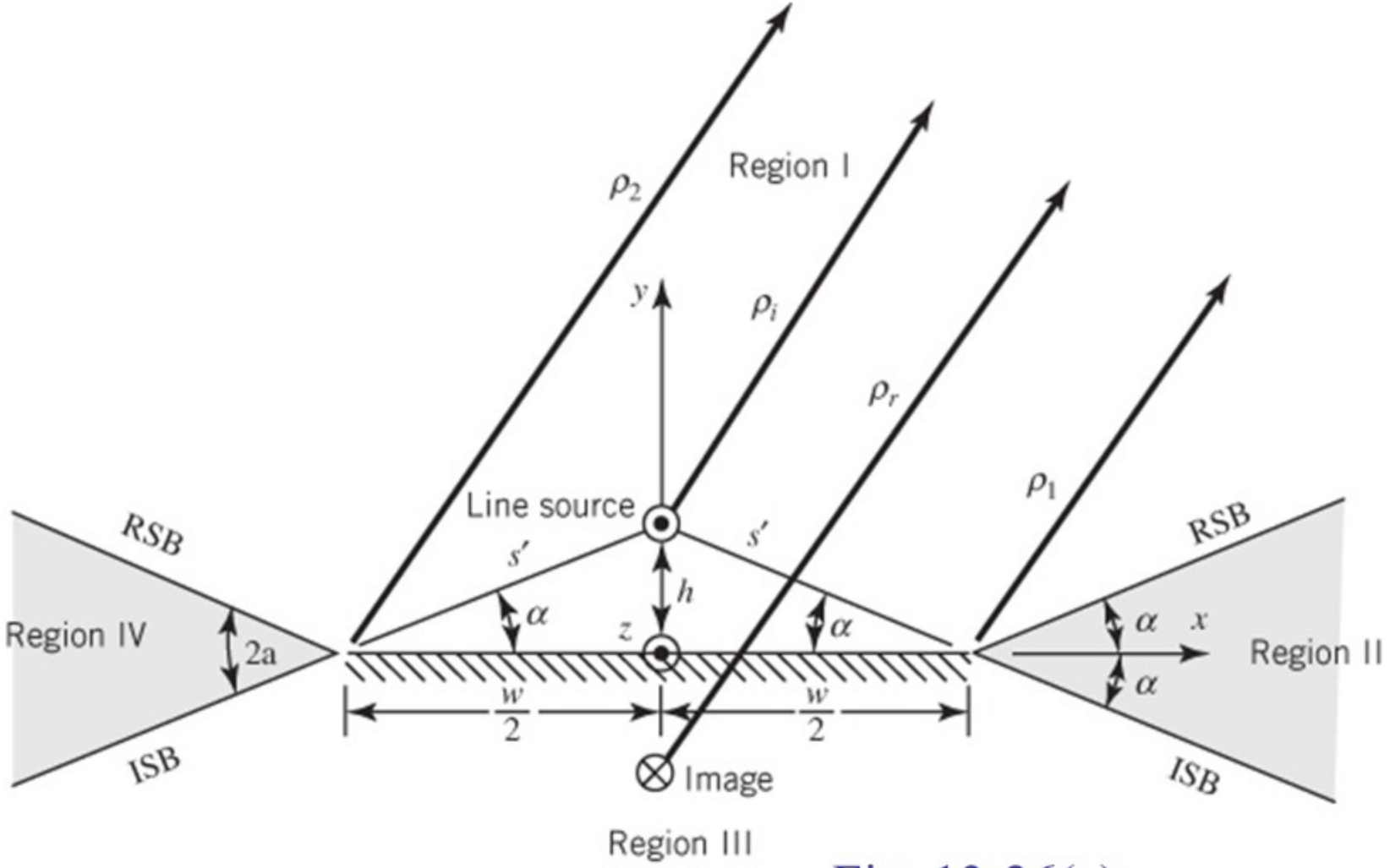

Fig. 13-26(a)

Geometry for Diffraction by Wedge

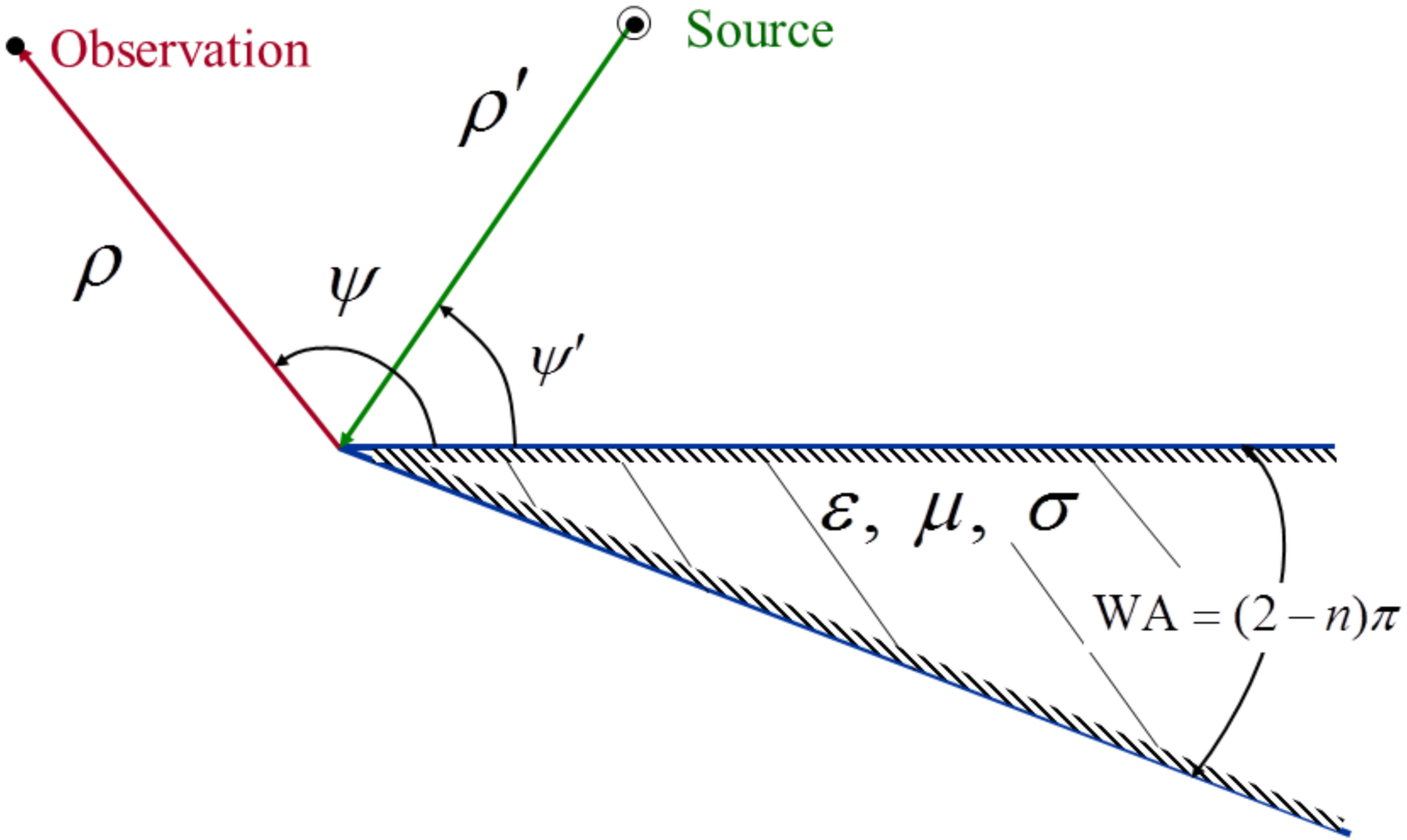

Diffraction by Edges 1 and 2

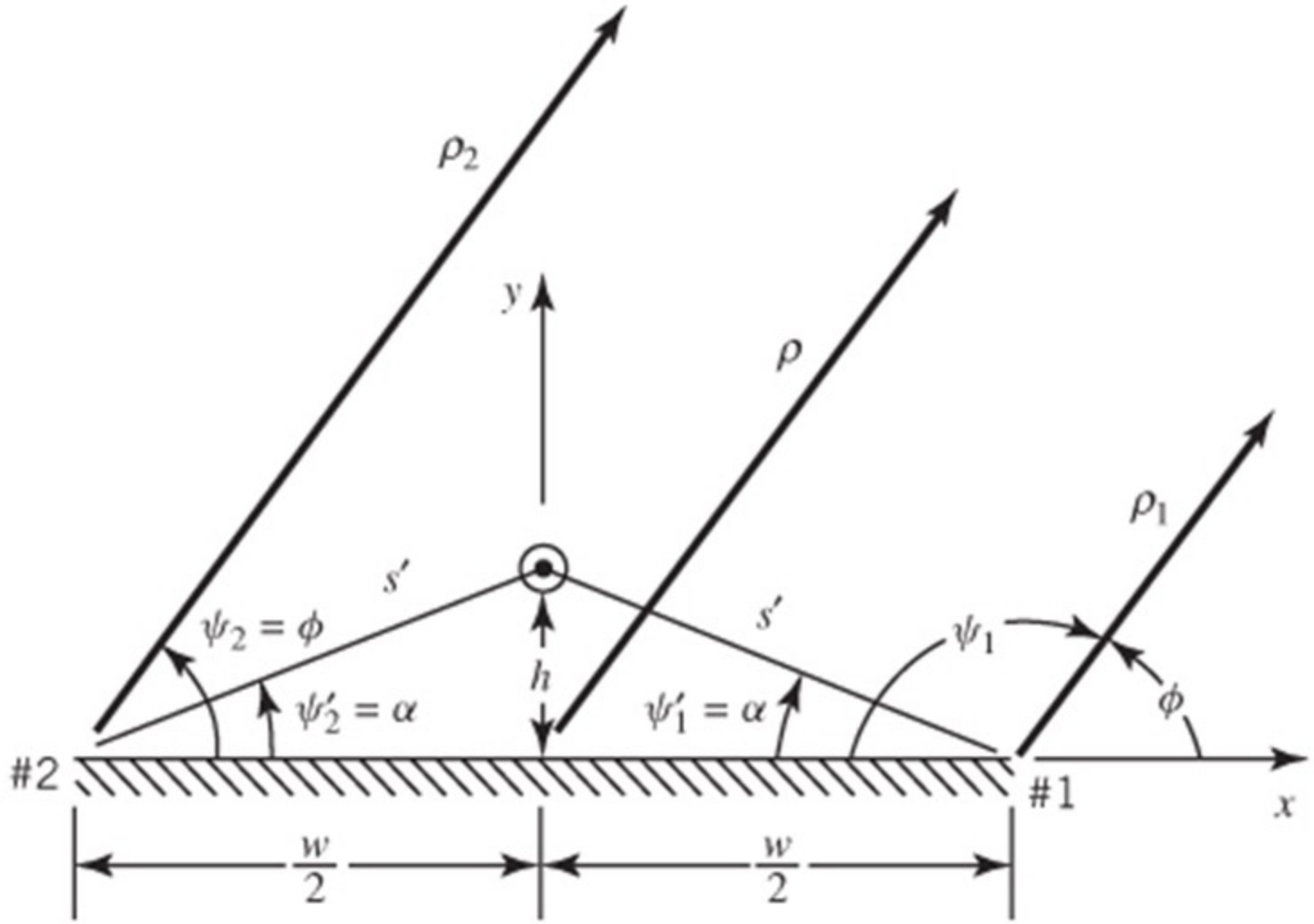

Fig. 13-26(b)

Diffracted Field from Wedge #1

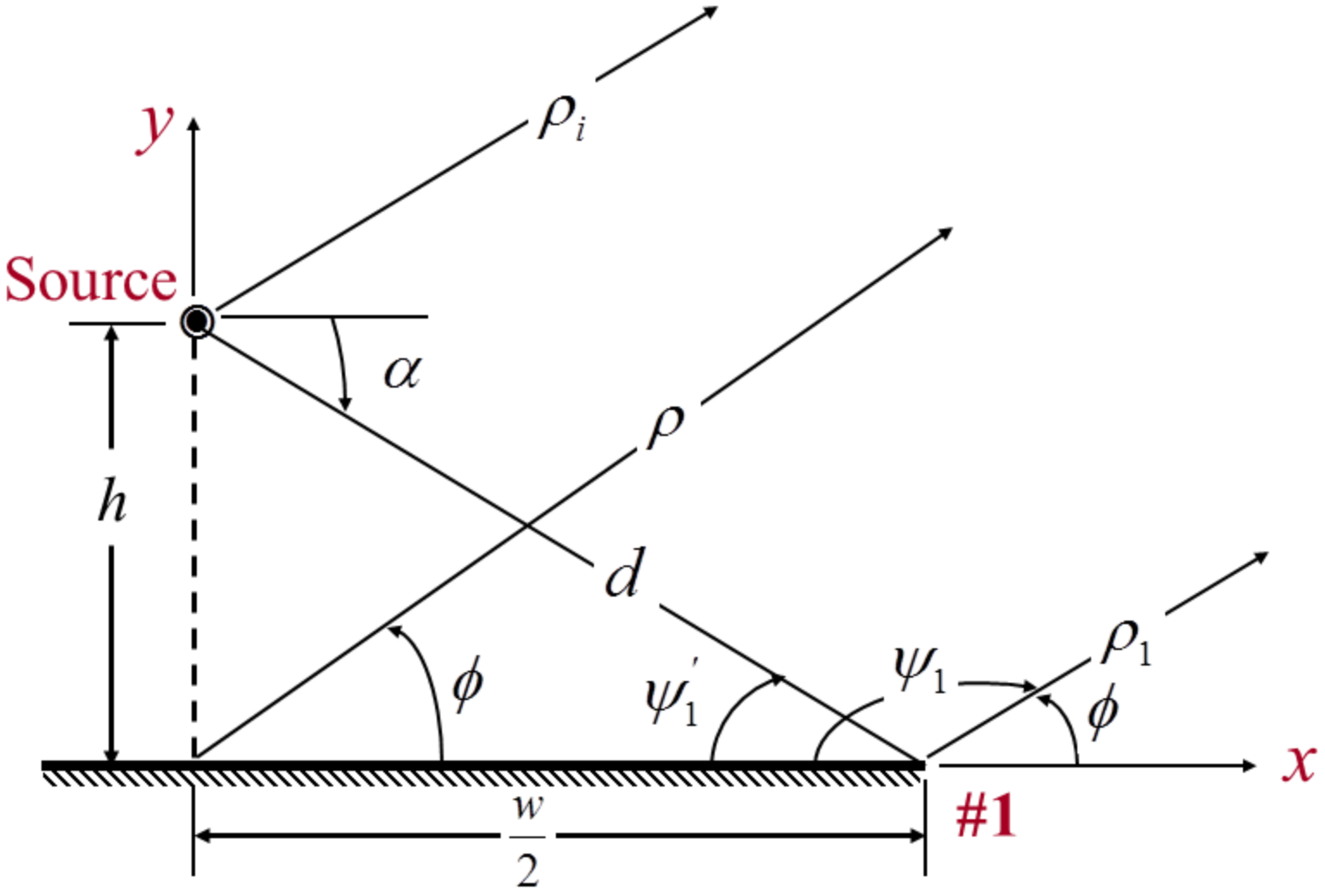

Diffraction by Edge #1 in Region $0^o \le \phi \le 180^o$

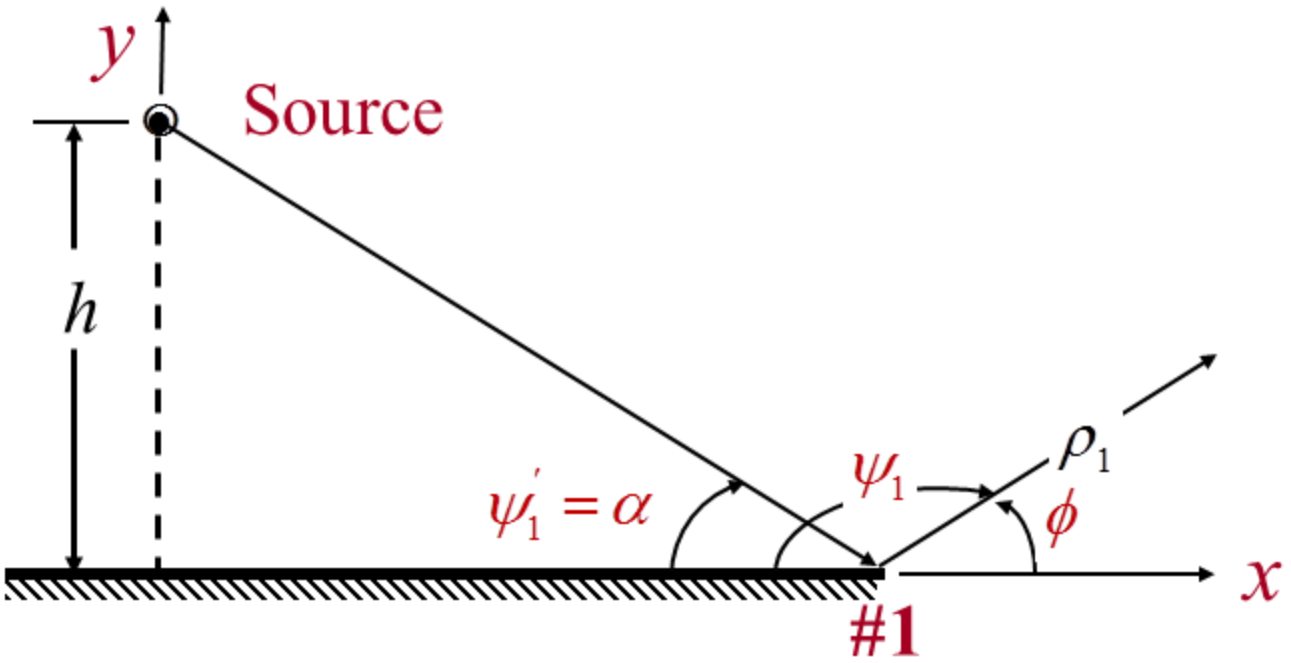

$$\left.\begin{aligned}
\psi_1' &= \alpha \\
\psi_1 &= \pi - \phi \\
\xi_1^- &= \psi_1 - \psi_1' = \pi - \phi - \psi_1' \\
\xi_1^+ &= \psi_1 + \psi_1' = \pi - \phi + \psi_1'
\end{aligned}\right\} 0^o \le \phi \le 180^o$$

Diffraction by Edge #1 in Region $180^o \le \phi \le 360^o$

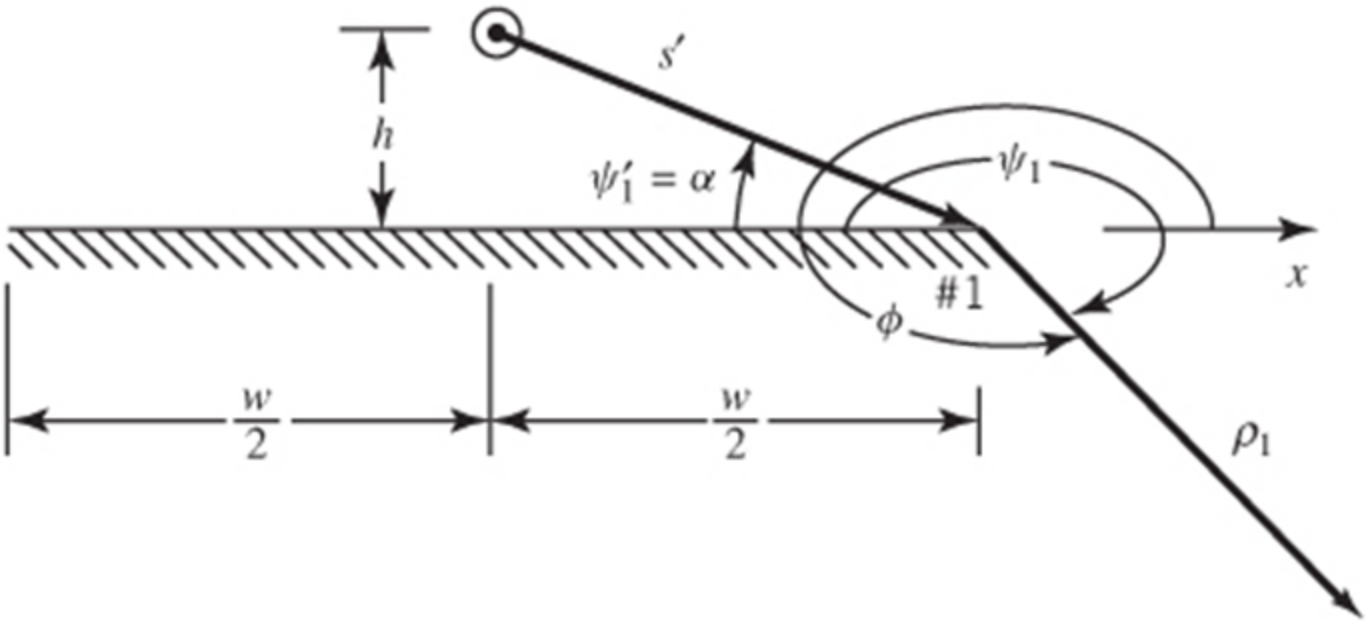

$$\left.\begin{aligned}
&\psi_1 = \alpha \\
&\psi_1 + \phi = 3\pi \Rightarrow \psi_1 = 3\pi - \phi \\
&\xi_1^- = \psi_1 - \psi_1' = 3\pi - \phi - \psi_1' \\
&\xi_1^+ = \psi_1 + \psi_1' = 3\pi - \phi + \psi_1'
\end{aligned}\right\} 180^o \le \phi \le 360^o$$

Fig. 13-26(c)

Diffraction by Edge #2 in Region $0^o \le \phi \le 360^o$

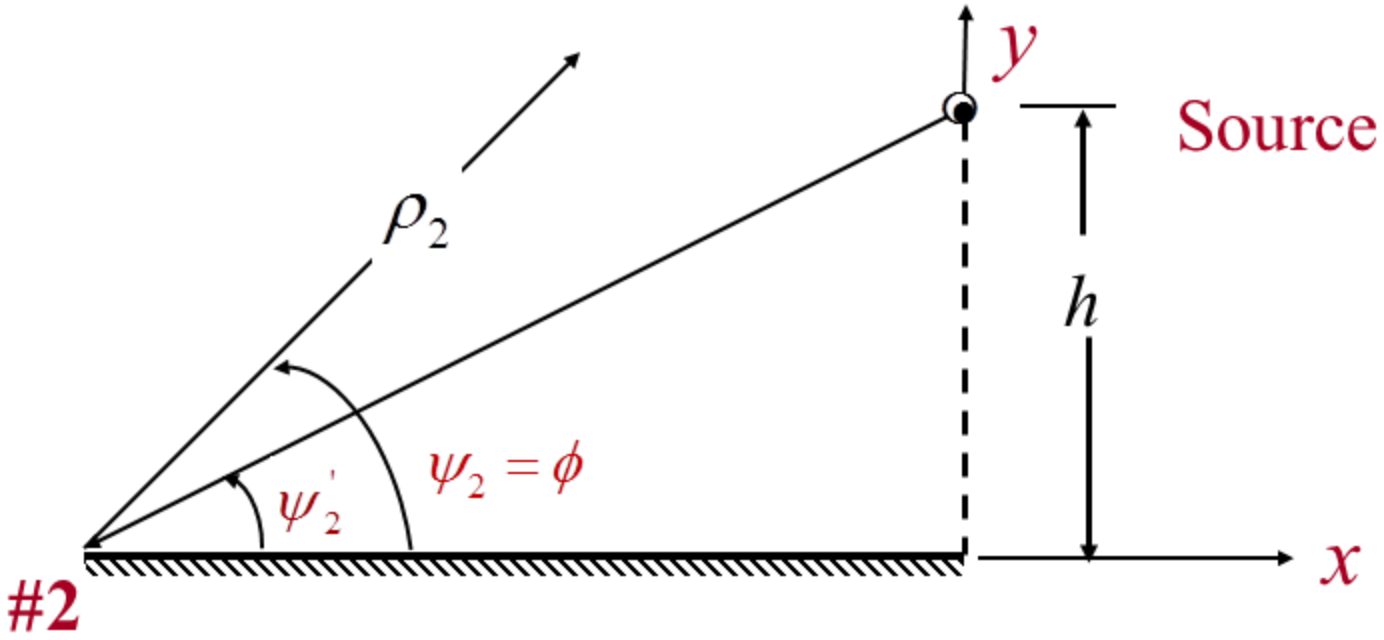

$$\left.\begin{aligned} \psi_2' &= \alpha \\ \psi_2 &= \phi \\ \xi_2^- &= \psi_2 - \psi_2' = \pi - \psi_2' \\ \xi_2^+ &= \psi_2 + \psi_2' = \phi + \psi_2' \end{aligned}\right\} 0^o \le \phi \le 360^o$$

Geometrical Optics (GO) Field

$$E_z^i(\beta\rho_i) = -\frac{\beta^2 I_o}{4\omega\varepsilon} H_0^{(2)}(\beta\rho_i) = -\eta\frac{\beta I_0}{4} H_0^{(2)}(\beta\rho_i)$$

$$E_z^r(\beta\rho_r) = +\frac{\beta^2 I_o}{4\omega\varepsilon} H_0^{(2)}(\beta\rho_r) = +\eta\frac{\beta I_0}{4} H_0^{(2)}(\beta\rho_r)$$

$$\eta = \sqrt{\frac{\mu}{\varepsilon}}$$

For large arguments

$$H_0^{(2)}(\beta\rho) \overset{\beta\rho\to\infty}{\simeq} \sqrt{\frac{2j}{\pi\beta\rho}} e^{-j\beta\rho}$$

Thus

$$E_z^i(\beta\rho_i) \simeq -\eta \frac{\beta I_o}{4}\sqrt{\frac{2j}{\pi\beta}}\frac{e^{-j\beta\rho_i}}{\sqrt{\rho_i}} = E_o \cdot \frac{e^{-j\beta\rho_i}}{\sqrt{\rho_i}}$$

$$E_z^r(\beta\rho_r) \simeq +\eta \frac{\beta I_o}{4}\sqrt{\frac{2j}{\pi\beta}}\frac{e^{-j\beta\rho_r}}{\sqrt{\rho_r}} = -E_o \cdot \frac{e^{-j\beta\rho_r}}{\sqrt{\rho_r}}$$

$$E_0 = -\eta \frac{\beta I_o}{4}\sqrt{\frac{2j}{\pi\beta}} = -\eta\beta I_o\sqrt{\frac{j}{8\pi\beta}}$$

$$D_{s1}^{i} = -\frac{e^{-j\pi/4}}{2n\sqrt{2\pi\beta}} \left\langle \left\{ C^{+}(\xi_1^{-}, n) F^{+}\left[\beta dg^{+}(\xi_1^{-})\right] + \left\{ C^{-}(\xi_1^{-}, n) F^{+}\left[\beta dg^{+}(\xi_1^{-})\right] \right\rangle \right|_{\xi^{-} = \psi_1 - \psi_1'}$$

$$D_{s1}^{r} = -\frac{e^{-j\pi/4}}{2n\sqrt{2\pi\beta}} \left\langle \left\{ C^{+}(\xi_1^{+}, n) F^{+}\left[\beta dg^{+}(\xi_1^{+})\right] + C^{-}(\xi_1^{+}, n) F^{-}\left[\beta dg^{-}(\xi_1^{+})\right] \right\} \right\rangle \Big|_{\xi^{+} = \psi_1 + \psi_1'}$$

$$D_{s1} = D_{s1}^{i} - D_{s1}^{r}$$

$$\left.\begin{aligned} \xi_1^- &= \psi_1 - \psi_1' = \pi - \phi - \psi_1' \\ \xi_1^+ &= \psi_1 + \psi_1' = \pi - \phi + \psi_1' \end{aligned}\right\} 0^o \le \phi \le 180^o$$

$$\left.\begin{aligned} \xi_1^- &= \psi_1 - \psi_1' = 3\pi - \phi - \psi_1' \\ \xi_1^+ &= \psi_1 + \psi_1 = 3\pi - \phi + \psi_1' \end{aligned}\right\} 180^o \le \phi \le 360^o$$

$$E_{z1}^{d} = E_z^{i}(\rho_i = d, \alpha_1) D_{s1}(d, \psi_1, \psi_1', n = 2)$$

$$\cdot A_1(d, \rho_1) e^{-j\beta\rho_1}$$

$$E_z^{i}(\rho_1 = d, \alpha_1) = E_0 \frac{e^{-j\beta d}}{\sqrt{d}}$$

$$D_{s1}(d, \psi_1, \psi_1', n = 2) = D_{s1}^{i}(d, \psi_1 - \psi_1', n = 2)$$

$$- D_{s1}^{r}(d, \psi_1 + \psi_1', n = 2)$$

$$A_1(d, \rho_1) = \frac{1}{\sqrt{\rho_1}}$$

$$C^{+}(\xi_1^{-},n)=\cot\left[\frac{\pi+\xi_1^{-},}{2n}\right]_{\xi_1^{-}=\psi_1-\psi_1'}$$

$$C^{-}(\xi_1^{-},n)=\cot\left[\frac{\pi-\xi_1^{-},}{2n}\right]_{\xi_1^{-}=\psi_1-\psi_1'}$$

$$C^{+}(\xi_1^{+},n)=\cot\left[\frac{\pi+\xi_1^{+},}{2n}\right]_{\xi_1^{+}=\psi_1+\psi_1'}$$

$$C^{-}(\xi_1^{+},n)=\cot\left[\frac{\pi-\xi_1^{+},}{2n}\right]_{\xi_1^{+}=\psi_1+\psi_1'}$$

$$E_{z1}^{d} = E_0 \underbrace{\left[\frac{e^{-jkd}}{\sqrt{d}} D_{s1} \right]} \frac{e^{-j\beta\rho_1}}{\sqrt{\rho_1}}$$

$$= E_0 \underbrace{\left[V_B^i(d, \xi_1^-, n=2) - V_B^r(d, \xi_1^+, n=2 \right]} \frac{e^{-j\beta\rho_1}}{\sqrt{\rho_1}}$$

$$\left.\begin{aligned} \xi_1^- &= \psi_1 - \psi_1' = \pi - \phi - \psi_1' \\ \xi_1^+ &= \psi_1 + \psi_1 = \pi - \phi + \psi_1' \end{aligned}\right\} 0^o \le \phi \le 180^o$$

$$\left.\begin{aligned} \xi_1^- &= \psi_1 - \psi_1' = 3\pi - \phi - \psi_1' \\ \xi_1^+ &= \psi_1 + \psi_1 = 3\pi - \phi + \psi_1' \end{aligned}\right\} 180^o \le \phi \le 360^o$$

Diffractions (Wedge #2)

In a similar manner

$$E_{z2}^{d} = E_0 \left[\frac{e^{-j\beta d}}{\sqrt{d}} D_{s2} \right] \frac{e^{-j\beta\rho_2}}{\sqrt{\rho_2}}$$

$$= E_0 \left[V_B^i(d, \xi_2^-, n=2) - V_B^r(d, \xi_2^+, n=2) \right] \frac{e^{-j\beta\rho_2}}{\sqrt{\rho_2}}$$

$$\left.\begin{aligned} \xi_2^- &= \psi_2 - \psi_2' = \phi - \psi_2' \\ \xi_2^+ &= \psi_2 + \psi_2' = \phi + \psi_2' \end{aligned}\right\} 0^\circ \le \phi \le 360^\circ$$

Reflection Geometry

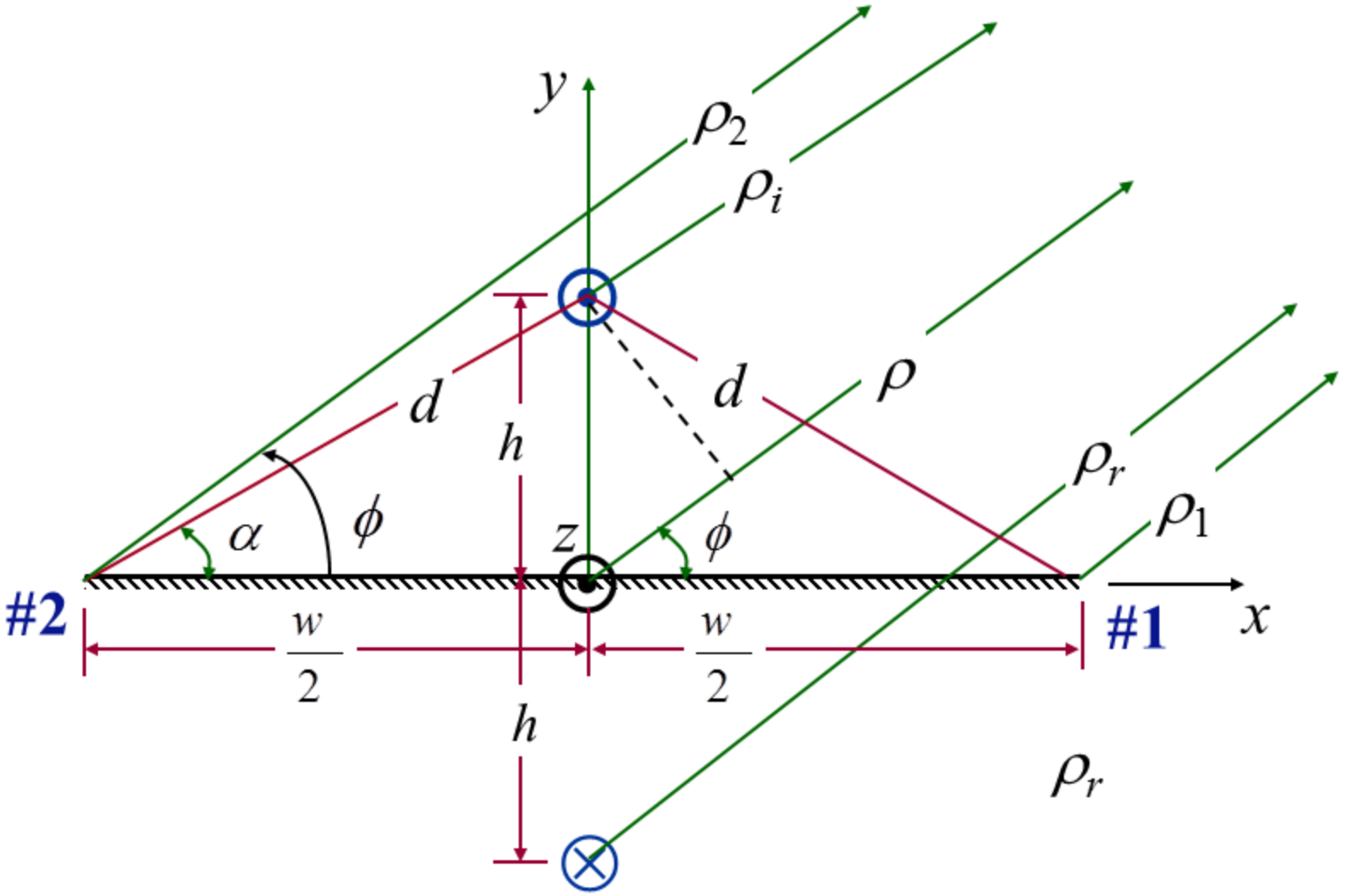

For Far-Field Observations

$$\rho_i \simeq \rho - h\cos\left(\frac{\pi}{2} - \phi\right) = \rho - h\sin\phi$$

$$\rho_r \simeq \rho + h\cos\left(\frac{\pi}{2} - \phi\right) = \rho + h\sin\phi$$

$$\rho_1 \simeq \rho - \frac{w}{2}\cos\phi$$

$$\rho_2 \simeq \rho + \frac{w}{2}\cos\phi$$

} For phase terms

$$\rho_i \simeq \rho_r \simeq \rho_1 \simeq \rho_2 \simeq \rho$$ } For amplitude terms

Thus in Far-Field (Summary)

$0^\circ \le \phi \le 360^\circ$

$$E_z^i = E_0 e^{+j\beta h \sin\phi}\left(\frac{e^{-j\beta\rho}}{\sqrt{\rho}}\right) \qquad \left\{\begin{array}{c} 0 \le \phi \le \pi + \psi_0 \\ 2\pi - \psi_0 \le \phi \le 2\pi \end{array}\right\}$$

$$E_z^r = -E_0 e^{-j\beta h \sin\phi}\left(\frac{e^{-j\beta\rho}}{\sqrt{\rho}}\right) \qquad \left\{\psi_0 \le \phi \le \pi - \psi_0\right\}$$

$$E_{z1}^d = E_0 V_{B1}^s e^{+j\frac{\beta w}{2}\cos\phi}\left(\frac{e^{-j\beta\rho}}{\sqrt{\rho}}\right) \qquad \left\{0 \le \phi \le 2\pi\right\}$$

$$E_{z2}^d = E_0 V_{B2}^s e^{-j\frac{\beta w}{2}\cos\phi}\left(\frac{e^{-j\beta\rho}}{\sqrt{\rho}}\right) \qquad \left\{0 \le \phi \le 2\pi\right\}$$

Note: The $E_0 e^{-j\beta\rho} / \sqrt{\rho}$ factor can be suppressed.

Normalized Pattern of Line Source Above Strip

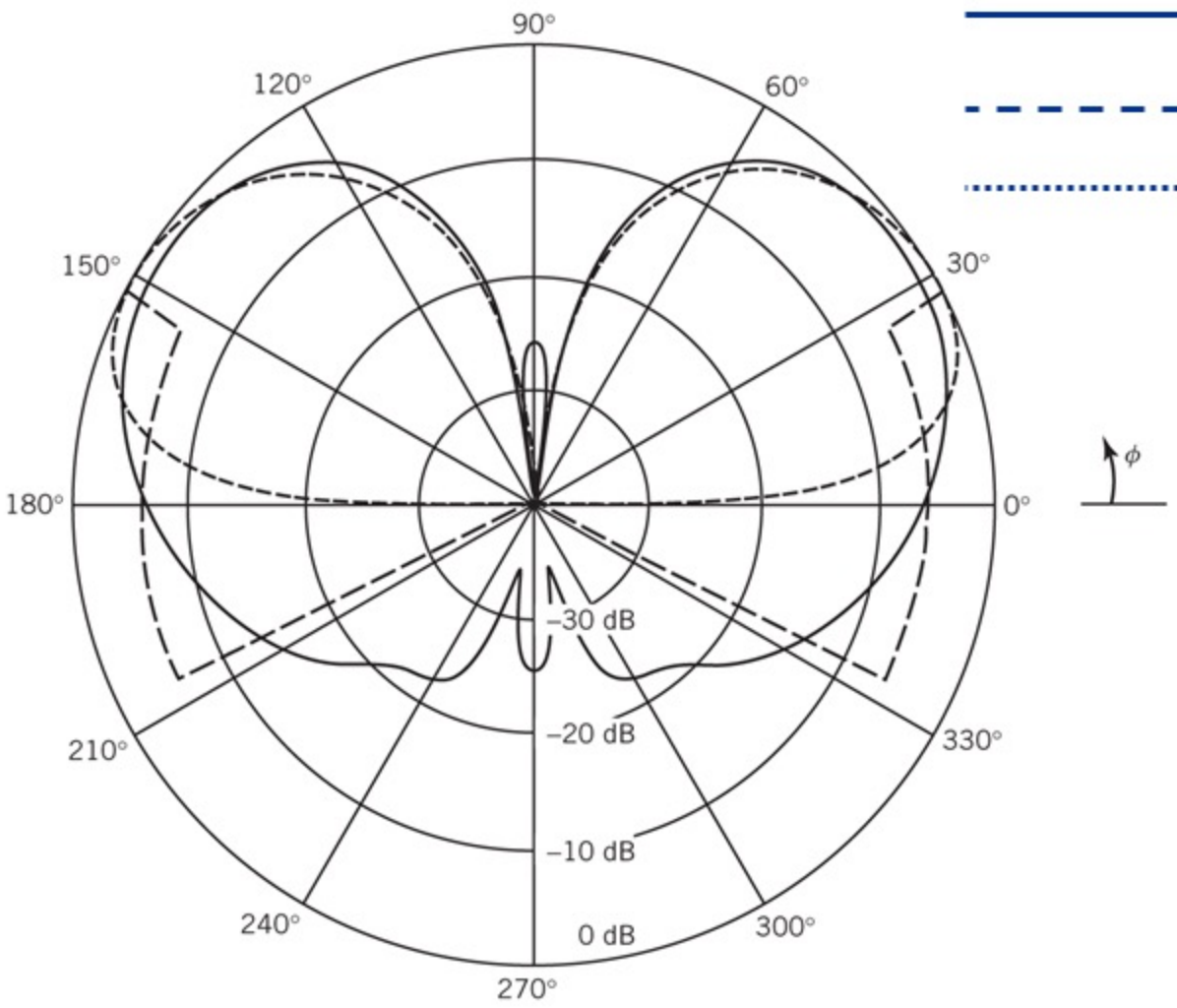

GTD $(w = 2\lambda,\ h = 0.5\lambda)$

GO $(w = 2\lambda,\ h = 0.5\lambda)$

GO $(w = \infty,\ h = 0.5\lambda)$

$$w = 2\lambda, \infty$$

$$h = 0.5\lambda$$

Scattering From Strip

Physical Optics

Chapter 13
Geometrical Theory of Diffraction

Finite Width Strip

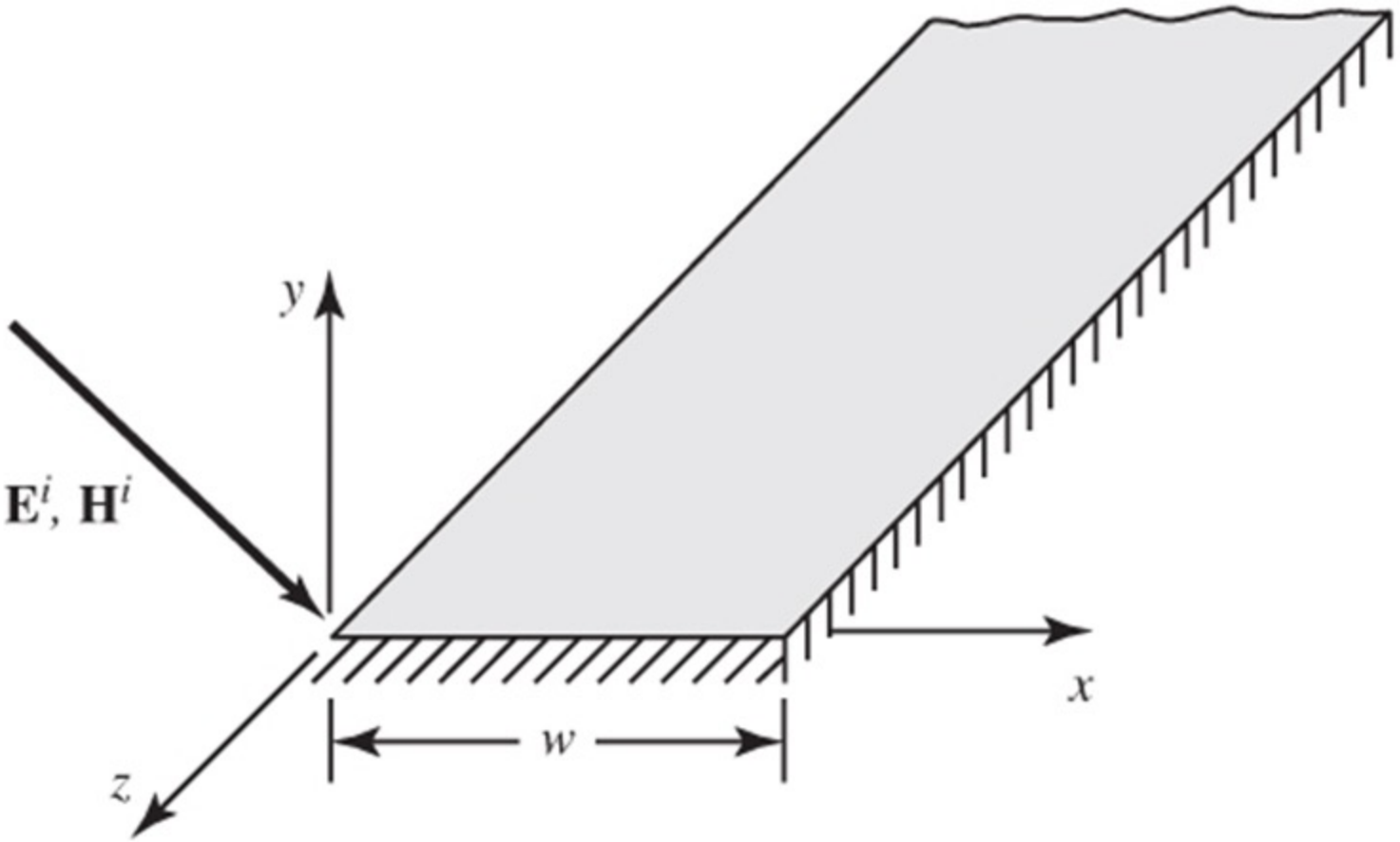

Fig. 11-4 (a)

TM^z Polarization

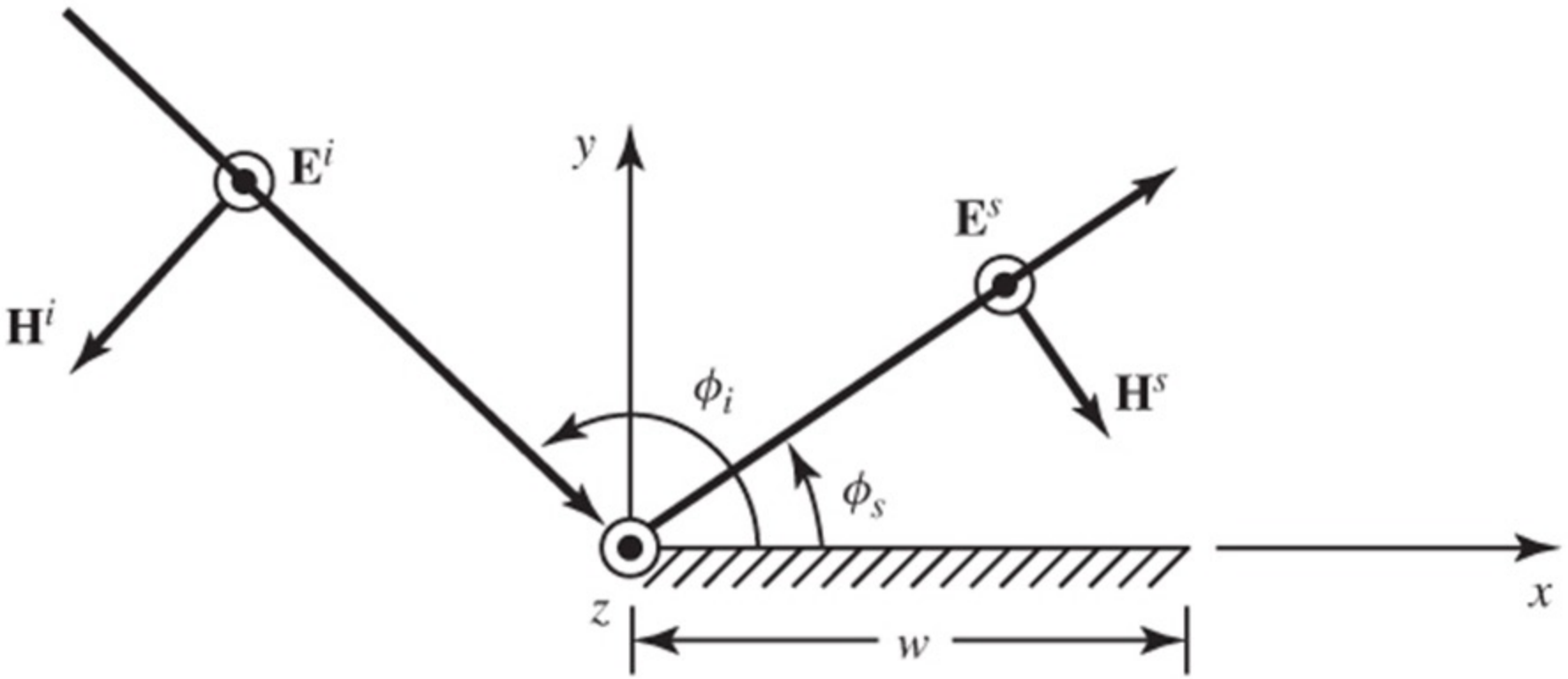

Fig. 11-4 (b)

TE^z Polarization

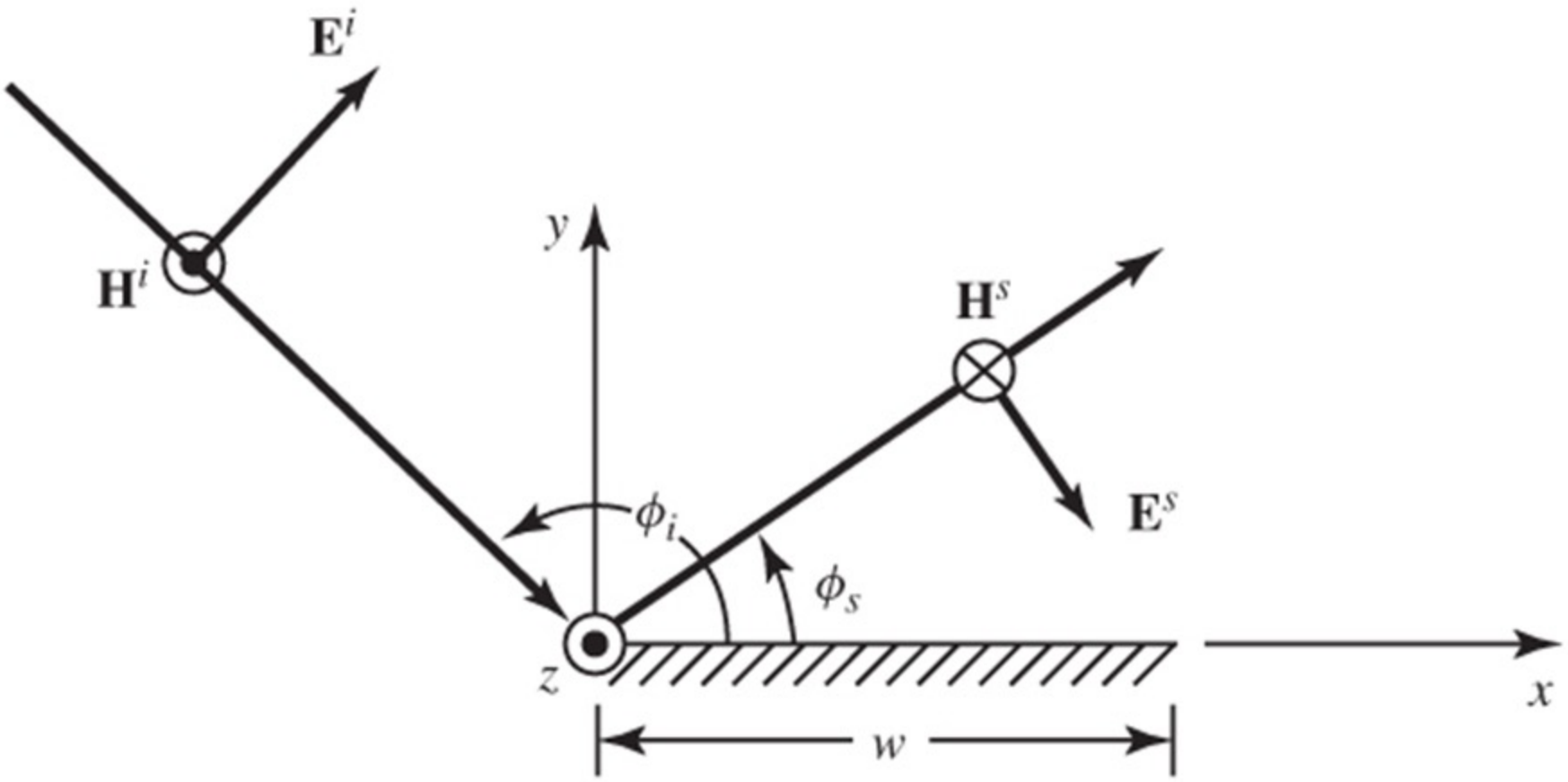

Fig. 11-4 (c)

Scattering by a Strip Using Diffractions

Example 13-5

Scattering From a PEC Strip

Example 13 – 5 :

A soft polarized uniform plane wave, whose electric field amplitude is E_o, is incident upon a two-dimensional PEC strip of width w, as shown in Figure 12-13a and Figure 13-28.

1. Determine the backscattered ($\phi = \phi'$) electric field and its backscattered scattering width (SW).
2. Compute and plot the normalized SW ($\sigma_{2\text{-D}}$) in dB/m (dBm) when $w = 2\lambda$ and $f = 10$ GHz.

Solution:

It follows.

Plane Wave Incidence

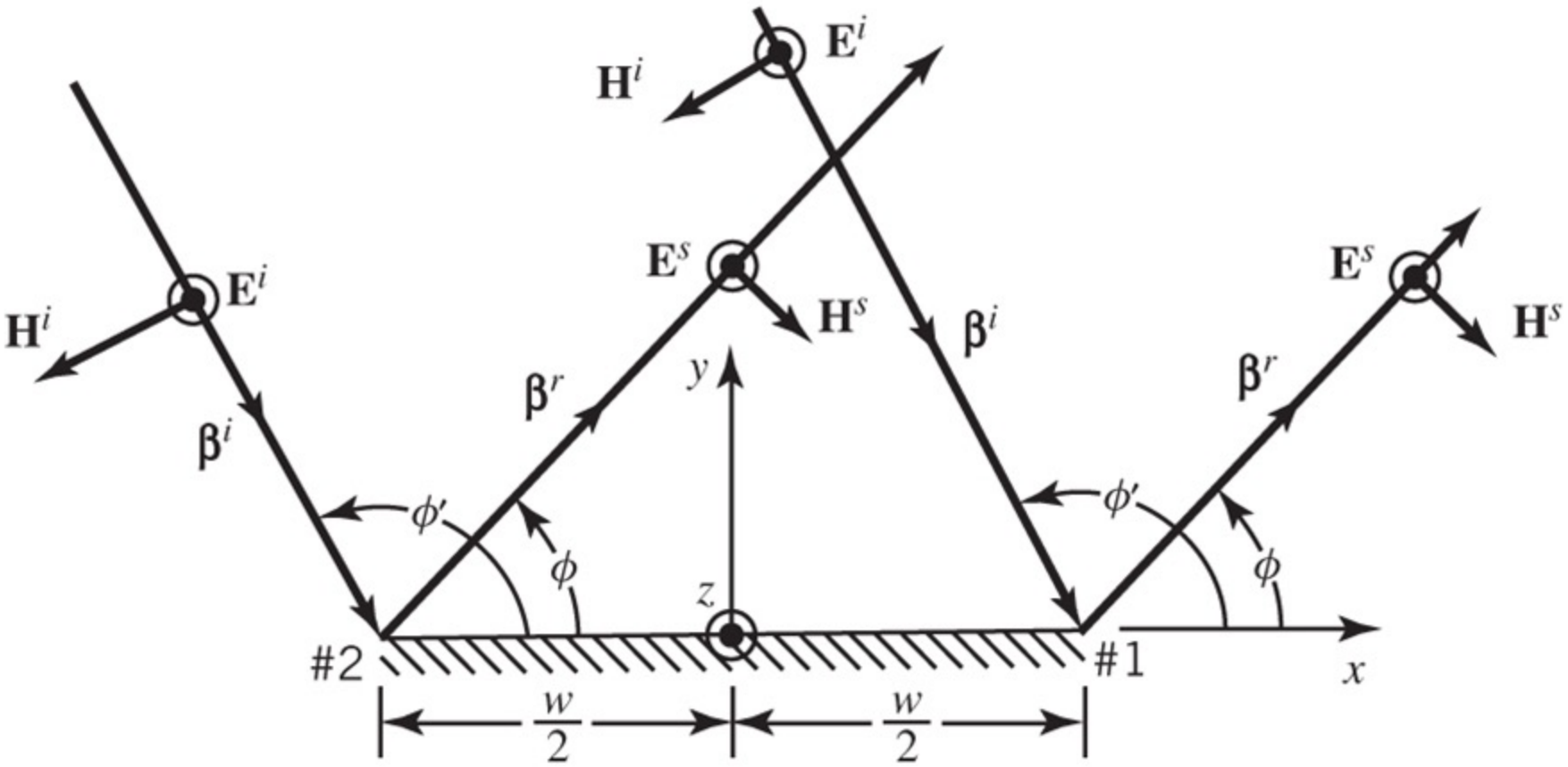

Fig. 13-28(a)

Plane Wave Diffraction

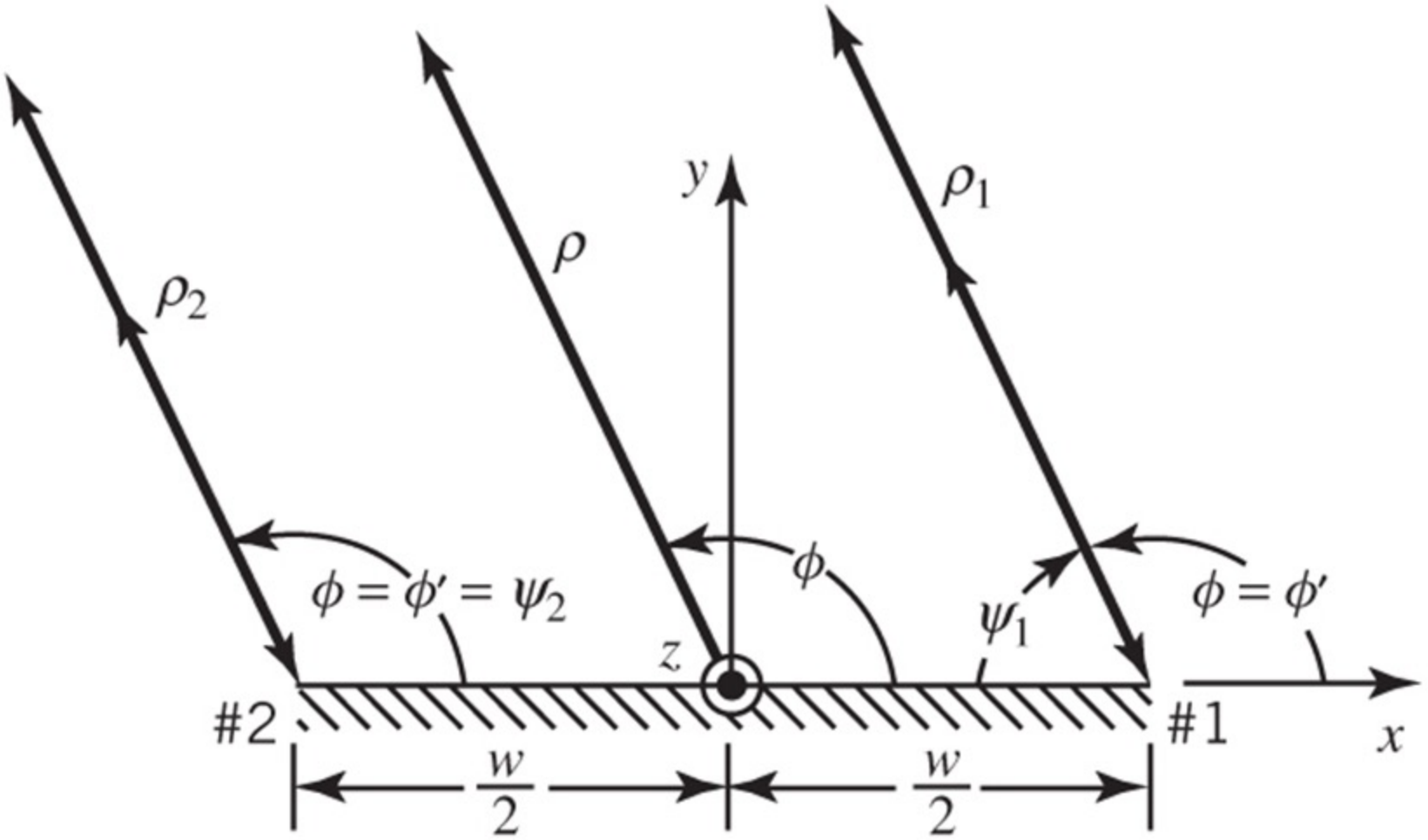

Fig. 13-28(b)

Geometry and Field Expressions

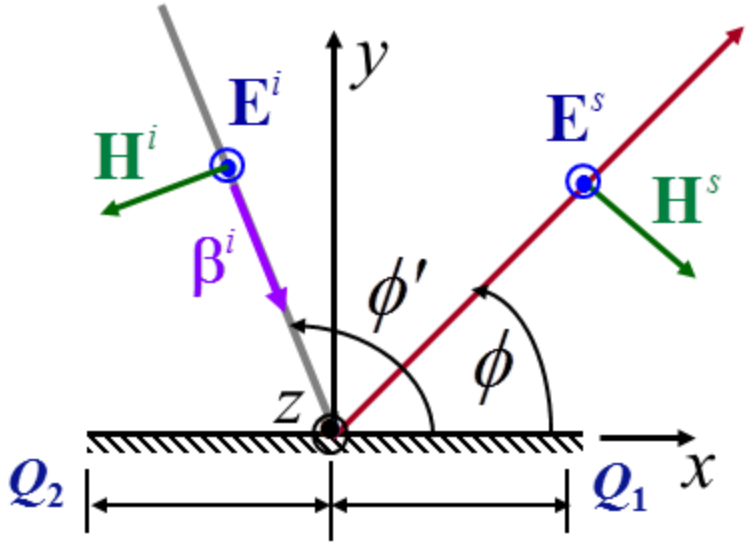

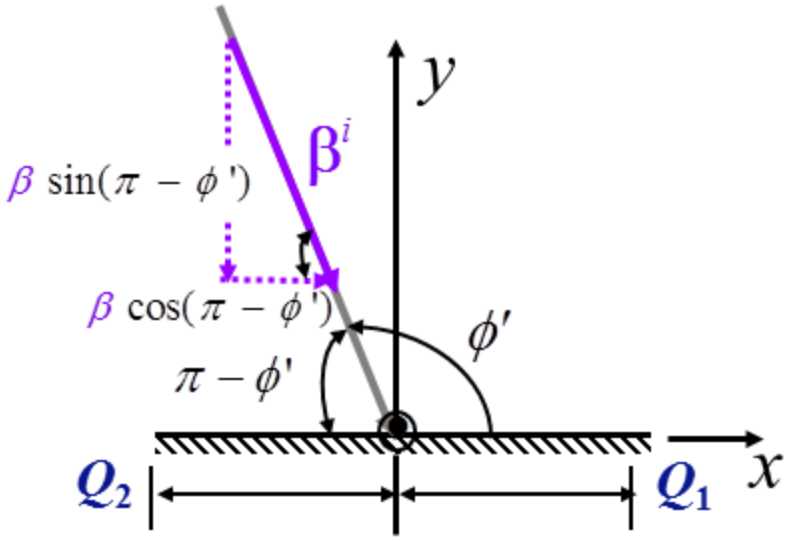

$$\mathbf{E}^i = \hat{a}_z E_o e^{-j\boldsymbol{\beta}^i \cdot \mathbf{r}}, \quad |\boldsymbol{\beta}^i| = \beta$$

$$\mathbf{E}^i = \hat{a}_z E_o e^{+j\beta(x\cos\phi' + y\sin\phi')}$$

$$\mathbf{E}^i(Q_1)\Big|_{x=\frac{w}{2}, y=0} = \hat{a}_z E_o e^{+j\frac{\beta w}{2}\cos\phi'}$$

$$\boldsymbol{\beta}^i = \hat{a}_x \beta \cos(\pi - \phi') + \hat{a}_y \beta \sin(\pi - \phi')$$

$$\boldsymbol{\beta}^i = \hat{a}_x \beta \cos\phi' - \hat{a}_y \beta \sin\phi'$$

$$\mathbf{r} = \hat{a}_x x + \hat{a}_y y + \hat{a}_z z$$

$$\boldsymbol{\beta}^i \cdot \mathbf{r} = \beta(x\cos\phi' + y\sin\phi')$$

For Backscattering

$$\underline{E}_1^d = \underline{E}^i(Q_1) \cdot \tilde{\overline{D}}_1^s A_1(\rho_1) e^{-j\beta\rho_1}$$

$$\underline{E}^i(Q_1) = \underline{E}^i \Big|_{\substack{x=\frac{w}{2} \\ y=0 \\ \phi=\phi'}} = \hat{a}_z E_o e^{j\frac{\beta w}{2}\cos\phi}$$

$$A_1(\rho_1) = \frac{1}{\sqrt{\rho_1}}$$

$$\widetilde{D}_1^s = \hat{a}_z \hat{a}_z \frac{e^{-j\frac{\pi}{4}} \sin\left(\frac{\pi}{n}\right)}{n\sqrt{2\pi\beta}} \left\{ \frac{1}{\cos\left(\frac{\pi}{n}\right) - \cos\left(\frac{\psi_1 - \psi_1'}{n}\right)} - \frac{1}{\cos\left(\frac{\pi}{n}\right) - \cos\left(\frac{\psi_1 + \psi_1'}{n}\right)} \right\}_{\substack{n=2 \\ \psi_1=\psi_1'=\pi-\phi}}$$

$$\widetilde{D}_1^s = -\hat{a}_z \hat{a}_z \frac{e^{-j\pi/4}}{2\sqrt{2\pi\beta}} \left[1 + \frac{1}{\cos\phi} \right]$$

Geometry For Backscattering

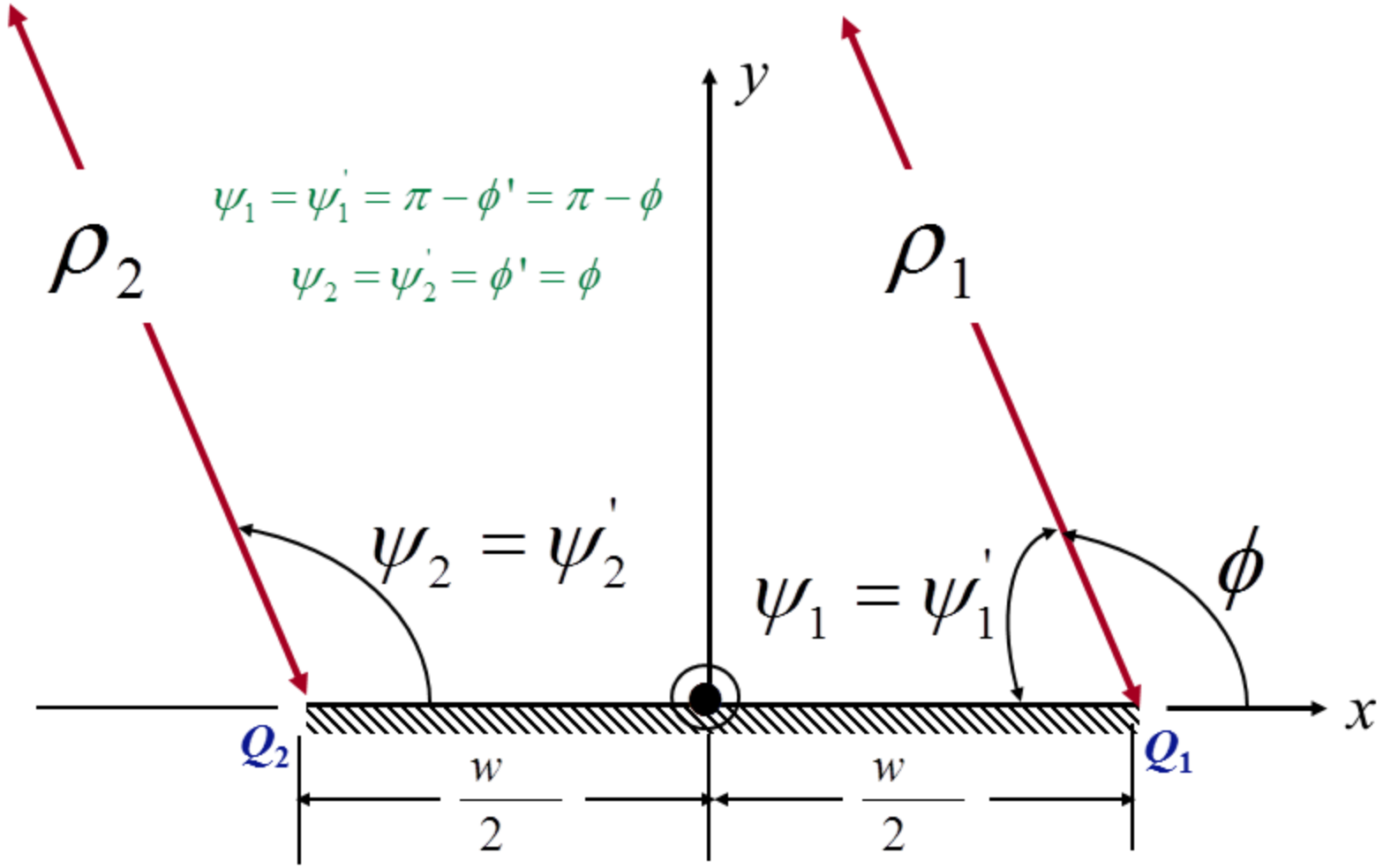

$$\underline{E}_1^d = -\hat{a}_z E_0 \frac{e^{-j\pi/4} e^{j\frac{\beta w}{2}\cos\phi}}{2\sqrt{2\pi\beta}} \left\{1 + \frac{1}{\cos\phi}\right\} \frac{e^{-j\beta\rho_1}}{\sqrt{\rho_1}}$$

Similarly, it can be shown that:

$$\underline{E}_2^d = -\hat{a}_z E_0 \frac{e^{-j\pi/4} e^{-j\frac{\beta w}{2}\cos\phi}}{2\sqrt{2\pi\beta}} \left\{1 - \frac{1}{\cos\phi}\right\} \frac{e^{-j\beta\rho_2}}{\sqrt{\rho_2}}$$

For far-field observations:

$$\left.\begin{aligned} \rho_1 &\simeq \rho + \frac{w}{2}\cos(\pi - \phi) = \rho - \frac{w}{2}\cos\phi \\ \rho_2 &\simeq \rho - \frac{w}{2}\cos\left(\frac{\pi}{2} - \phi\right) = \rho + \frac{w}{2}\cos\phi \end{aligned}\right\} \text{For phase terms}$$

$$\rho_1 \simeq \rho_2 \simeq \rho \qquad \text{For amplitude terms}$$

Geometry For Backscattering

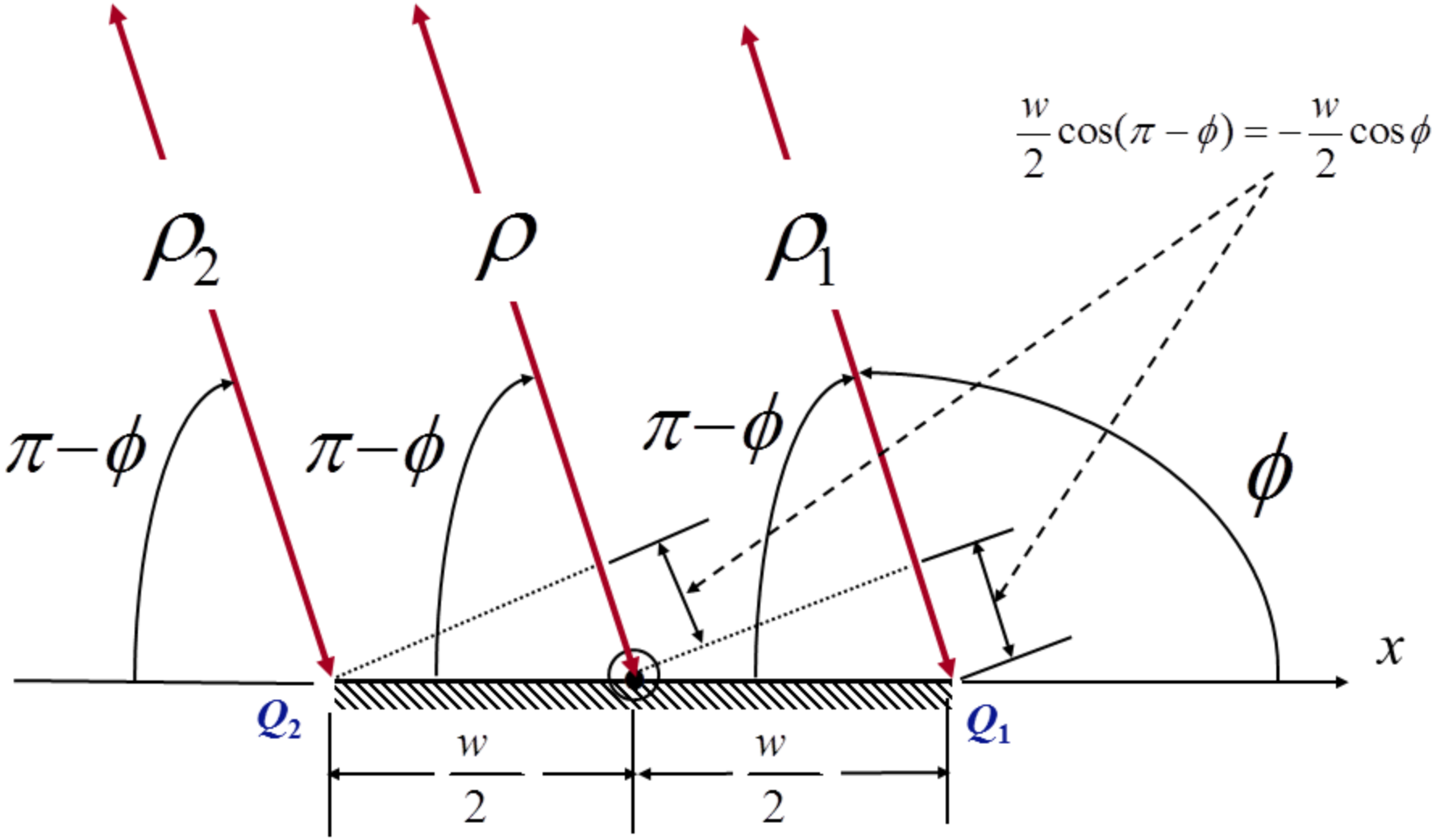

$$\underline{E}_1^d = -\hat{a}_z E_0 \frac{e^{-j\pi/4}}{2\sqrt{2\pi\beta}} \left\{ 1 + \frac{1}{\cos\phi} \right\} e^{j\beta w \cos\phi} \frac{e^{-j\beta\rho}}{\sqrt{\rho}}$$

$$\underline{E}_2^d = -\hat{a}_z E_0 \frac{e^{-j\pi/4}}{2\sqrt{2\pi\beta}} \left\{ 1 - \frac{1}{\cos\phi} \right\} e^{-j\beta w \cos\phi} \frac{e^{-j\beta\rho}}{\sqrt{\rho}}$$

$$\underline{E}_t^d = E_1^d + E_2^d$$

$$E_t^d = -\hat{a}_z E_o \frac{e^{-j\pi/4}}{\sqrt{2\pi\beta}} \left[\cos(\beta w \cos\phi) + j(\beta w) \frac{\sin(\beta w \cos\phi)}{\beta w \cos\phi} \right] \frac{e^{-j\beta\rho}}{\sqrt{\rho}}$$

Since there are no GO fields in the baskcattered direction (Snell's Law is not satisfied) when $\phi = \phi' \neq \pi/2$, the total diffracted field also represents the total field. In the limit as $\phi = \phi' = \pi/2$, each diffracted field exhibits a singularity; however, the total diffracted field is finite because the singularity of one diffracted field compensates for the singularity of the other.

This is also evident at normal incidence as long as the edges of the two diffracted wedges are parallel to each other, even though the included angles of the two wedges are not necessarily the same [39]. In addition, the limiting value of the diffracted field at normal incidence reduces and represents also the GO scattered field.

$$\left|\underline{E}_t^d\right|^2 = \frac{\left|E_o\right|^2}{2\pi\beta\rho}\left\{\cos^2(\beta w\cos\phi) + (\beta w)^2\left[\frac{\sin(\beta w\cos\phi)}{\beta w\cos\phi}\right]^2\right\}$$

$$\sigma_{2-D} = \lim_{\rho\to\infty}\left\{2\pi\rho\frac{\left|E_t^d\right|^2}{\left|E^i\right|^2}\right\}$$

$$\sigma_{2-D} = \frac{\lambda}{2\pi}\left\{\cos^2(\beta w\cos\phi) + (\beta w)^2\left[\frac{\sin(\beta w\cos\phi)}{\beta w\cos\phi}\right]^2\right\}$$

$$\sigma_{2-D}\Big|_{\phi=\frac{\pi}{2}} = \frac{\lambda}{2\pi}\left\{1+(\beta w)^2\right\} \overset{\beta w>>1}{\simeq} \beta(w)^2$$

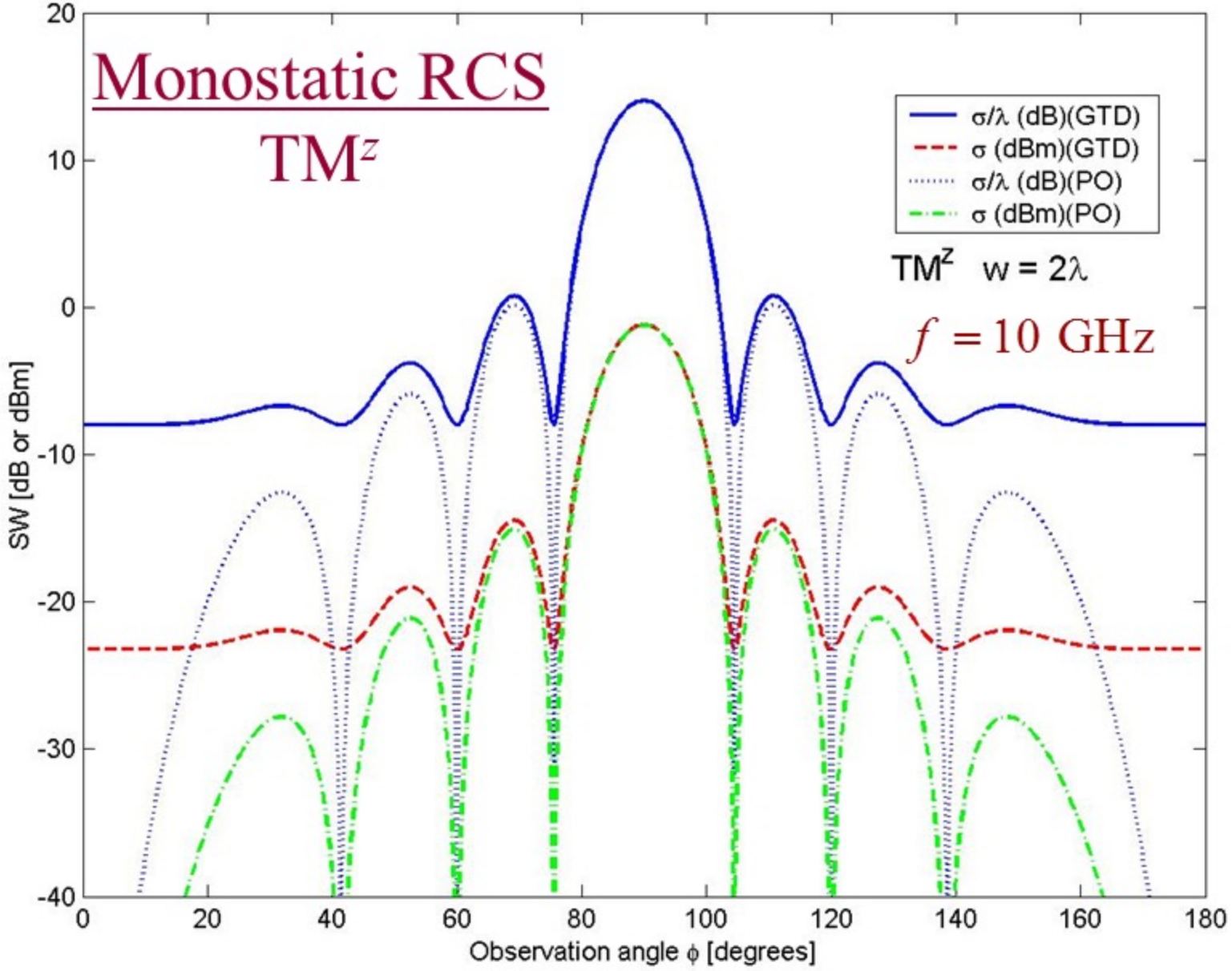

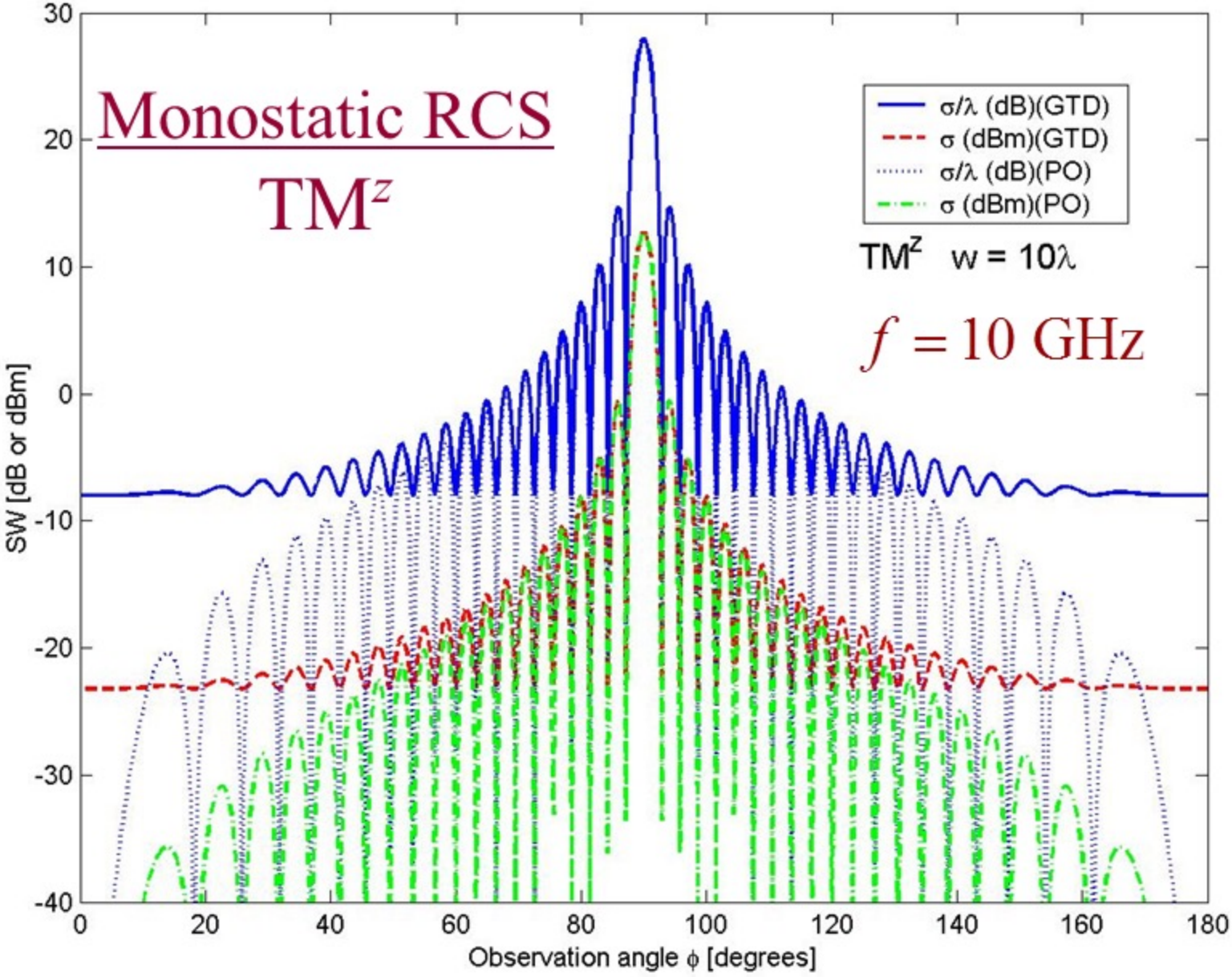

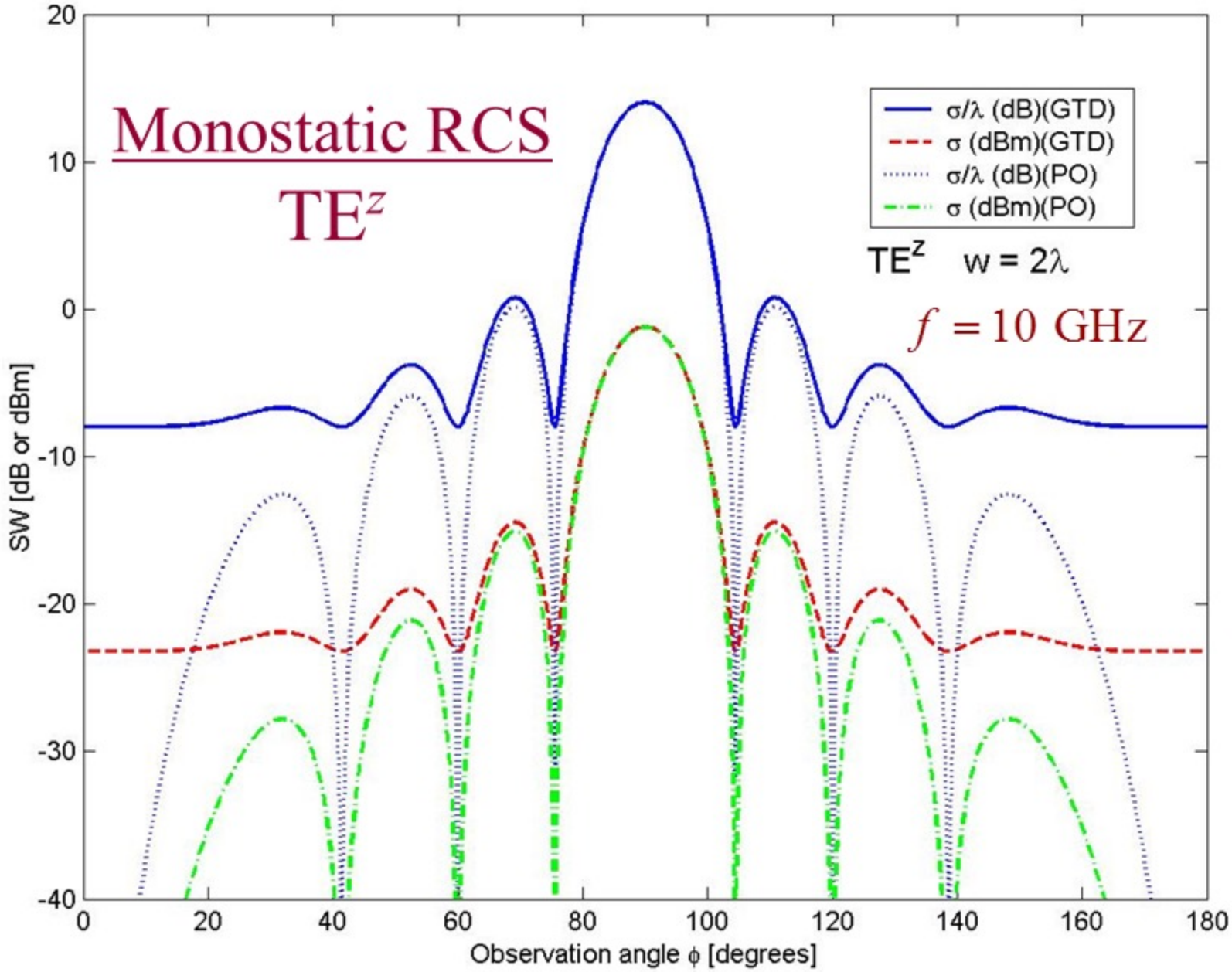

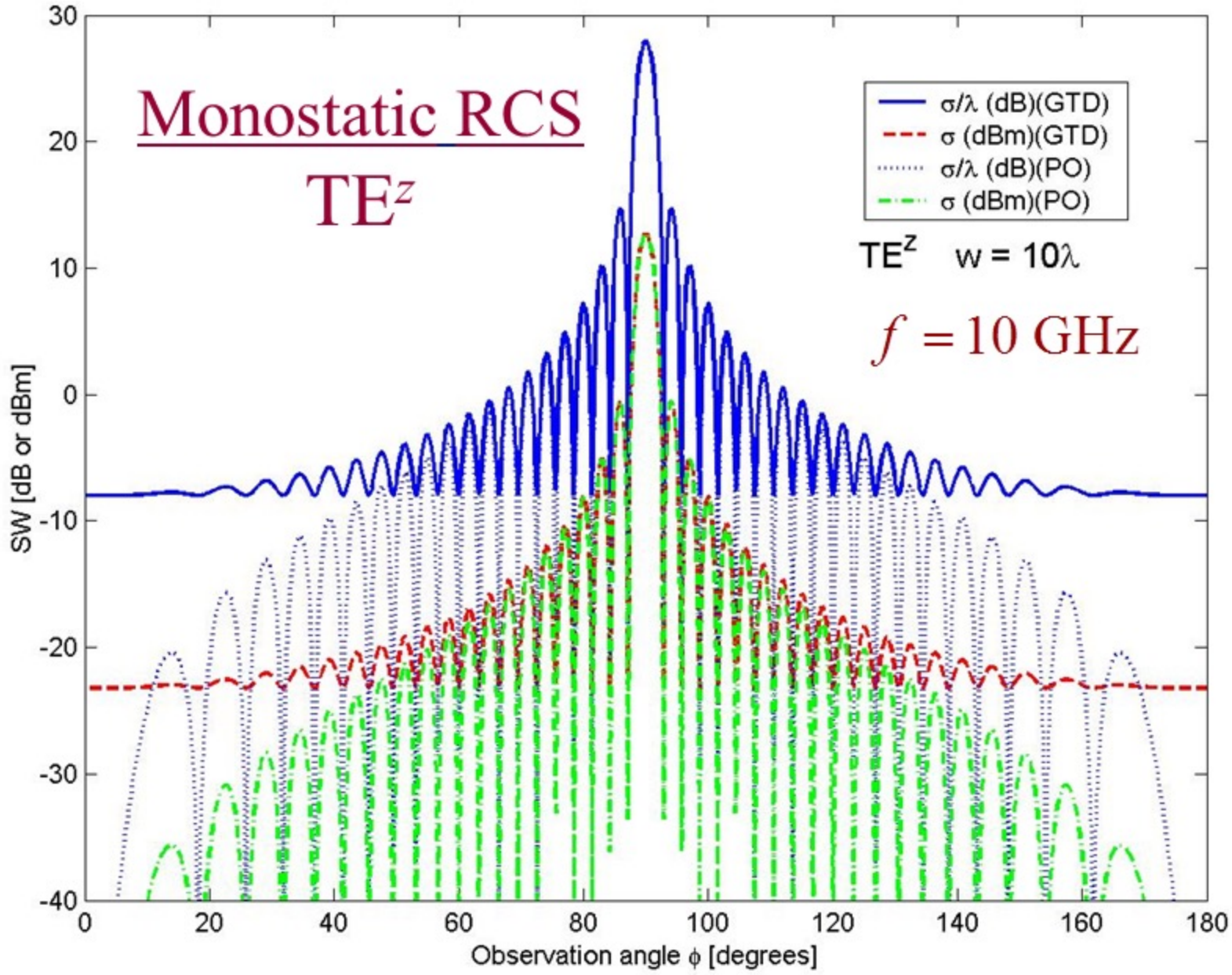

Monostatic RCS

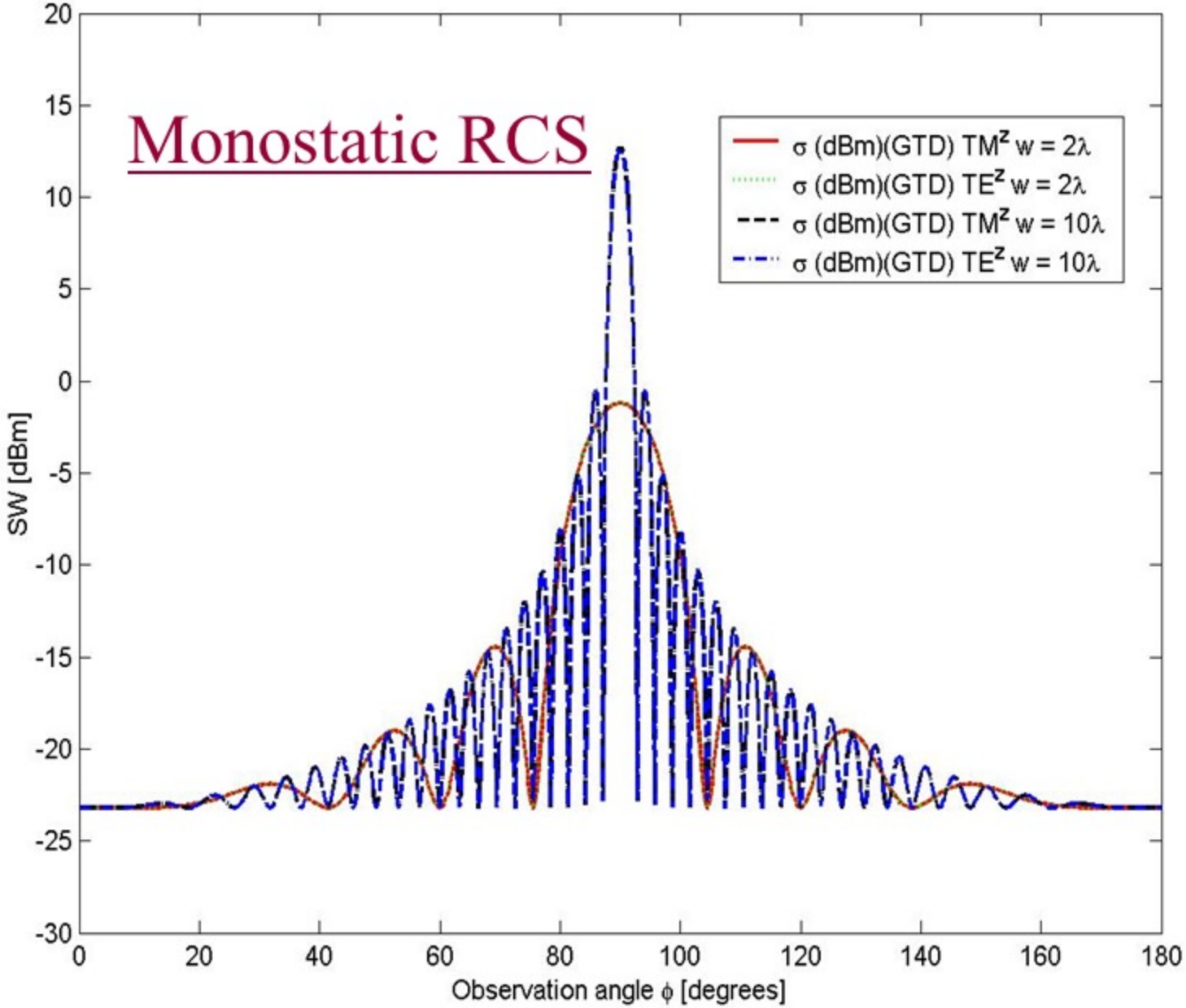

Monostatic: Soft (TM^z) ($w = 2\lambda, f = 10$ GHz)

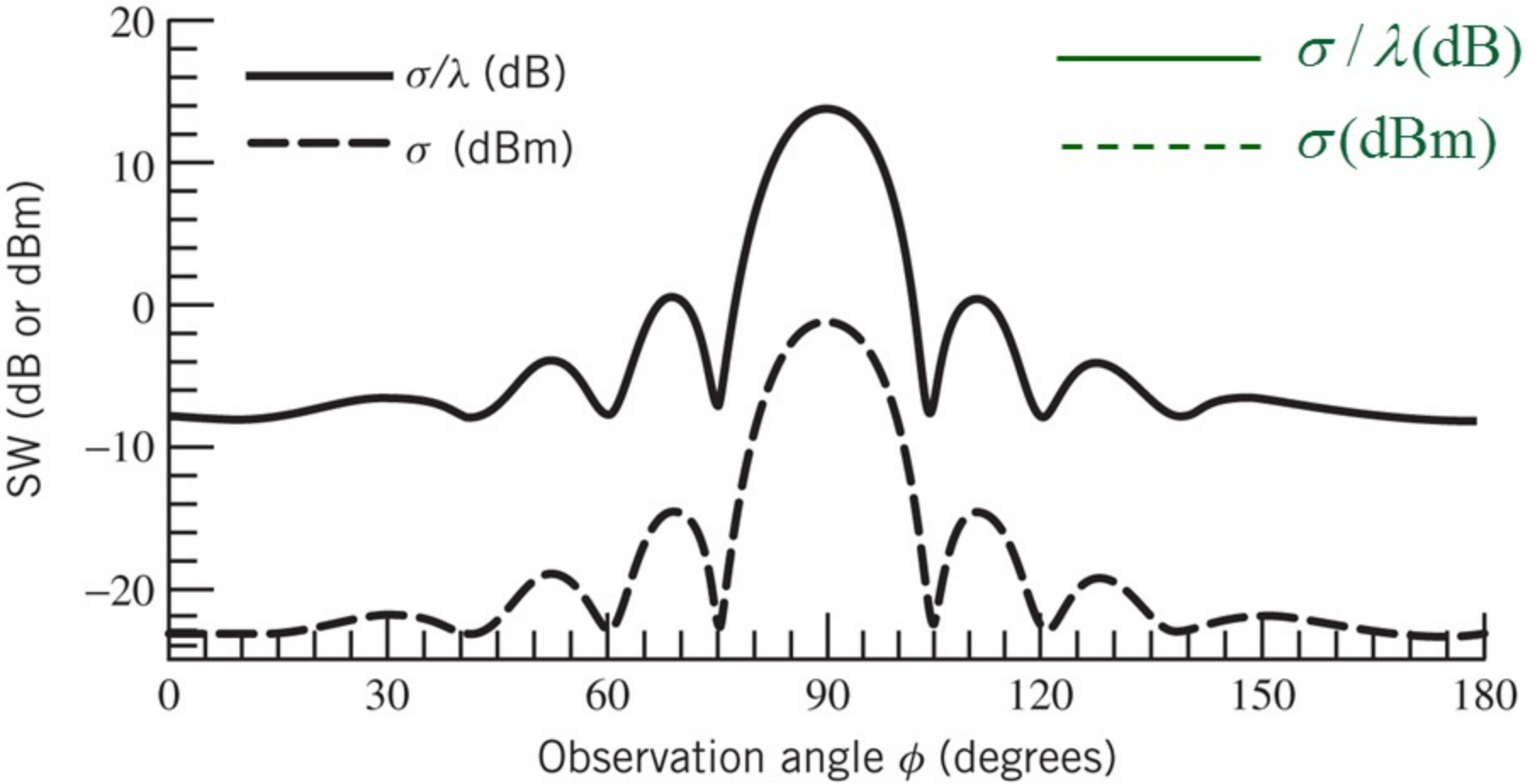

Fig. 13-29

Problem 13.36 (end of chapter problem):

A hard polarized uniform plane wave, whose magnetic field amplitude is H_o, is incident upon a two-dimensional PEC strip of width w, as shown in Figure 12-13b.

1. Determine the backscattered ($\phi = \phi'$) electric field and its bascattered scattering width (SW).
2. Compute the plot the normalized SW ($\sigma_{2\text{-D}}$) in dB/m (dBm) when $w=2\lambda$ and $f=10$ GHz.

Distance Parameter *L*

When both the source and observation are at a finite distance. Near-field observations.

Distance Parameter L

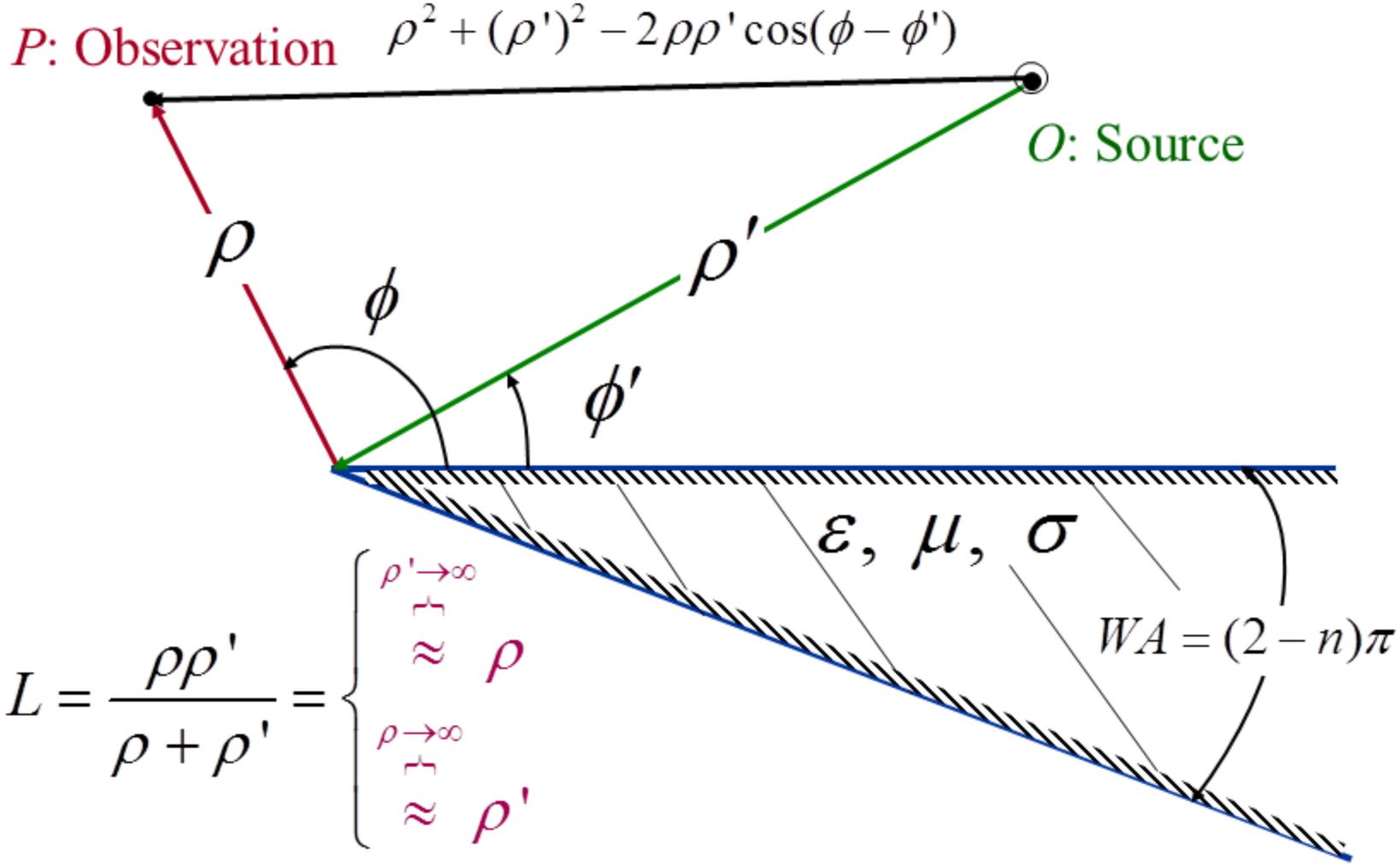

$$L = \frac{\rho\rho'}{\rho + \rho'} = \begin{cases} \overset{\rho' \to \infty}{\downarrow} \\ \approx \rho \\ \overset{\rho \to \infty}{\downarrow} \\ \approx \rho' \end{cases}$$

$$V_B^i(L,\phi-\phi',n)=V_B^i(L,\xi^-,n)$$

$$=\frac{e^{-j\beta\rho}}{\sqrt{\rho}}D^i(L,\xi^-,n) \qquad (13\text{-}84a)$$

$$V_B^r(L,\phi+\phi',n)=V_B^r(L,\xi^+,n)$$

$$=\frac{e^{-j\beta\rho}}{\sqrt{\rho}}D^r(L,\xi^+,n) \qquad (13\text{-}84b)$$

$$L=\frac{\rho\rho'}{\rho+\rho'}=\begin{cases}\overset{\rho'\to\infty}{\approx}\ \rho\\ \overset{\rho\to\infty}{\approx}\ \rho'\end{cases} \qquad (13\text{-}84)$$

Distance Parameter *L*

When both the source and observation are at a infinite distance, like in plane wave scattering; i.e., both source and observations are at far-field.

Distance Parameter L

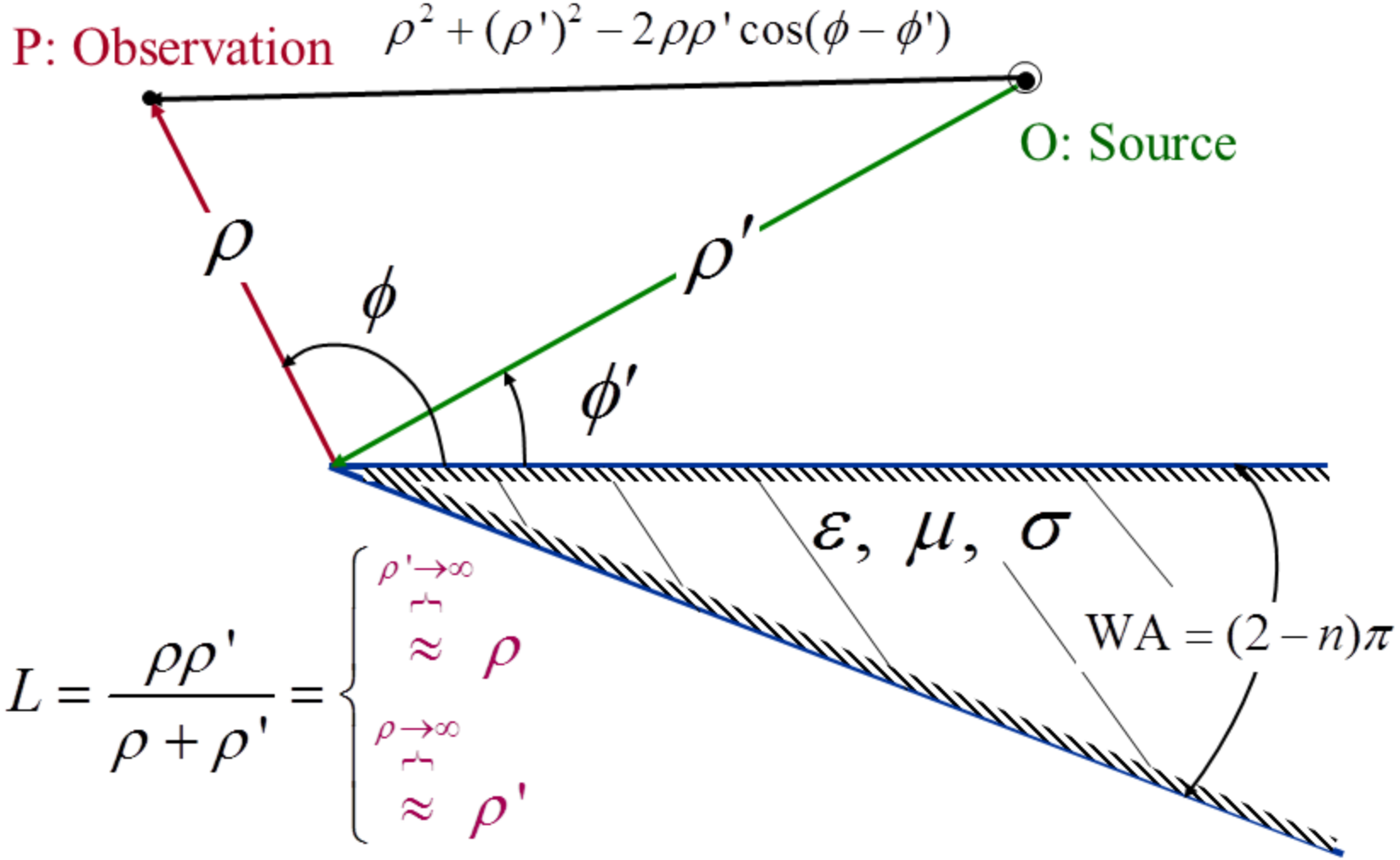

$$L = \frac{\rho\rho'}{\rho + \rho'} = \begin{cases} \overset{\rho' \to \infty}{\approx} \rho \\ \overset{\rho \to \infty}{\approx} \rho' \end{cases}$$

$$V_B^i(L,\phi-\phi',n)=V_B^i(L,\xi^-,n)$$

$$=\frac{e^{-j\beta\rho}}{\sqrt{\rho}}D^i(L,\xi^-,n) \qquad (13\text{-}84a)$$

$$V_B^r(L,\phi+\phi',n)=V_B^r(L,\xi^+,n)$$

$$=\frac{e^{-j\beta\rho}}{\sqrt{\rho}}D^r(L,\xi^+,n) \qquad (13\text{-}84b)$$

$$L=\frac{\rho\rho'}{\rho+\rho'} \overset{\rho'\to\infty,\ \rho\to\infty}{=} \infty \qquad (13\text{-}84)$$

In that case, UTD reduces to GTD and you have to use GTD because the UTD algorithm requires finite distances (L).

In order for the Keller diffraction functions and coefficients to be valid $\beta\rho g^{\pm} >> 1$. This can be achieved by one of the following conditions:

1. $\beta\rho$ and $g^{\pm}$ are large. These are satisfied if the distance ρ to the observation point is large and the observation angle ϕ is far away from either of the two shadow boundaries.

$$g^{\pm}\left(\xi^{\mp}\right) = 1 + \cos\left[\left(\phi \mp \phi'\right) - 2\pi n N^{\pm}\right]$$

2. $\beta\rho$ large and $g^{\pm}$ small. This is satisfied if the distance ρ to the observation point is large and observation angle ϕ is near either one or both of the shadow boundaries.

3. $\beta\rho$ small and $g^{\pm}$ large. This is satisfied if the distance ρ to the observation point is small and observation angle ϕ is far away from either of the two shadow boundaries.

GTD Can/Should Be Used When:

1. Observations are NOT AT or NEAR the ISB or RSB, no matter what the distances of the source or observation are.
2. The incident wave is uniform plane wave and the observations are made at distances far away from the edge of the wedge; many wavelengths (ideally at infinity) because the Transition Region along both the ISB and RSB shrink.

UTD Should/Can Be Used When:

1. Observations are made AT or NEAR the ISB or RSB, especially when the distances of the source and observation are small.
2. The incident wave is uniform plane wave and the observations are made at short distance.
3. The source is located at short distances but the observations are made at far distances (ideally at infinity).

Oblique Incidence Diffraction

E- and H-plane Diffraction by Rectangular Waveguide and Pyramidal Horn

Waveguide

Horn

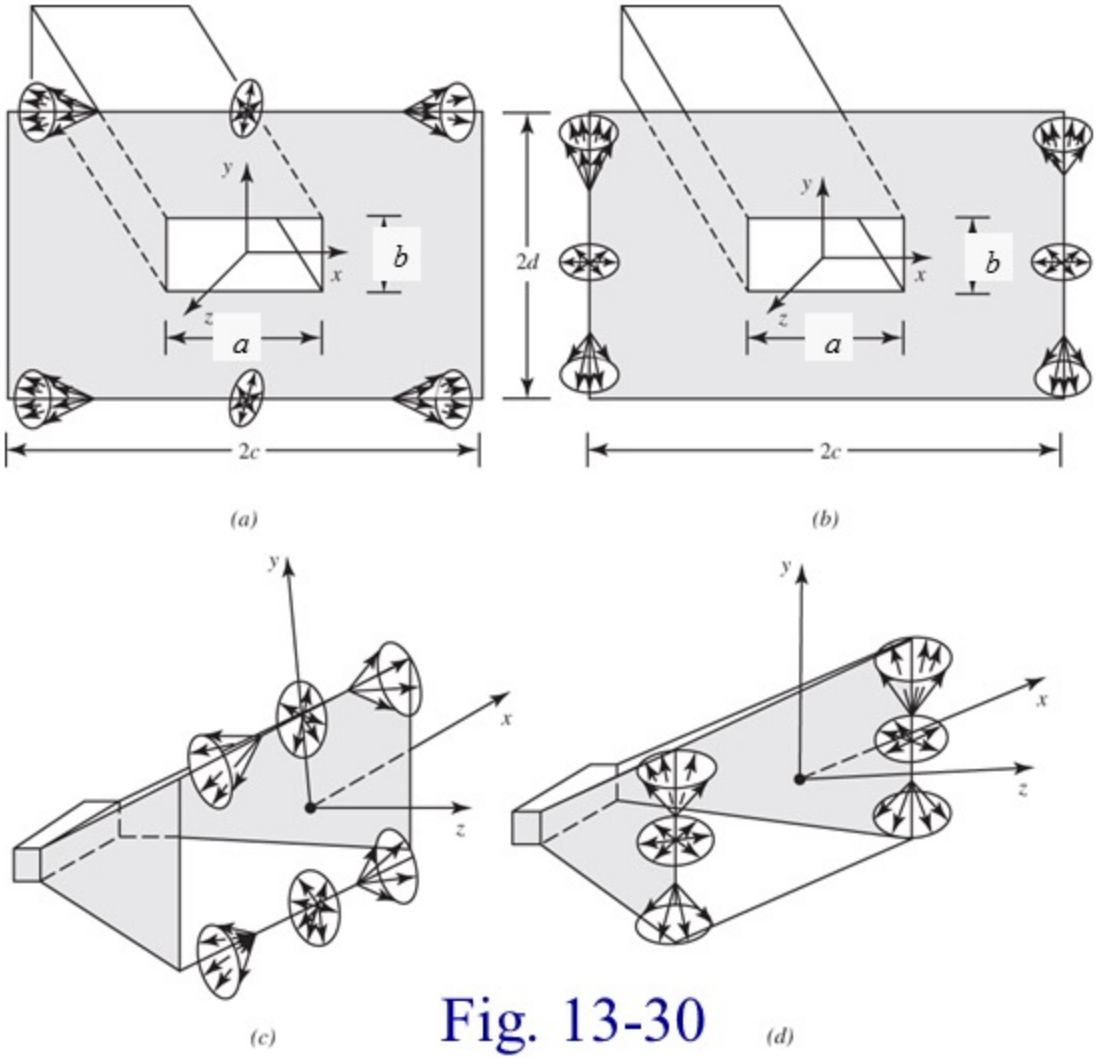

Fig. 13-30

For oblique incidence diffraction, we adopt ray-fixed coordinate systems (s', β_o', ϕ') for the source and (s, β_o, ϕ) for the observation point, in contrast to the edge-fixed cordinate system $(\rho', \phi', z'; \rho, \phi, z)$.

The diffraction coefficient for ray-fixed coordinate system can be expressed as a dyad (or 2 x 2 matrix, with 2 nonvanishing elements), whereby for an edge-fixed coordinate system it is expressed as a dyad (or 3 x 3 matrix, with 7 nonvanishing elements).

Oblique Incidence Wedge Diffraction

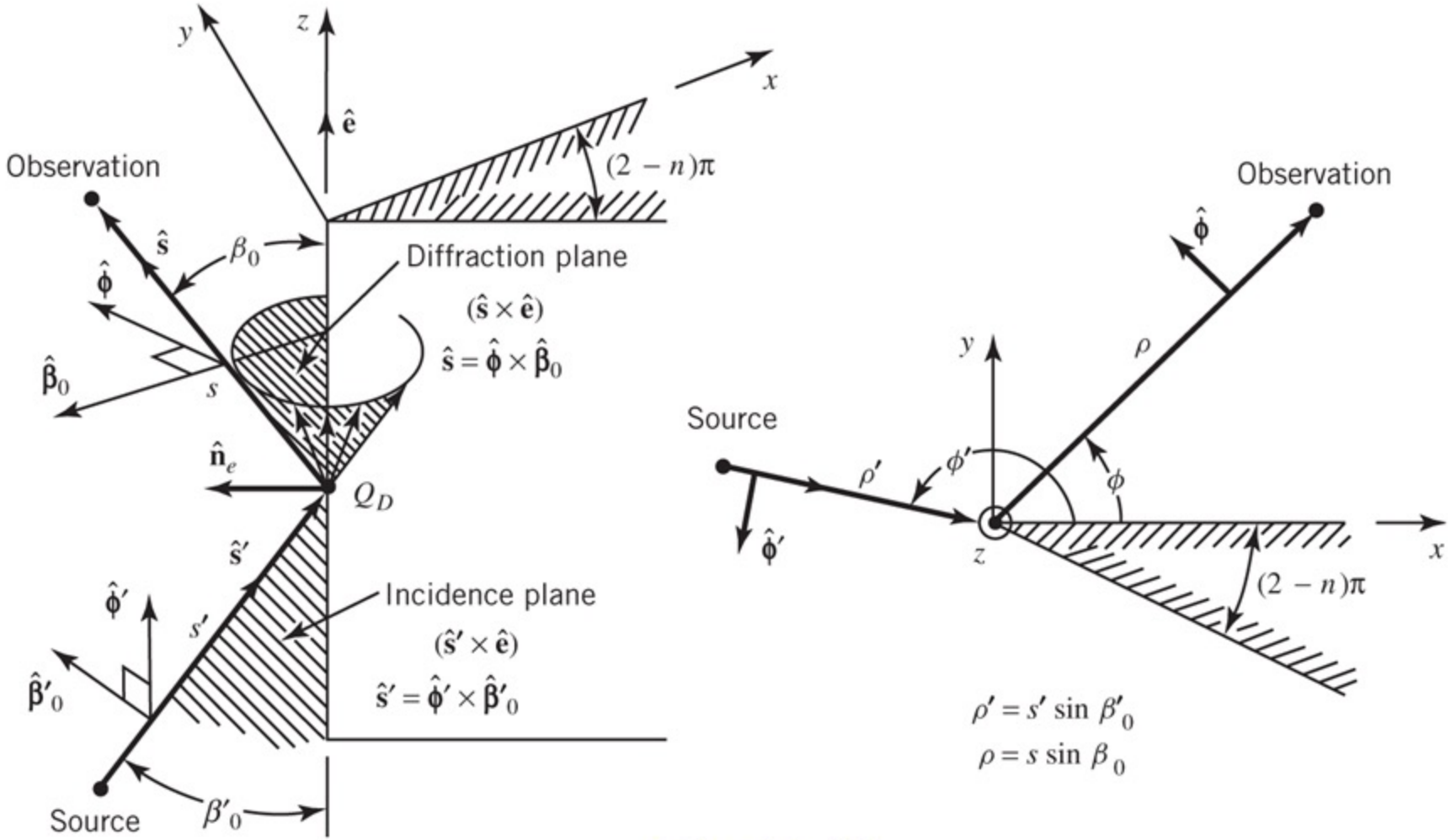

Fig. 13-31

(a) Oblique Incidence

(b) Top View

Oblique Incidence Wedge Diffraction

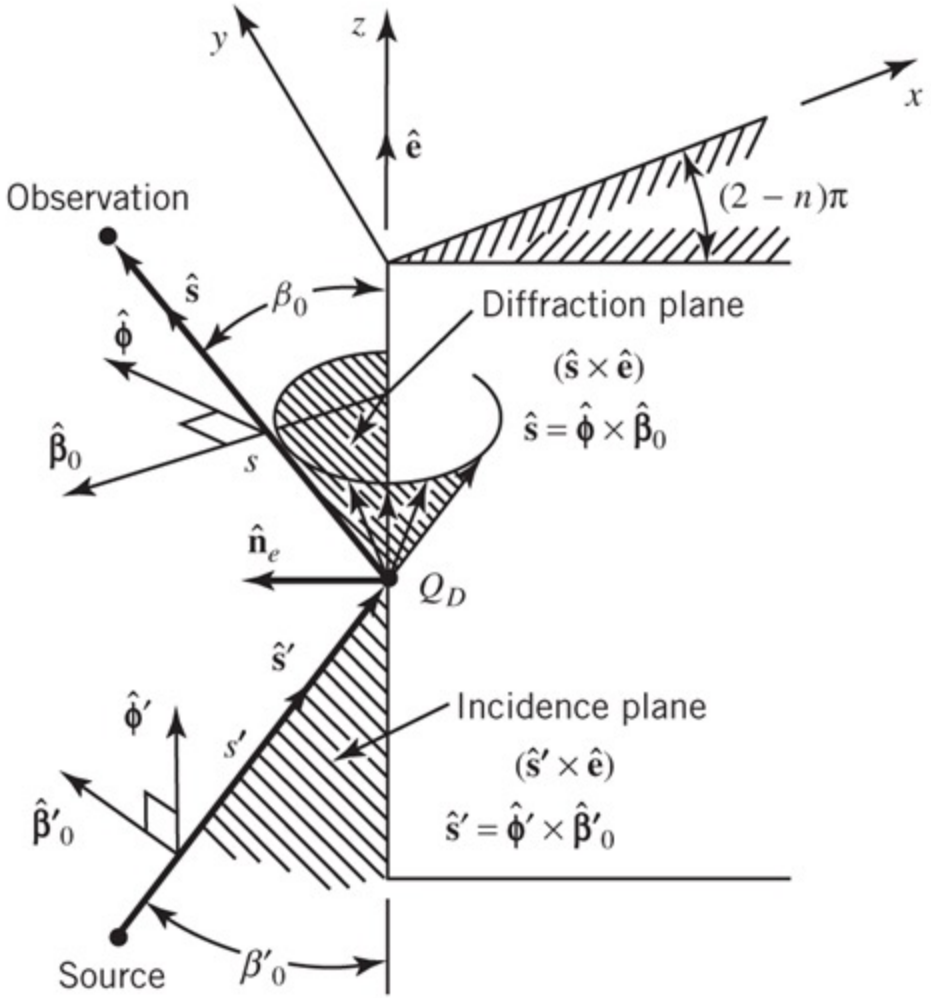

(a) Oblique Incidence

Fig. 13-31

Oblique Incidence Wedge Diffraction

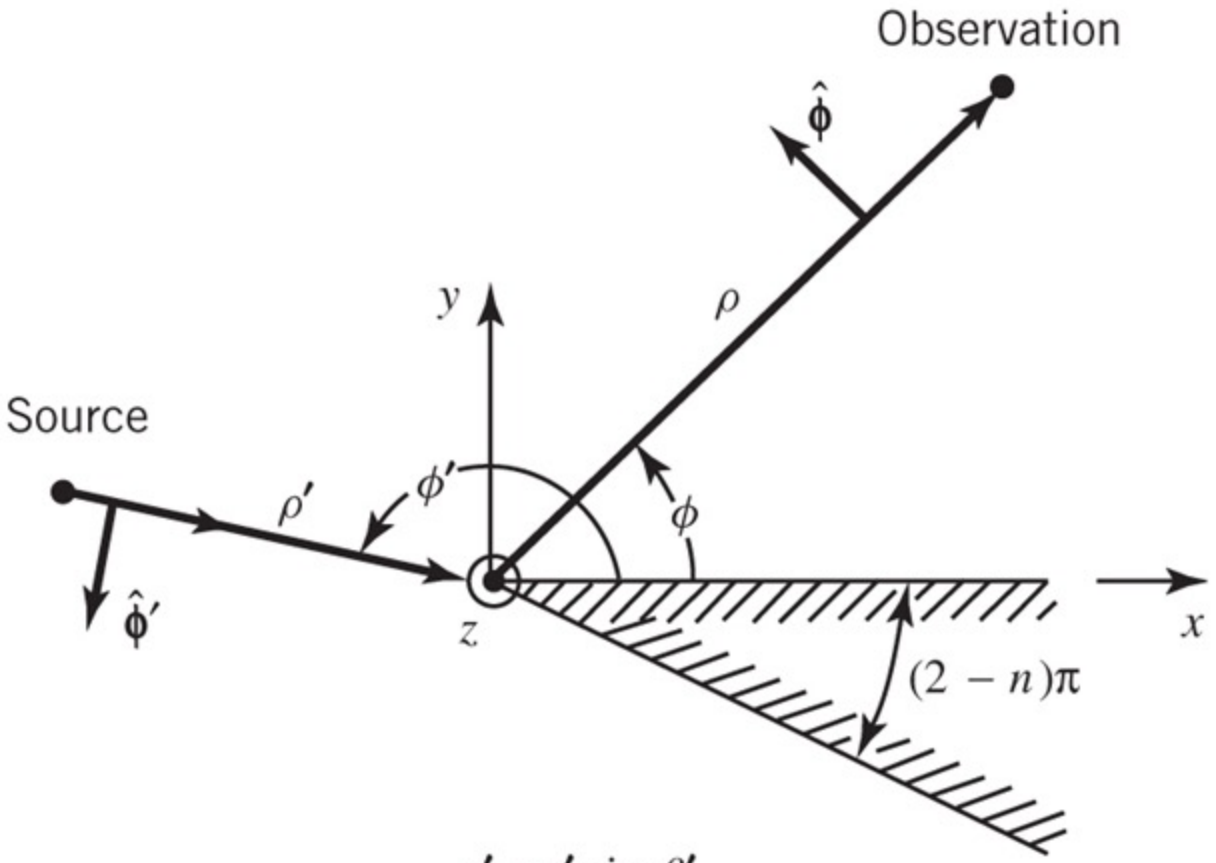

$$\rho' = s' \sin \beta'_0$$

$$\rho = s \sin \beta_0$$

(b) Top View

Fig. 13-31

General Form of Diffracted Field

$$\underline{E}^d(s) = \underline{E}^i(Q_D) \cdot \underline{\underline{D}}(L;\phi,\phi';n;\beta_0')\, A(s,s')e^{-j\beta s}$$

$$A(s,s') = \sqrt{\frac{s'}{s(s'+s)}} \qquad (13\text{-}85)$$

Edge-fixed plane of incidence with the unit vectors

$$\hat{s}' = \hat{\phi}' \times \hat{\beta}_0' \qquad (13\text{-}86a)$$

where $\hat{\beta}_0'$ is $\parallel$ to plane of incidence

$\hat{\phi}'$ is $\perp$ to plane of incidence

Edge-fixed plane of diffraction with the unit vectors

$$\hat{s} = \hat{\phi} \times \hat{\beta}_0 \qquad (13\text{-}86b)$$

where $\hat{\beta}_0$ is $\parallel$ to plane of diffraction

$\hat{\phi}$ is $\perp$ to plane of diffraction

$$\underline{E}^d(s) = \underline{E}^i(Q_D) \cdot \underline{\underline{D}}(L;\phi,\phi';n;\beta_0')A(s,s')e^{-j\beta s}$$

(13-85)

$$\hat{s}' = \hat{\phi}' \times \hat{\beta}_0'$$

(13-86a)

where $\hat{\beta}_0'$ is $\|$ to plane of incidence

$\hat{\phi}'$ is $\perp$ to plane of incidence

$$\hat{s} = \hat{\phi} \times \hat{\beta}_0$$

(13-86b)

where $\hat{\beta}_0$ is $\|$ to plane of diffraction

$\hat{\phi}$ is $\perp$ to plane of diffraction

Incident Field At Diffraction Point

$$\underline{E}^i(Q_D) = \hat{\beta}_0' E^i_{\beta' 0}(Q_D) + \hat{\phi}' E^i_{\phi'}(Q_D)$$

$$\underline{E}^i_{\beta_0}(Q_D) = \hat{\beta}_0' \cdot \underline{E}^i(Q_D) \qquad \text{(13-88a)}$$

$$\underline{E}^i_{\phi'}(Q_D) = \hat{\phi}' \cdot \underline{E}^i(Q_D) \qquad \text{(13-88b)}$$

$\underset{\sim}{D}(L;\phi,\phi';n;\beta_0') = \text{Dyadic Diffraction Coefficient}$

$$\underset{\sim}{D}(L;\phi,\phi';n;\beta_0') = -\hat{\beta}_0'\hat{\beta}_0 D_s(L;\phi,\phi';n;\beta_0') - \hat{\phi}'\hat{\phi} D_h(L;\phi,\phi';n;\beta_0') \tag{13-87}$$

$$D_s(L;\phi,\phi';n;\beta_0') = D^i(L,\phi-\phi',n,\beta_0') - D^r(L,\phi+\phi',n,\beta_0') \tag{13-89a}$$

$$D_h(L;\phi,\phi';n;\beta_0') = D^i(L,\phi-\phi',n,\beta_0') + D^r(L,\phi+\phi',n,\beta_0') \tag{13-89b}$$

$$\begin{bmatrix} E^d_{\beta_0}(s) \\ E^d_{\phi}(s) \end{bmatrix} = -\begin{bmatrix} D_s & 0 \\ 0 & D_h \end{bmatrix} \begin{bmatrix} E^i_{\beta_0'}(Q_D) \\ E^i_{\phi'}(Q_D) \end{bmatrix} A(s',s)e^{-j\beta s} \tag{13-88}$$

$$E^i_{\beta_0'}(Q_D) = \hat{\beta}_0' \cdot \underline{E}^i(Q_D) \tag{13-88a}$$

$$E^i_{\phi'}(Q_D) = \hat{\phi}' \cdot \underline{E}^i(Q_D) \tag{13-88b}$$

$$E^d_{\beta_0}(s) = -D_s E^i_{\beta_0'}(Q_D) A(s',s)e^{-j\beta s}$$

$$E^d_{\phi}(s) = -D_h E^i_{\phi'}(Q_D) A(s',s)e^{-j\beta s}$$

$$D^i(L,\phi-\phi',n,\beta_0') = -\frac{e^{-j\pi/4}}{2n\sqrt{2\pi\beta}\sin\beta_0'}\times$$

$$\times\left\{\cot\left[\frac{\pi+(\phi-\phi')}{2n}\right]F^+\left[\beta Lg^+(\phi-\phi')\right]\right.$$

$$\left.+\cot\left[\frac{\pi-(\phi-\phi')}{2n}\right]F^-\left[\beta Lg^-(\phi-\phi')\right]\right\}$$

(13-90a)

$$D^r(L,\phi+\phi',n,\beta_0') = -\frac{e^{-j\pi/4}}{2n\sqrt{2\pi\beta}\sin\beta_0'}\times$$

$$\times\left\{\cot\left[\frac{\pi+(\phi+\phi')}{2n}\right]F^+\left[\beta Lg^+(\phi+\phi')\right]\right.$$

$$\left.+\cot\left[\frac{\pi-(\phi+\phi')}{2n}\right]F^-\left[\beta Lg^-(\phi+\phi')\right]\right\}$$

(13-90b)

For Straight-Edge, Oblique Incidence

$$L = \frac{s(\rho_e^i + s)\rho_1^i \rho_2^i}{\rho_e^i(\rho_1^i + s)(\rho_2^i + s)} \sin^2 \beta_0 \qquad (13\text{-}91)$$

ρ_e^i = incident wave radius of curvature

ρ_1^i, ρ_2^i = principal radii of curvature of incident wave

$$\rho_e^i = \begin{cases} \infty \text{ for plane and cylindrical waves} \\ s' \text{ for spherical and conical waves} \end{cases}$$

$$\rho_1^i, \rho_2^i = \begin{cases} \infty \text{ for plane wave incidence} \\ \rho_1^i, \rho_2^i = \infty; \text{ or } \rho_1^i = \infty, \ \rho_2^i = \rho' \text{ or vice-versa} \\ \text{for cylindrical wave incidence} \\ s' \text{ for spherical and conical wave incidence} \end{cases}$$

Then L reduces to

$$L = \begin{cases} s \sin^2 \beta_0 & \text{for plane wave incidence} \\ & (\rho_e^i = \rho_1^i = \rho_2^i = \infty) \\ \dfrac{\rho\rho'}{\rho + \rho'} & \text{for cylindrical wave incidence} \\ & (\rho_e^i = \infty, s = \rho, \beta_0 = 90^\circ) \\ & (\rho_1^i = \rho', \rho_2^i = \infty \text{ or } \rho_1^i = \infty, \rho_2^i = \rho') \\ & (\text{Also } \rho = s \sin\beta_0, \rho' = s' \sin\beta_0') \\ \dfrac{ss'}{s + s'} \sin^2 \beta_0 & \text{for spherical and conical wave incidence} \\ & (\rho_e^i = \rho_1^i = \rho_2^i = s') \end{cases} \qquad (13\text{-}92)$$

The spatial attenuation (amplitude spreading) factor is:

$$A(s',s) \simeq \begin{cases} \dfrac{1}{\sqrt{s}} & \text{Plane \& conical wave inc.} \\ \dfrac{1}{\sqrt{\rho}}, \rho = s \sin\beta_0 & \text{Cylindrical wave inc.} \\ \dfrac{\sqrt{s'}}{s} & \text{Spherical wave inc.} \end{cases} \qquad (13\text{-}93)$$

If $s >> s',\ \rho >> \rho'$

$$L \simeq \begin{cases} s \sin^2\beta_0' & \text{Plane wave incidence} \\ \rho' & \text{Cylindrical wave incidence} \\ & (\rho' = s' \sin\beta_0') \\ s' \sin^2\beta_0' & \text{Conical \& spherical} \\ & \text{wave incidence} \end{cases} \tag{13-94}$$

Example 13-6

λ/4 Monopole Above Square Ground Plane

Example 13 – 6 :

To determined the far-zone elevation plane pattern, in the principal planes, of a $\lambda/4$ monopole mounted on a finite size square ground plane of width w on each of its sides, refer to Figure 13-32a. Examine contributions from all four edges.

Solution:

It follows.

Vertical Monopole on a Square Ground-Plane, and Reflection and Diffraction Mechanisms

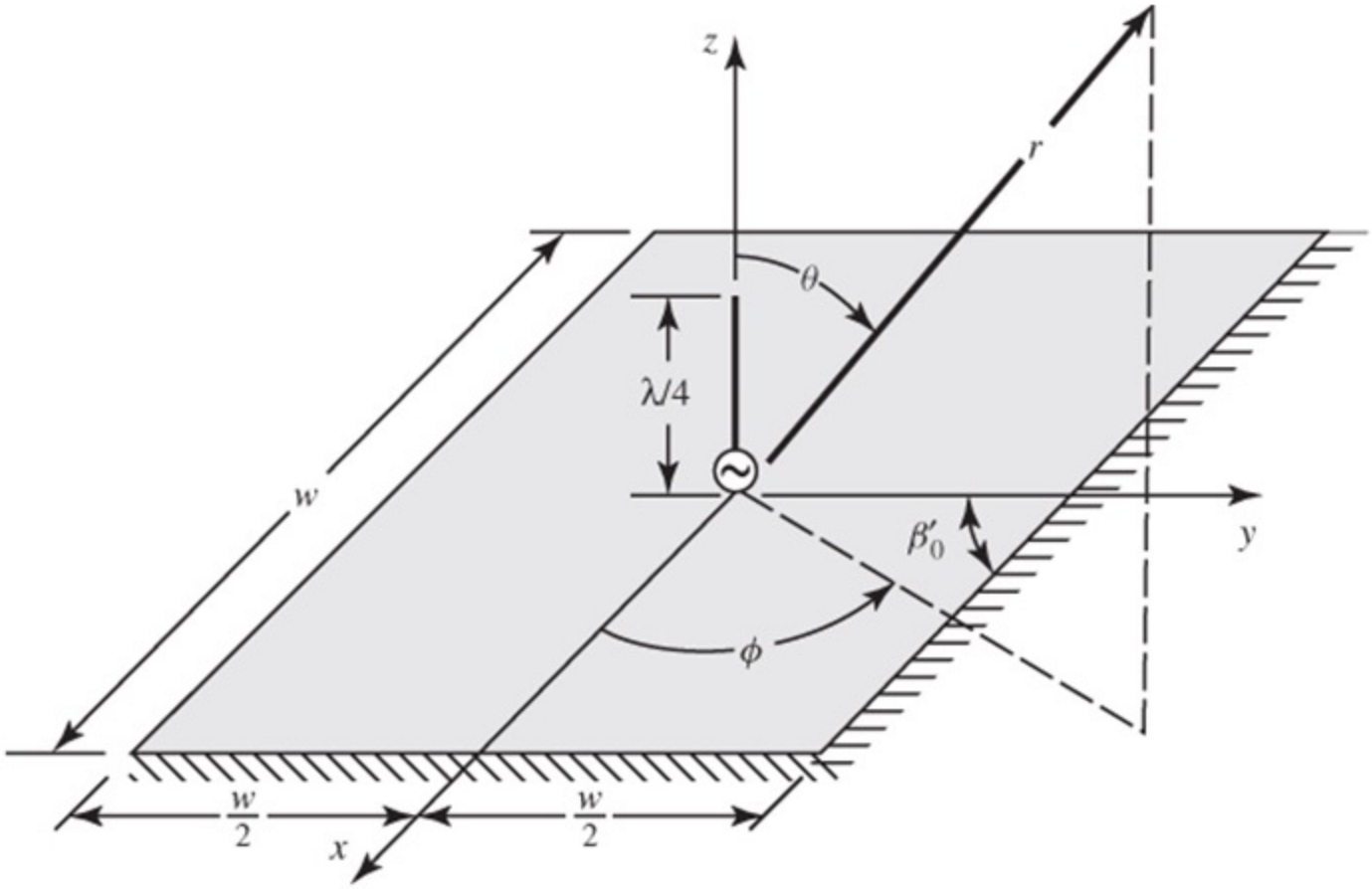

(a) Monopole on ground plane

Fig. 13-32

Normal Incidence Diffraction of Vertical Monopole on a Square Ground-Plane

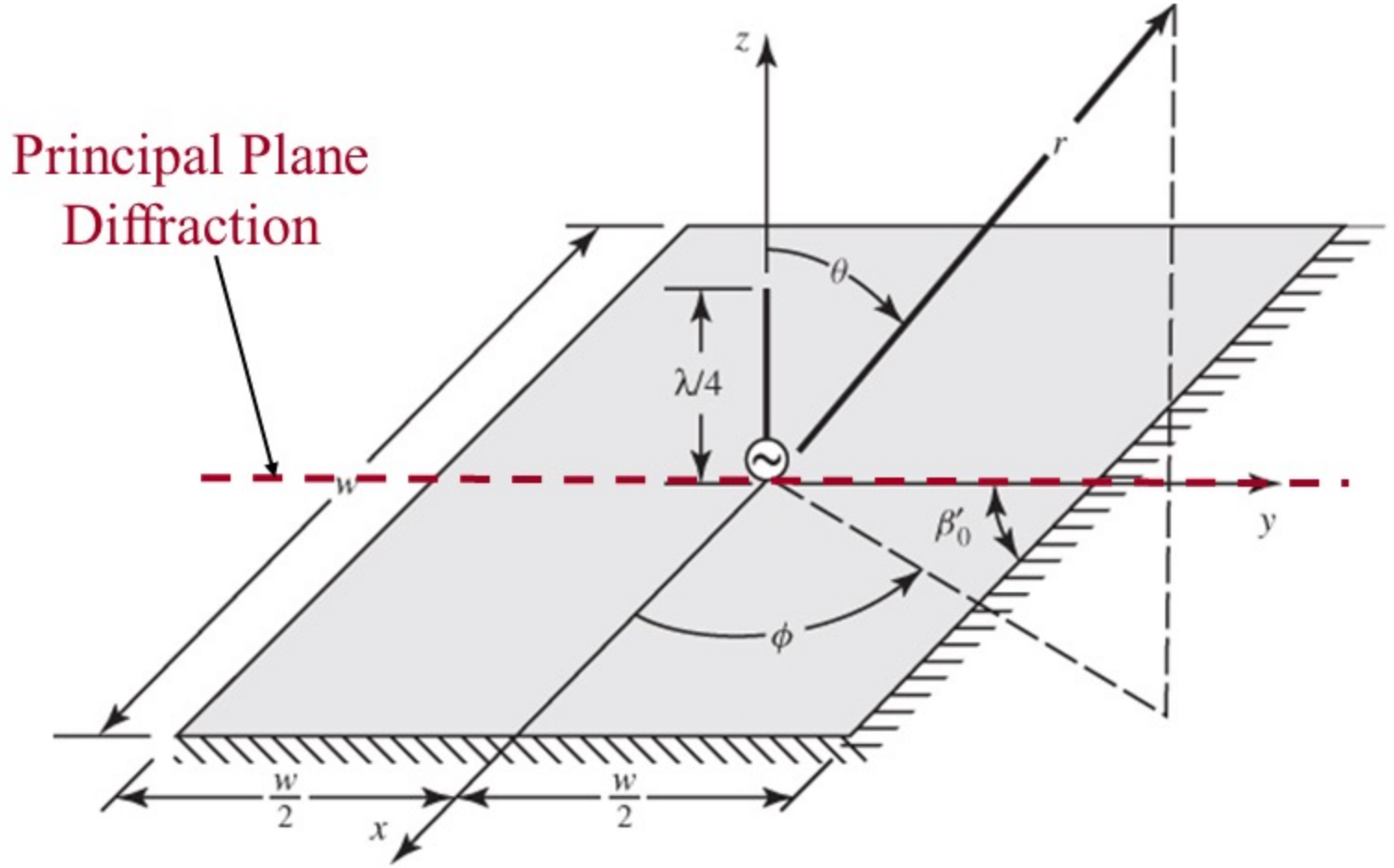

Fig. 13-32

Normal Incidence Diffraction of Vertical Monopole on a Square Ground-Plane

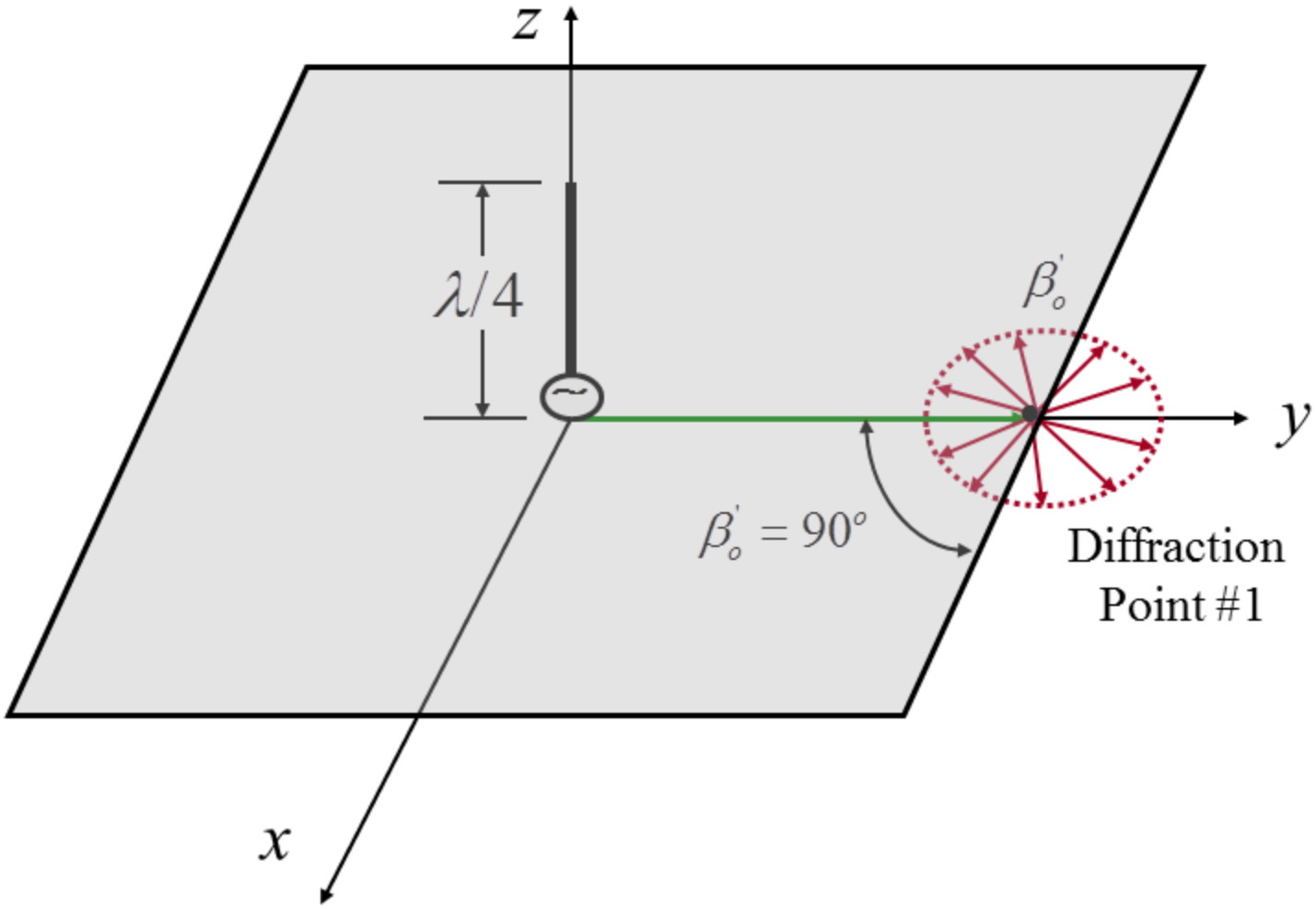

Normal and Oblique Incidence Diffraction of Vertical Monopole on a Square Ground-Plane

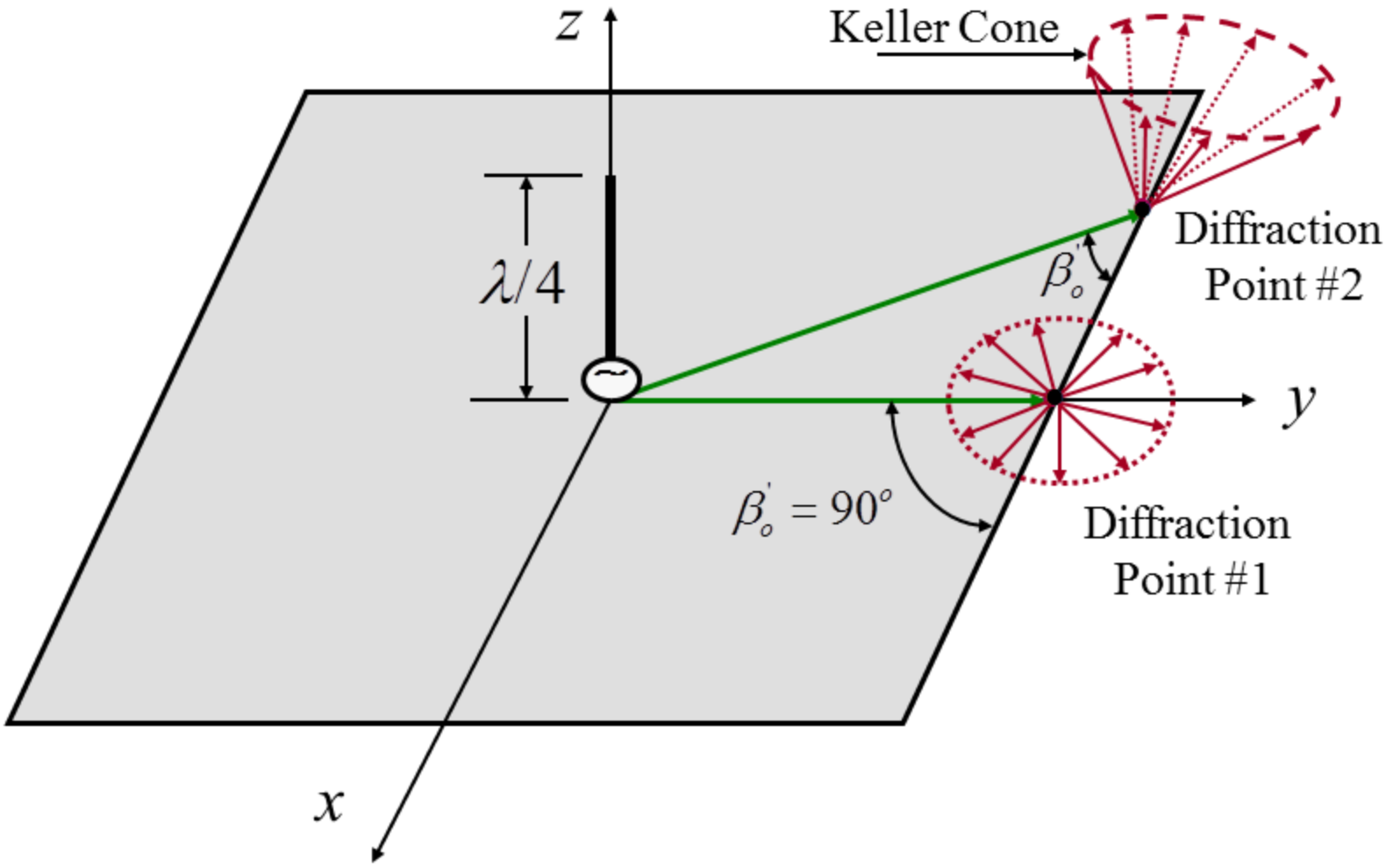

Wedge Diffraction: Normal Incidence

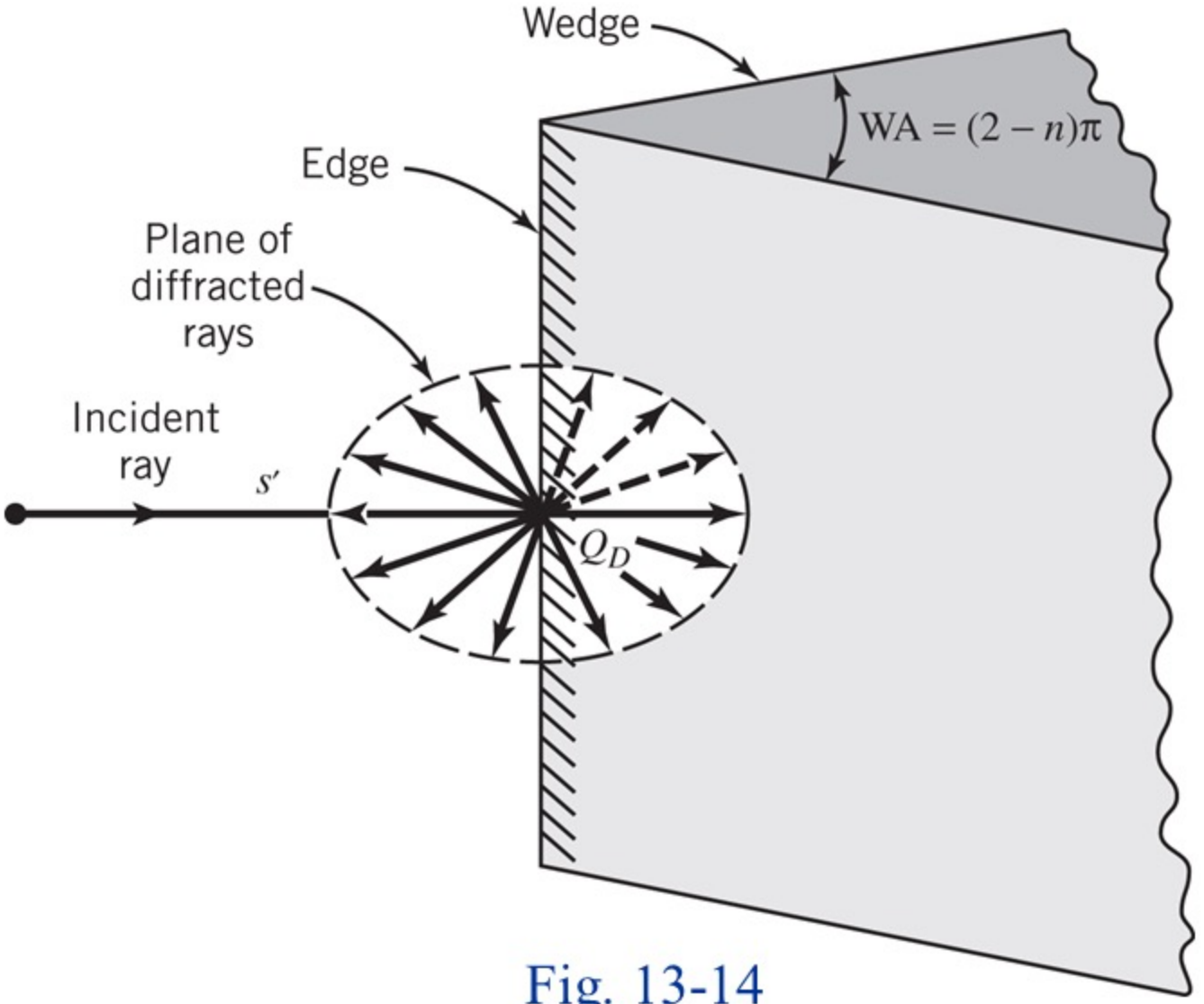

Fig. 13-14

Polarization of Incident and Diffracted Fields

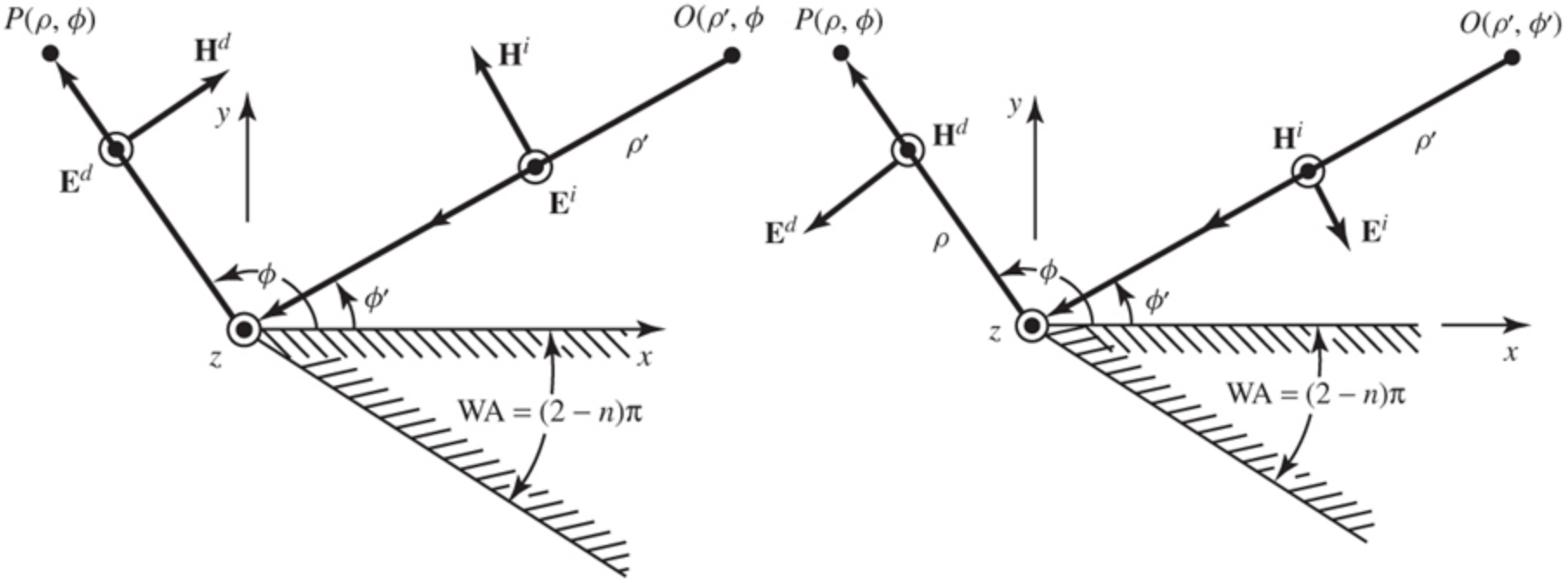

(a) Soft Polarization

(b) Hard Polarization

Fig. 13-22

Vertical Monopole on a Square Ground-Plane, and Reflection and Diffraction Mechanisms

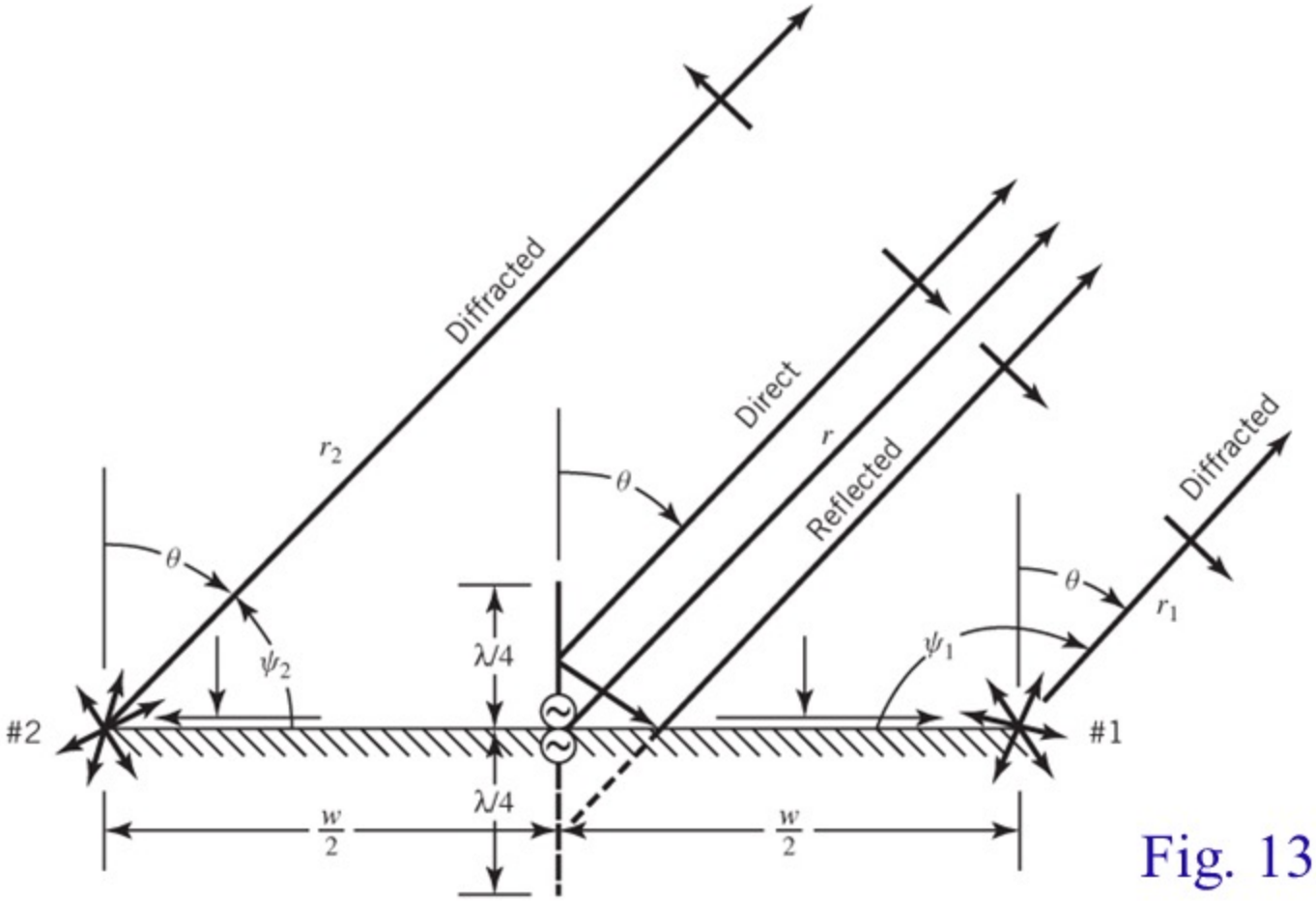

Fig. 13-32

(b) Reflection and diffraction mechanisms

GO Electric Field of a Monopole

$$E_{\theta G} = E_{\theta G}^{i} + E_{\theta G}^{r} = E_{\theta G} = E_0 \left[\frac{\cos\left(\frac{\pi}{2} \cos\theta \right)}{\sin\theta} \right] \frac{e^{-j\beta r}}{r}$$

$$E_{\theta G}\Big|_{\theta=\frac{\pi}{2}} = E_{\theta G}^{i}\Big|_{\theta=\frac{\pi}{2}} + E_{\theta G}^{r}\Big|_{\theta=\frac{\pi}{2}} = E_{\theta G}\Big|_{\theta=\frac{\pi}{2}} = E_0 \frac{e^{-j\beta r}}{r}$$

$$E_{\theta G}\Big|_{\theta=\frac{\pi}{2}} = 2E_{\theta G}^{i}\Big|_{\theta=\pi/2} = 2E_{\theta G}^{r}\Big|_{\theta=\pi/2}$$

$$E_{\theta G}^{i}\Big|_{\theta=\frac{\pi}{2}} = \frac{1}{2} E_{\theta G}\Big|_{\theta=\frac{\pi}{2}} = \frac{1}{2} E_0 \frac{e^{-j\beta r}}{r}$$

$$E_{1\theta}^{d}(r_1,\theta) = E^{i}(Q_1)D^{h}(L,\xi_1^{\pm},n=2,\beta_0^{'}=\frac{\pi}{2})$$

$$\cdot A_1(w,r_1)e^{-j\beta r_1}$$

$$E^{i}(Q_1) = \frac{1}{2}E_{\theta G}\left(\theta=\frac{\pi}{2},r=\frac{w}{2}\right)$$

$$E^{i}(Q_1) = \frac{1}{2}E_0\frac{\cos\left(\frac{\pi}{2}\cos\theta\right)}{\sin\theta}\frac{e^{-j\beta r}}{r}\Bigg|_{\substack{\theta=\pi/2\\ r=w/2}} = \frac{E_0}{2}\frac{e^{-j\beta w/2}}{w/2}$$

$$E^{i}(Q_1) = \frac{E_0}{2}\frac{e^{-j\beta w/2}}{w/2}$$

Diffracted Electric Field of a Monopole From Edge #1

$$E_{\theta 1}^{d} = E^{i}(Q_1) D_{1h} A_1 e^{-j\beta r_1}$$

$$= \frac{1}{2} E_{\theta G}^{t} \Big|_{\theta=\frac{\pi}{2}} 2D^{i}(L,\phi,n) A_1 e^{-j\beta r_1}$$

$$= \frac{1}{2} E_0 \frac{e^{-j\beta\frac{w}{2}}}{\frac{w}{2}} 2D^{i}(L,\phi,n) A_1 e^{-j\beta r_1}$$

$$E_{\theta 1}^{d} = E_0 \frac{e^{-j\beta\frac{w}{2}}}{\frac{w}{2}} D^{i}(L,\phi,n) A_1 e^{-j\beta r_1}$$

$$D_h\left(L,\xi_1^{\pm},n=2,\beta_0^{'}=\frac{\pi}{2}\right)$$

$$=D^i\left(L,\xi_1^{\pm},n=2,\beta_0^{'}=\frac{\pi}{2}\right)$$

$$+D^r\left(L,\xi_1^{\pm},n=2,\beta_0^{'}=\frac{\pi}{2}\right)$$

$$L\simeq s'\sin^2\beta_o^{'}\;\Big|_{\substack{\beta_0^{'}=\frac{\pi}{2}\\ s'=w/2}}=s'=w/2$$

Amplitude Spreading Factor

$$A = \begin{cases} \dfrac{1}{\sqrt{s}}, & \text{plane wave incidence} \\ \dfrac{1}{\sqrt{\rho}}, \ \rho = s \sin \beta_0', & \text{cylindrical wave incidence} \\ \dfrac{\sqrt{s'}}{s}, & \text{spherical wave incidence} \end{cases}$$

s' = distance (source to edge)

s = distance (edge to observation)

$$\left.\begin{aligned} \xi_1^- &= \psi_1 - \psi_1' = \frac{\pi}{2} + \theta \\ \xi_1^+ &= \psi_1 + \psi_1' = \frac{\pi}{2} + \theta \end{aligned}\right\} \Rightarrow \begin{aligned} \xi_1^- &= \xi_1^+ = \xi_1 \\ \xi_1 &= \frac{\pi}{2} + \theta \end{aligned}$$

$$A_1(w, r_1) \simeq \frac{\sqrt{s'}}{s}\Big|_{\substack{s'=w \\ s=r_1}} = \frac{\sqrt{w/2}}{r_1}$$

$$E_{\theta 1}^{d}(r_1,\theta) = \frac{E_o}{2}\frac{e^{-j\beta w/2}}{w/2}$$

$$\cdot\left[D^{i}\left(\frac{w}{2},\xi_1,n=z,\beta_o^{'}=\frac{\pi}{2}\right)\right.$$

$$\left.+D^{r}\left(\frac{w}{2},\xi_1,n=z,\beta_o^{'}=\frac{\pi}{2}\right)\right]$$

$$\cdot\frac{\sqrt{w/2}}{r_1}e^{-j\beta r_1}$$

$$D^i\left(\frac{w}{2},\xi_1,n=2,\beta_o^{'}=\frac{\pi}{2}\right)=D^r\left(\frac{w}{2},\xi_1,n=2,\beta_o^{'}=\frac{\pi}{2}\right)$$

$$E_{\theta 1}^d(r_1,\theta)=\frac{E_o}{2}\left\{\frac{e^{-j\beta w}}{\sqrt{w/2}}\left[2D^{i,r}\left(\frac{w}{2},\xi_1,n=2,\beta_o^{'}=\frac{\pi}{2}\right)\right]\right\}\frac{e^{-j\beta r_1}}{r_1}$$

$$=E_0\underbrace{\left\{\frac{e^{-j\beta w}}{\sqrt{w/2}}\left[D^{i,r}\left(\frac{w}{2},\xi_1,n=2,\beta_o^{'}=\frac{\pi}{2}\right)\right]\right\}}_{V_B^{i,r}\left(\frac{w}{2},\xi_1,n=2,\beta_o^{'}=\frac{\pi}{2}\right)}\frac{e^{-j\beta r_1}}{r_1}$$

$$E_{\theta 1}^{d}(r_1,\theta) = E_0\left[V_B^{i,r}\left(\frac{w}{2},\xi_1,n=2,\beta_0{}' = \frac{\pi}{2}\right)\right]\frac{e^{-j\beta r_1}}{r_1}$$

$$= E_0\left[V_B^{i,r}\left(\frac{w}{2},\xi_1,n=2,\beta_0{}' = \frac{\pi}{2}\right)\right]\frac{e^{-j\beta r_1}}{r_1}$$

$$E_{\theta 1}^{d}(r_1,\theta) = E_0\left[V_B^{i,r}\left(\frac{w}{2},\xi_1,n=2,\beta_0^{'}=\frac{\pi}{2}\right)\right]\frac{e^{-j\beta r_1}}{r_1}$$

$$E_{\theta 2}^{d}(r_2,\theta) = -E_0\left[V_B^{i,r}\left(\frac{w}{2},\xi_2,n=2,\beta_0^{'}=\frac{\pi}{2}\right)\right]\frac{e^{-j\beta r_2}}{r_2}$$

$$\xi_1 = \frac{\pi}{2}+\theta; \qquad \xi_2 = \begin{cases} \dfrac{\pi}{2}-\theta, & 0 \le \theta \le \dfrac{\pi}{2} \\ \dfrac{5\pi}{2}-\theta, & \dfrac{\pi}{2} \le \theta \le \pi \end{cases}$$

For far-field observations

$$r_1 \simeq r - \frac{w}{2}\cos\left(\frac{\pi}{2} - \theta\right) = r - \frac{w}{2}\sin\theta$$

$$r_2 \simeq r - \frac{w}{2}\cos\left(\frac{\pi}{2} - \theta\right) = r + \frac{w}{2}\sin\theta$$

} for ϕ terms

$$r_1 \simeq r_2 \simeq r$$ for amplitude terms

$$E_{\theta 1}^{d}(r,\theta) = E_0 \left[V_B^{i,r}\left(\frac{w}{2}, \xi_1, n=2, \beta_0^{'} = \frac{\pi}{2} \right) \right] \cdot e^{j\beta \frac{w}{2}\sin\theta} \frac{e^{-j\beta r}}{r}$$

$$E_{\theta 2}^{d}(r,\theta) = -E_0 \left[V_B^{i,r}\left(\frac{w}{2}, \xi_2, n=2, \beta_0^{'} = \frac{\pi}{2} \right) \right] \cdot e^{-j\beta \frac{w}{2}\sin\theta} \frac{e^{-j\beta r}}{r}$$

Amplitude Pattern: Square Ground Plane

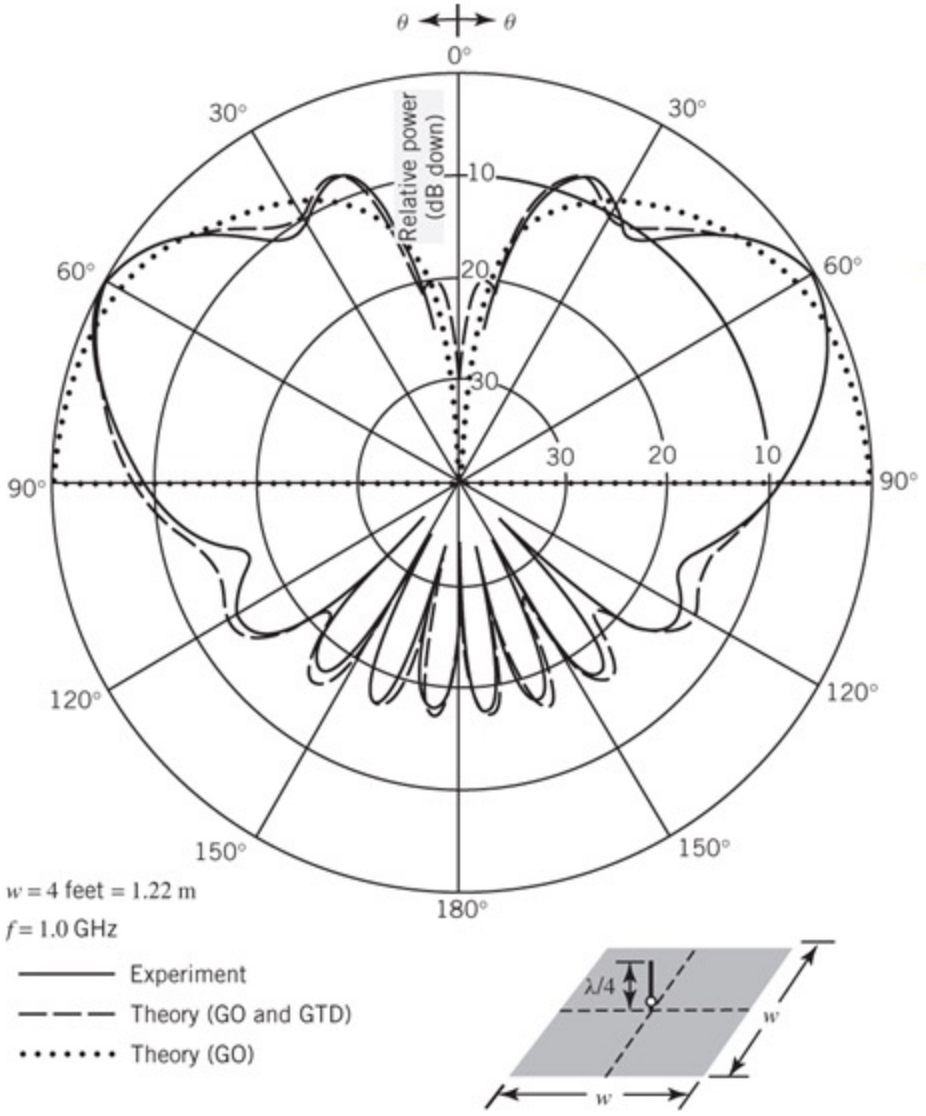

$w = 4$ ft

$w = 1.22$ m

$f = 1$ GHz

Fig. 13-33

Curved-Edge Diffraction

Diffraction by Curved-Edge Structures

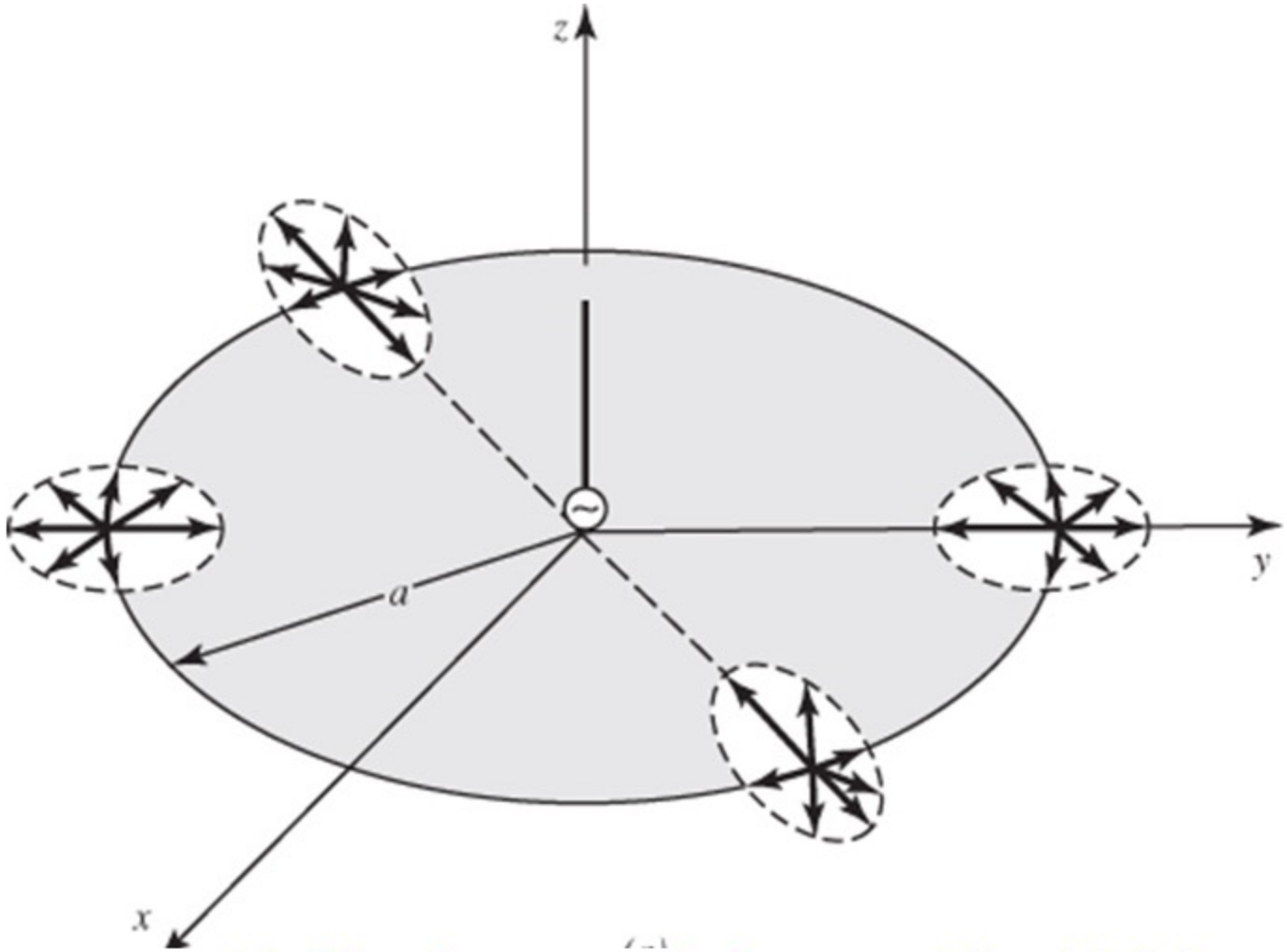

(a) Circular ground plane

Fig. 13-34

Diffraction by Curved-Edge Structures

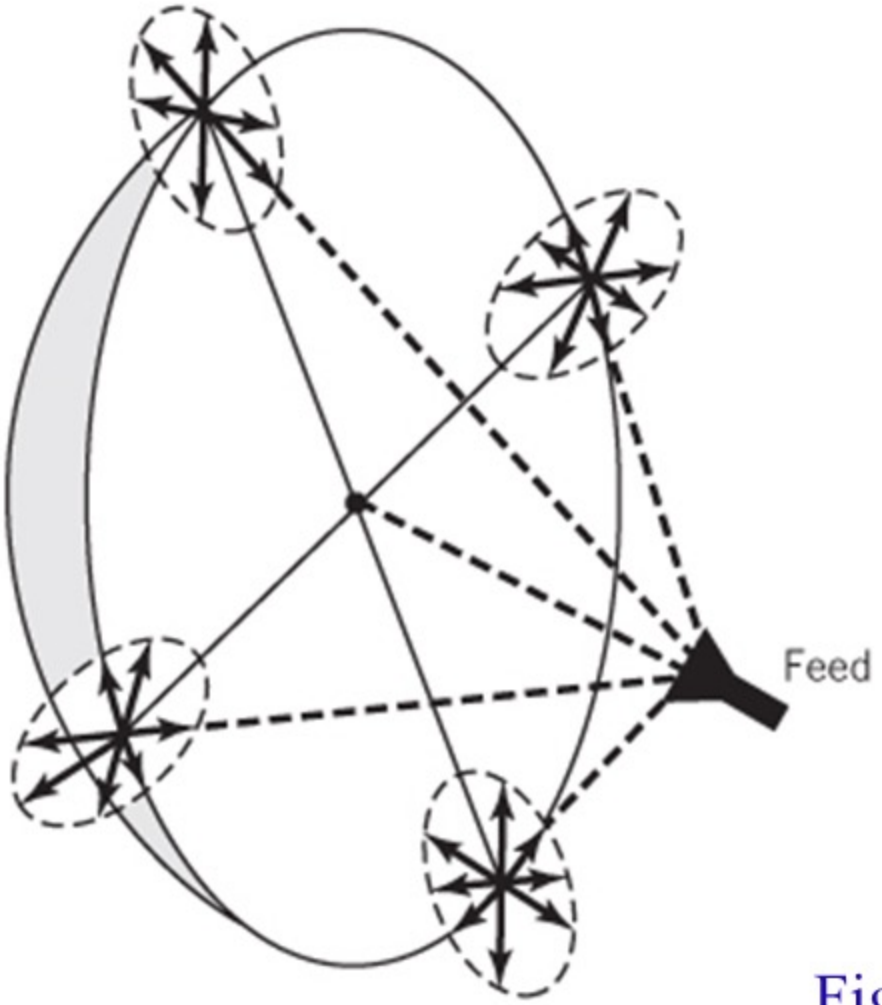

Fig. 13-34

(b) Paraboloidal Reflector

Diffraction by Curved-Edge Structures

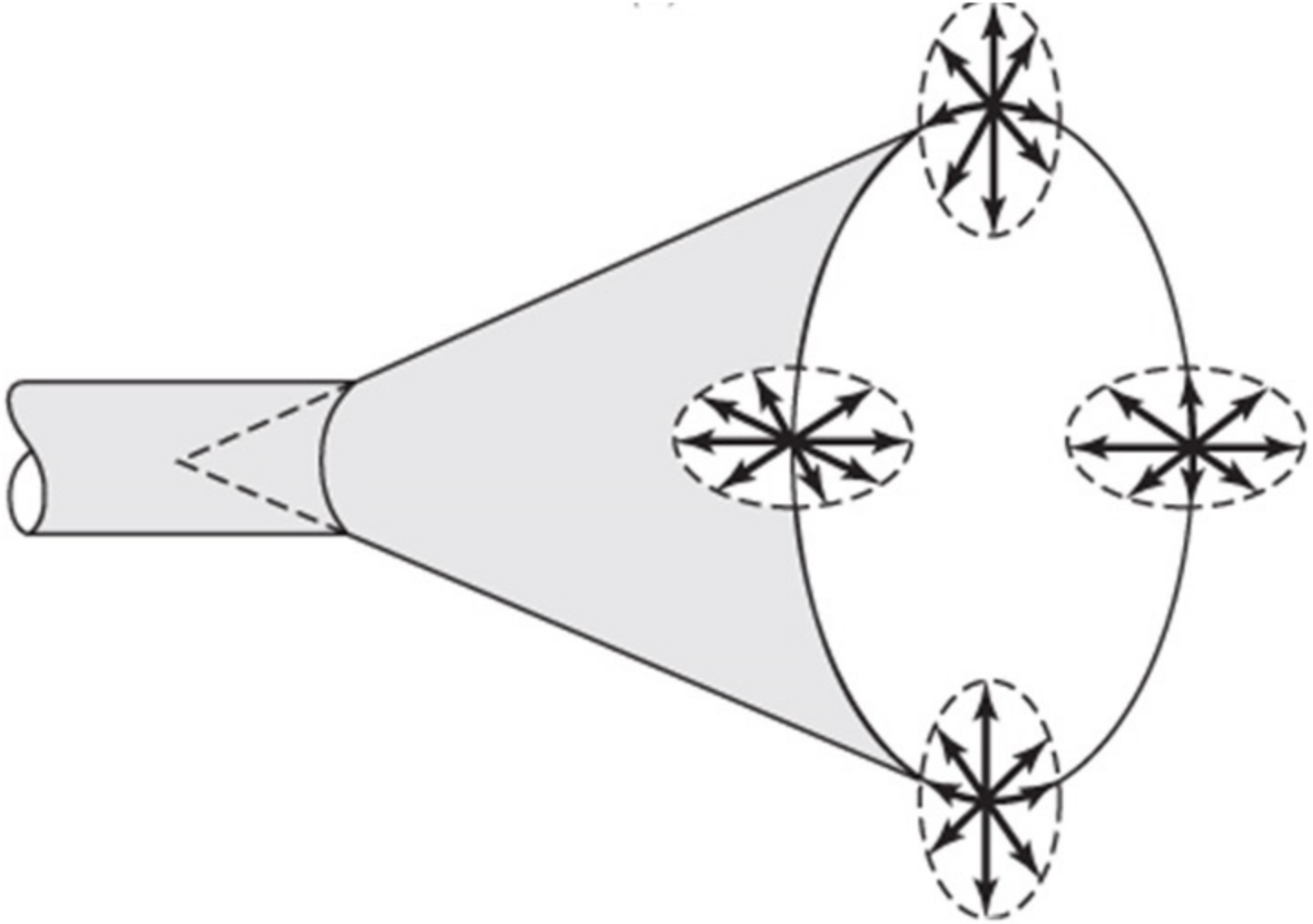

(c) Conical Horn

Fig. 13-34

Oblique Incidence Diffraction by a Curved Edge

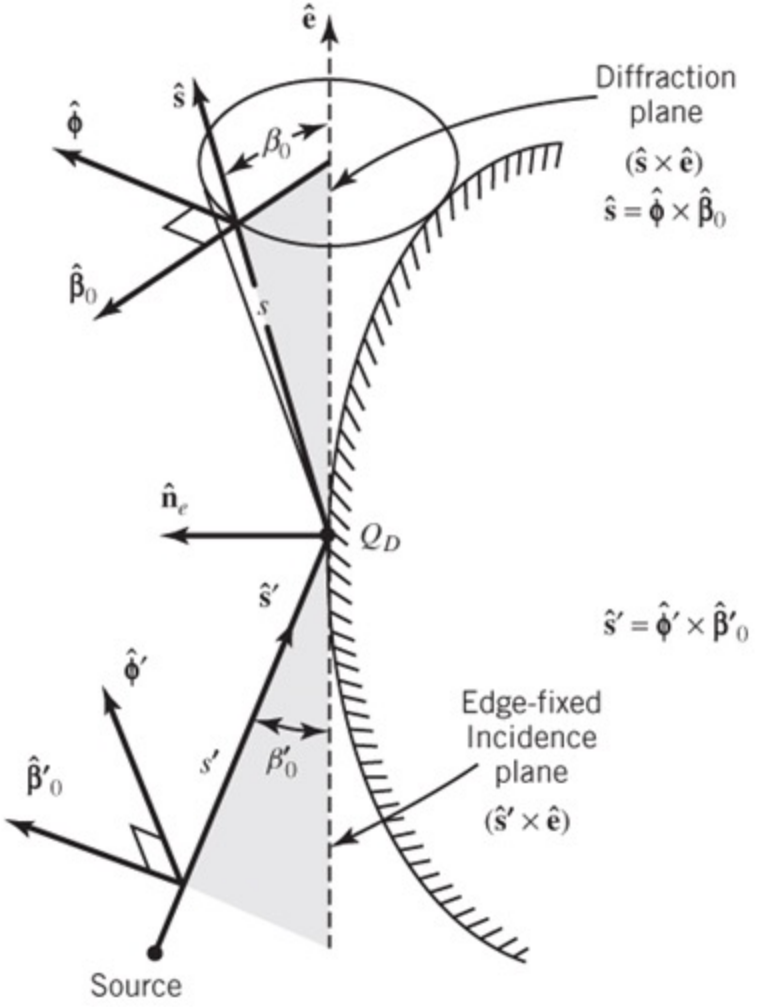

(a) Oblique Incidence

Fig. 13-35

Oblique Incidence Diffraction by a Curved Edge

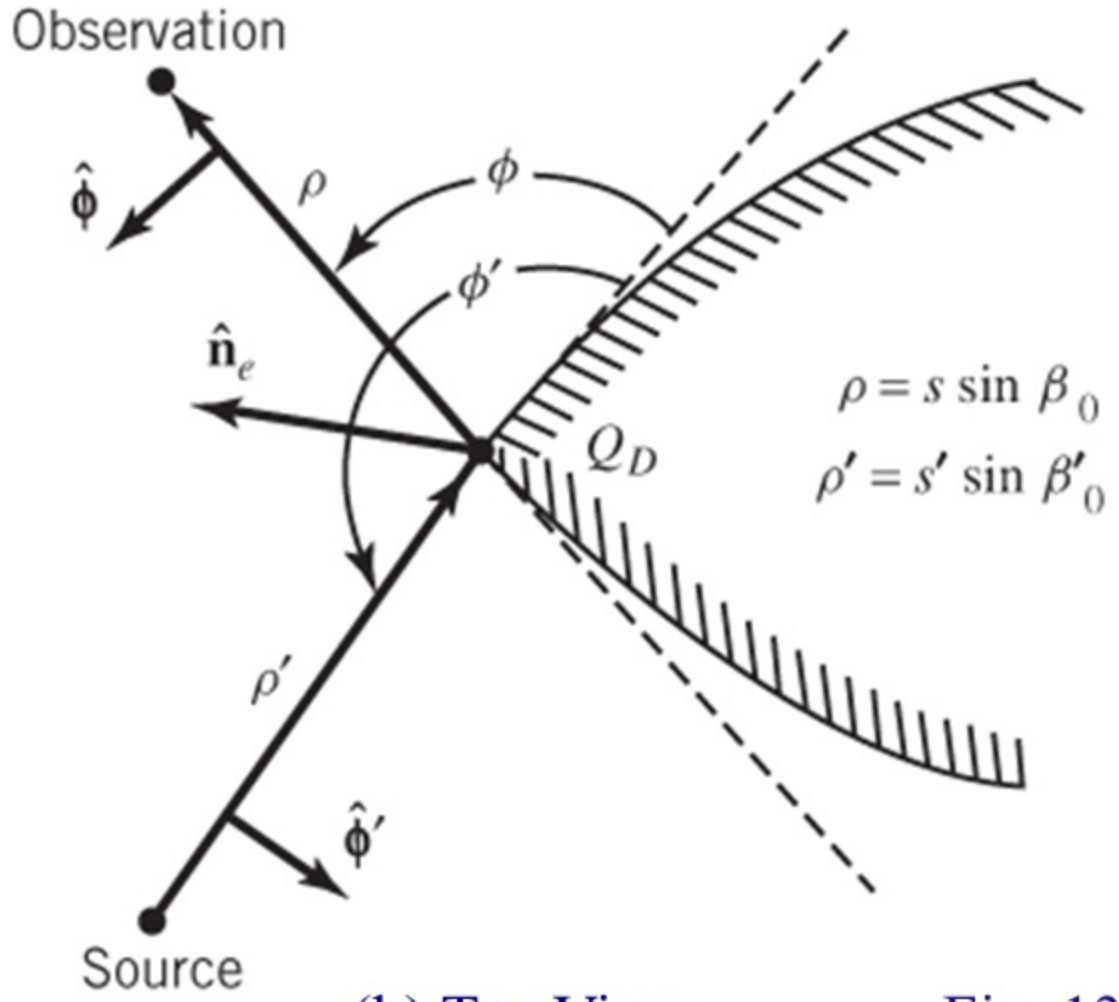

(b) Top View

Fig. 13-35

Curved Edge (Screen)

$$\underline{E}^d(s) = \underline{E}^i(Q_D)\cdot \tilde{D}(L^i, L^r; \phi, \phi'; n; \beta_0) A(s, \rho_c) e^{-j\beta s}$$

$$A(s,\rho_c) = \underbrace{\sqrt{\frac{s'}{s(s'+s)}}}_{(13\text{–}35c)}\Bigg|_{s'=\rho_c} = \sqrt{\frac{\rho_c}{s(\rho_c+s)}} \overset{s>>\rho_c}{\simeq} \frac{\sqrt{\rho_c}}{s} \qquad (13\text{-}100)$$

$$\frac{1}{\rho_c} = \frac{1}{\rho_e^i} - \frac{\hat{n}_e\cdot(\hat{s}'-\hat{s})}{\rho_g \sin^2\beta_0'} = \frac{1}{\rho_e^i} - \frac{\hat{n}_e\cdot\hat{s}'-\hat{n}_e\cdot\hat{s}}{\rho_g \sin^2\beta_0'} \qquad (13\text{-}100a)$$

ρ_c = distance between caustic at edge and second caustic of diffracted ray

ρ_e^i = radius of curvature of incidence wavefront in edge-fixed plane of incidence

$\rho_e^i = \infty$ for plane, cylindrical and conical waves

$\rho_e^i = s'$ for spherical waves

ρ_g = radius of curvature of edge at diffraction point

$\hat{n}_e$ = unit vector normal to edge at Q_D and directed away from the center of curvature

$\hat{s}'$ = unit vector in direction of incidence

$\hat{s}$ = unit vector in direction of diffraction

β_0' = angle between $\hat{s}'$ and tangent to the edge at point of diffraction

$\hat{e}$ = unit vector tangent to the edge at the point of diffraction

$$D^i(L^i,\xi^-,n,\beta_0)=-\frac{e^{-j\pi/4}}{2n\sqrt{2\pi\beta}\sin\beta_0}$$

$$\cdot\left\{C^+(\xi^-)F^+\left[\beta L^i g^+(\xi^-)\right]\right.$$

$$\left.+C^-(\xi^-)F^-\left[\beta L^i g^-(\xi^-)\right]\right\} \qquad (13\text{-}96a)$$

$$D^r(L^r,\xi^+,n,\beta_0)=-\frac{e^{-j\pi/4}}{2n\sqrt{2\pi\beta}\sin\beta_0}$$

$$\cdot\left\{C^+(\xi^+)F^+\left[\beta L^{rn} g^+(\xi^+)\right]\right.$$

$$\left.+C^-(\xi^+)F^-\left[\beta L^{ro} g^-(\xi^+)\right]\right\} \qquad (13\text{-}96b)$$

$$D_s(L^i, L^r, \xi^-, \xi^+, n, \beta_0)$$

$$= D^i(L^i, \xi^-, n, \beta_0) - D^r(L^{rn,ro}, \xi^-, n, \beta_0)$$

$$D_h(L^i, L^r, \xi^-, \xi^+, n, \beta_0)$$

$$= D^i(L^i, \xi^+, n, \beta_0) + D^r(L^{rn,ro}, \xi^+, n, \beta_0)$$

For Curved-Edge Diffraction

$$L^i = \frac{s(\rho_e^i + s)\rho_1^i \rho_2^i}{\rho_e^i(\rho_e^i + s)(\rho_2^i + s)} \sin^2 \beta_0' \qquad \text{(13-97a)}$$

$$L^{ro,rn} = \frac{s(\rho_e^r + s)\rho_1^r \rho_2^r}{\rho_e^r(\rho_e^r + s)(\rho_2^r + s)} \sin^2 \beta_0' \qquad \text{(13-97b)}$$

For Curved-Edge Diffraction

$\rho_e^i =$ radius of curvature of incident wavefront in the edge-fixed plane of incidence

$$\rho_e^i = \begin{cases} \infty & \text{for plane and cylindrical waves} \\ s' & \text{for spherical and conical waves} \end{cases}$$

$\rho_e^r =$ radius of curvature of diffracted wavefront in the edge-fixed plane of incidence

$$\rho_e^r = \begin{cases} \infty & \text{for plane and cylindrical waves} \\ s' & \text{for spherical and conical waves} \end{cases}$$

Caustic Distance and Center of Curvature for Curved-Edge Diffraction

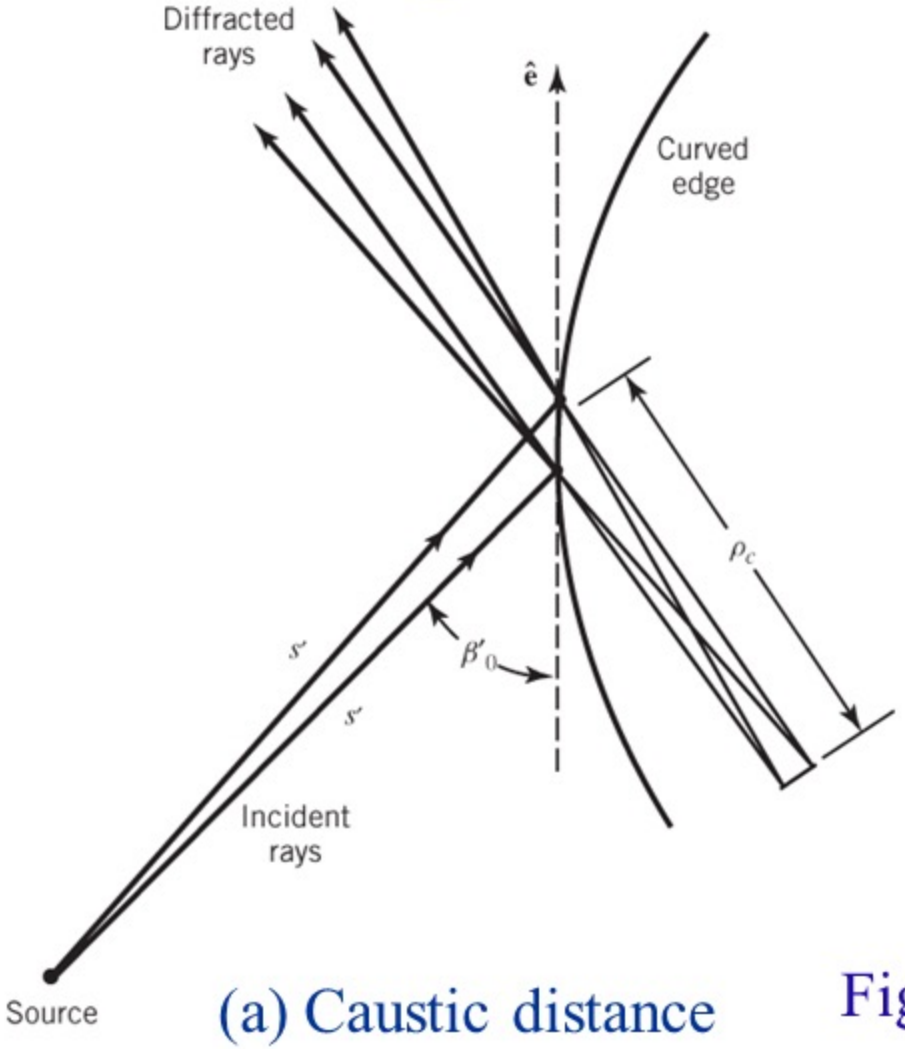

(a) Caustic distance

Fig. 13-36

Caustic Distance and Center of Curvature
Curved-Edge Diffraction

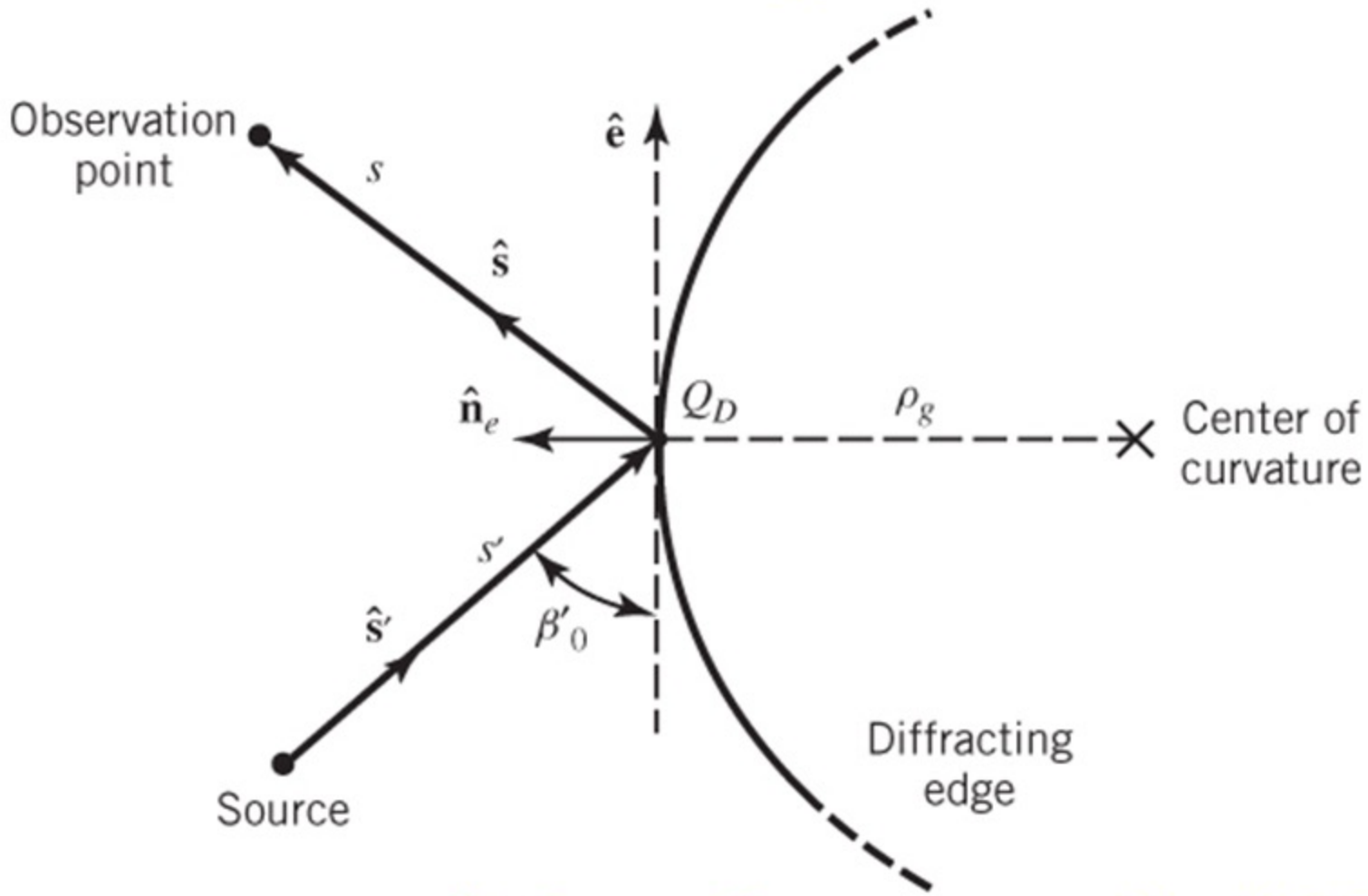

(b) Center of curvature

Fig. 13-36

Curved Edge (Screen)

$$\underline{E}^d(s) = \underline{E}^i(Q_D)\cdot \tilde{D}(L^i, L^r; \phi, \phi'; n; \beta_0) A(s, \rho_c) e^{-j\beta s}$$

$$A(s,\rho_c) = \underbrace{\sqrt{\frac{s'}{s(s'+s)}}}_{(13\text{–}35c)}\Bigg|_{s'=\rho_c} = \sqrt{\frac{\rho_c}{s(\rho_c+s)}} \overset{s>>\rho_c}{\simeq} \frac{\sqrt{\rho_c}}{s} \qquad (13\text{-}100)$$

$$\frac{1}{\rho_c} = \frac{1}{\rho_e^i} - \frac{\hat{n}_e\cdot(\hat{s}'-\hat{s})}{\rho_g \sin^2\beta_0'} = \frac{1}{\rho_e^i} - \frac{\hat{n}_e\cdot\hat{s}'-\hat{n}_e\cdot\hat{s}}{\rho_g \sin^2\beta_0'} \qquad (13\text{-}100a)$$

ρ_c = distance between caustic at edge and second caustic of diffracted ray

ρ_e^i = radius of curvature of incidence wavefront in edge-fixed plane of incidence

$\rho_e^i = \infty$ for plane, cylindrical and conical waves

$\rho_e^i = s'$ for spherical waves

ρ_g = radius of curvature of edge at diffraction point

$\hat{n}_e$ = unit vector normal to edge at Q_D and directed away from the center of curvature

$\hat{s}'$ = unit vector in direction of incidence

$\hat{s}$ = unit vector in direction of diffraction

β_0' = angle between $\hat{s}'$ and tangent to the edge at point of diffraction

$\hat{e}$ = unit vector tangent to the edge at the point of diffraction

$\rho_1^i, \rho_2^i =$ principal radii of curvature of the incident wavefront

$\rho_e^r =$ radius of curvature of the reflected wavefront in the plane containing the diffracted ray and edge

The subscripts *ro*,*rn* in (13-96b) and (13-97b) denote that the radii of curvature ρ_1^i, ρ_2^i and ρ_e^r must be calculated for *ro* at the reflection boundary $\pi - \phi'$ of Figure 13-24a and for *rn* at the reflection boundary $(2n-1)\pi - \phi'$ of Figure 13-24b.

For far-field observation where $s >> \rho_e^i, \rho_1^i, \rho_2^i, \rho_e^r, \rho_1^r, \rho_2^r$, (13-97a) and (13-97b) simplify to

$$L^i = \frac{\rho_1^i \rho_2^i}{\rho_e^i} \sin^2 \beta_0' \tag{13-98a}$$

$$L^{ro,rn} = \frac{\rho_1^r \rho_2^r}{\rho_e^r} \sin^2 \beta_0' \tag{13-98b}$$

If the intersecting curved surfaces forming the curved edge in Figure 13-34 are plane surfaces that form an ordinary wedge, then the distance parameters in (13-97a) and (13-97b) or (13-98a) and (13-98b) are equal, that is,

$$L^{ro} = L^{rn} = L^i \tag{13-99}$$

Curved Edge (Screen)

$$\underline{E}^d(s) = \underline{E}^i(Q_D)\cdot \tilde{D}(L^i, L^r; \phi, \phi'; n; \beta_0) A(s, \rho_c) e^{-j\beta s}$$

$$A(s,\rho_c) = \underbrace{\sqrt{\frac{s'}{s(s'+s)}}}_{(13\text{–}35c)}\Bigg|_{s'=\rho_c} = \sqrt{\frac{\rho_c}{s(\rho_c+s)}} \overset{s>>\rho_c}{\simeq} \frac{\sqrt{\rho_c}}{s} \qquad (13\text{-}100)$$

$$\frac{1}{\rho_c} = \frac{1}{\rho_e^i} - \frac{\hat{n}_e\cdot(\hat{s}'-\hat{s})}{\rho_g \sin^2\beta_0'} = \frac{1}{\rho_e^i} - \frac{\hat{n}_e\cdot\hat{s}'-\hat{n}_e\cdot\hat{s}}{\rho_g \sin^2\beta_0'} \qquad (13\text{-}100a)$$

Curved-Edge Diffraction Example

Example 13-7

λ/4 Dipole Above Circular Ground Plane Diffraction

Example 13 – 7 :

Determined the far-zone elevation plane pattern of a $\lambda/4$ monopole mounted on a circular PEC ground plane of radius a, as shown in Figure 13-37a.

Solution:

It follows.

$\lambda/4$ Monopole Above Circular Plate

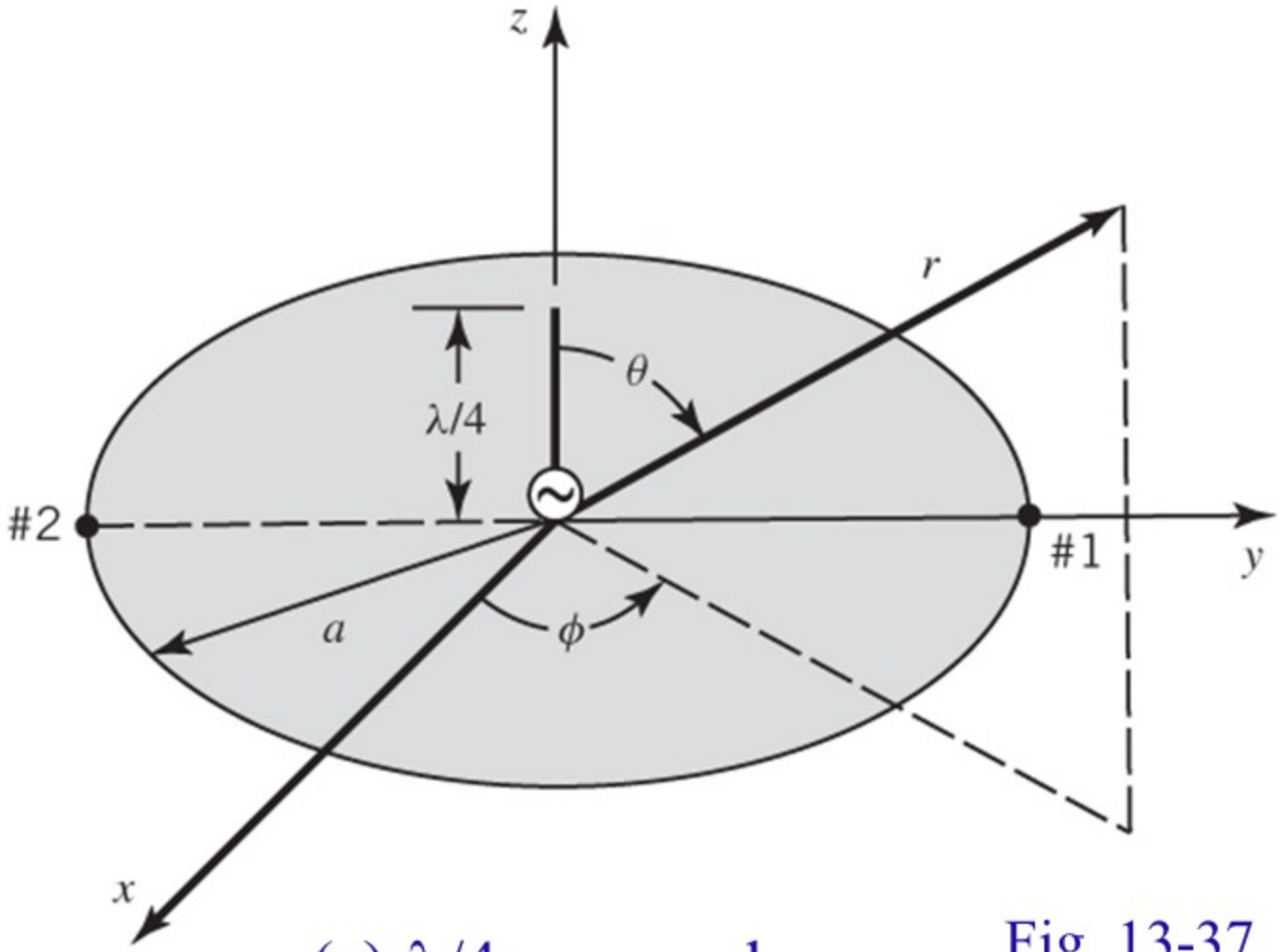

(a) $\lambda/4$ monopole

Fig. 13-37

Two-Point Diffraction

Circular Ground Plane

$$\psi_2 = \begin{cases} \dfrac{\pi}{2} - \theta & 0 \le \theta \le 90^\circ \\ \dfrac{5\pi}{2} - \theta & 90^\circ \le \theta \le 180^\circ \end{cases}$$

$$\psi_1 = \frac{\pi}{2} + \theta$$

$$0^\circ \le \theta \le 180^\circ$$

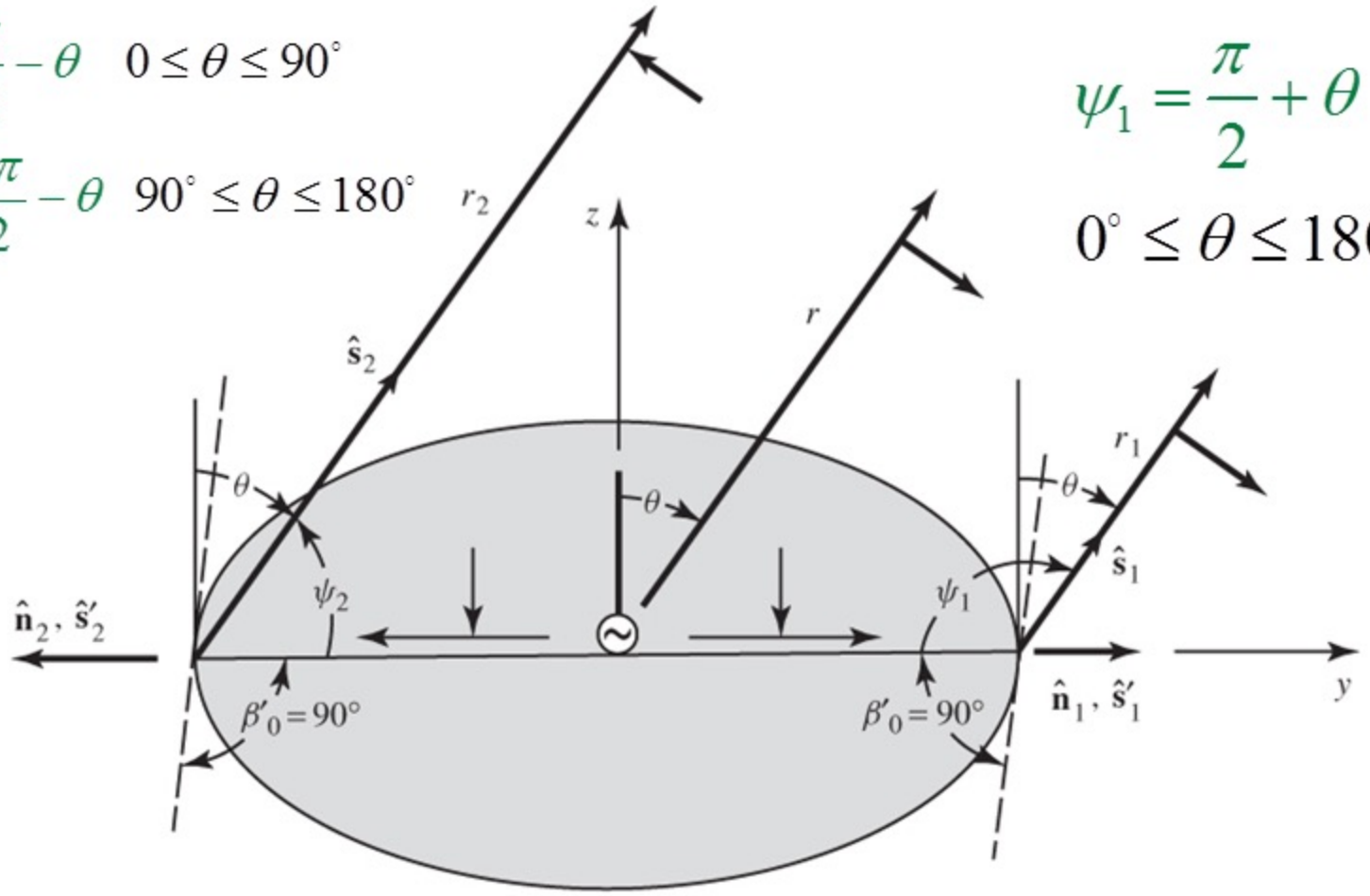

(b) Diffraction mechanism

Fig. 13-37

Diffracted Fields from Diffraction Points #1 and #2

Circular Ground Plane

Diffraction Point #1:

$$E_1^d(r_1) = E_{GO}^i(Q_1) D_1^h(L_1^i, L_1^r) A_1(r_1, \rho_{c1}) e^{-j\beta r_1}$$

Diffraction Point #2:

$$E_2^d(r_2) = E_{GO}^i(Q_2) D_2^h(L_2^i, L_2^r) A_2(r_2, \rho_{c2}) e^{-j\beta r_2}$$

Diffraction Point #1

Geometrical Optics
Field of λ/4 Monopole

Geometrical Optics Field

Quarter-Wavelength Monopole (same as that of $\lambda/2$ dipole)

$$E_{\theta G}(r,\theta) = E^{i}_{\theta G} + E^{r}_{\theta G} = E_{\theta G}$$

$$E_{\theta G}(r,\theta) = E_0 \left[\frac{\cos\left(\frac{\pi}{2}\cos\theta\right)}{\sin\theta} \right] \frac{e^{-j\beta r}}{r} \qquad (4\text{-}84)$$

Incident Geometrical Optics Field Toward Diffraction Point #1 ($r = a,\ \theta = 90^{o}$)

GO Field Toward Diffraction Point #1

Quarter-Wavelength Monopole

$$E_{\theta G}(r,\theta) = E_0 \left[\frac{\cos\left(\frac{\pi}{2}\cos\theta\right)}{\sin\theta} \right] \frac{e^{-j\beta r}}{r}$$

$$E_{\theta G}\Big|_{\theta=90^\circ} = E^i_{\theta G}\Big|_{\theta=90^\circ} + E^r_{\theta G}\Big|_{\theta=90^\circ} = E_{\theta G}\Big|_{\theta=90^\circ} = E_0 \frac{e^{-j\beta r}}{r}$$

$$E_{\theta G}\Big|_{\theta=90^\circ} = 2E^i_{\theta G}\Big|_{\theta=90^\circ} = 2E^r_{\theta G}\Big|_{\theta=90^\circ}$$

$$E^i_{\theta G}\Big|_{r=a,\theta=90^\circ} = \frac{1}{2}E_{\theta G}\Big|_{r=a,\theta=90^\circ} = \frac{1}{2}E_0 \frac{e^{-j\beta r}}{r}\Big|_{r=a,\theta=90^\circ} = \frac{1}{2}E_0 \frac{e^{-j\beta a}}{a}$$

Amplitude Spreading Factor

$$A_1(s_1 = r_1, \rho_{c1}) = \underbrace{\sqrt{\frac{s_1'}{s_1(s_1' + s_1)}}}_{(13\text{–}35c)}\Bigg|_{s_1' = \rho_{c1}} = \sqrt{\frac{\rho_{c1}}{s_1(\rho_{c1} + s_1)}} \overset{s_1 \gg \rho_{c1}}{\simeq} \frac{\sqrt{\rho_{c1}}}{s_1}\Bigg|_{s = r_1} = \frac{\sqrt{\rho_{c1}}}{r_1}$$

$$\frac{1}{\rho_{c1}} = \frac{1}{\rho_e^i} - \frac{\hat{n}_1 \cdot (\hat{s}_1' - \hat{s}_1)}{\rho_g \sin^2 \beta_0'}\Bigg|_{\rho_e^i = \rho_g = a,\, \beta_0' = 90^\circ} = \frac{1}{a} - \frac{\hat{n}_1 \cdot \hat{s}_1' - \hat{n}_1 \cdot \hat{s}_1}{a \sin^2(90^\circ)}$$

$$\hat{n}_1 \cdot \hat{s}_1' = \left|\hat{n}_1\right|\left|\hat{s}_1'\right| \cos(0^\circ) = 1$$

$$\hat{n}_1 \cdot \hat{s}_1 = \left|\hat{n}_1\right|\left|\hat{s}_1\right| \cos\left(\frac{\pi}{2} - \theta\right) = \sin\theta$$

$$\frac{1}{\rho_{c1}} = \frac{1}{a} - \frac{1 - \sin\theta}{a} = \frac{1 - 1 + \sin\theta}{a} = \frac{\sin\theta}{a} \Rightarrow \rho_{c1} = \frac{a}{\sin\theta}$$

Diffraction Coefficient
Edge #1

Circular Ground Plane

$$\psi_2 = \begin{cases} \dfrac{\pi}{2} - \theta & 0 \le \theta \le 90^\circ \\ \dfrac{5\pi}{2} - \theta & 90^\circ \le \theta \le 180^\circ \end{cases}$$

$$\psi_1 = \frac{\pi}{2} + \theta$$

$$0^\circ \le \theta \le 180^\circ$$

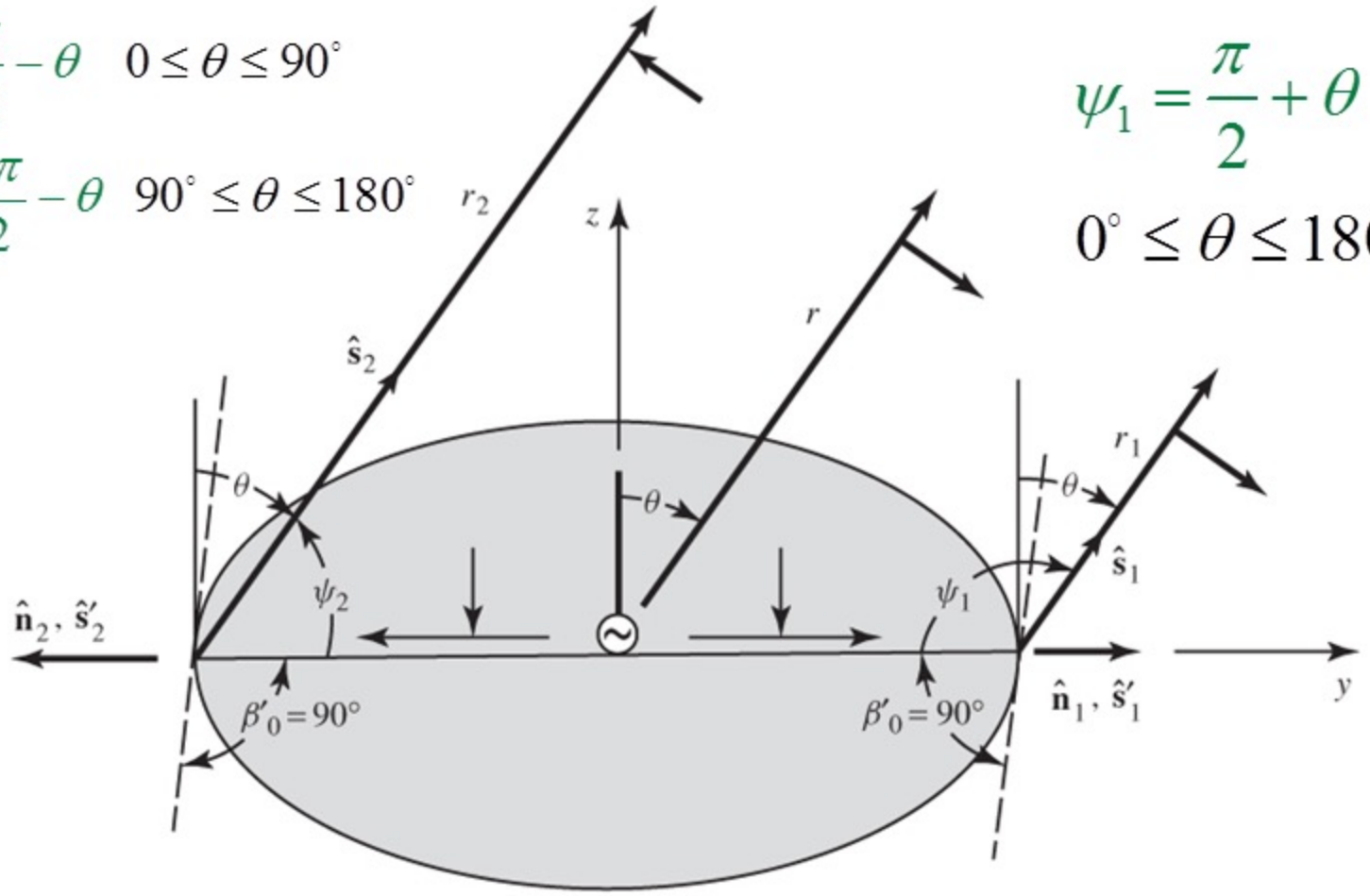

(b) Diffraction mechanism

Fig. 13-37

Distance Parameters

$$L_1^i,\ L_1^r$$

$$D_1^h(L_1^i, L_1^r, \psi_1, \psi_1', n) = D_1^i(L_1^i, \psi_1 - \psi_1', n = 2)$$
$$+ D_1^r(L_1^r, \psi_1 + \psi_1', n = 2)$$

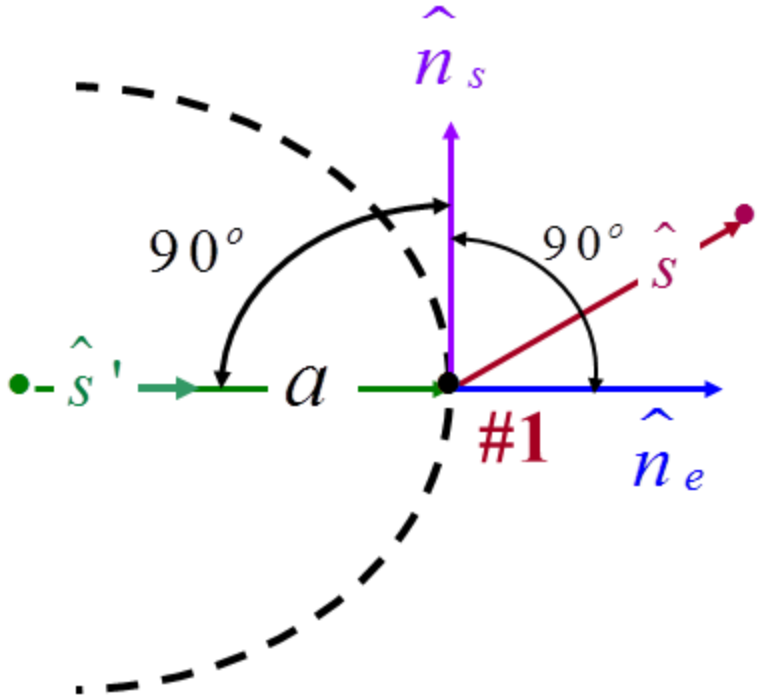

$$L_1^i = \frac{s(\rho_e^i + s)\rho_1^i \rho_2^i}{\rho_e^i(\rho_1^i + s)(\rho_2^i + s)} \sin^2 \beta_0' \Big|_{\beta_0'=90^\circ}$$

$$L_1^r = \frac{s(\rho_e^r + s)\rho_1^r \rho_2^r}{\rho_e^r(\rho_1^r + s)(\rho_2^r + s)} \sin^2 \beta_0' \Big|_{\beta_0'=90^\circ}$$

Distance Parameter

$$L_1^i$$

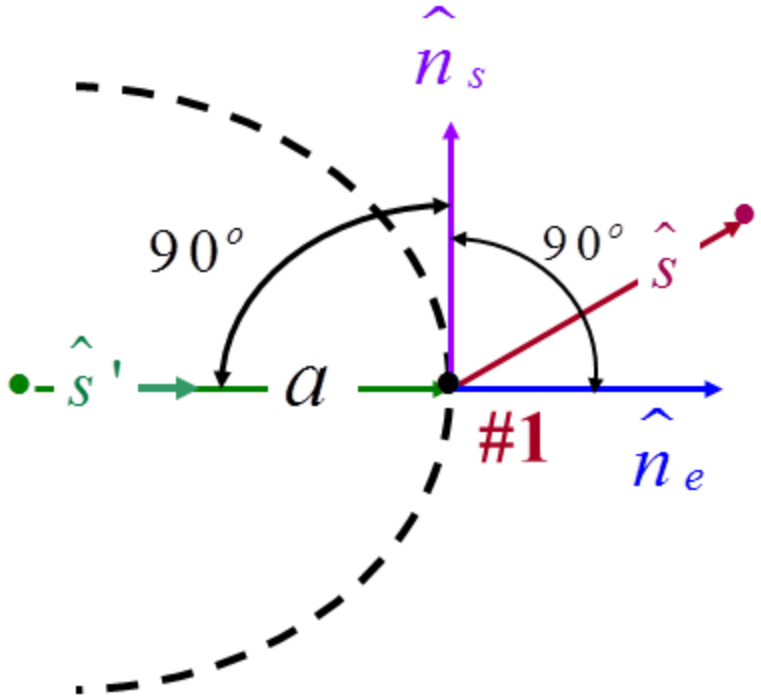

$$L_1^i = \frac{s(\rho_e^i + s)\rho_1^i \rho_2^i}{\rho_e^i(\rho_1^i + s)(\rho_2^i + s)} \sin^2 \beta_0' \Big|_{\beta_0'=90^\circ}$$

$$L_1^r = \frac{s(\rho_e^r + s)\rho_1^r \rho_2^r}{\rho_e^r(\rho_1^r + s)(\rho_2^r + s)} \sin^2 \beta_0' \Big|_{\beta_0'=90^\circ}$$

For Ground Plane Curved Edge

Since the wave from the $\lambda/4$ monopole is spherical, $\rho_1^i = \rho_2^i = s' = a$. Therefore

$$L_1^i = \left. \frac{s(\rho_e^i + s)\rho_1^i \rho_2^i}{\rho_e^i(\rho_1^i + s)(\rho_2^i + s)} \sin^2 \beta_0' \right|_{\beta_0' = 90^\circ}$$

$$\rho_e^i = s' = a; \quad \rho_1^i = \rho_2^i = s' = a$$

$$L_1^i = \left. \frac{s(s' + s)(s')^2}{s'(s' + s)(s' + s)} \sin^2 \beta_0' \right|_{\beta_0' = 90^\circ}$$

$$L_1^i = \frac{ss'}{s' + s} \overset{s >> s'}{\simeq} s' = a$$

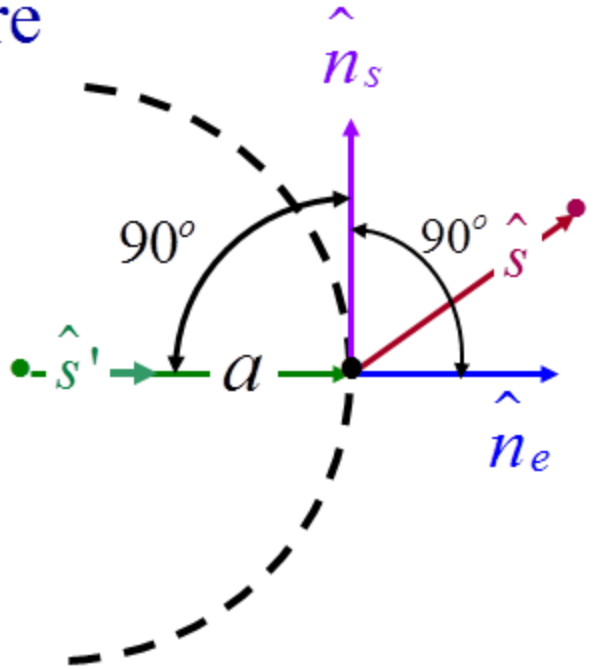

Distance Parameter

$$L_1^r$$

For Ground Plane Curved Edge

$$L_1^r = \frac{s(\rho_e^r + s)\rho_1^r \rho_2^r}{\rho_e^r(\rho_1^r + s)(\rho_2^r + s)} \sin^2 \beta_0^2$$

$$\rho_e^r = \rho_1^r = \rho_2^r = s' = a$$

$$L_1^r = \frac{s(s'+s)(s')^2}{s'(s'+s)(s'+s)} \sin^2 \beta_0'$$

$$L_1^r = \frac{ss'}{s'+s} \sin^2 \beta_0' \Big|_{\substack{\beta_0' = 90^\circ \\ s>>s'}} \overset{s>>s'}{=} s' = a$$

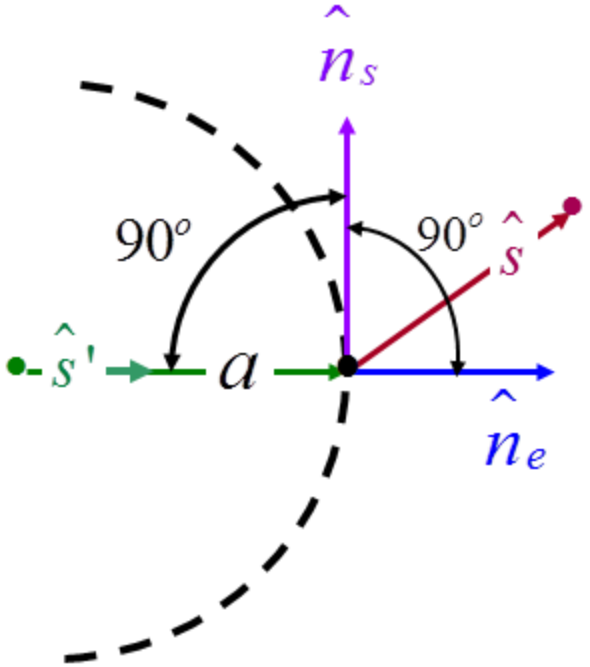

$$D_1^h(L_1^i, L_1^r, \psi_1, \psi_1', n) = D_1^i(L_1^i, \psi_1 - \psi_1', n = 2)$$
$$+ D_1^r(L_1^r, \psi_1 + \psi_1', n = 2)$$

$$\psi_1 = \frac{\pi}{2} + \theta, \quad \psi_1' = 0 \qquad 0^\circ \le \theta \le 180^\circ$$

$$\psi_1 - \psi_1' = \psi_1; \quad \psi_1 + \psi_1' = \psi_1$$

$$\Rightarrow \psi_1 - \psi_1' = \psi_1 + \psi_1' = \psi_1 = \psi_1 = \frac{\pi}{2} + \theta$$

Since

$$\psi_1 - \psi_1' = \psi_1 + \psi_1' = \psi_1 = \psi_1 = \frac{\pi}{2} + \theta$$

then

$$D_1^i(L_1^i, \psi_1 - \psi_1', n = 2) = D_1^r(L_1^r, \psi_1 + \psi_1', n = 2)$$

$$D_1^i(L_1^i, \psi_1, n = 2) = D_1^r(L_1^r, \psi_1, n = 2)$$

and

$$D_1^h(L_1^i, L_1^r, \psi_1, \psi_1', n) = 2D_1^i(L_1^i, \psi_1, n = 2)$$

$$= 2D_1^r(L_1^r, \psi_1, n = 2)$$

$$L_1^i = L_1^r = s' = a; \qquad \psi_1 = \frac{\pi}{2} + \theta,$$

Summary for Diffractions from Edge #1

$$E_1^d(r_1) = E_{GO}^i(Q_1) D_1^h(L_1^i, L_1^r) A_1(r_1, \rho_{c1}) e^{-j\beta r_1}$$

$$E_{GO}^i(Q_1) = \frac{1}{2} E_0 \frac{e^{-j\beta a}}{a}$$

$$D_1^h(L_1^i, L_1^r) = 2D_1^i(L_1^i, \psi_1, n=2) = 2D_1^r(L_1^r, \psi_1, n=2)$$

$$L_1^i = L_1^r = s' = a; \qquad \psi_1 = \frac{\pi}{2} + \theta$$

$$A_1(r_1, \rho_{c1}) = \frac{\sqrt{\rho_{c1}}}{r_1}; \quad \rho_{c1} = \frac{a}{\sin\theta}$$

Summary for Diffractions from Edge #1

$$E_1^d(r_1) = E_{GO}^i(Q_1) D_1^h(L_1^i, L_1^r) A_1(r_1, \rho_{c1}) e^{-j\beta r_1}$$

$$E_1^d(r_1) = \left(\frac{1}{2} E_0 \frac{e^{-j\beta a}}{a} \right) \left[2D_1^{i,r}(L_1^{i,r}, \psi_1, n=2) \right] \sqrt{\frac{a}{\sin\theta}} \frac{e^{-j\beta r_1}}{r_1}$$

$$E_1^d(r_1) = E_0 \underbrace{\left(\frac{e^{-j\beta a}}{\sqrt{a}} \right) \left[D_1^{i,r}\left(a, \frac{\pi}{2} + \theta, n=2 \right) \right]}_{V_B^{i,r}} \sqrt{\frac{1}{\sin\theta}} \frac{e^{-j\beta r_1}}{r_1}$$

$$E_1^d(r_1) = E_0 \left[V_B^{i,r}\left(a, \frac{\pi}{2} + \theta, n=2 \right) \right] \sqrt{\frac{1}{\sin\theta}} \frac{e^{-j\beta r_1}}{r_1}$$

Following a similar procedure, it can be shown that:

Diffraction Point #2:

$$E_2^d(r_2) = E_{GO}^i(Q_2) D_2^h(L_2^i, L_2^r) A_2(r_2, \rho_{c2}) e^{-j\beta r_2}$$

$$E_1^d(r_2) = -E_0 \underbrace{\left(\frac{e^{-j\beta a}}{\sqrt{a}} \right) \left[D_2^{i,r}\left(a, \xi_2, n=2\right) \right]}_{V_B^{i,r}} e^{j\frac{\pi}{2}} \sqrt{\frac{1}{\sin\theta}} \frac{e^{-j\beta r_1}}{r_1}$$

$$E_1^d(r_1) = -E_0 \left[V_B^{i,r}\left(a, \xi_2, n=2\right) \right] e^{j\frac{\pi}{2}} \sqrt{\frac{1}{\sin\theta}} \frac{e^{-j\beta r_2}}{r_2}$$

$$\xi_2 = \begin{cases} \dfrac{\pi}{2} - \theta, & \theta_o \le \theta \le \dfrac{\pi}{2} \\ \dfrac{5\pi}{2} - \theta, & \dfrac{\pi}{2} \le \theta \le \pi - \theta_o \end{cases}$$

$$A_2(r_2,\rho_{c2}) \simeq \frac{\sqrt{\rho_{c2}}}{r_2}$$

$$\frac{1}{\rho_{c2}} = \frac{1}{\rho_e^i} - \frac{\hat{n}_2 \cdot (\hat{s}_2' - \hat{s}_2)}{\rho_g \sin^2 \beta_0'}$$

$$\frac{1}{\rho_{c2}} = \frac{1}{a} - \frac{\hat{n}_2 \cdot \hat{s}_2' - \hat{n}_2 \cdot \hat{s}_2}{a \sin^2(90^\circ)}$$

$$\hat{n}_2 \cdot \hat{s}_2' = \left|\hat{n}_2\right|\left|\hat{s}_2'\right| \cos(0^\circ) = 1$$

$$\hat{n}_2 \cdot \hat{s}_2 = \left|\hat{n}_2\right|\left|\hat{s}_2\right| \cos\left(\frac{\pi}{2} + \theta\right) = -\sin\theta$$

$$\frac{1}{\rho_{c2}} = \frac{1}{a} - \frac{\hat{n}_2 \cdot \hat{s}_2' - \hat{n}_2 \cdot \hat{s}_2}{a \sin^2(90^\circ)}$$

$$\frac{1}{\rho_{c2}} = \frac{1}{a} - \frac{1-(-\sin\theta)}{a}$$

$$= \frac{1-1-\sin\theta}{a} = -\frac{\sin\theta}{a}$$

$$\Rightarrow \rho_{c2} = -\frac{a}{\sin\theta}$$

$$A_2(r_2,\rho_{c2}) \simeq \frac{\sqrt{\rho_{c2}}}{r_2} = \frac{1}{r_2}\sqrt{-\frac{a}{\sin\theta}}$$

$$= \frac{e^{j\pi/2}}{r_2}\sqrt{\frac{a}{\sin\theta}}$$

$$E_d^2(r_2) = E_{\theta G}^i(Q_2) D_2^h(L_2^i, L_2^r)$$

$$\cdot \sqrt{\frac{a}{\sin\theta}} e^{j\pi/2} \frac{e^{-j\beta r_2}}{r_2}$$

For far-field observations

$$\left.\begin{aligned} r_1 &\simeq r - a\cos\left(\frac{\pi}{2} - \theta\right) = r - a\sin\theta \\ r_2 &\simeq r - a\cos\left(\frac{\pi}{2} - \theta\right) = r + a\sin\theta \end{aligned}\right\} \text{for } \phi \text{ terms}$$

$$r_1 \simeq r_2 \simeq r \qquad \text{for amplitude terms}$$

Using the results from Example 13-6 we can write

$$E_{\theta G}(r,\theta) = E_0 \left[\frac{\cos\left(\frac{\pi}{2}\cos\theta\right)}{\sin\theta} \right] \frac{e^{-j\beta r}}{r} \qquad 0 \le \theta \le \pi/2$$

$$E^d_{\theta 1}(r,\theta) = E_0 \left[V_B^{i,r}\left(a, \theta + \frac{\pi}{2}, n=2\right)\right] \frac{e^{j\beta a \sin\theta}}{\sqrt{\sin\theta}} \frac{e^{-j\beta r}}{r}$$

$$\theta_o \le \theta \le \pi - \theta_o$$

$$E^d_{\theta 2}(r,\theta) = -E_0 \left[V_B^{i,r}\left(\frac{w}{2}, \xi_2, n=2\right)\right] e^{j\pi/2} \frac{e^{j\beta a \sin\theta}}{\sqrt{\sin\theta}} \frac{e^{-j\beta r}}{r}$$

$$\theta_o \le \theta \le \pi - \theta_o$$

$$\xi_2 = \begin{cases} \dfrac{\pi}{2} - \theta, & \theta_o \le \theta \le \dfrac{\pi}{2} \\ \dfrac{5\pi}{2} - \theta, & \dfrac{\pi}{2} \le \theta \le \pi - \theta_o \end{cases}$$

Amplitude Pattern: Circular Ground Plane

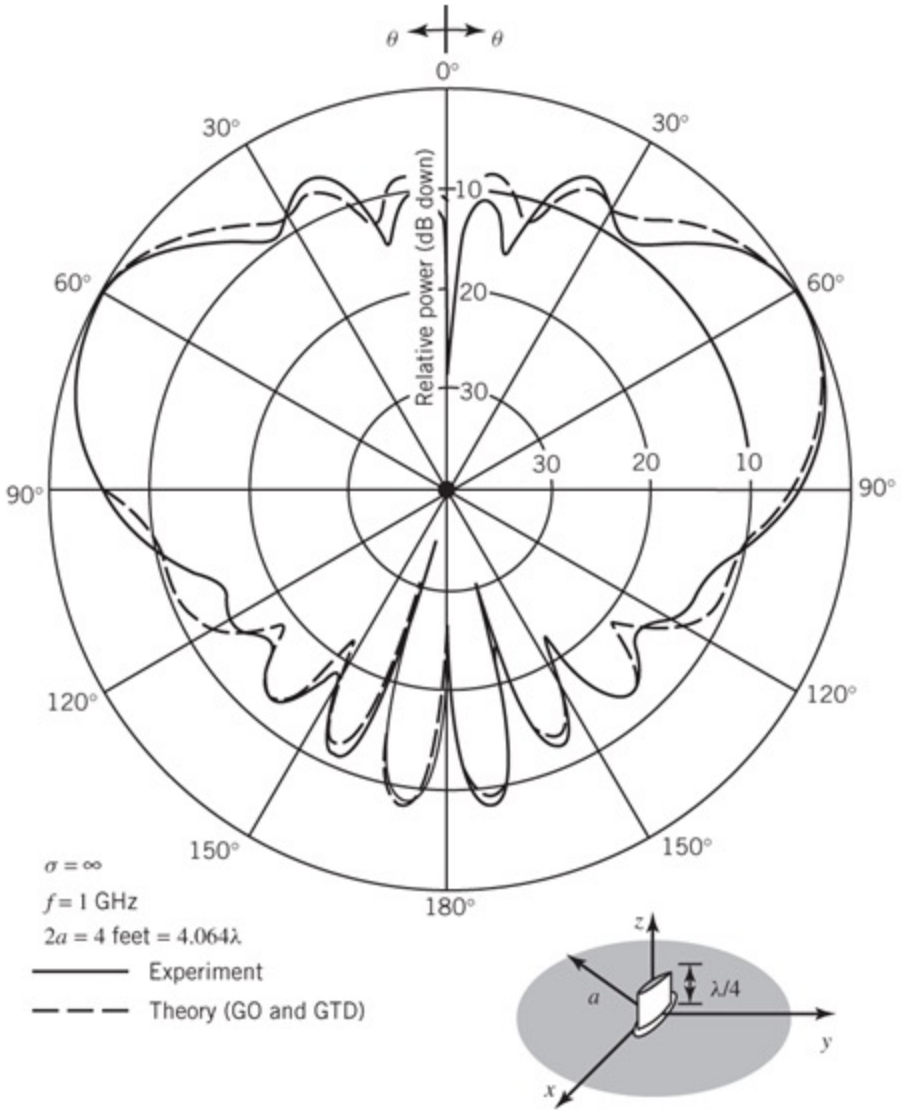

Fig. 13-39

It is noted that at $\theta = 0^{o}$ or 180^{o} the diffracted fields become singular because along these directions there are an infinite number of rays that contribute caustics for the diffracted fields. Along these directions, these rays form "a ring source radiator".

The infinite number of diffracted rays from the rim are identical in amplitude and phase and lead to the caustics.

Ring Radiator on a Circular Ground Plane

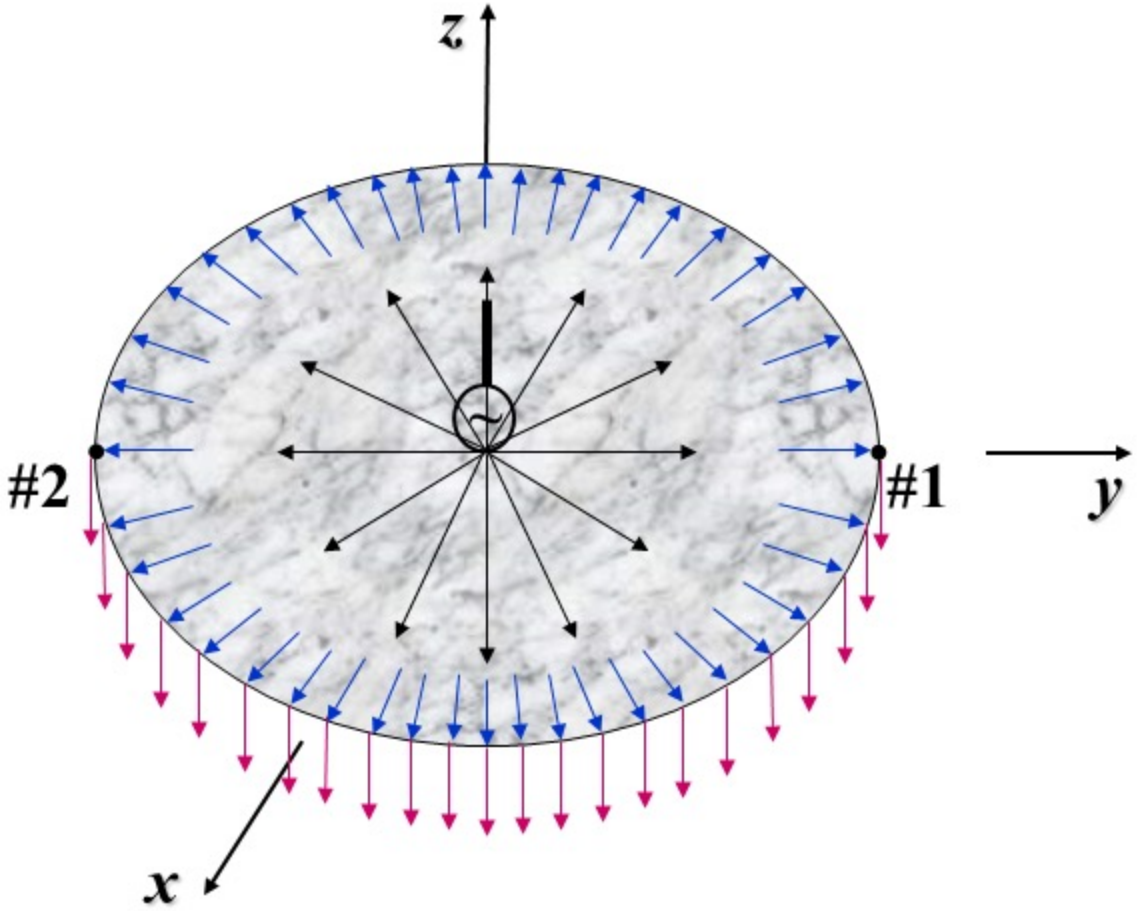

Fig. 13-38

Therefore the diffracted fields from the aforementioned two points of the rim are invalid within a cone of half included angle of θ_o which is primarily a function of the radius of curvature of the rim. For most moderate size ground planes, θ_o is in the range of $10^o < \theta_o < 30^o$.

To make corrections for the diffracted field singularity and inaccuracy at and near the symmetry axis ($\theta = 0^\circ$ or 180°) due to axial caustics, the rim of the ground plane must be modeled as a "ring radiator". This is accomplished by using the Method of Equivalent Currents (MEC) concepts in diffraction which will be discussed next. The ring radiator at and near the symmetry axis ($\theta = 0^\circ$ or 180°) leads to higher field intensity compared to the two-point diffraction. This is demonstrated in the next two graphs for circular and square ground planes.

By modeling the ring radiator by "equivalent currents" for the field at and near the symmetry axis ($\theta = 0^\circ$ or 180°), which will be in the form of an integral, it can be shown that by applying the *Method of Steepest Descent* (*Saddle Point Method*), which was discussed previously, that for points not close to the symmetry axis, the diffracted field can be included by assuming that only two points on the edge of the cone, which are contained in the plane of diffraction and are diametrical to each other, are sufficient to predict the overall radiation pattern very accurately.

Amplitude Pattern: Circular Ground Plane

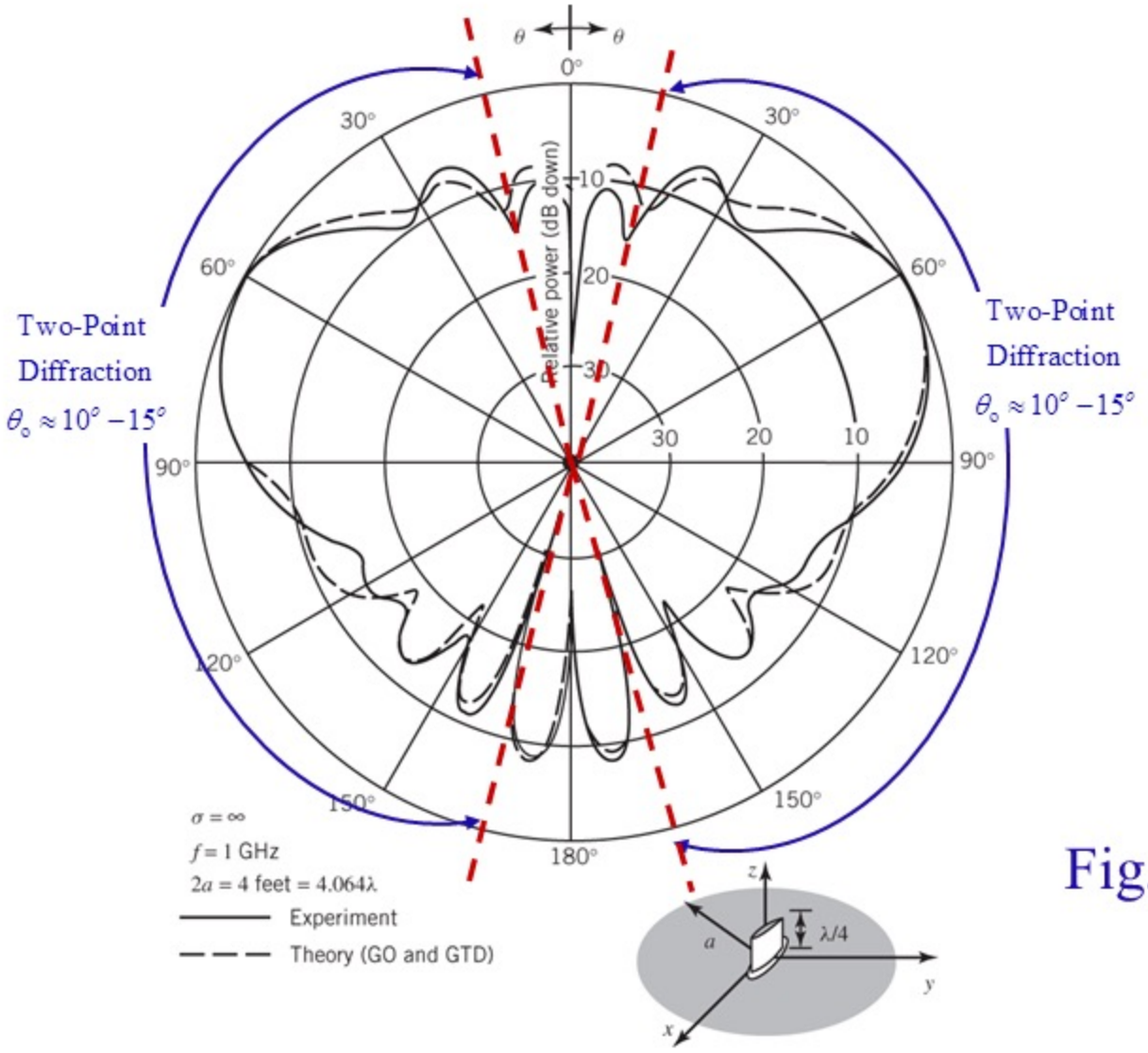

Fig. 13-39

Method of Equivalent Currents (MEC)

Normal Incidence Equivalent Currents (EC)

Wedge Diffraction at Normal Incidence and its Equivalent

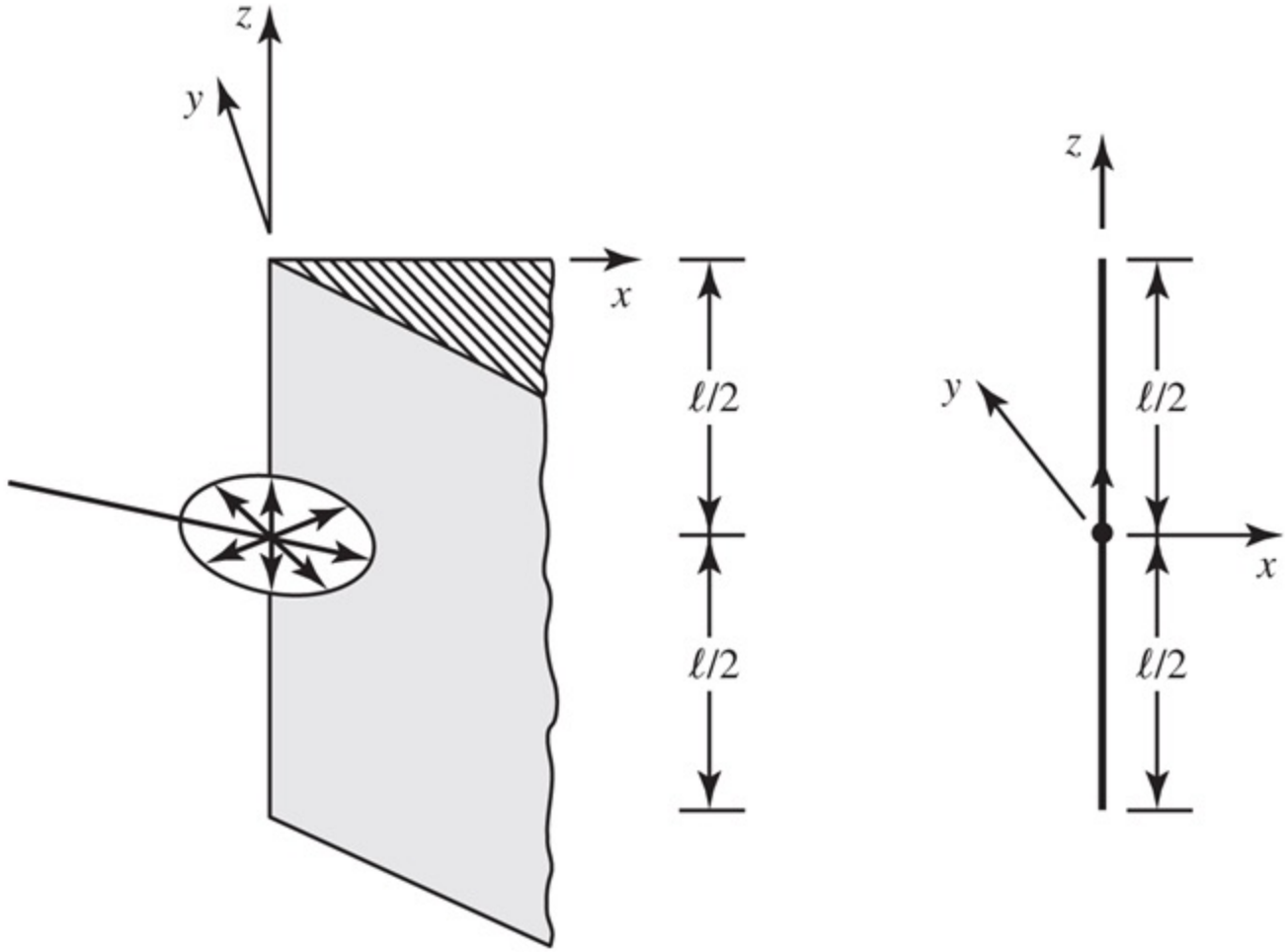

(a) Actual Wedge

Fig. 13-40

(b) Equivalent

Ideal Current Distribution on a Dipole Antenna [38]

$$I_z^e(z') = \begin{cases} I_o \sin\left[\beta\left(\frac{\ell}{2} - z'\right)\right] & 0 \le z' \le +\ell/2 \\ I_o \sin\left[\beta\left(\frac{\ell}{2} + z'\right)\right] & -\ell/2 \le z' \le 0 \end{cases}$$

Electric Field Radiated by a Dipole of Length ℓ [38]

$$E_\theta^e = j\eta \frac{\beta e^{-j\beta r}}{4\pi r} \sin\theta \int_{-\ell/2}^{\ell/2} I_z^e(z') e^{j\beta z' \cos\theta} dz'$$

$$E_\theta^e = j\eta \frac{I_o e^{-j\beta r}}{2\pi r} \left[\frac{\cos\left(\frac{\beta\ell}{2}\cos\theta\right) - \cos\left(\frac{\beta\ell}{2}\right)}{\sin\theta} \right]$$

Half-Wavelength Dipole ($\ell=\lambda/2$) [38]

$$E_\theta^e \overset{\ell=\lambda/2}{=} E_\theta \simeq j\eta \frac{I_0 e^{-j\beta r}}{2\pi r} \frac{\cos\left(\frac{\pi}{2}\cos\theta\right)}{\sin\theta}$$

Infinitesimal Dipole ($\ell << \lambda$) [38]

$$E_\theta^e \overset{\ell<<\lambda}{=} j\eta \frac{I_0 \beta \ell e^{-j\beta r}}{4\pi r} \sin\theta$$

Elevation Plane Amplitude Patterns for a Thin Dipole [38]

($l = << \lambda, \lambda/4, \lambda/2, 3\lambda/4, \lambda$)

HPBW

1. $\ell \leq \dfrac{\lambda}{50}$: HPBW = 90°

2. $\ell \leq \dfrac{\lambda}{2}$: HPBW = 74.93°

3. $\ell \leq \lambda$: HPBW = 47.8°

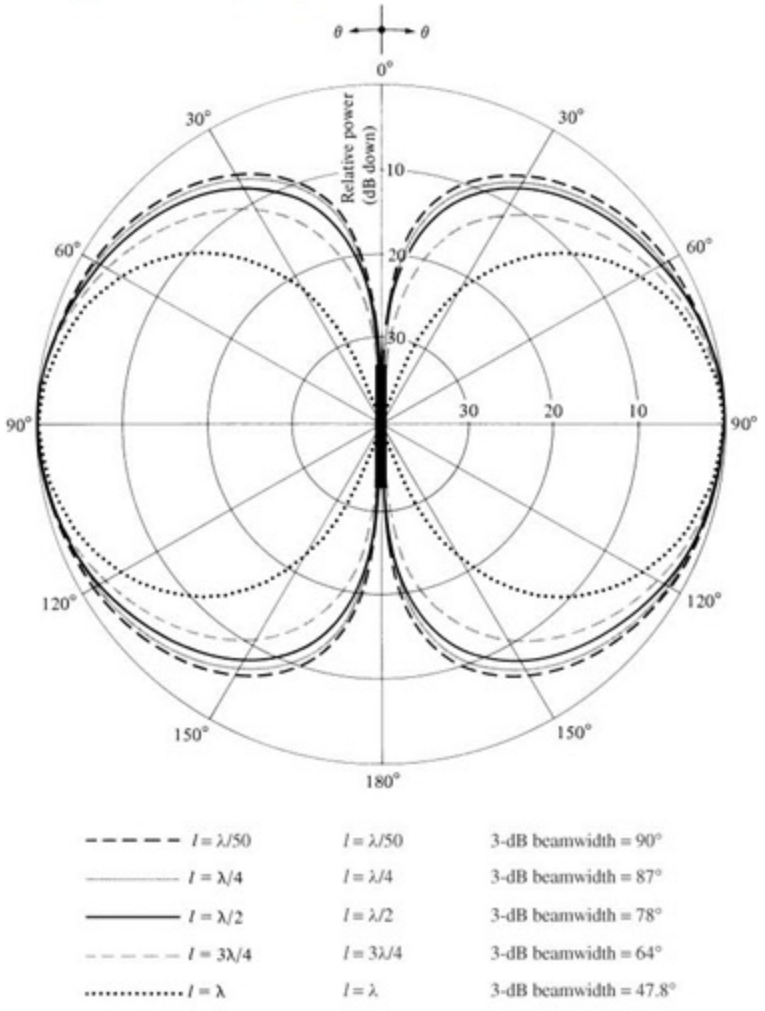

Two-Dimensional Pattern [38] (l=1.25λ)

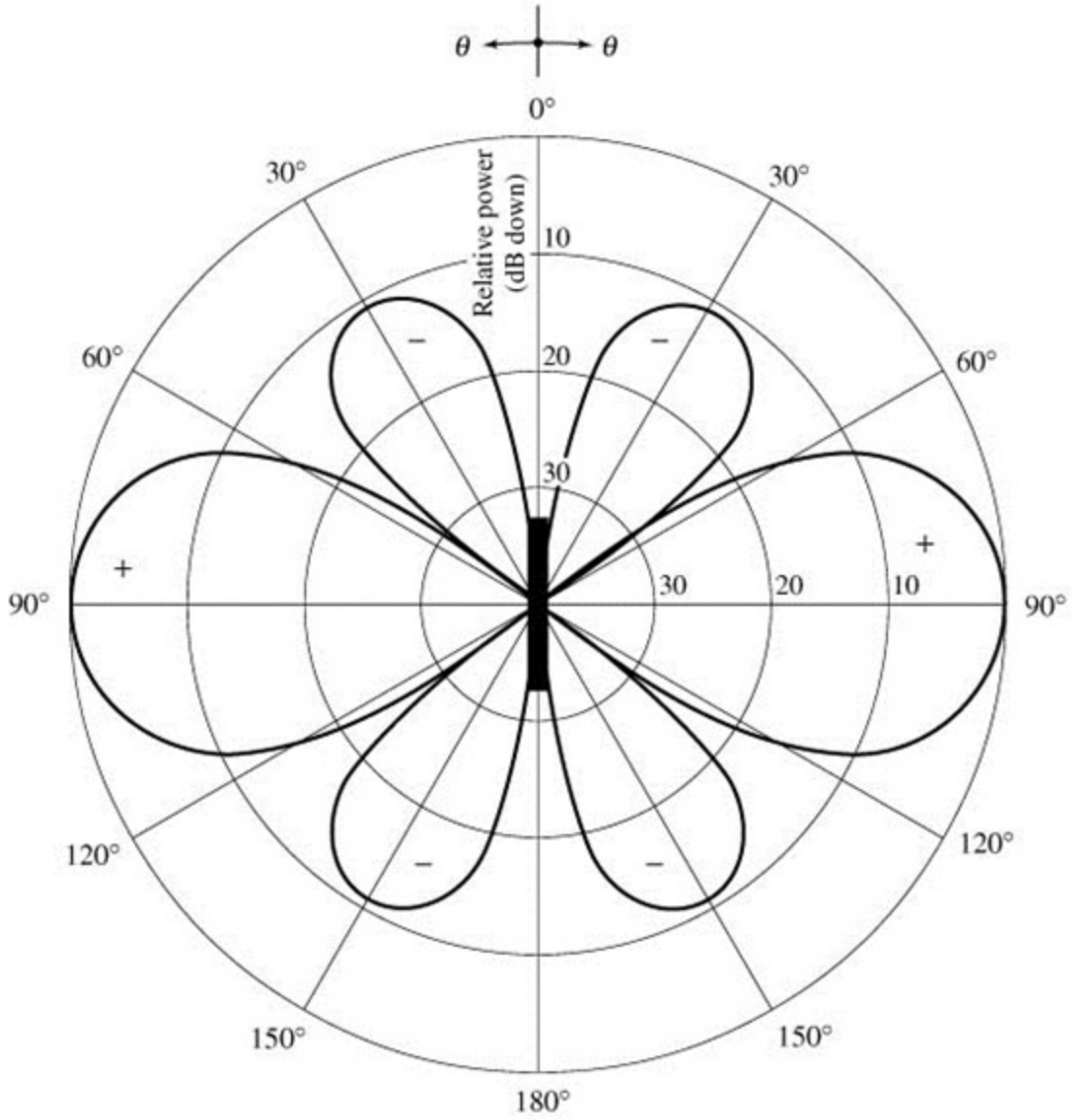

Electric Line Source:

The electric field radiated by an electric line source is

$$E_z^e = -\frac{\beta^2 I_z^e}{4\omega\varepsilon} H_0^{(2)}(\beta\rho)$$

For far-field observations

$$H_0^{(2)}(\beta\rho) \overset{\beta\rho\to\infty}{\simeq} \sqrt{\frac{2}{\pi\beta\rho}} e^{-j\left(\beta\rho+\frac{\pi}{4}\right)}$$

the electric field reduces to

$$E_z^e \overset{\beta\rho\to\infty}{\simeq} -I_z^e \frac{\eta\beta}{2}\sqrt{\frac{j}{2\pi\beta}}\frac{e^{-j\beta\rho}}{\sqrt{\rho}} \qquad \text{(13-101a)}$$

Electric:

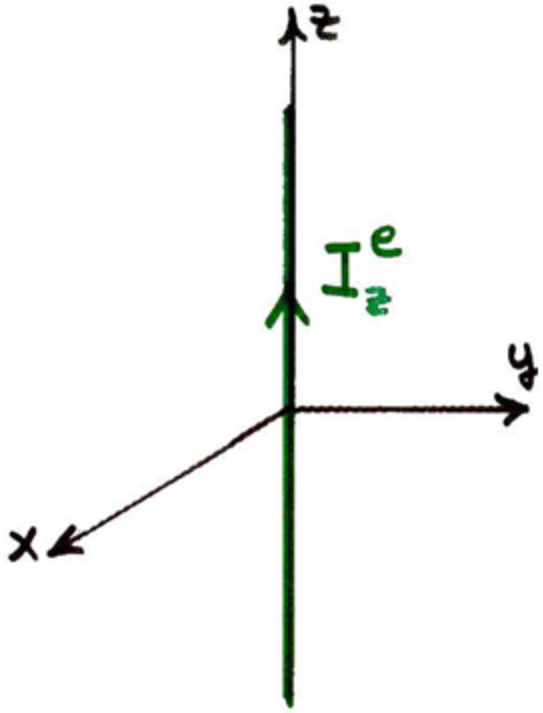

Magnetic Line Source:

The magnetic field radiated by a magnetic line source is

$$H_z^m = -\frac{\beta^2 I_z^m}{4\omega\mu} H_0^{(2)}(\beta\rho)$$

For far-field observations

$$H_0^{(2)}(\beta\rho) \overset{\beta\rho\to\infty}{\simeq} \sqrt{\frac{2}{\pi\beta\rho}} e^{-j\left(\beta\rho+\frac{\pi}{4}\right)}$$

the magnetic field reduces to

$$H_z^m \overset{\beta\rho\to\infty}{\simeq} -I_z^m \frac{\beta}{2\eta}\sqrt{\frac{j}{2\pi\beta}}\frac{e^{-j\beta\rho}}{\sqrt{\rho}}$$

(13-101b)

Magnetic:

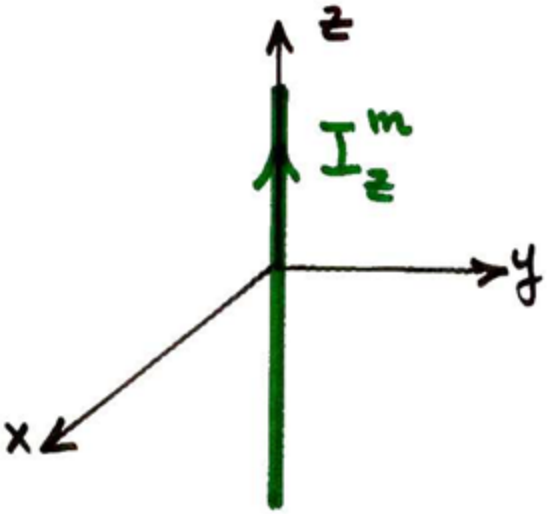

Using (13-34), (13-34a), (13-101a) and (13-101b), and assuming normal incidence ($\beta' = \pi / 2$), we can write the electric field diffracted from a wedge as:

Soft Polarization:

$$E_z^d = E_z^i(Q_D) D_s(L, \xi^-, \xi^+, n) \frac{1}{\sqrt{\rho}} e^{-j\beta\rho} \quad \text{(diffraction)}$$

while the electric field radiated by an electric line source is

$$E_z^e \simeq -I_z^e \frac{\eta\beta}{2} \sqrt{\frac{j}{2\pi\beta}} \frac{e^{-j\beta\rho}}{\sqrt{\rho}} \quad \text{(electric line source)}$$

By equating the previous two equations:

$$\underbrace{E_z^d = E_z^i(Q_D) D_s(L, \xi^-, \xi^+, n) \frac{1}{\sqrt{\rho}} e^{-j\beta\rho}}_{\text{from diffraction}} \qquad (13\text{-}102a)$$

$$= \underbrace{E_z^e \simeq -I_z^e \frac{\eta\beta}{2} \sqrt{\frac{j}{2\pi\beta}} \frac{e^{-j\beta\rho}}{\sqrt{\rho}}}_{\text{from electric line source}}$$

and solving for I_z^e, it leads to the electric EC of

$$I_z^e = -\frac{\sqrt{8\pi\beta}}{\eta\beta} e^{-j\pi/4} E_z^i(Q_D) D^s(L, \xi^-, \xi^+, n) \qquad (13\text{-}103a)$$

Using (13-34), (13-34a), (13-101a) and (13-101b), and assuming normal incidence ($\beta' = \pi / 2$), we can write the magnetic field diffracted from a wedge as:

Hard Polarization:

$$H_z^d = H_z^i(Q_D) D^h(L, \xi^-, \xi^+, n) \frac{1}{\sqrt{\rho}} e^{-j\beta\rho} \quad \text{(diffraction)}$$

while the magnetic field radiated by a magnetic line source is

$$H_z^m \simeq -I_z^m \frac{\beta}{2\eta} \sqrt{\frac{j}{2\pi\beta}} \frac{e^{-j\beta\rho}}{\sqrt{\rho}} \quad \text{(magnetic line source)}$$

By equating the previous two equations:

$$\underbrace{E_z^d = E_z^i(Q_D) D_s(L,\xi^-,\xi^+,n)\frac{1}{\sqrt{\rho}} e^{-j\beta\rho}}_{\text{from diffraction}} = \underbrace{E_z^e \simeq -I_z^e \frac{\eta\beta}{2}\sqrt{\frac{j}{2\pi\beta}}\frac{e^{-j\beta\rho}}{\sqrt{\rho}}}_{\text{from magnetic line source}} \quad (13\text{-}102b)$$

and solving for I_z^m, it leads to the magnetic EC of

$$\boxed{I_z^m = -\eta\frac{\sqrt{8\pi\beta}}{\beta} e^{-j\pi/4} H_z^i(Q_D) D^h(L,\xi^-,\xi^+,n)} \quad (13\text{-}103b)$$

If the wedge of Figure 13-40 is of finite length ℓ, its equivalent current will also be of finite length. The far-zone field radiated by each can be obtained by using techniques similar to those of Chapter 4 of [38]. Assuming the edge is along the z axis, the far-zone electric field radiated by an electric line source of length ℓ can be written using (4-58a) of [38] as

$$E_\theta^e = j\eta \frac{\beta e^{-j\beta r}}{4\pi r} \sin\theta \int_{-\ell/2}^{\ell/2} I_z^e(z') e^{j\beta z' \cos\theta} dz' \qquad (13\text{-}104a)$$

Electric

$$E_\theta^e = j\eta \frac{\beta e^{-j\beta r}}{4\pi r} \sin\theta \int_{-l/2}^{+l/2} I_z^e(z') e^{j\beta z' \cos\theta} dz' \qquad \text{(13-104a)}$$

$$I_z^e = \text{constant} = I_z^e(z')$$

$$E_\theta^e = j\eta \frac{\beta e^{-j\beta r}}{4\pi r} \sin\theta \, I_z^e \int_{-l/2}^{+l/2} e^{j\beta z' \cos\theta} dz'$$

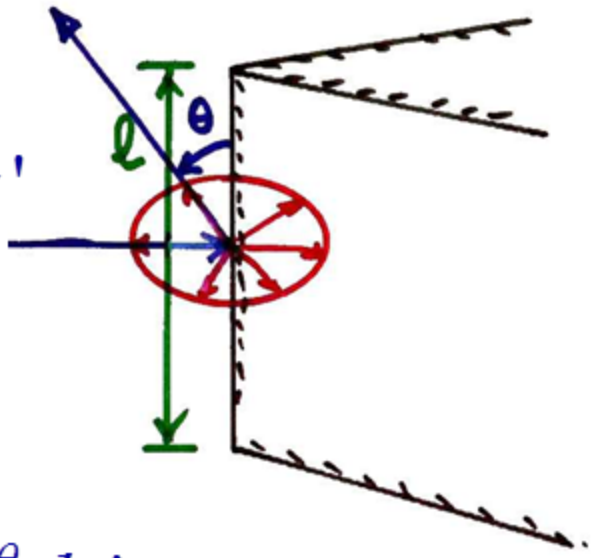

Magnetic

$$H_\theta^m = j \frac{\beta e^{-j\beta r}}{4\pi r} \sin\theta \int_{-l/2}^{+l/2} I_z^m(z') e^{j\beta z' \cos\theta} dz' \qquad \text{(13-104b)}$$

Using duality, the far-zone magnetic field radiated by a magnetic line source of finite length can be written as

$$H_\theta^m = j\frac{\beta e^{-j\beta r}}{4\pi r}\sin\theta \int_{-l/2}^{+l/2} I_z^m(z')e^{j\beta z'\cos\theta}dz' \qquad (13\text{-}104a)$$

For a constant equivalent current, the integrals of (13-104a) and (13-104b) reduce to a sinc function.

$$\frac{\sin(\zeta)}{\zeta}$$

Oblique Plane Wave Incidence EC

For oblique plane wave incidence diffraction by a finite length ℓ wedge, as shown in Figure 13-41, the equivalent currents of (13-103a) and (13-103b) take the form of:

Oblique Incidence Diffraction a Finite Length Wedge

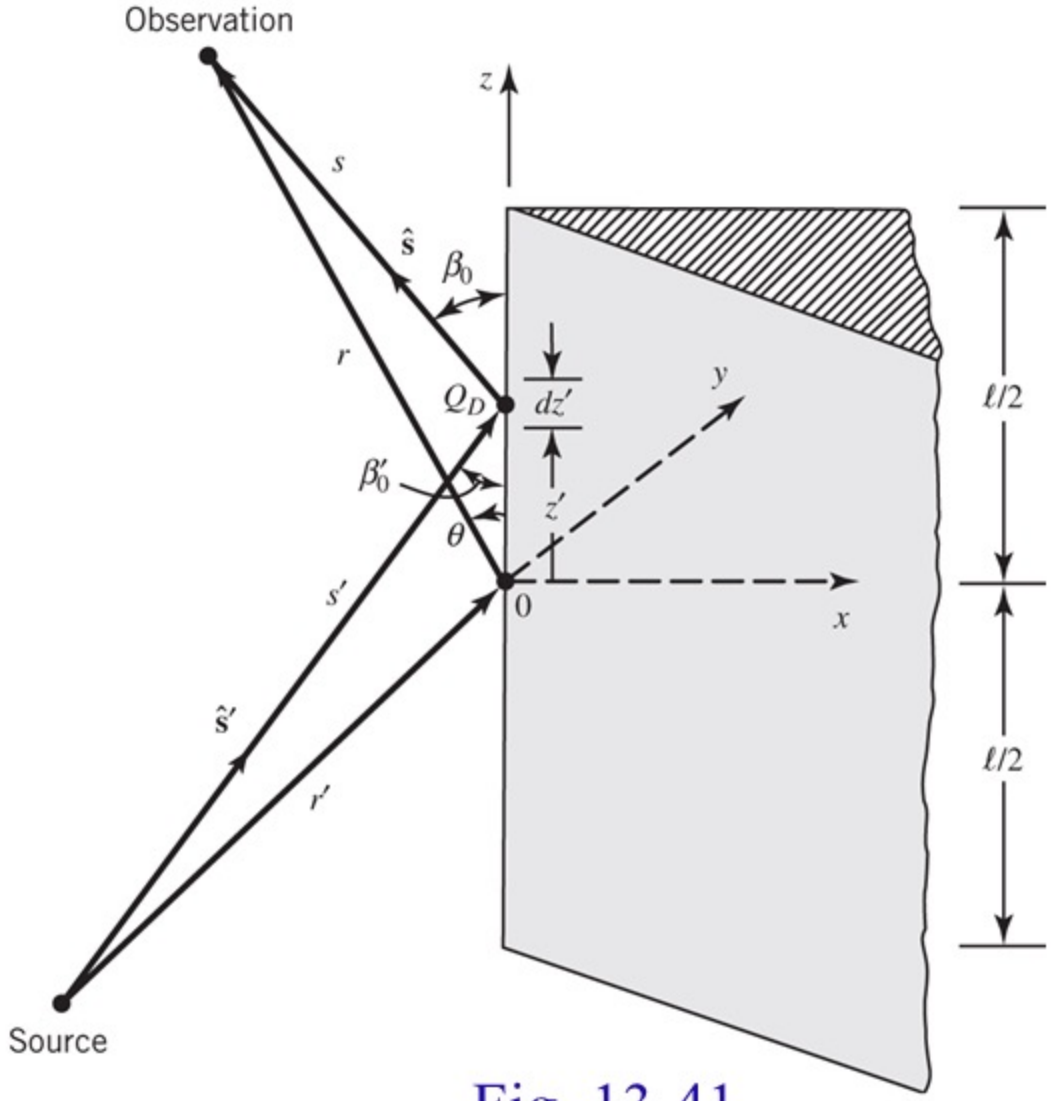

Fig. 13-41

Electric Line Source: Soft Polarization

$$I_z^e = -\frac{\sqrt{8\pi\beta}}{\pi\beta} e^{-j\pi/4} E_z^i(Q_D) D_s(\xi^-, \xi^+, n; \beta_0')$$

$$I_z^e \overset{s'>>z'}{\simeq} -\frac{\sqrt{8\pi\beta}}{\pi\beta} e^{-j\pi/4} E_z^i(0) D_s(\xi^-, \xi^+, n; \beta_0') e^{-j\beta z' \cos\beta_0'}$$

(13-107a)

Magnetic Line Source: Hard Polarization

$$I_z^m = -\frac{\eta\sqrt{8\pi\beta}}{\beta} e^{-j\pi/4} H_z^i(Q_D) D_h(\xi^-, \xi^+, n; \beta_0')$$

$$I_z^m \overset{s'>>z'}{\simeq} -\frac{\eta\sqrt{8\pi\beta}}{\beta} e^{-j\pi/4} H_z^i(0) D_h(\xi^-, \xi^+, n; \beta_0') e^{-j\beta z' \cos\beta_0'}$$

(13-107b)

Circular Loop Equivalent Currents (EC)

Circular Loop Equivalent Currents

If the equivalent current is distributed along a circular loop of radius a and it is parallel to the *xy*-plane, as shown in the figure that follows, the field radiated by each of the equivalent currents can be obtained using the techniques of Chapter 5, Section 5.3, of [38].

Geometry for Circular Loop [38]

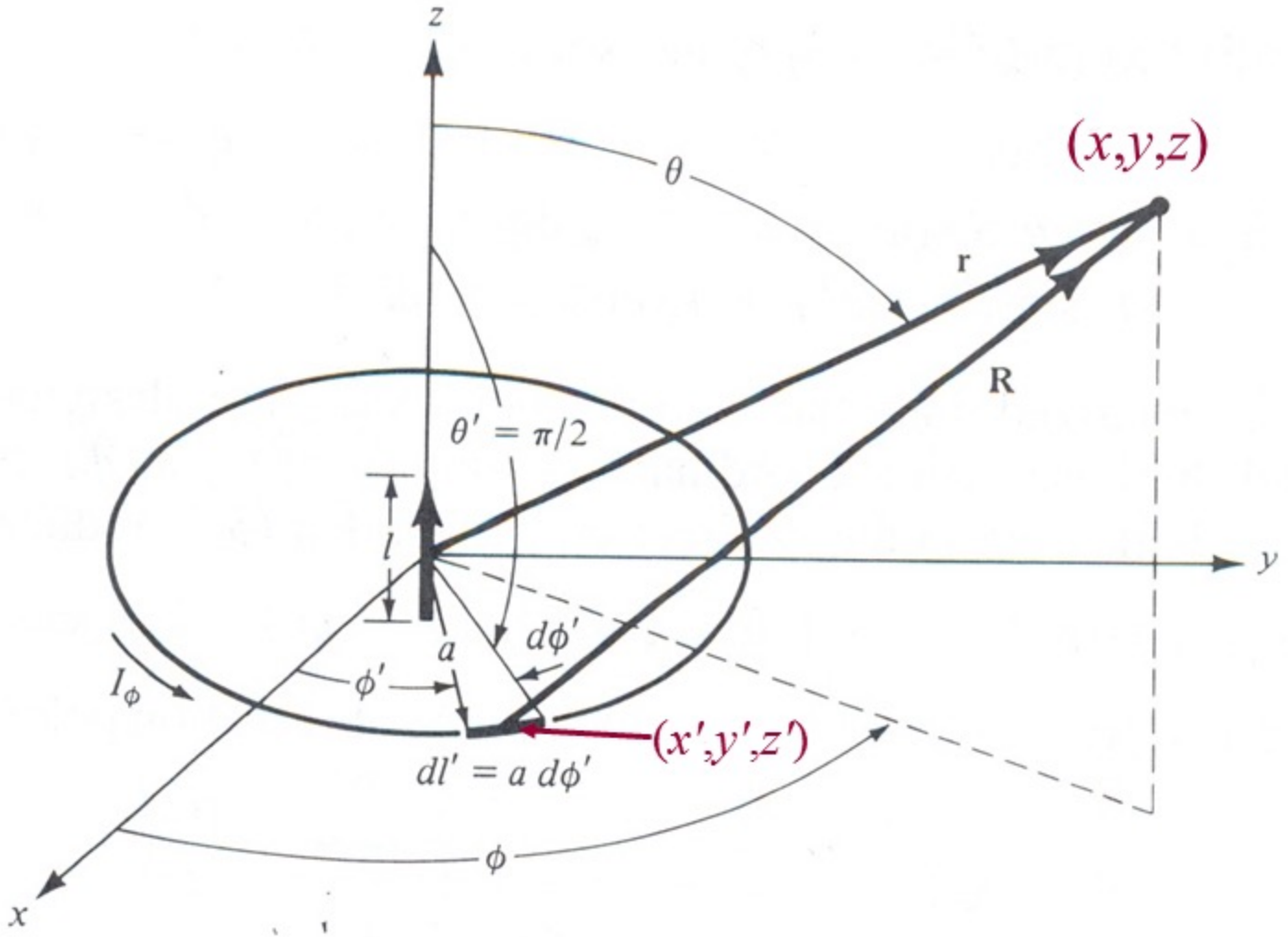

Geometrical Arrangement for Far Field Radiation [38]

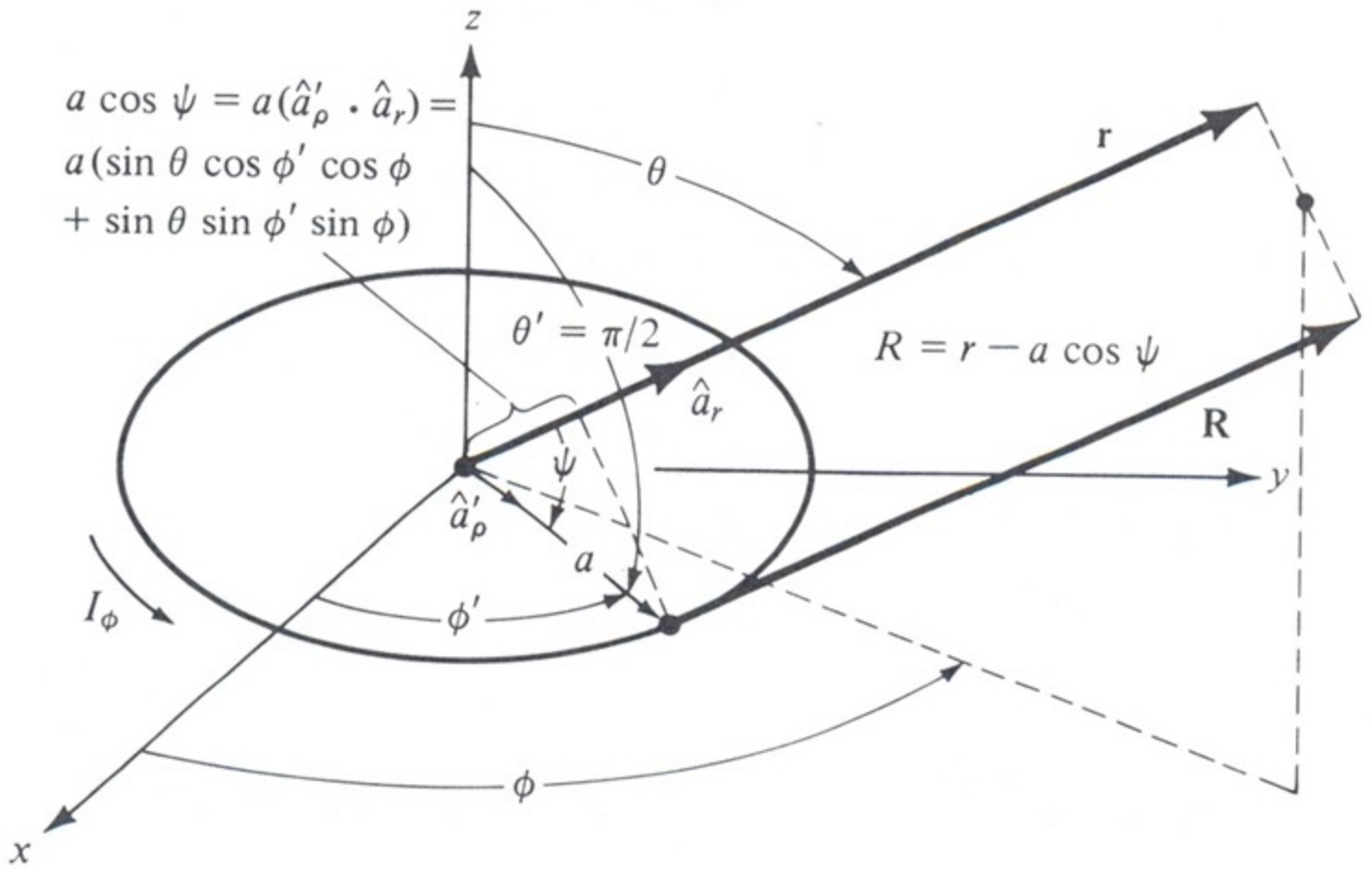

Electric Equivalent Current

$$E_\phi^e = -j\frac{\omega\mu a e^{-j\beta r}}{4\pi r}\int_0^{2\pi} I_\phi^e(\phi')\cos(\phi-\phi')e^{j\beta a\sin\theta\cos(\phi-\phi')}d\phi' \qquad (13\text{-}105a)$$

If the current $I_\phi^e(\phi')$ is constant, $I_\phi^e(\phi') = I_\phi^e$

$$E_\phi^e = -j\frac{\omega\mu a e^{-jkr}}{4\pi r} I_\phi^e \int_0^{2\pi} \cos(\phi')e^{j\beta a\sin\theta\cos\phi'}d\phi'$$

$$E_\phi^e = -j\frac{\omega\mu a e^{-j\beta r}}{4\pi r} I_\phi^e \left[2\pi j J_1(\beta a\sin\theta)\right]$$

$$E_\phi^e = \frac{\omega\mu a e^{-j\beta r}}{2r} I_\phi^e J_1(\beta a\sin\theta) \qquad (13\text{-}106a)$$

Magnetic Equivalent Current

$$H_\phi^m = j\frac{\omega\varepsilon a e^{-j\beta r}}{4\pi r} \cdot \int_0^{2\pi} I_\phi^m(\phi')\cos(\phi-\phi')e^{j\beta a\sin\theta\cos(\phi-\phi')}d\phi' \qquad (13\text{-}105b)$$

$$H_\phi^m = \frac{\omega\varepsilon a e^{-j\beta r}}{2r} I_\phi^m J_1(\beta a\sin\theta) \qquad (13\text{-}106b)$$

$$E_\theta^m = \eta H_\phi^m = \eta\frac{a\omega\varepsilon e^{-j\beta r}}{2r} I_\phi^m J_1(\beta a\sin\theta)$$

Amplitude Pattern: Circular Ground Plane

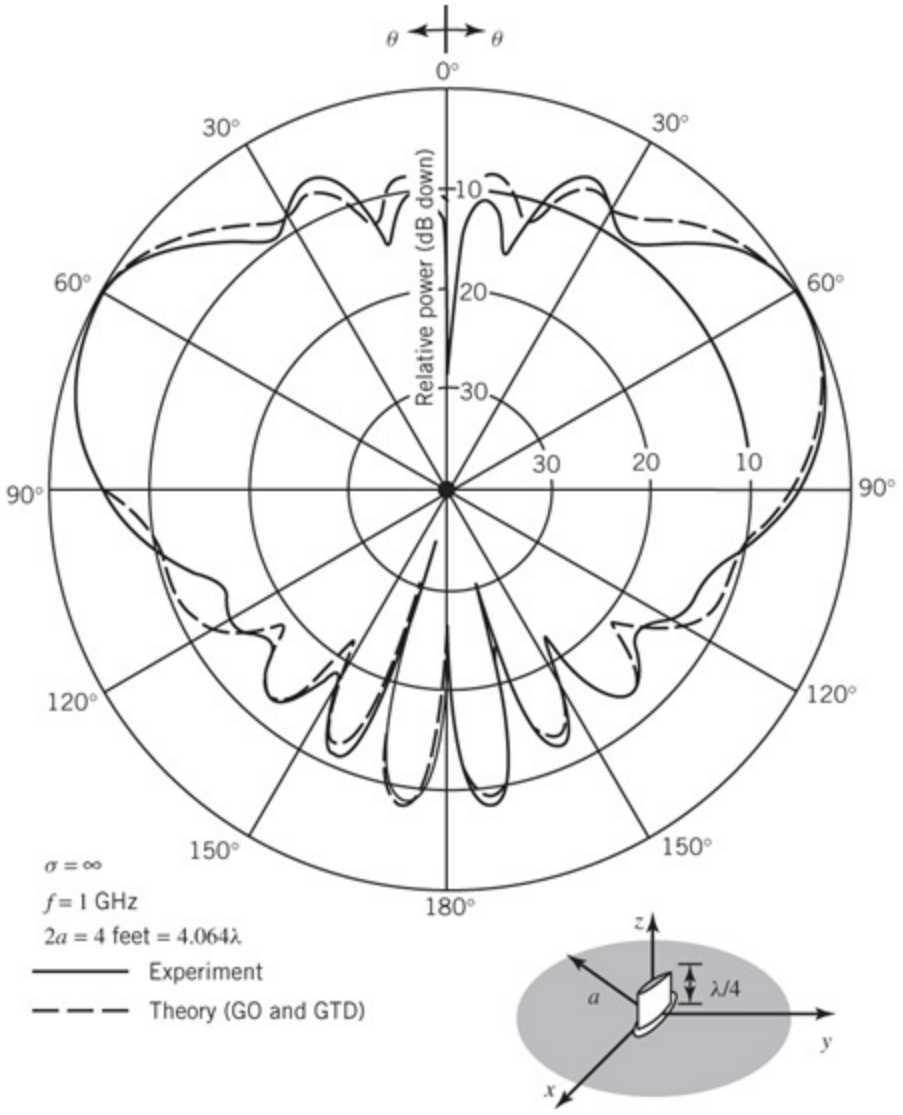

Fig. 13-39

Slope Diffraction

Slope Diffraction

When $\phi' = 0$ or $n\pi$ (grazing angle), the soft polarization diffraction coefficient $D^s = 0$. Thus the diffracted field, for this polarization based on the regular diffraction coefficient D^s, according to the following equation

$$E_D^s = \underline{E}^i(Q) \cdot \widetilde{D}^s \; A(s', s) \; e^{-j\beta s}$$

is equal to zero. There are higher-order diffraction coefficients that account for diffraction based on the rate of change (*slope*) of the field at the point of diffraction. These coefficients are referred to as *slope diffraction coefficients*, and will be introduced later.

Slope diffracted fields are not significant for hard polarization cases, in which higher-order regular diffractions are more significant than slope diffractions; however they contribute in soft polarization cases because this polarization does not usually support higher-order diffractions. The general formulation for slope diffracted fields is to determine the slope of the incident field at the point of interest and the multiply it by the appropriate UTD slope diffraction coefficient.

Wedge Geometry for Slope Diffraction

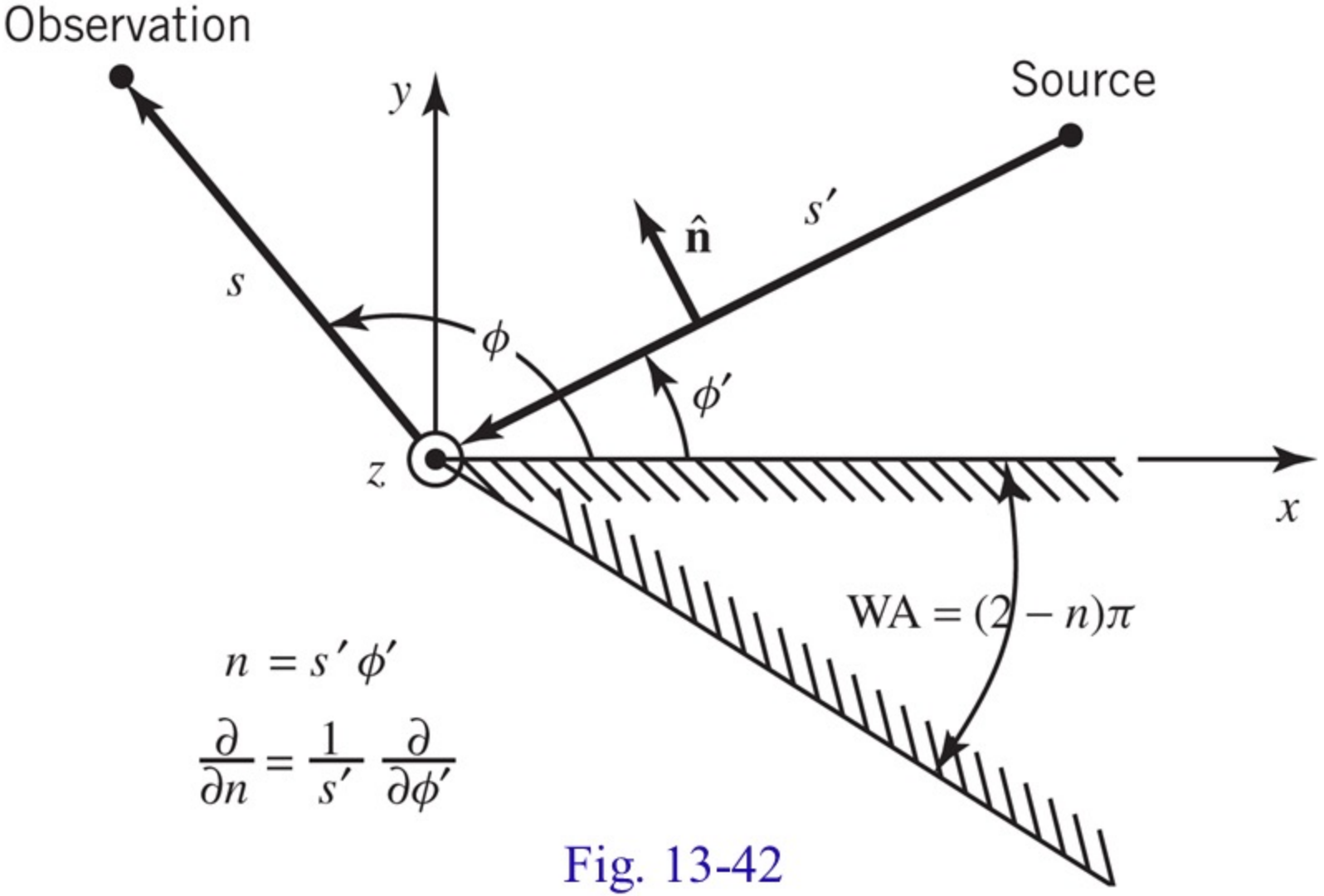

Fig. 13-42

Slope Diffraction

$$U_{s,h}^{d} = \frac{1}{j\beta}\left[\frac{\partial U^{i}(Q_D)}{\partial n}\right]\left[\frac{\partial D_{s,h}}{\partial \phi'}\right]\sqrt{\frac{\rho_c}{s(\rho_c + s)}}\, e^{-j\beta s} \qquad (13\text{-}108)$$

$$\frac{\partial U^{i}(Q_D)}{\partial n} = \frac{1}{s'}\frac{\partial U^{i}}{\partial \phi'}\bigg|_{Q_D} = \text{slope of incident field} \qquad (13\text{-}108a)$$

$$\frac{\partial D_{s,h}}{\partial \phi'} = \text{slope diffraction coefficient} \qquad (13\text{-}108c)$$

U represent E (for soft) and H (for hard).

Slope Diffraction

$$E^d = \frac{1}{j\beta}\left[\frac{\partial E^i(Q_D)}{\partial n}\right]\left[\frac{\partial D_s}{\partial \phi'}\right]\sqrt{\frac{\rho_c}{s(\rho_c + s)}}e^{-j\beta s}$$

(13-108)

$$\frac{\partial E^i(Q_D)}{\partial n} = \frac{1}{s'}\frac{\partial E^i}{\partial \phi'}\bigg|_{Q_D} = \text{slope of incident field}$$

(13-108a)

$$\frac{\partial D_s}{\partial \phi'} = \text{slope diffraction coefficient}$$

(13-108c)

Slope Diffraction

$$H^d = \frac{1}{j\beta}\left[\frac{\partial H^i(Q_D)}{\partial n}\right]\left[\frac{\partial D_h}{\partial \phi'}\right]\sqrt{\frac{\rho_c}{s(\rho_c + s)}}e^{-j\beta s}$$

(13-109)

$$\frac{\partial H^i(Q_D)}{\partial n} = \frac{1}{s'}\frac{\partial H^i}{\partial \phi'}\bigg|_{Q_D} = \text{slope of incident field}$$

(13-109a)

$$\frac{\partial D_h}{\partial \phi'} = \text{slope diffraction coefficient}$$

(13-109c)

Slope Diffraction

In general, the total diffracted field can be found using

$$U_d^{s,h} = \left\{ U^i(Q_D) D_{s,h} + \frac{1}{j\beta} \left[\frac{\partial U^i(Q_D)}{\partial n} \right] \left[\frac{\partial D_{s,h}}{\partial \phi'} \right] \right\} \times \sqrt{\frac{\rho_c}{s(\rho_c + s)}} e^{-j\beta s} \tag{13-110}$$

where the first term represents the contribution to the total diffracted field due to the magnitude of the incident field and the second accounts for the contribution due to the slope (rate of change) of the incident field. U represents either the electric for the soft polarization and the magnetic field for the hard polarization.

Slope Diffraction Coefficient for Soft (Hard) Polarization

$$\left[\frac{\partial D_{s,h}}{\partial \phi'}(\phi,\phi',n;\beta_o')\right] = -\frac{e^{-j\pi/4}}{4n^2\sqrt{2\pi\beta}\sin\beta_0'}\times$$

$$\times\left\{\left[\csc^2\left[\frac{\pi+(\phi-\phi')}{2n}\right]F_s\left[\beta Lg^+(\phi-\phi')\right]\right.\right.$$

$$\left.-\csc^2\left[\frac{\pi-(\phi-\phi')}{2n}\right]F_s\left[\beta Lg^-(\phi-\phi')\right]\right]$$

$$\pm\left\{-\left[\csc^2\left[\frac{\pi+(\phi+\phi')}{2n}\right]F_s\left[\beta Lg^+(\phi+\phi')\right]\right.\right.$$

$$\left.\left.-\csc^2\left[\frac{\pi-(\phi+\phi')}{2n}\right]F_s\left[\beta Lg^-(\phi+\phi')\right]\right]\right\}\right\} \quad \text{(13-111a,b)}$$

Fresnel Transition Function

$$F_s(X) = 2jX\left[X - j2\sqrt{X}e^{jX}\int_{\sqrt{X}}^{\infty} e^{-j\tau^2}\,d\tau\right]$$

$$= 2jX\left[1 - F(X)\right]$$

\+ for soft polarization

\- for hard polarization

(13-111c)

Computer Program (SWDC)

Slope Wedge Diffraction Coefficients

SWDC (SCDCS, SCDCH, R, PHID, PHIPD, BTD, FN)

SCDCS = Complex Diffraction Coefficient (Soft)

SCDCH = Complex Diffraction Coefficient (Hard)

R = Distance Parameter ρ or ρ' (in λ)

PHID = ϕ (in degrees)

PHIPD = ϕ' (in degrees)

BTD = β' (incidence angle; *in degrees*)

FN = n [WA = $(2\text{-}n)\pi$]

Higher-Order Diffractions

For structures with multiple edges, coupling is introduced in the form of higher-order diffractions. To illustrate this point, let us refer to Figure 13-43a where a plane wave of hard polarization, represented magnetic field component parallel to the edge of the wedges, is incident upon a two-dimensional PEC structure composed of three wedges.

Higher-Order Diffractions from 2-D Wedge

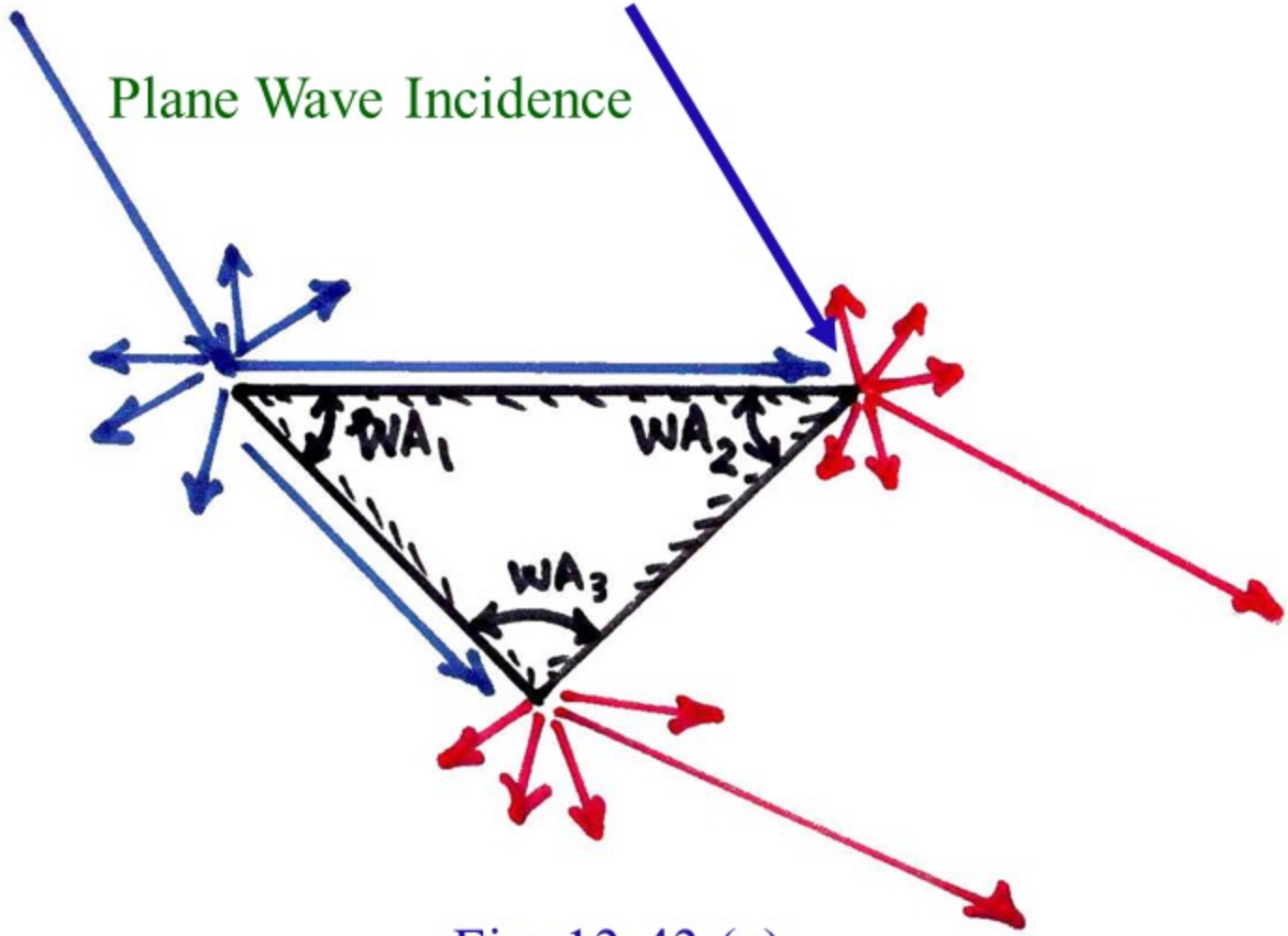

Fig. 13-43 (a)

Higher-Order Diffractions from 2-D Wedge

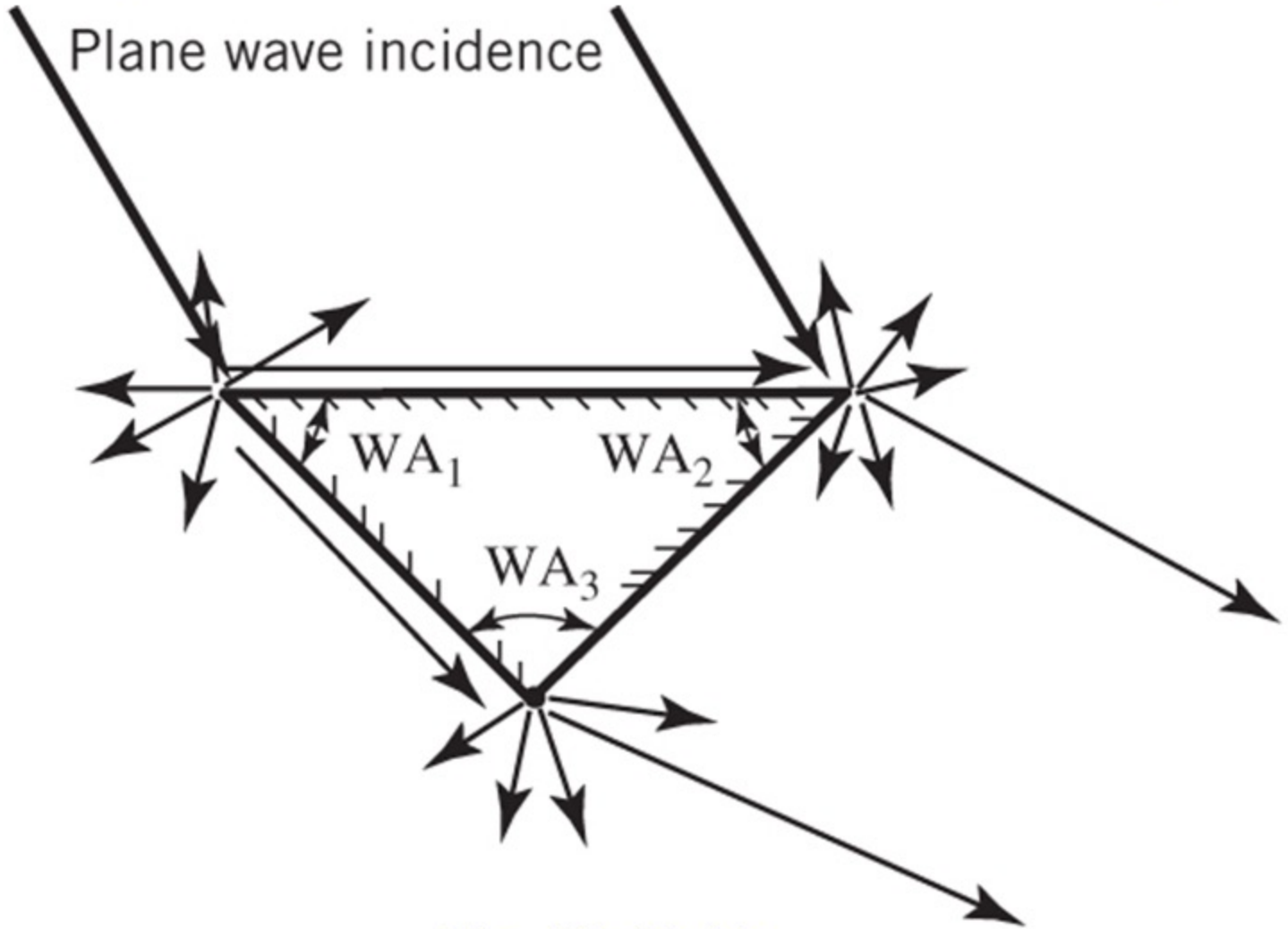

Fig. 13-43 (a)

The diffraction mechanism of this system can be outlined as follows: The plane wave incident on wedge 1, represented by wedge angle WA1, will be diffracted as shown in the Figure 13-43a. This is referred to as *first-order diffraction*. The field diffracted by wedge 1 in the direction of wedge 2, represented by wedge angle WA2, will be diffracted again, as shown in Figures 13-43a and 13-43b. This is referred to as *second-order diffraction*, because it is the result of diffraction from diffraction. In turn the field diffracted from wedge 2 toward wedges 1 and 3 will be diffracted again.

The same procedure can be followed for second-order diffractions from wedge 3 due to first-order diffractions from wedge 1. Second- and higher-order diffractions are all referred to as *higher-order diffractions*, and they account for coupling between the edges and are more important for bistatic than monostatic scattering.

First-Order Diffractions From Edge #1

Higher-Order Diffractions from 2-D Wedge

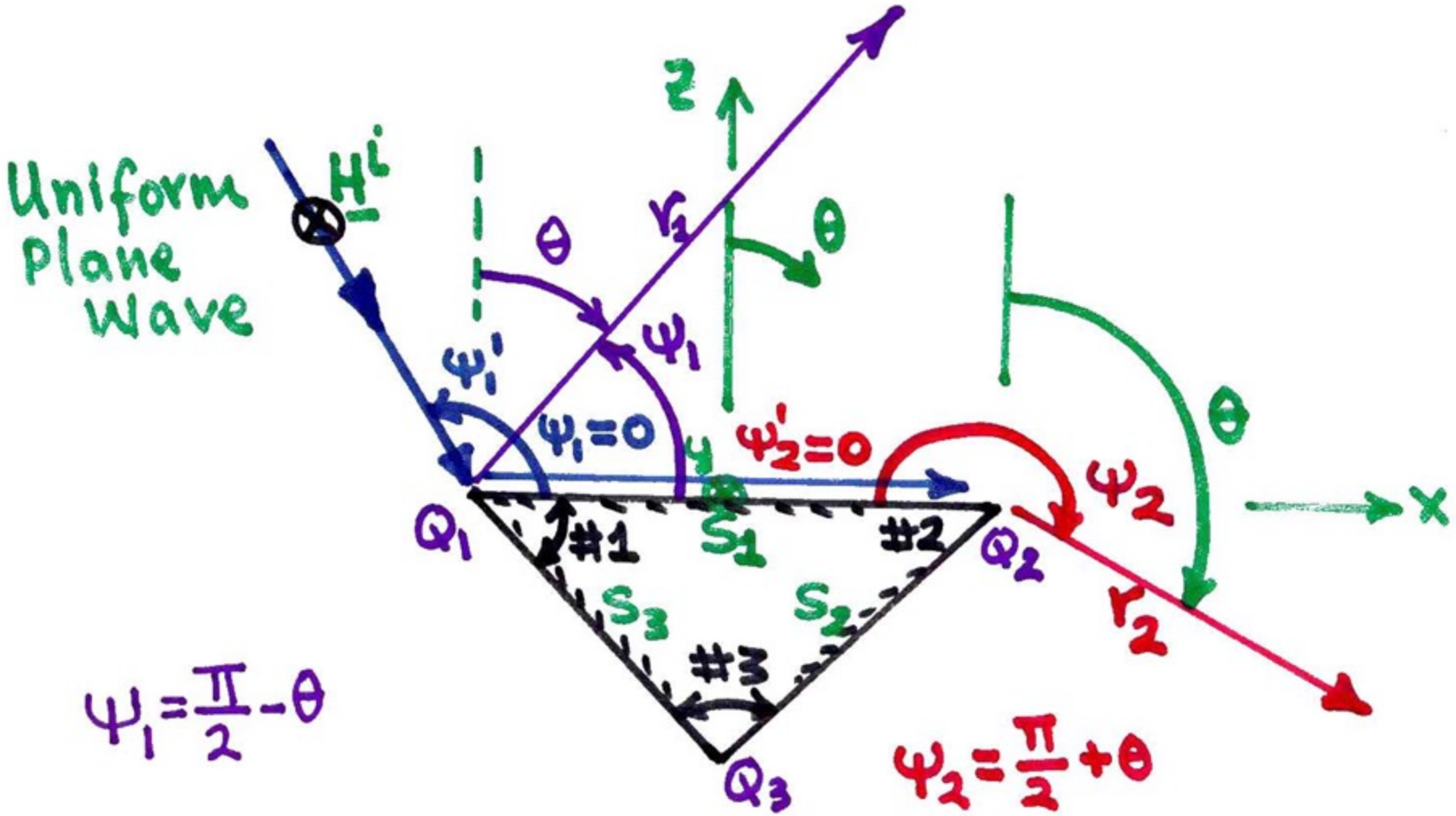

Fig. 13-43 (b)

Higher-Order Diffractions from 2-D Wedge

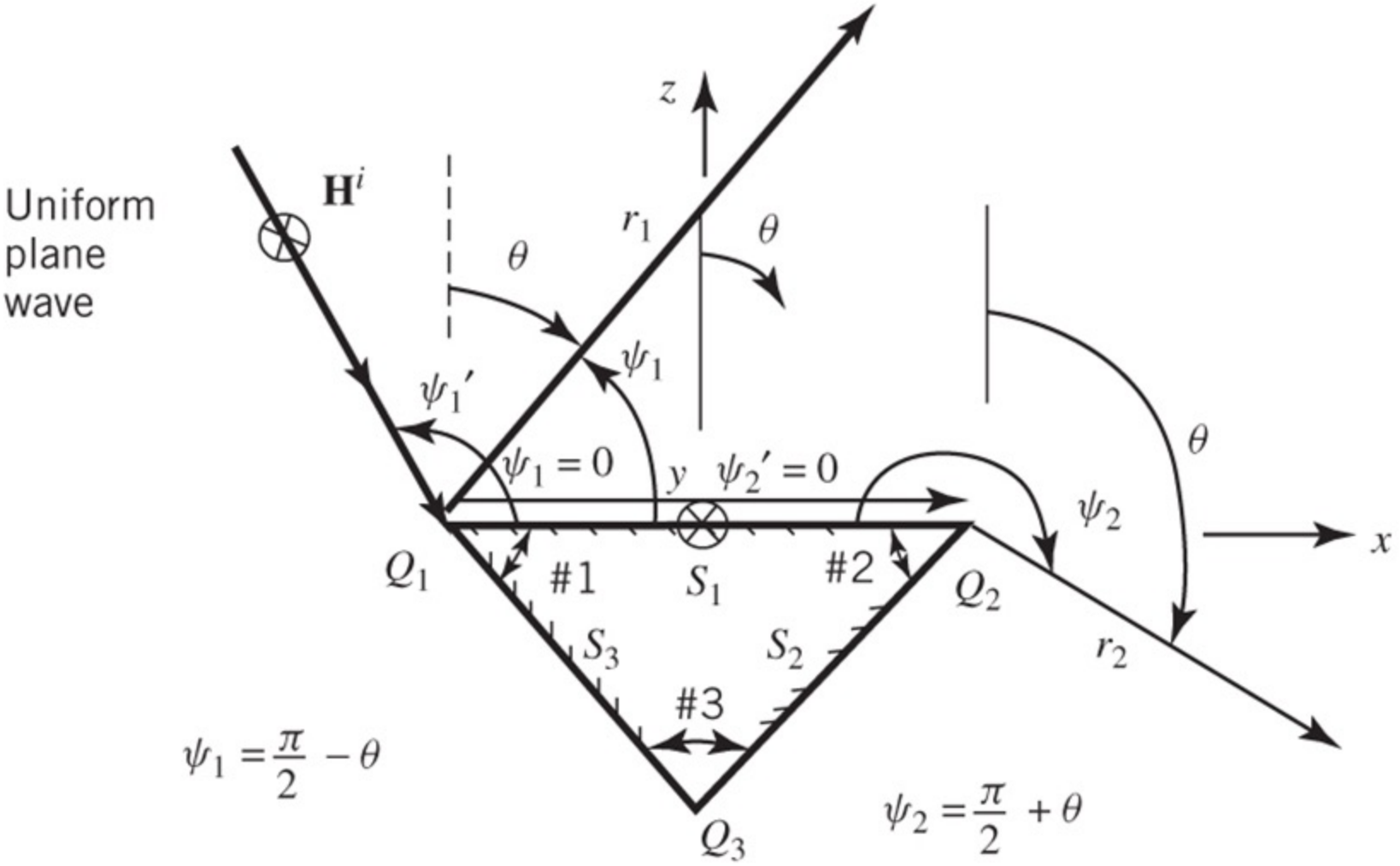

Fig. 13-43 (b)

Following the procedures that have been outlined for diffractions from two-dimensional PEC wedges, the first-order diffractions from wedge 1, first-order diffractions from wedge 1 toward wedge 2, and second-order diffractions from wedge 2 due to first-order diffractions from wedge 1, can be written, using the geometries of Figures 13-43a and 13-43b, as:

Uniform Plane Wave
Hard Polarization (2-D)
First-Order Diffraction Edge #1

$$\underline{H}_{y1}^{d1} = \underline{H}_1^i(Q_1)\cdot\left[\hat{a}_y\hat{a}_y D_1^h(r_1,\psi_1,\psi_1^{'},n_1)\right]\frac{1}{\sqrt{r_1}}e^{-j\beta r_1}$$

$$= \hat{a}_y H_1^i(Q_1)\cdot\left[\hat{a}_y\hat{a}_y\begin{Bmatrix} D_1^i(r_1,\psi_1-\psi_1^{'},n_1) \\ +D_1^r(r_1,\psi_1+\psi_1^{'},n_1)\end{Bmatrix}\right]\frac{1}{\sqrt{r_1}}e^{-j\beta r_1}$$

$$\underline{H}_{y1}^{d1} = +\hat{a}_y H_1^i(Q_1)\begin{Bmatrix} D_1^i(r_1,\psi_1-\psi_1^{'},n_1) \\ +D_1^r(r_1,\psi_1+\psi_1^{'},n_1)\end{Bmatrix}\frac{e^{-j\beta r_1}}{\sqrt{r_1}} \qquad \text{(13-112a)}$$

First-Order Diffractions From Edge #1 Toward Edge #2

First-Order Diffraction Edge #1 Toward Edge #2

$$\underline{H}_{y1}^{d1}(r_1 = s_1, \psi_1 = 0, n_1)\Big|_{r_1=s_1,\psi_1=0}$$

$$= + \hat{a}_y H_1^i(Q_1) \begin{Bmatrix} D_1^i(s_1, -\psi_1', n_1) \\ + D_1^r(s_1, \psi_1', n_1) \end{Bmatrix} \frac{e^{-j\beta s_1}}{\sqrt{s_1}}$$

$$\underline{H}_{y1}^{d1}(r_1 = s_1, \psi_1 = 0, n_1)\Big|_{r_1=s_1,\psi_1=0}$$

$$= + \hat{a}_y H_1^i(Q_1) \begin{Bmatrix} V_1^i(s_1, -\psi_1', n_1) \\ + V_1^r(s_1, \psi_1', n_1) \end{Bmatrix} \qquad (13\text{-}112b)$$

Equation 13-112b represents the total diffracted field; half of it is the incident diffracted field and the other half is the reflected diffracted field.

Second-Order Diffractions From Edge #2 Due to First-Order Diffractions from Edge #1

Second-Order Diffraction from Edge #2

$$\underline{H}_{y2}^{d2} = \underline{H}_{21}^{i}(Q_2)\cdot \hat{a}_y \hat{a}_y D_2^h(s_2,\psi_2,\psi_2^{'},n_2)\frac{1}{\sqrt{r_2}}e^{-j\beta r_2}$$

$$\psi_2^{'} = 0, \quad \psi_2 = \frac{\pi}{2}+\theta$$

$$\underline{H}_{y2}^{d2} = \frac{\underline{H}_{y1}^{d1}(r_1 = s_1,\psi_1 = 0,n_1)}{2}\cdot\left[\hat{a}_y \hat{a}_y D_2^h(s_2,\psi_2,\psi_2^{'},n_2)\right]\frac{e^{-j\beta r_2}}{\sqrt{r_2}}$$

$$\underline{H}_{y2}^{d2} = +\hat{a}_y \frac{H_1^i(Q_1)}{2}\left\{V_{B1}^i(s_1,-\psi_1^{'},n_1)+V_B^r(s_1,\psi_1^{'},n_1)\right\}$$

$$\cdot \hat{a}_y \hat{a}_y\left[D_2^i(s_2,\psi_2,n_2)+D_2^r(s_2,\psi_2,n_2)\right]\frac{e^{-j\beta r_2}}{\sqrt{r_2}}$$

$$\underline{\underline{H}}_{y2}^{d2} = +\hat{a}_y \frac{H_1^i(Q_1)}{2}\left[V_{B1}^i(s_1,-\psi_1^{'},n_1)+V_B^r(s_1,\psi_1^{'},n_1)\right]$$

$$\cdot\left[D_2^i(s_2,\psi_2,n_2)+D_2^r(s_2,\psi_2,n_2)\right]\frac{e^{-j\beta r_2}}{\sqrt{r_2}}$$

$$\underline{\underline{H}}_{y2}^{d2} = +\hat{a}_y \frac{1}{2}H_1^i(Q_1)\left[V_{B1}^i(s_1,-\psi_1^{'},n_1)+V_B^r(s_1,\psi_1^{'},n_1)\right]$$

$$\cdot\left[2D_2^i(s_2,\psi_2,n_2)\right]\frac{e^{-j\beta r_2}}{\sqrt{r_2}}$$

$$\underline{\underline{H}}_{y2}^{d2} = +\hat{a}_y H_1^i(Q_1)\left[V_B^i(s_1,-\psi_1^{'},n_1)+V_B^r(s_1,\psi_1^{'},n_1)\right]$$

$$\cdot D_2^i(s_2,\psi_2,n_2)\frac{e^{-j\beta r_2}}{\sqrt{r_2}} \qquad (13\text{-}112c)$$

The ½ factor in the development of (13-112c) is used to represent the incident diffracted field of (13-112b) from wedge 1 toward wedge 2.

The procedure needs to the repeated for first- and second-order diffractions due to the direct incidence of the plane wave to wedge 2. The method was developed for hard polarization as there are no higher-order diffractions for soft polarization since the diffracted field from any of the wedges toward the others will be zero due to the vanishing of the tangential electric field along the PEC surface of the structure.

Higher-Order Diffractions

Self-Consistent Method

or

Successive Scattering Procedure

Finite Thickness Edge for Multiple Diffractions

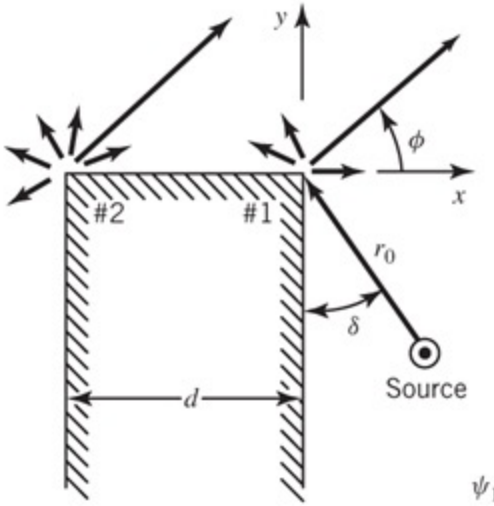

$\psi_{10} = \frac{\pi}{2} + \phi$

$\psi'_{10} = \delta$

$\psi_{12} = \pi - \phi$

$\psi'_{12} = 0$

(a) Source Incidence

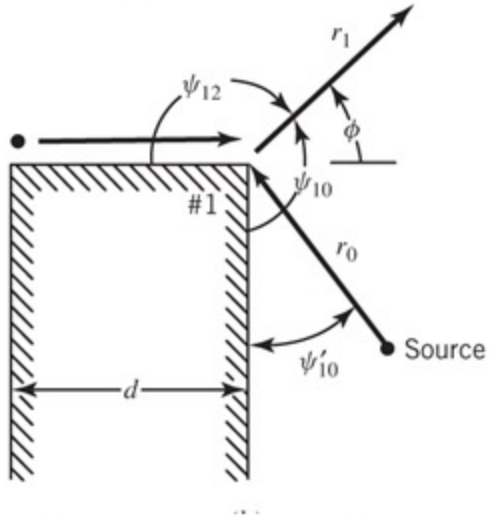

(b) Diffraction By Edge #1

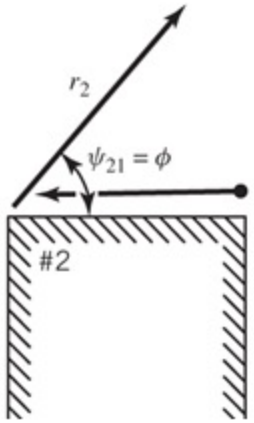

$\psi_{21} = \phi$

$\psi'_{21} = 0$

(c) Diffraction By Edge #2

Fig. 13-44

Diffractions From Edge #1

$$U_1^{s,h}(r_1,\phi) = U_0^{s,h}(Q_1)$$

$$\cdot D_{10}^{s,h}\left(L_{10},\psi_{10}=\frac{\pi}{2}+\phi,\psi_{10}^{'}=\delta,n_1\right)A_{10}e^{-j\beta r_1}$$

$$+\frac{1}{2}U_2^{s,h}(r_2=d,\phi=0)$$

$$\cdot D_{12}^{s,h}\left(L_{12},\psi_{12}=\pi-\phi,\psi_{12}^{'}=0,n_1\right)A_{12}(r_1)e^{-j\beta r_1}$$

(13-113a)

Diffractions From Edge #2

$$U_2^{s,h}(r_2,\phi)=\frac{1}{2}U_1^{s,h}(r_1=d,\phi=\pi)$$
$$\cdot D_{21}^{s,h}\left(L_{21},\psi_{21}=\phi,\psi_{21}^{'}=0,n_2\right)A_{21}(r_2)e^{-j\beta r_2} \qquad \text{(13-113b)}$$

$$U_1^{s,h}(r_1,\phi)=\left[\begin{array}{l} U_0^{s,h}(Q_1) \\ \quad \cdot D_{10}^{s,h}\left(L_{10},\psi_{10}=\dfrac{\pi}{2}+\phi,\psi_{10}^{'}=\delta,n_1\right)A_{10}e^{-j\beta r_1} \\ +\dfrac{1}{2}U_2^{s,h}(r_2=d,\phi=0) \\ \quad \cdot D_{12}^{s,h}\left(L_{12},\psi_{12}=\pi-\phi,\psi_{12}^{'}=0,n_1\right)A_{12}(r_1)e^{-j\beta r_1} \end{array}\right]_{\substack{r_1=d \\ \phi=\pi}}$$

(13-113a)

$$U_1^{s,h}(r_1 = d, \phi = \pi) = U_0^{s,h}(Q_1)$$

$$\cdot D_{10}^{s,h}\left(L_{10}, \psi_{10} = \frac{3\pi}{2}, \psi_{10}^{'} = \delta, n_1\right) A_{10} e^{-j\beta d}$$

$$+ \frac{1}{2} U_2^{s,h}(r_2 = d, \phi = 0) \qquad (13\text{-}114a)$$

$$\cdot D_{12}^{s,h}\left(L_{12}, \psi_{12} = 0, \psi_{12}^{'} = 0, n_1\right) A_{12}(r_1 = d) e^{-j\beta d}$$

$$U_2^{s,h}(r_2 = d, \phi = 0) = U_1^{s,h}(r_1 = d, \phi = \pi)$$

$$\cdot \left\{ \frac{1}{2} D_{21}^{s,h}\left(L_{21}, \psi_{21} = 0, \psi_{21}^{'} = 0, n_2\right) A_{21}(r_2 = d) e^{-j\beta d} \right\}$$

(13-114b)

Equations (13-114a) and (13-114b) can be written, respectively, in simplified form as

$$\left[U_1^{s,h}(r_1 = d, \phi = \pi)\right] = U_0^{s,h}(Q_1)T_{10}^{s,h} + \left[U_2^{s,h}(r_2 = d, \phi = 0)R_{12}^{s,h}\right] \tag{13-115a}$$

$$\left[U_2^{s,h}(r_2 = d, \phi = 0)\right] = \left[U_1^{s,h}(r_1 = d, \phi = \pi)R_{21}^{s,h}\right] \tag{13-115b}$$

where

$$T_{10}^{s,h} = D_{10}^{s,h}\left(L_{10}, \psi_{10} = \frac{3\pi}{2}, \psi_{10}^{'} = \delta, n_1\right) \cdot A_{10}(r_1 = d)e^{-j\beta d} \tag{13-115c}$$

$T_{10}^{s,h}$ = transmission coefficient from wedge 1 toward wedge 2 due to radiation from main source

$$R_{12}^{s,h} = \frac{1}{2} D_{12}^{s,h}\left(L_{12}, \psi_{12} = 0, \psi_{12}^{'} = 0, n_1\right) \cdot A_{12}(r_1 = d)e^{-j\beta d} \tag{13-115d}$$

$R_{12}^{s,h}$ = reflection coefficient from wedge 1 toward wedge 2 due to diffractions from wedge 2

$$R_{21}^{s,h} = \frac{1}{2} D_{21}^{s,h}\left(L_{21}, \psi_{21} = 0, \psi_{21}^{'} = 0, n_2\right) \cdot A_{21}(r_2 = d) e^{-j\beta d} \tag{13-115e}$$

$R_{21}^{s,h}$ = reflection coefficient from wedge 2 toward wedge 1 due to diffractions from wedge 1

The self-consistent pair of (13-115a) and (13-115b) constains the two unknowns $U_1^{s,h}(r_1 = d, \phi = \pi)$ and $U_2^{s,h}(r_2 = d, \phi = 0)$ that are needed to predict the total diffracted field as given by (13-113a) and (13-113b). That is:

$$\left[U_1^{s,h}(r_1 = d, \phi = \pi)\right] = U_0^{s,h}(Q_1)T_{10}^{s,h} + \left[U_2^{s,h}(r_2 = d, \phi = 0)R_{12}^{s,h}\right] \quad (13\text{-}115a)$$

$$\left[U_2^{s,h}(r_2 = d, \phi = 0)\right] = \left[U_1^{s,h}(r_1 = d, \phi = \pi)R_{21}^{s,h}\right] \quad (13\text{-}115b)$$

$$\left[U_1^{s,h}(r_1 = d, \phi = \pi)\right] = U_0^{s,h}(Q_1)T_{10}^{s,h} + \left[U_2^{s,h}(r_2 = d, \phi = 0)R_{12}^{s,h}\right] \quad \text{(13-115a)}$$

Rearranging the terms in (13-115a) we can rewrite (13-115a) as

$$\left[U_1^{s,h}(r_1 = d, \phi = \pi)\right] - \left[U_2^{s,h}(r_2 = d, \phi = 0)R_{12}^{s,h}\right] = U_0^{s,h}(Q_1)T_{10}^{s,h}$$

$$U_1^{s,h}(r_1 = d, \phi = \pi) - R_{12}^{s,h}U_2^{s,h}(r_2 = d, \phi = 0) = U_0^{s,h}(Q_1)T_{10}^{s,h}$$

$$U_1^{s,h}(r_1 = d, \phi = \pi) - R_{12}^{s,h} U_2^{s,h}(r_2 = d, \phi = 0)$$
$$= U_0^{s,h}(Q_1) T_{10}^{s,h}$$

$$U_2^{s,h}(r_2 = d, \phi = 0) = U_1^{s,h}(r_1 = d, \phi = \pi) R_{21}^{s,h} \qquad \text{(13-115b)}$$

Substituting $U_2^{s,h}(r_2 = d, \phi = 0)$ from (13-115b) into first equation, we can write it as

$$U_1^{s,h}(r_1 = d, \phi = \pi) - R_{12}^{s,h} R_{21}^{s,h} U_1^{s,h}(r_1 = d, \phi = \pi)$$
$$= U_0^{s,h}(Q_1) T_{10}^{s,h}$$

which when solved for $U_1^{s,h}(r_1 = d, \phi = \pi)$ reduces to

$$U_1^{s,h}(r_1 = d, \phi = \pi) = U_0^{s,h}(Q_1) \frac{T_{10}^{s,h}}{1 - R_{12}^{s,h} R_{21}^{s,h}} \qquad \text{(13-116a)}$$

When (13-116a)

$$U_1^{s,h}(r_1 = d, \phi = \pi) = U_0^{s,h}(Q_1)\frac{T_{10}^{s,h}}{1 - R_{12}^{s,h}R_{21}^{s,h}} \qquad \text{(13-115a)}$$

is substituted into (13-115b)

$$U_2^{s,h}(r_2 = d, \phi = 0) = U_1^{s,h}(r_1 = d, \phi = \pi)R_{21}^{s,h} \qquad \text{(13-115b)}$$

reduces it to

$$U_2^{s,h}(r_2 = d, \phi = 0) = U_0^{s,h}(Q_1)\frac{T_{10}^{s,h}R_{21}^{s,h}}{1 - R_{21}^{s,h}R_{12}^{s,h}} \qquad \text{(13-116b)}$$

Summary

$$U_1^{s,h}(r_1 = d, \phi = \pi) = U_0^{s,h}(Q_1)\frac{T_{10}^{s,h}}{1 - R_{21}^{s,h}R_{12}^{s,h}}$$

(13-116a)

$$U_2^{s,h}(r_2 = d, \phi = 0) = U_0^{s,h}(Q_1)\frac{T_{10}^{s,h}R_{21}^{s,h}}{1 - R_{21}^{s,h}R_{12}^{s,h}}$$

(13-116b)

Another way to get (13-116a) and (13-116b) is to solve (13-115a) and (13-115b) simultaneously.

$$U_1^{s,h}(r_1 = d, \phi = \pi) - R_{12}^{s,h} U_2^{s,h}(r_2 = d, \phi = 0) = U_0^{s,h}(Q_1) T_{10}^{s,h} \tag{13-115a}$$

$$R_{21}^{s,h} U_1^{s,h}(r_1 = d, \phi = \pi) - U_2^{s,h}(r_2 = d, \phi = 0) = 0 \tag{13-115b}$$

which reduce to

$$U_1^{s,h}(r_1 = d, \phi = \pi) = U_0^{s,h}(Q_1) \frac{T_{10}^{s,h}}{1 - R_{21}^{s,h} R_{12}^{s,h}} \tag{13-116a}$$

$$U_2^{s,h}(r_2 = d, \phi = 0) = U_0^{s,h}(Q_1) \frac{T_{10}^{s,h} R_{21}^{s,h}}{1 - R_{21}^{s,h} R_{12}^{s,h}} \tag{13-116b}$$

When expanded, it can be shown that (13-116a) and (13-116b) can be written, by letting $x_0 = R_{21}^{s,h} R_{12}^{s,h}$, as a geometrical progression series of the form

$$\frac{1}{1-x_0} = 1 + x_0 + x_0^2 + x_0^3 + \ldots\ldots$$

$$U_1^{s,h}(r_1 = d, \phi = 0) = U_0^{s,h}(Q_1) T_{10}^{s,h} \cdot \left[1 + x_0 + x_0^2 + x_0^3 + \ldots..\right] \tag{13-117a}$$

$$U_2^{s,h}(r_2 = d, \phi = 0) = U_0^{s,h}(Q_1) T_{10}^{s,h} R_{21}^{s,h} \cdot \left[1 + x_0 + x_0^2 + x_0^3 + \ldots..\right] \tag{13-117b}$$

Each term of the geometrical series can be related to an order of diffraction by the corresponding wedge.

In matrix form, the self-consistent set of equations, (13-115a) and (13-115b), can be written as

$$\begin{bmatrix} 1 & -R_{12}^{s,h} \\ -R_{21}^{s,h} & 1 \end{bmatrix} \begin{bmatrix} U_1^{s,h}(r_1 = d, \phi = \pi) \\ U_2^{s,h}(r_2 = d, \phi = \pi) \end{bmatrix} = \begin{bmatrix} U_0^{s,h}(Q_1)T_{10} \\ 0 \end{bmatrix} \tag{13-118}$$

which can be solved using standard matrix inversion.

Overlap Transition Region

The field diffracted by Edge #1 towards Edge #2 creates a Transition Region (TR), as shown in Figure 12-45, over which the diffracted field is non-ray optical and the second-order and successive diffractions are not accurately predicted using the traditional GTD/UTD. The same is true for diffractions from other wedges, as shown in the graphs that follow.

Transition Region

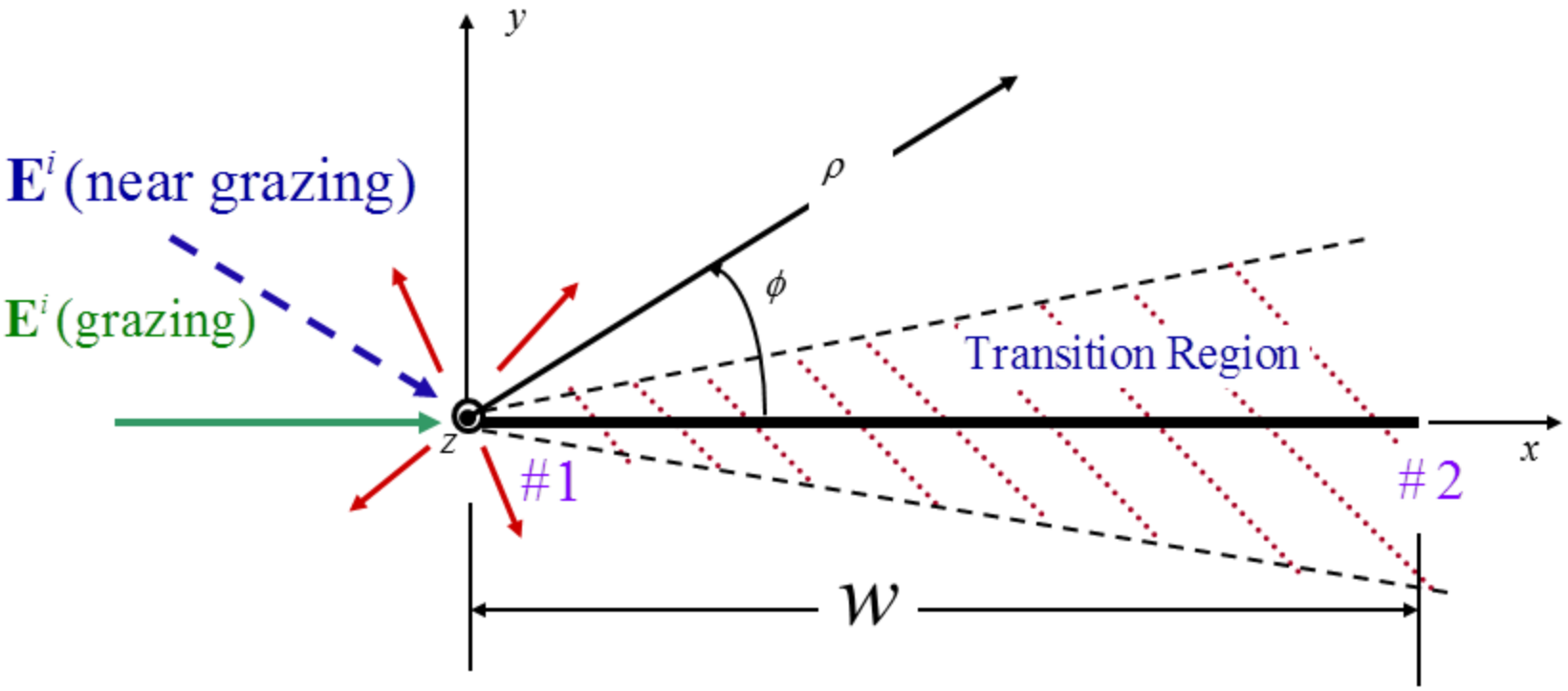

Fig. 13-45

Transition Region

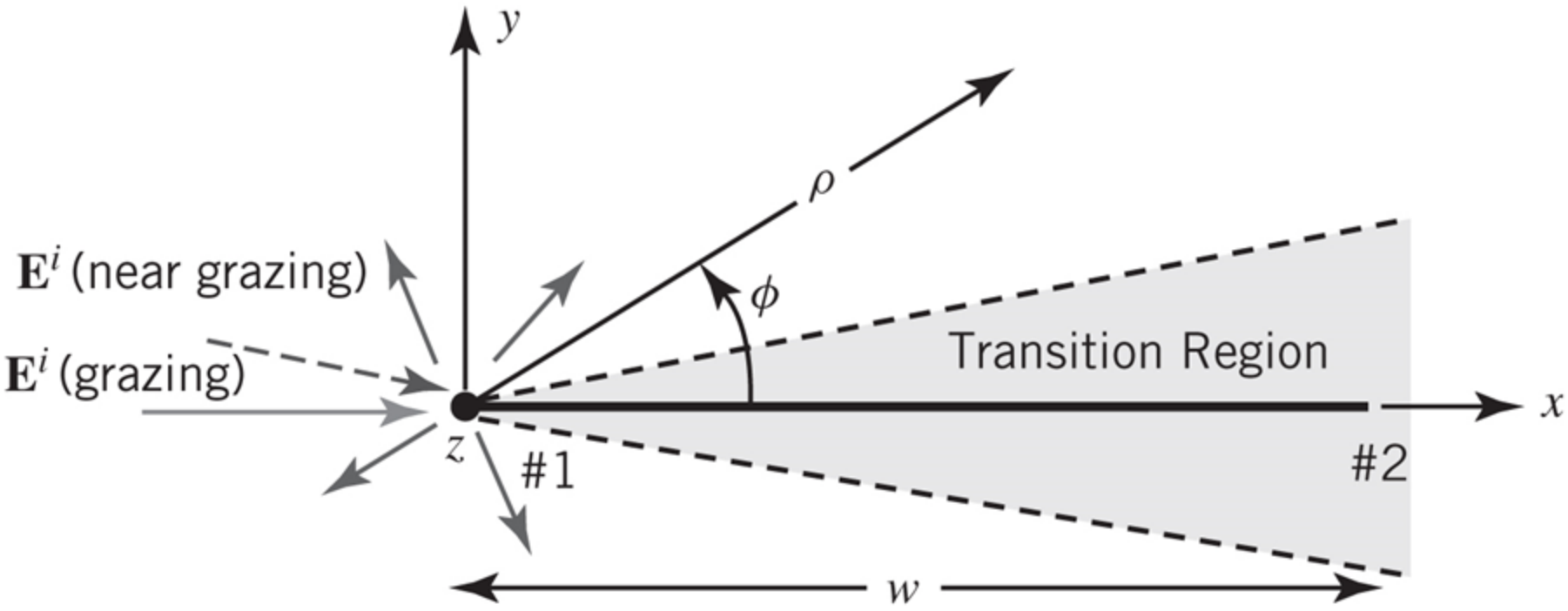

Fig. 13-45

To resolve the issue of the non-ray optical nature of the first-order diffractions, and the inaccurate predictions by standard GTD/UTD of the higher-order successive diffractions by wedges, the following two methods can be used.

1. Extended Spectral Theory of Diffraction (ESTD) [64]
2. Extended Physical Theory of Diffraction (EPTD) [65]

* GTD and UTD are considered to be somewhat heuristic, but more general and less cumbersome in their application to multiple diffractions.
* ESTD [64] and EPTD [65] are more rigorous and accurate, although less general and more complex.
* The use of GTD/UTD for multiple diffractions has already been addressed and illustrated.

The use of the GTD/UTD for multiple diffractions has already been addressed and illustrated.

The GTD/UTD fails in overlapping transition regions which occur for incidence at and near grazing and observation in the forward scatter region. For these cases, other methods must be utilized; two of those are the ESTD [64] and EPTD [65]. Both of these methods are considered as spectral methods, and both involve formulating appropriate high-frequency approximations for the double-diffracted field of a double wedge.

The ESTD [64] is an extension of the STD [66]. Using the ESTD, the current density induced on the scatter of interest is transformed in the spectral domain. The radiation integral is then asymptotically evaluated in the spectral domain after the induced current density is multiplied by a spectral diffraction coefficient. The original STD was limited to a half-plane and aperture scattering for plane wave incidence. The ESTD extends the STD to general double-wedge configuration, and it can be used for plane, cylindrical and spherical wave incidence for both normal and oblique incidence.

The EPTD [65] is an alternative transition region method based upon a different evaluation of the surface radiation integral. The induced current density is approximated using the PTD fringe currents [67], whereas the ESTD used the UTD diffraction coefficients. The resulting radiation integral is evaluated asymptotically to obtain the second-order field diffracted by the double wedge structure. The EPTD formulation is limited to plane-wave incidence, far-field observation in the normal plane of the structure. As with the ESTD, the EPTD doubly-diffracted field expression can be greatly simplified for certain geometries, such as for the strip.

To demonstrate the concepts of near grazing angle incidence diffraction, a numbers of examples are considered for monostatic and bistatic scattering for both soft (TM^z) and hard (TE^z) polarizations [68],[69]. For monostatic scattering the patterns are illustrated in Figures 13-46(a,b) for a strip of width $w = 2\lambda$. A width of 2λ is chosen for all cases so that the GTD/UTD diffraction coefficients are valid. For the soft polarization only first-order UTD diffractions are considered since higher-orders are not applicable; however for the hard polarization up to fourth-order UTD diffractions are included. It is clear that the results of all three methods (MM, EPTD, UTD) for both monostatic cases are in very good agreement.

Monostatic RCS by a 2-D PEC Strip

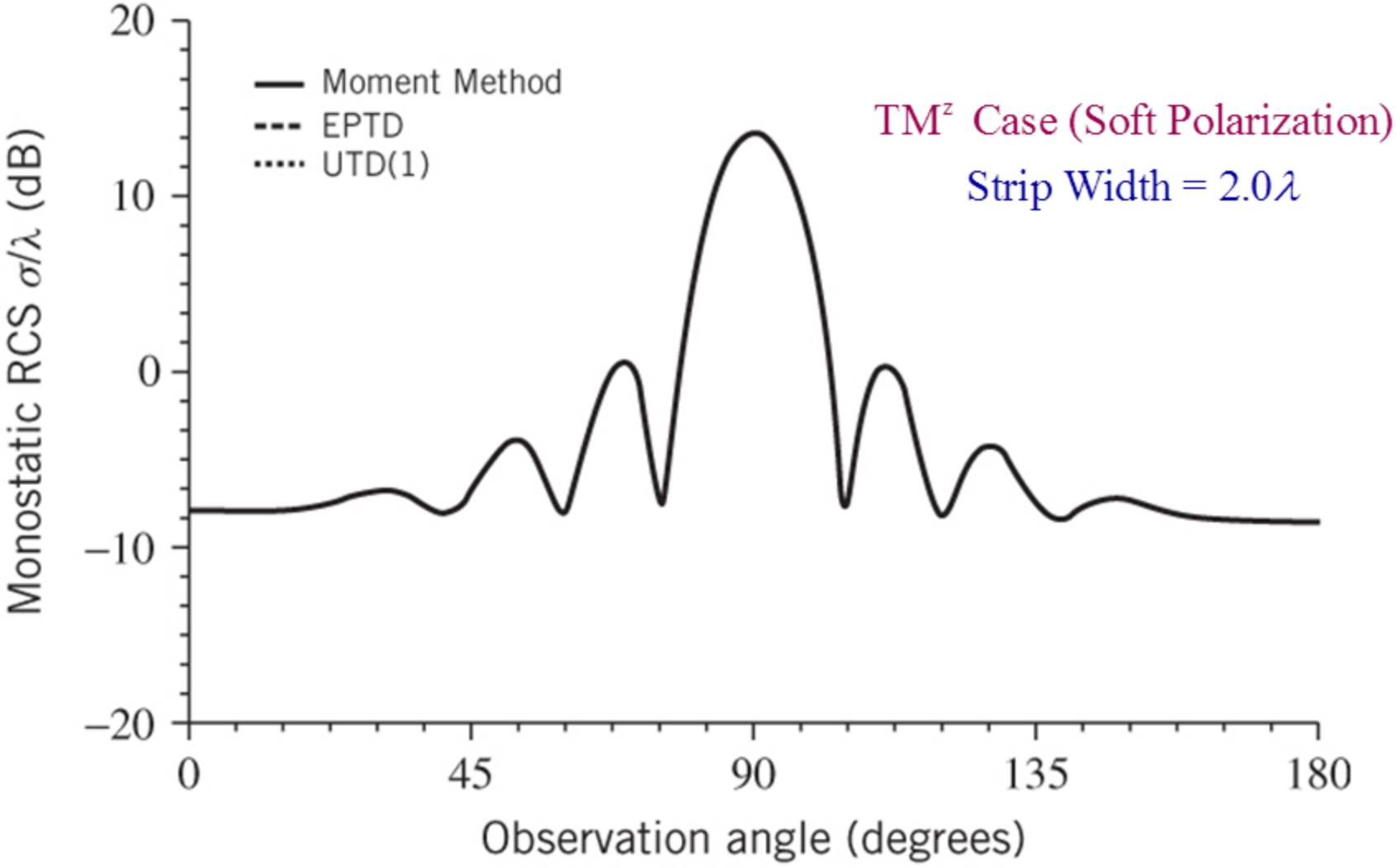

Fig. 13-46(a)

Monostatic RCS by a 2-D PEC Strip

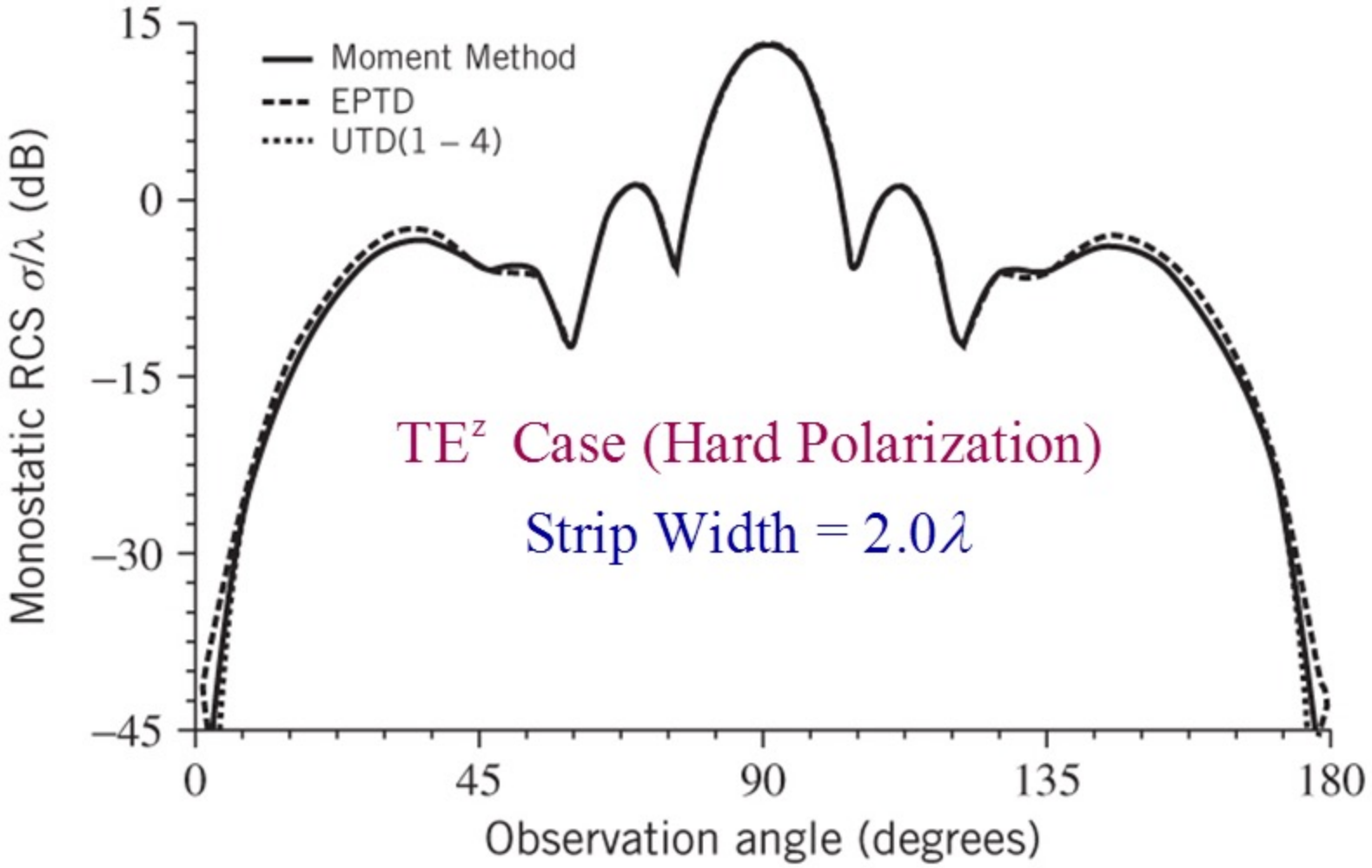

Fig. 13-46(b)

The bistatic scattering results for incidence angles of near grazing (ϕ_i =170°) and away from grazing (ϕ_i =135°) are shown in Figures 13-47(a,b) and 13-48(a,b), respectively. As expected, because of the UTD diffracted fields near grazing angle (ϕ_i =170°) are non-ray optical, the patterns of the UTD results are not in very good agreement with those of the MM and EPTD as indicated in Figures 13-47(a,b) for both polarizations. However the comparison of not near-grazing incidence (ϕ_i =135°) the agreement of all three methods is very good for both polarizations, as indicted in Figures 13-48(a,b).

Bistatic RCS by a 2-D PEC Strip

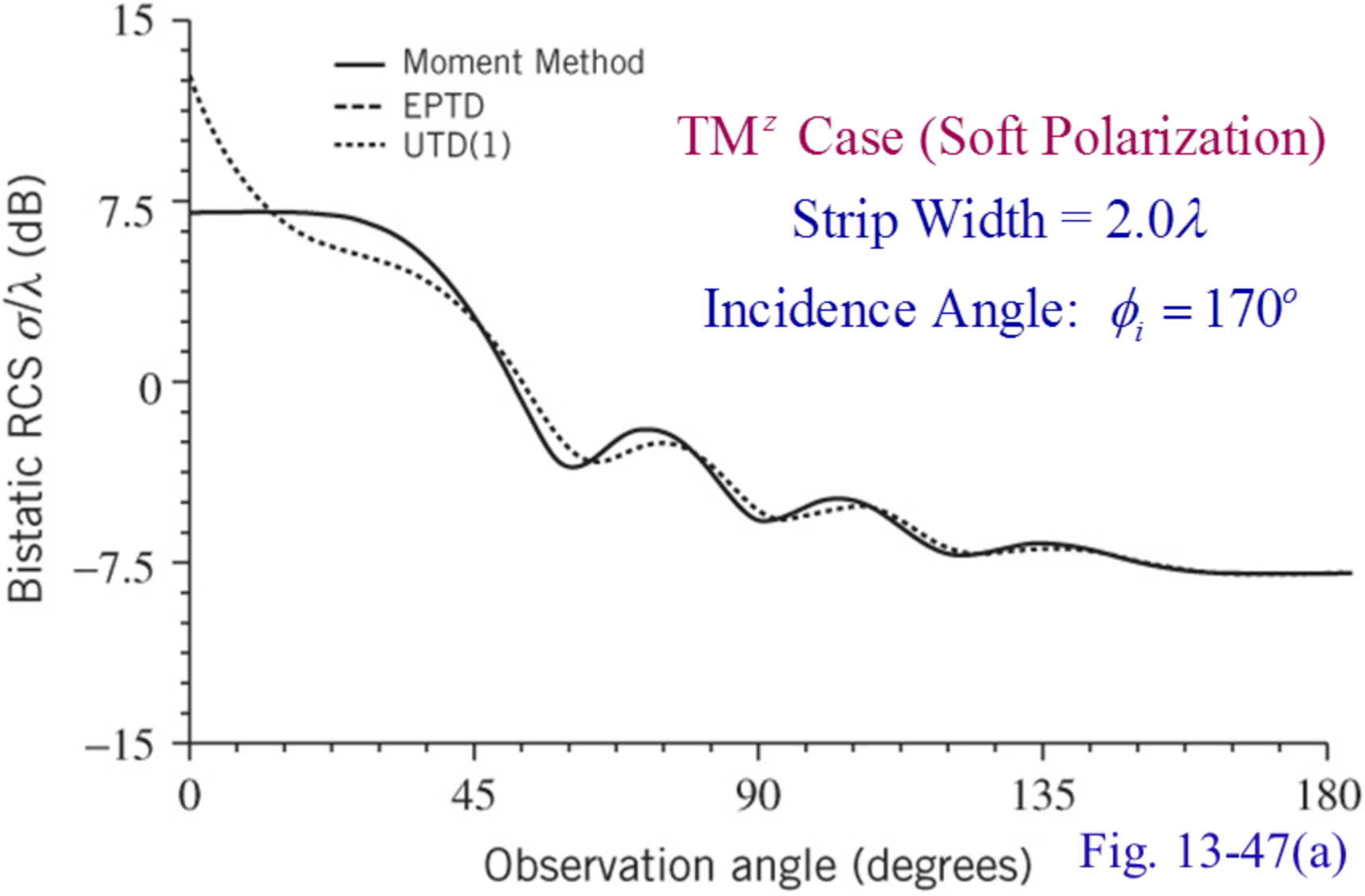

TM^z Case (Soft Polarization)

Strip Width = 2.0λ

Incidence Angle: $\phi_i = 170^o$

Fig. 13-47(a)

Bistatic RCS by a 2-D PEC Strip

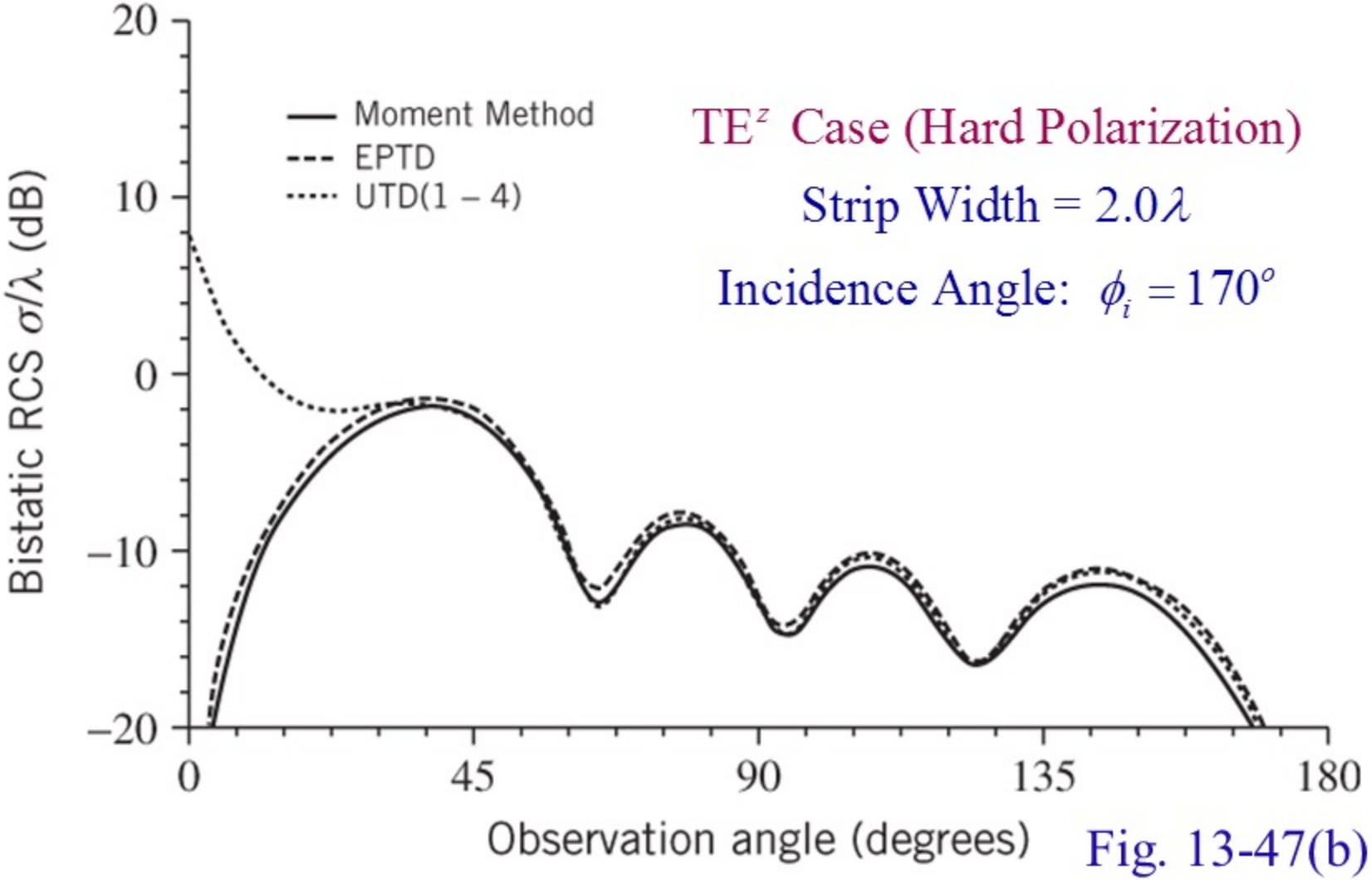

TE^z Case (Hard Polarization)

Strip Width = 2.0λ

Incidence Angle: $\phi_i = 170^o$

Fig. 13-47(b)

Bistatic RCS by a 2-D PEC Strip

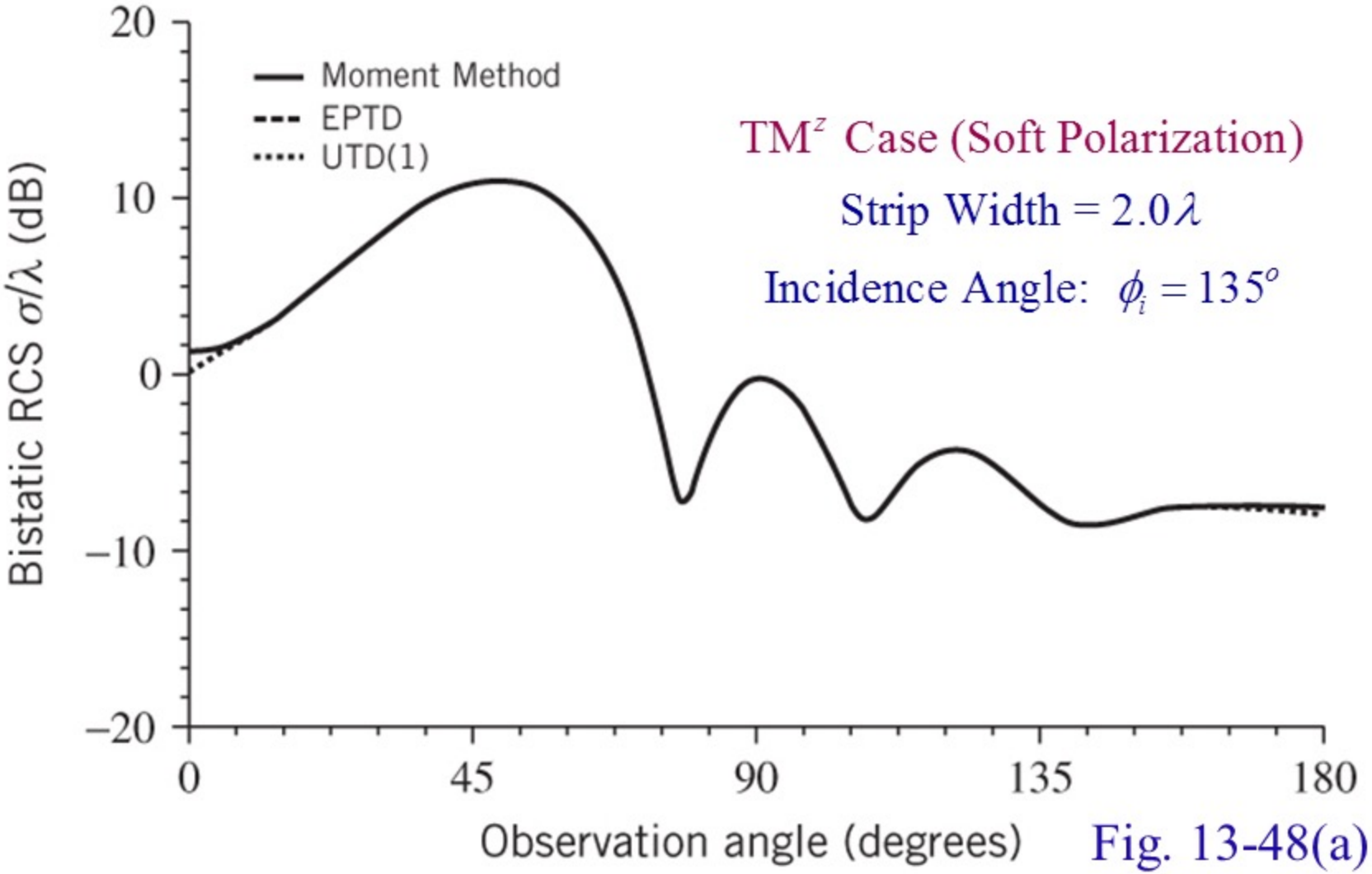

Fig. 13-48(a)

Bistatic RCS by a 2-D PEC Strip

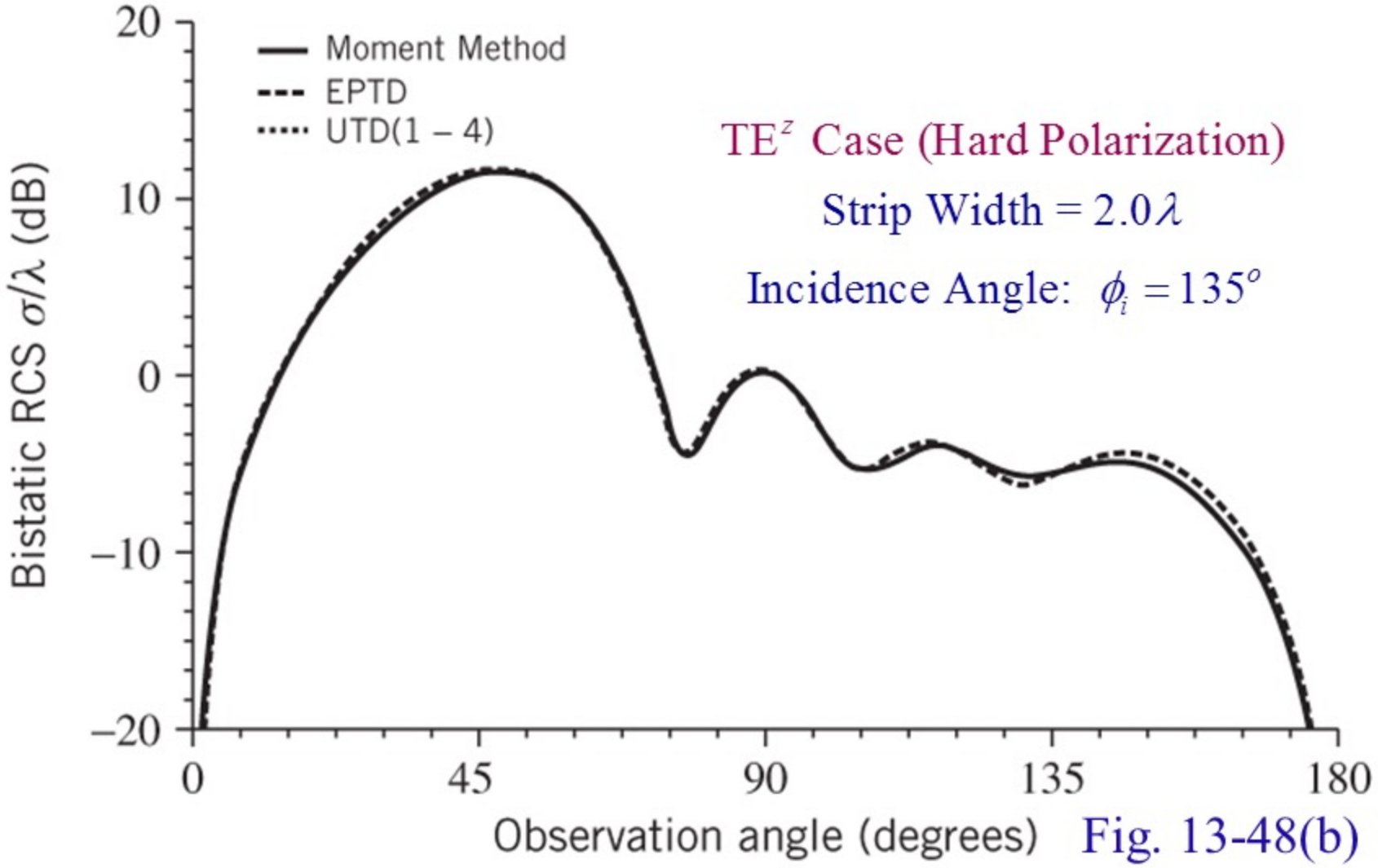

TE^z Case (Hard Polarization)

Strip Width $= 2.0\lambda$

Incidence Angle: $\phi_i = 135^o$

Fig. 13-48(b)

13.5 MULTIMEDIA

On the website that accompanies this book, the following multimedia resources are included for the review, understanding and presentation of the material of this chapter.

- **Matlab computer programs:**
  - **a. WDC:** (Both Matlab and Fortran). Computes the first order wedge diffraction coefficient based on (13-89a)-(13-90b). The initial Fortran algorithm was developed and reported in [53].
  - **b. SWDC:** (Both Matlab and Fortran). Computes the first slope wedge diffraction coefficient based on (13-111a)-(13-111c). The initial Fortran algorithm was developed and reported in [53].
  - **c. PEC_Wedge:** Computes, based on the exact solution of (13-40a), the normalized amplitude pattern of a uniform plane wave incident upon a two-dimensional PEC wedge of Figure 13-13.
  - **d. PEC_Strip_Line_UTD**: Computes, using UTD, the normalized amplitude radiation pattern of a line source based on the UTD of Example 13-4. It is compared with that based of the Integral Equation (IE) of Sections 12.2.2-12.2.8 and Physical Optics (PO) of Section 11.2.3.

e. **PEC_Strip_SW_UTD:** Computes, using UTD, the TM^z and TE^z 2D scattering width (SW), monostatic and bistatic, of a PEC strip of finite width, based on the UTD of Example 13-5. It is compared with that of the Integral Equation (IE) of Section 12.3.1 and Physical Optics of Section 11.3.1, and Figures 12-13 and 11-4.

f. **Monopole_GP_UTD:** Computes, using UTD, the normalized amplitude radiation pattern of a l/4 monopole on a rectangular or circular ground plane based on UTD and Figures 13-32 and 13-37.

g. **Aperture_GP_UTD**: Computes, using UTD, the normalized amplitude radiation pattern of a rectangular or circular aperture, with either a uniform or dominant mode aperture field distribution, on a rectangular ground plane based on UTD and Figure 13-32 where the monopole is replaced by an aperture as shown in Figure P13-41.

h. **PEC_Rect_RCS_UTD**: Computes, using UTD, the TE^x and TM^x bistatic and monostatic RCS of a PEC rectangular plate using UTD. It is compared with the Physical Optics (PO) of Section 11.2.3.

i. **PEC_Circ_RCS_UTD:** Computes the TE^x and TM^x monostatic RCS of a PEC circular plate using UTD. It is compared with the Physical Optics (PO) of Chapter 11 and Problem 11.24.

j. **PEC_Square_Circ_RCS_UTD.** Computes, using UTD, the TE^x and TM^x monostatic RCS of PEC square and circular plates, which have the same area and equal maximum monostatic RCS at normal incidence. The UTD patterns of the two plates, square and circular, are compared with the Physical Optics (PO) of Chapter 11.

- **Power Point (PPT) viewgraphs, in multicolor.**